

Project Number: ECC-A082



---

# Engine Hydrostatic-lock Mitigation

---

A Major Qualifying Project  
Submitted to the Faculty  
of the  
**WORCESTER POLYTECHNIC INSTITUTE**  
in partial fulfillment of the requirements for the  
Degree of Bachelor of Science

by

Steven Danley

---

Christopher Egan

---

Christopher Lyons

---

Submitted:

---

Professor Eben C. Cobb, Advisor

## Abstract

Hydrostatic-lock occurs when an incompressible fluid replaces air entering an internal combustion engine. As the piston attempts to compress this fluid, the engine will stall, potentially resulting in catastrophic failure of various components. This project sought to develop a system to mitigate and prevent hydrostatic-lock. Following analysis of engine dynamics and pressures, two systems were developed to work in conjunction with each other. The first system measures pressure in the engine's intake. If a spike in negative pressure is detected, indicating the presence of water, the intake is closed off. Should water enter the combustion chamber, the second system, a valve in the engine head, will react to the pressure spike and allow the excess pressure to be relieved. Following computer simulation, a prototype of each system was manufactured and validated through testing.

## Executive Summary

In the last century society has been reliant on the use of internal combustion engines to fuel a growing need. While the concept behind such engines has not changed the operational control has yet some conditions have been inadequately researched. Following a friends experience with hydrostatic-lock the team came to a conclusion that a system could be developed to prevent, or mitigate the condition. The introduction of this system into both modern and preceding engines seeks to eliminate the condition or reduce the detrimental effects.

Hydrostatic lock is a term used to describe the introduction of any incompressible fluid, which exceeds the maximum volume at top dead center (TDC). Research determined that while the risk is rare in the Northeast and other northern areas of the country, states and countries with inadequate water management systems frequently experience the condition. Derived from a need, attention was turned towards developing two independent or concurrently functioning systems, eliminating the possibility of experiencing hydrostatic-lock. Several companies have recently addressed this need; producing a system to block the entry of water with a rubber diaphragm, routing the intake to a higher level. As a result, water is prevented from entering the intake, however, if the product is also submersed the engine is no longer protected.

To develop a system that would allow for protection during a complete submersion, the team focused on prototyping two systems. One system is implemented within the engine head, with the other attached to the intake tubing. To thwart hydro locking, the engine head system

exhausts pressure beyond the nominal threshold, thereby relieving pressure that may cause engine damage. The intake system works to prevent the intake of water through continuous monitoring of pressure; if a large negative spike is registered the intake is blocked off, stalling the engine.

To design the engine head it was required that the team analyzes the nominal operating conditions of the engine. To evaluate both the non-running/running pressures a pressure transducer was fitted into a custom built head. Once fitted, a circuit was developed to amplify and power the transducer. The data was acquired through a 12-bit Digital-Analog-Converter used in conjunction with NI labview; this setup resulted in a sampling rate of 10,000 samples per second exported into excel for analysis. The resulting data allowed the team to redesign and build the engine head, including a portion necessary to properly seat a valve as well as a valve guide. Additionally, the team calculated the required spring constant and necessary spring required to hold the running engine pressure.

The intake system was designed as a stand-alone system used to detect and prevent hydrostatic lock conditions. Concurrent design allowed the team to build a single circuit, which would allow the recording of both the engine and intake pressure. The necessary intake data was then transferred to a circuit, which would analyze and compare pressure. If the intake pressure dropped below normal conditions the circuit would signal a solenoid to close, blocking off the intake. By stopping airflow to the engine the system effectively stalls the engine while blocking water from entering the combustion chambers, preventing hydrostatic-lock.

Independently, each system works to reduce the chance of hydrostatic-locking by means of preventing the compression of incompressible fluids. To reduce overall cost many considerations were taken into account, allowing for ease of manufacturing, decreased mold costs, and other modifications to reduce overall cost. With performance unaffected they allow the general public to purchase and implement a design to prevent the condition. While no system is perfect, together the prototypes offer a viable solution to reduce the chance of engine failure due to hydrostatic lock.

## Acknowledgements

We would like to thank our advisor, Professor E.C. Cobb, for all the guidance and motivation over the course of the project. Thanks to the guidance we received we were able to truly get a sense of how real world engineering projects function.

The members of the team would also like to express appreciation to the secretaries and staff of the mechanical engineering department, for all the help provided over the year. A special thanks to Professor Taskin Padir from the ECE department, as well as Wayne Haase from Summit Safety for the extensive help and guidance developing our circuits. We would also like to thank the staff of the WPI Washburn Shops, Toby Berstrom, Adam Sears, and Dan Flavin, their assistance and teaching allowed us to develop the skills needed to manufacture our prototype systems. The Design studio staff, Randy Robinson, Sia Najafi, and Adriana Hera, for providing the software and facilities needed to design and analyze our systems, as well as Russell Morin for his help making the Rapid Prototype parts.

And finally for helping us get started, Professor Norton for his initial belief in the project and advice on how to get started, as well as Dick Deterra of Polaris a Lockheed Martin Company, for providing the Briggs and Stratton Engine for us to test on. Without everyone's help this project would not have been possible.

## Table of Contents

<b>Abstract</b>	<b>i</b>
<b>Executive Summary</b>	<b>ii</b>
<b>Acknowledgements</b>	<b>v</b>
Table of Figures	vii
<b>Chapter 2 : Introduction</b>	<b>2-1</b>
<b>Chapter 3 : Background</b>	<b>3-3</b>
Internal Combustion Engine	3-3
Our Engine	3-4
Engine Theory	3-7
<b>Chapter 4 : Project Objective</b>	<b>4-12</b>
3.1 Goal Statement	4-12
3.2 Task Specifications	4-12
<b>Chapter 5 : Design Concepts</b>	<b>5-13</b>
4.1: Spring Controlled Valve	5-13
4.2: Intake system	5-15
4.3: Valve System on Exhaust Valve	5-17
4.4: Pressure relief valve in the piston	5-19
4.5 Actuated Valve in Cylinder	5-21
<b>Chapter 6 : Design Selection</b>	<b>6-24</b>
<b>Chapter 7 : Engine Analysis and Testing</b>	<b>7-26</b>
<b>Chapter 8 : Detailed Design</b>	<b>8-34</b>
Intake System	8-34
Circuit design and development	8-37
Spring Valve	8-40
The final valve:	8-43
The final combustion chamber:	8-44
<b>Chapter 9 : Prototype Construction</b>	<b>9-51</b>
Intake system	9-53
Valve system	9-54
<b>Chapter 10 : Prototype Testing</b>	<b>10-57</b>
<b>Chapter 11 : Conclusions</b>	<b>11-61</b>
<b>Chapter 12 : Recommendations</b>	<b>12-65</b>
Alternative Water Detection and ECU Integration	12-65

Valve Seating and Sealing .....	12-67
System Improvement and modification .....	12-67
Adaptation for Manufacturing .....	12-68
<b>Chapter 13 : Appendices.....</b>	<b>13-69</b>
Appendix A: Drawings .....	13-69
Appendix B: Data.....	13-83
Ungrounded Tests.....	13-83
Grounded tests .....	13-84
Intake Pressure Tests .....	13-86
Appendix C: Data Sheets .....	13-88
Appendix D: Calculations .....	13-157
Appendix E: Analysis .....	13-160
Appendix F: Analysis .....	13-163

## Table of Figures

<b>Figure 3-1: Engine Head without Head.....</b>	<b>3-5</b>
<b>Figure 3-2: Combustion chamber of the Engine Head.....</b>	<b>3-5</b>
<b>Figure 3-3: Throttle Arm.....</b>	<b>3-6</b>
<b>Figure 3-4: Carburetor .....</b>	<b>3-6</b>
<b>Figure 3-5: Volumetric Efficiency, Honda S2000 .....</b>	<b>3-8</b>
<b>Figure 3-6: Volumetric Efficiency, Mustang GT .....</b>	<b>3-8</b>
<b>Figure 3-7: Mass Fraction Burned vs. Crank Angle.....</b>	<b>3-10</b>
<b>Figure 3-8: Cylinder Pressure vs. Crank Angle.....</b>	<b>3-11</b>
<b>Figure 7-1: 3 Op-Amp Instrumentation Amplifier .....</b>	<b>7-27</b>
<b>Figure 7-2: LabView Block Diagram.....</b>	<b>7-29</b>
<b>Figure 7-3: LabView Front Panel .....</b>	<b>7-29</b>
<b>Figure 7-4: Engine Pressure over Time .....</b>	<b>7-30</b>



Figure 7-5: Engine Pressure for One Revolution .....	7-30
Figure 7-6: Intake Pressure over Time.....	7-31
Figure 7-7: Intake Pressure over Time during Hydrostatic-Lock .....	7-31
Figure 7-8: Pressure vs. Time .....	7-32
Figure 8-1: Final Intake System Design.....	8-35
Figure 8-2: Intake System Cutaway.....	8-37
Figure 8-3: Circuit Diagram .....	8-40
Figure 8-4: Engine Head Cutaway .....	8-42
Figure 8-5: Max Stress in Valve .....	8-44
Figure 8-6: Deformation in Valve .....	8-44
Figure 8-7: Stress in Combustion Chamber.....	8-45
Figure 8-8: Deformations in Combustion Chamber.....	8-45
Figure 8-9: Velocity Magnitude Contours.....	8-47
Figure 8-10: Velocity Path Lines.....	8-48
Figure 8-11: Pressure Contour .....	8-49
Figure 9-1: Final Machined Engine Head .....	9-56
Figure 11-1: CAD Model of Intake System .....	11-62
Figure 11-2: Final Prototype of Intake System.....	11-62
Figure 11-3: CAD Model of Engine Valve System .....	11-63
Figure 11-4: Final Prototype of Engine Valve System.....	11-63
Figure 11-5: Both Systems Installed on the Engine .....	11-64
Figure 13-1: Engine Pressure Test 1 .....	13-83
Figure 13-2: Engine Pressure Test 2 .....	13-83
Figure 13-3: Engine Pressure Test 3 .....	13-84
Figure 13-4: Engine Pressure Test 4 .....	13-84
Figure 13-5: Engine Pressure Test 5 .....	13-84
Figure 13-6: Engine Pressure Test 6 .....	13-85

<b>Figure 13-7: Engine Pressure Test 7 .....</b>	<b>13-85</b>
<b>Figure 13-8: Engine Pressure Test 8 .....</b>	<b>13-85</b>
<b>Figure 13-9: Engine Pressure Test 9 .....</b>	<b>13-86</b>
<b>Figure 13-10: Intake Pressure with Short Hydrostatic-Lock Simulation .....</b>	<b>13-86</b>
<b>Figure 13-11: Intake Pressure with Full Hydrostatic-Lock Simulation .....</b>	<b>13-86</b>
<b>Figure 13-12: Intake Pressure Normal.....</b>	<b>13-87</b>
<b>Figure 13-13: Intake Pressure with Hydrostatic-Lock Simulation .....</b>	<b>13-87</b>
<b>Figure 13-14: Valve Variation 1.....</b>	<b>13-160</b>
<b>Figure 13-15: Valve Variation 2.....</b>	<b>13-160</b>
<b>Figure 13-16: Valve Variation 3.....</b>	<b>13-161</b>
<b>Figure 13-17: Valve Variation 4.....</b>	<b>13-161</b>
<b>Figure 13-18: Final Valve .....</b>	<b>13-162</b>

## Chapter 2 : Introduction

Hydrostatic lock, more commonly referred to as Hydrostatic-lock is a phenomenon resulting from the introduction of an incompressible fluid into the cylinder of an internal combustion engine. The effects of hydrostatically locking were initially discovered with the advent of steam engines; excess steam within the cylinder would prevent the compression stroke, often causing the connecting rod to puncture the firebox. Such catastrophes led engineers to develop cylinder drain cocks, which would allow the engineer to exhaust excess steam before such condensation would occur. Hydrostatic lock occurs if the volume of the introduced fluid exceeds that of the combustion chamber in the engine. As a result, the pistons in a 4-stroke engine are prevented from rotating through the compression stroke, leading to catastrophic failure. Typically, the force caused by the stroke termination often exceeds the materials yield strength, resulting in the failure of different parts, most commonly the connecting rod, piston, or cylinder head. Often the damage is enough to require a new engine to be purchased by the consumer and/or many hours of extra labor from the manufacture.

While the effects of hydrostatic-locking on steam engines have been prevented through the addition of drain cocks, allowing the engineer to exhaust excess pressure, modern internal combustion engines are susceptible to its effects. As a result, this project focuses on the development of a system that would prevent such effects and be feasibly implemented on any internal combustion engine. Although the addition of several parts may increase the existing engine retail price, the viable cost savings for a consumer is easily justified.

In effort to develop a suitable system the team will start by performing tests on a single cylinder Briggs and Stratton engine model number 98901. Required for the design and development of a viable system is the maximum internal pressures experienced during normal operation and at the moment of hydrostatic lock. Upon evaluation, the team will evaluate multiple designs and develop a system that will automatically prevent or exhaust the buildup of excessive pressure. Once a determination has been made as to which design is the most appropriate the team will begin fabricating a prototype. The Prototype will then be tested, and improved as needed.

## Chapter 3 : Background

### Internal Combustion Engine

Initially the term “engine” described any device that produced an output force from a given input. Derived from the French word *engin*, related to the Latin definition of ingenious, the English word “engine” portrayed any device which was thought of as ingenious. In modern usage, the word engine is used to describe a device that converts chemical or electrical energy into mechanical work. Sir Samuel Morland designed the first modern internal combustion during the 17<sup>th</sup> century; by using gunpowder Morland was able to drive water pumps. In 1858 Jean Joseph Étienne developed the first electric-spark ignition engine fueled by coal gas. Once proven as a possible source of mechanical work, engineers began to improve on past designs; and in 1876 engineers Nikolaus August Otto and Sir Dougald Clerk produced the first four and two stroke engines, seen as the modern production engines of today.

Nikolaus Otto’s engine standardized modern engine production, developing the first 4-stroke combustion engine cycle. Although the 2-stroke engine provided more power for a given weight, it required oil to be added to the fuel, increasing emissions; for this reason 2-stroke engines are being replaced in many applications. Once standardized, many engineers began to improve on Otto’s design. Karl Benz designed the first engine with multiple and horizontally opposed pistons. By horizontally opposing the cylinders the engine would be self-balancing, each piston reaching top-dead center simultaneously. As power demands increased, engineers began to experiment with increasing the relative size of the engine by adding pistons, increasing the engine speed, and expanding the cylinders volume. Growing emphasis on

emissions has led the development of more fuel efficient and smaller engines. Through improvements in modern engine control systems the fuel efficiency and emissions performance has drastically increased, leading the continuance for the internal combustion engine.

## Our Engine

We are using a single cylinder engine from Briggs and Stratton, specifically the 98901 model. This is a horizontally oriented engine. It has the following specifications:

Model	98901
Displacement	9.02ci (148cc)
Bore	2.562in (65.08mm)
Stroke	1.75in (44.45mm)
Oil Capacity	18-20oz (.54-.59L)

Table 3-1: Engine Specifications

The engine has valves that run parallel to the piston as shown in Figure 3-1.



**Figure 3-1: Engine Head without Head**

The combustion chamber is offset from the top of the piston, as show in Figure 3-2.



**Figure 3-2: Combustion chamber of the Engine Head**

The throttle is self-regulating using an arm and air speed as shown in Figure 3-3, controlling the throttle following the carburetor in Figure 3-4.

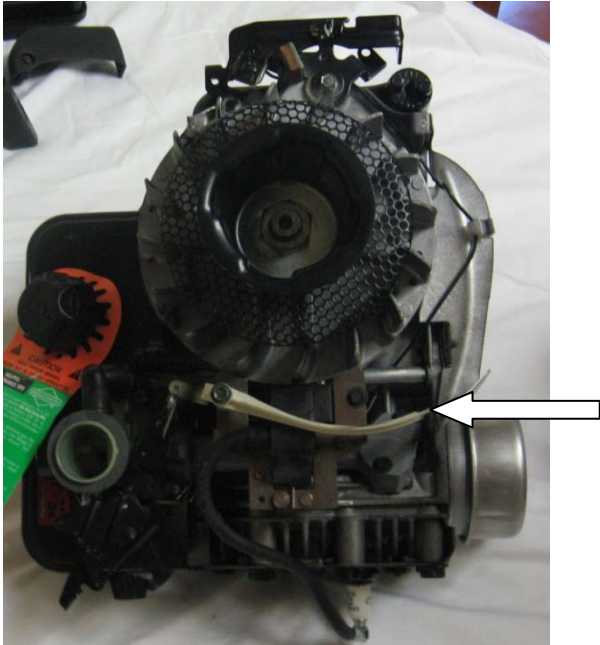


Figure 3-3: Throttle Arm



Figure 3-4: Carburetor



## Engine Theory

An engine may be referred to as anything that converts chemical energy into mechanical movement. Modern engines have typical efficiencies of 40%, with much of the inefficiency due to drive train and heat losses. In order for an engine to operate three elements must be present, air, fuel and ignition.

The more air you can force into the engine the more power you can make, the more efficient it will be. The amount of air you are pulling into the cylinder is referred to as volumetric efficiency; defined by the volume of air that is pulled into the cylinder verse the maximum volume of the cylinder itself. This theoretical amount is calculated using the formula  $(\pi \times \text{bore}^2 / 4 \times \text{stroke})$ .

If you are able to introduce a larger volume of air than the cylinder can hold it is possible to achieve efficiencies of over 100%. Typically, normal cars will not achieve this; however many high performance cars can, as shown in Figure 3-5 showing the VE of a Honda S2000.

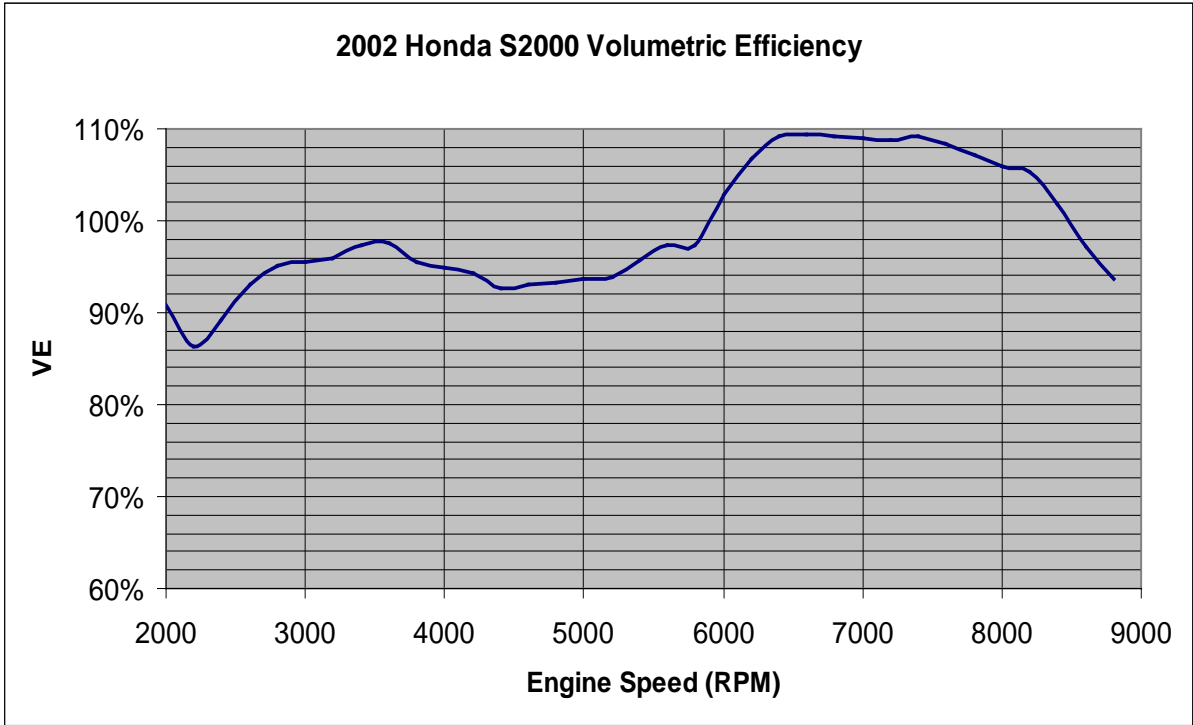


Figure 3-5: Volumetric Efficiency, Honda S2000

We can see a more typical curve in Figure 3-6 for the Mustang GT

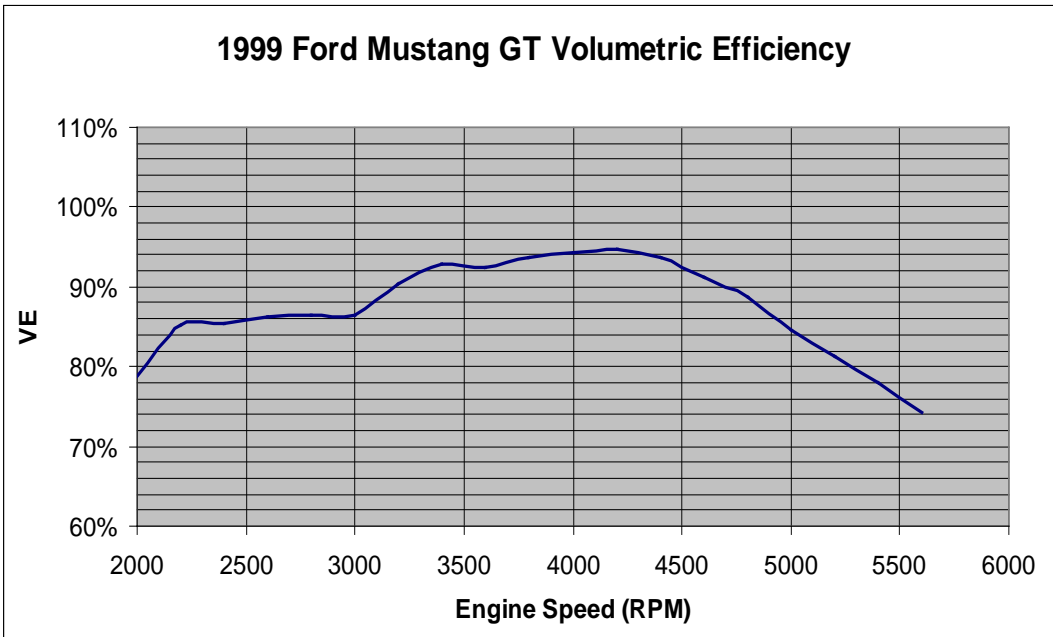


Figure 3-6: Volumetric Efficiency, Mustang GT

Another way to achieve over 100% efficiency is to use forced induction, through the introduction of a supercharger or turbocharger. This will force extra air into the cylinder, allowing for a more complete burn, increasing power.

You also want to consider compression ratio. This is calculated using the total volume of the cylinder and combustion chamber at bottom dead center; versus the total area at top dead center. Typical engines run between 8:1 and 10:1, with high performance engines typically being between 10:1 and 14:1 and diesel engine run around 22:1.

In order to achieve a complete combustion the air to fuel ratio must be accurately controlled. Modern engines strive to achieve a 14.7:1 air to fuel ratio, the ideal stoichiometric ratio required for a theoretically complete burn. Essentially, to achieve maximum power it is necessary to match the mass amount of fuel to the mass amount of air. If the stoichiometric ratio is greater than recommended 14.7:1 the engine will be running lean and rich for any ratio less than that.

In a lean burn you are introducing less fuel than required for a complete burn. The reduction of fuel decreases the flame front, essentially creating a high explosive force. This instantaneous burn may cause component damage if run for an extended period of time. However, a car's management system may lean out the mixture to limit power under certain conditions to protect the engine from damaging itself.

Running a rich mixture may damage parts of the engine and exhaust due to the introduction of more fuel than can be burnt. Since the engine is unable to intake enough air unburnt fuel is being introduced into the exhaust. This fuel enters the catalytic converter and

combusts; these explosions will decrease the efficacy of the converter and eventually lead to its failure. Additionally, the engines performance will be reduced to the incomplete burn reducing power and decreasing gas mileage.

The final element needed for operation is spark. Since it takes time for the fuel to combust and travel the engine must employ a spark advance, meaning you set the spark to go off before the piston reaches top dead center. This allows the flame front to start early, developing maximum combustion power around top dead center, providing maximum torque. You want about 50% of the burn occurring just past top dead center as shown in Figure 3-7

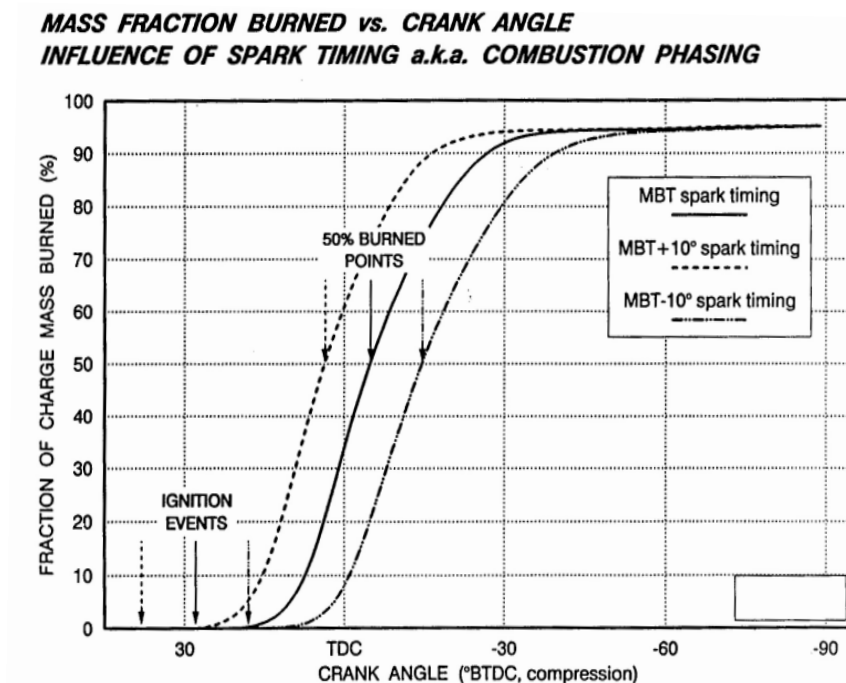


Figure 3-7: Mass Fraction Burned vs. Crank Angle

Which results in the following pressures in the cylinders

**CYLINDER PRESSURE vs. CRANK ANGLE  
INFLUENCE OF SPARK TIMING**

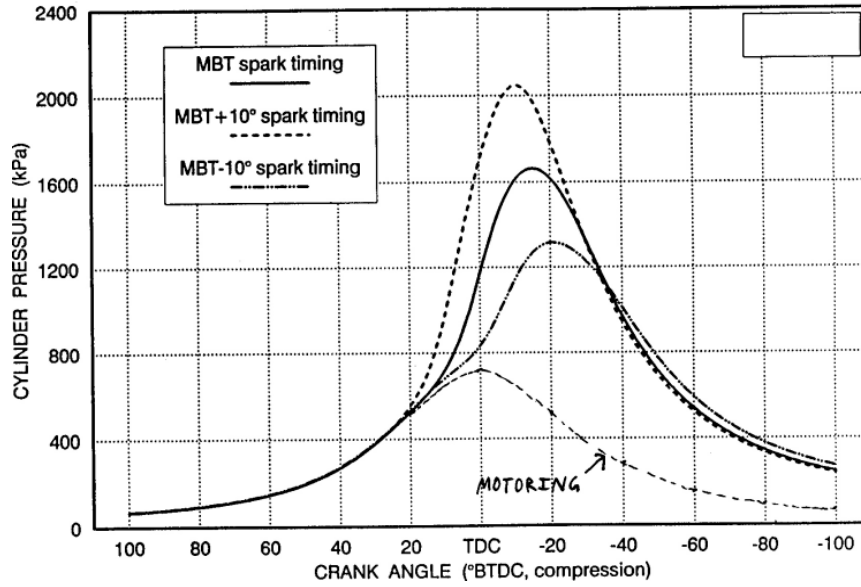


Figure 3-8: Cylinder Pressure vs. Crank Angle

## Chapter 4 : Project Objective

### 3.1 Goal Statement

Design a system that will prevent a 4-stroke engine from entering into hydrostatic lock after an incompressible liquid has been introduced to the engine system.

### 3.2 Task Specifications

1. The design must be able to prevent an engine from entering hydrostatic lock
2. The design must survive an extended engine service interval, 6,000 miles (for car engines) or 10 hours (lawnmower style engines) without failure.
3. The design must remain functional after extended normal engine operation.
4. The design must remain functional after prolonged exposure to the elements.
5. The design must not compromise or hinder in anyway normal engine performance when not in use.
6. The design must be scalable to many different styles of internal combustion engines.
7. The design must be able to respond to a sensed excess in pressure within a complete rotation of the crank
8. The design must be capable of allowing the entire volume causing the excess pressure to exit the engine before closing
9. The design must not cause damage to any engine components when in use
10. The design should not cost more than \$100<sup>1</sup> to implement on an engine.

---

<sup>1</sup> \*The cost of \$100 is a relative number based on current economic conditions, the relative cost may increase or decrease due to fluctuations in economy and therefore cannot be accurately accounted for.

## Chapter 5 : Design Concepts

As the backbone to the industrial revolution, the internal combustion engine has played a vital role in the development and expansion of modern society. While the design of this engine has not dramatically changed since the mid 1800's modern technology has allowed for major advances in efficiency, power and weight reduction. However, even as modern technology drives the development of new engines future designs will still be susceptible to a variety of hazardous conditions. The focus of this MQP is to analyze and implement a system that would act as a pressure release on modern engines to prevent a phenomenon known as hydrostatic lock.

### 4.1: Spring Controlled Valve

#### Overview

A system consisting of a Pressure Relief Valve (PRV) within the cylinder head would be installed within the engine head to prohibit the effects of hydrostatic lock.

#### Details

A PRV is a valve used to control the pressure within a confined space; implemented on many devices, our goal is to use such a valve to limit the pressure within the cylinder. The design will consist of a spring-controlled valve, calibrated to open at a pressure above that of normal compression. If the cylinder experiences increased pressure as the result of locking, the spring will open, exhausting the pressure outside of the head, keeping the material within its

yield strength. Once the pressure has been exhausted the engine may function as normal and the operator may resume normal operation.

### **Required Parts**

- Custom designed valve assembly
- Specific k-constant spring

### **Benefits**

Since the system employs a valve that has been calculated to open at any pressure above normal compression any water within the compression chamber will be exhausted at the time of a significant pressure increase. The benefit to such a system is that once the pressure has been exhausted the engine may continue to operate normally post hydrostatic lock conditions.

### **Negatives**

Due to the implementation of the system within the head itself the valve has to be manufactured with tight tolerances to prevent the exhausting of gases during normal operation. Additionally, modern engines are tuned for optimum performance and efficiency, by implementing a valve that increases the combustion area the performance and efficiency may be reduced.

### **Challenges**

This system requires the drilling of a hole into the engine head to install the PRV. The valve must be machined with very tight tolerances to maintain engine compression needed for normal running. The valve must also be resistant to temperature extremes as well as variable loading conditions.



## 4.2: Intake system

### Brief overview

The intake system is a standalone design that may be implemented onto the existing intake tubing. By constantly monitoring pressure the system will be able to detect the instant of hydrostatic-lock and close of the intake tube to prevent water flow. To effectively prevent water flow the system must utilize a watertight butterfly valve, and a system that would detect pressure changes and output a signal to close off the intake.

### Details

The throttle of a vehicle is a butterfly valve that controls to amount of air entering the engine. As the valve is opened more air is allowed to enter the engine, increasing the power and Rotations per Minute (RPM). Through the introduction of a second valve that is independently controlled, air, or any other fluid, may be prevented from entering the engine, reducing the chance of hydrostatic-locking.

Since the design requires that pressure be constantly monitored a circuit must be created to observe any pressure changes within the intake. When entering a hydrostatic-lock condition the engine must pull a vacuum greater than that of normal running conditions, creating a large negative spike. By creating a circuit to monitor the intake pressure the system can be designed to close the intake if such a spike is detected.

### Required Parts

- Butterfly Valve
- Pressure sensor
- Control system

## Benefits

The system requires no modification of vital engine parts such as the head or piston. This means that there are no parts that could potentially fail during engine operation and cause damage. Instead there is a system in place in the intake that will close when necessary. In a worst case scenario the valve will close unexpectedly, causing the engine to stall due to deficient air intake.

## Negatives

The addition of this system would increase the length of the intake tube slightly. Since the intake on some cars is tuned to a certain length to provide maximum power the addition of the system may cause a slight decrease in power. The length actually controls pressure waves created when the moving air hits a closing valve. By changing the length you start to alter this design. However, most modern cars are not tuned for this and altering the length won't negatively affect most cars.

## Combinations

This system could be used in conjunction with a valve system in the cylinder head. Since it is possible that the butterfly valve might not stop all water getting through a second system could be set up to insure protection. The intake system would provide an initial block while the head valve would release any water that was forced past the butterfly valve.

## Steps to implement

In order to implement the system the intake would require be modification or a new system manufactured. Once adapted to the intake the device must be powered through an

existing connector on the engine's wiring harness or powered from a 12-Volt battery. Following installation the design requires no user interference and functions only to detect and prevent a hydrostatic-lock condition.

### **4.3: Valve System on Exhaust Valve**

#### **Design Description**

The Valve system on Exhaust Valve would include the use of pressure transducers in the engine cylinder that would monitor pressure in the cylinder and if/when it detects a pressure that is above normal operating pressures it would trigger an actuator that would force open the exhaust valve allowing the normal motion of the piston to force out anything in the cylinder, specifically any water, out through the exhaust valve and out of the cylinder.

#### **Benefits**

Benefits of this design are the engine could continue to run normally after the exhaust relief valve ran. Because the valve would only act to force open the engines exhaust value for as long as there is an excess pressure, as soon as the excess pressure is relived, the engine could resume normal running. Due to the constant evacuation of pressure the engine may stall as the four-stroke cycle will be interrupted. However, after the excess pressure is evacuated the exhaust valve will close and the camshaft can actuate the valve in accordance with normal engine timing. There is also significantly less work required, if any, after the valve runs than in other designs.

## Drawbacks

Drawbacks of this design are the complexity of actuating the exhaust valve with a separate system than the normal camshaft that will not interfere with or harm the exhaust valves normal running. There is also an issue of scalability. Ultimately we would like to scale this design to as many engines as possible. Using this design will pose significant problems with interference engines. Interference engines cannot have the valves open at top dead center because the valve would interfere with the piston. In order for this design to work, the exhaust valve needs to stay open for an entire compression cycle. With an interference engine however, the piston would collide into the valve and in all likelihood break the valve.

## Challenges

The Challenges of implementing this design are finding a way of constantly monitoring the pressure of the cylinder. This will require drilling a hole into the engine's head and installing a pressure sensor. The pressure sensor will need to have an extremely tight fit to maintain the compression of the engine that is needed for normal running. It will have to resist very high pressures and temperatures normally experienced during normal running. Another more significant challenge is the placement of the mechanism that will actually open and hold the exhaust valve. It will require mounting in extremely tight spaces with low torque angles that may lead to excessive wear, and unreliability. There are two potential locations on which to mount the actuator; the two locations are either where the cam makes contact with the spring that pushes the valve open normally or in an engine with pushrods, somewhere at the rocker arm. Because of the tight space and close proximity to parts that are in constant motion, tolerances on location will have to be extremely tight. Implementation could prove to be very

challenging, however if the design proves to be reliable it could be a very good solution to the problem.

### **Detailed Design Description**

The design calls for a pressure transducer to be installed in the head of the engine. The pressure transducer will need to be connected to a small computer or circuit that will recognize when the pressure is above a specified value, determined by testing the engine. It will then need to actuate a spring or an actuated cylinder that will force and hold open the exhaust valve. The method of opening and holding the valve open is where most of the design problems will occur. The team may use an actuated cylinder to push up on the valve spring (the same place the camshaft pushes) however, the mechanism would have to work submersed in engine oil and cannot interfere with engine oil flow. An alternative is to have the actuated cylinder directly above (or below depending on the engine) the exhaust valve. This would require, modifying the exhaust port to allow room for a valve to fit in. The problem with having the actuator connected directly to the valve is that it would have to allow the valve to function normally, with no excess friction that would decrease performance and still be able to, when triggered force open and hold the valve in the open position.

### **4.4: Pressure relief valve in the piston**

#### **Overview**

A PRV located in the piston would allow pressure to be exhausted into the crankcase should the engine enter hydrostatic lock.

## Details

The pressure relief valve, not unlike the spring controlled one described earlier would be inserted into the piston of an internal combustion engine. When an engine enters hydrostatic lock the valve would open, opening a path through the piston into the crankcase. The water would be exhausted, into the crankcase, eventually making it to the oil pan. Once the pressure is exhausted the valve would close, allowing the engine to continue to run, provided certain things are taken into account, discussed below.

## Required parts

- Modified piston
- Custom designed valve
- Specific k-constant spring

## Benefits

No electronics are needed to control the system, reducing the electrical complexity of the system. Since the valve will close post hydrostatic-lock, normal operation may resume shortly thereafter.

## Negatives

Since you are exhausting fluid into the crankcase, you are releasing water into the oil. The introduction of water into the crankcase creates a problem, due to the sudden viscous change and reduction in lubrication, possibly leading to component failure. While the engine may continue to operate it is unadvisable to do so until the fluid is removed. Within the system, if a single use release valve is employed the engine must be rebuilt to replace the failed part.

## Challenges

The piston is designed to be very strong; altering the design to contain a valve may induce stress fractures, thereby reducing the yield strength of the part. Additionally, care must be taken into the balance of the piston as to not reduce premature wear or damage. If hydrostatic-lock occurs the user must disassemble the engine to replace the failed component.

## 4.5 Actuated Valve in Cylinder

### Brief Design Description

A design consisting of an actuated valve installed within the cylinder. The design is similar in operation to the engine head valve, replacing mechanical components for a detection circuit and actuator. A pressure transducer would be implemented in the cylinder, monitoring the contained pressure. If the transducer detects a pressure that is above normal operating pressures it would trigger an actuator to open a valve in the engine head, releasing excess pressure.

### Benefits

Benefits of this design are that the engine can continue to run after the valve has been actuated. Because the system would only act to open the valve for as long as there is an excess pressure, once the excess pressure is relieved, the engine could resume normal running without any detrimental effects. Due to the interruption of the four-stroke cycle and compressions, the engine may stall while the valve is held open. After the pressure is exhausted and the valve closes, the engine may run under normal operation. There is also significantly less work required, if any, after the valve runs than in other designs.

## Drawbacks

Drawbacks of this design are the complexity of implementing the design. The design requires machining the engines head to create the hole for the actuated valve. If there is a failure of the valve, the repairs could be very complicated, costly and could even require a new engine head. Because the design calls for drilling into the head of the engine, the scalability of the design would be challenging due to the diversity of engine configurations. The design also has the disadvantage of requiring special machining, and accommodation of the valve systems outside of the head; there may be cooling fins that will have to be cut away or left out, which can effect prolonged operation.

## Challenges

The challenges of implementing this design are finding a way of constantly monitoring the pressure in the cylinder. This will require drilling a second hole into the engine's head and installing a pressure transducer. Alternatively, if a pressure transducer could be installed in the spark plug this challenge could be avoided. Regardless of its location, the pressure transducer will need to have an extremely tight fit to maintain the compression of the engine that is needed for normal running. It will have to be resistant to very high pressures and temperatures that are experienced inside an engine during normal running. Another challenge will be to redesign and machine the head itself, which depending on head design may be very difficult.

## Detailed Design Description

The design calls for a pressure transducer in the head of the engine. A circuit must be developed to actively compare pressure within the engine. If the pressure exceeds a predetermined value, through testing, a valve would be actuated to relieve excess pressure.



The valve itself is contained within the engine head, manufactured by drilling a small hole in the head itself and placing the valve either in the hole or placed closely outside the head to maintain the same volume combustion chamber. The valve is required to trigger only if the pressure exceeds nominal operation and therefore must be very robust as to not fail during general operation causing sudden decompression loss.

## Chapter 6 : Design Selection

Required for the design and implementation of a suitable system, the team must develop a series of designs and evaluate the expected performance through a design matrix. A design matrix incorporates a number of specific goals such as performance, reliability, and other specific goals that are unique to the design alternatives. To determine the decision factor, the goals and designs are assigned numeric ratings, a weighing factor and rating factor from zero to 100 and zero to ten respectively, relative to the solutions ability to perform the desired task. The results of the decision factors allow for a determination as to which designs may more suitable to succeed in this particular application. Six designs were considered for the project, each based on seven goals (performance, work required post hydrostatic-lock, implementation, cost, adaptability, complexity, and reliability). By applying weighing factors two designs were selected to be prototyped, due to their high totals, observed as the intake system, and spring controlled valve.

## Goals

Design Alternatives	Weighing Factors							Total
	Performance	Work required post hydrostatic-lock	Implementation	Cost	Adaptability	Complexity	Reliability	
	100	90	85	0	70	50	0	4
<b>Actuated Valve in Cylinder head</b>	8/80 0	9/8 10	5/425	/480	8/56 0	4/2 00	7/ 280	3 555
<b>Spring controlled valve</b>	9/90 0	9/8 10	6/510	/640	8/56 0	8/4 00	9/ 360	4 180
<b>failure mechanism in piston</b>	7/70 0	1/9 0	6/510	/640	9/63 0	5/2 50	9/ 360	3 180
<b>valve system on exhaust valve</b>	5/50 0	10/ 900	3/255	/480	5/35 0	3/1 50	8/ 320	2 955
<b>intake system</b>	10/1 000	10/ 900	7/595	/560	10/7 00	6/3 00	7/ 280	4 335

## Chapter 7 : Engine Analysis and Testing

In order to correctly design and development both systems the team needed to determine the running pressure of the engine, as well as the intake pressure. Once both pressures were determined, the designs could be finalized with the correct data from our engine. To determine the pressures, two pressure transducers were implemented to actively read data, which once amplified would provide the running pressures.

Initial testing relied on the proper operation of the Briggs and Stratton engine. Given to the team as a donation, for safety reasons, the engine was donated without a flywheel. As a lawnmower engine the rotational energy required to properly operate was provided through the blades. For safety reasons the team adapted a Suzuki gs500 brake rotor to function as a flywheel, that, if spinning would not result in bodily harm due to failure. Initially the adapter was modeled and machined of 6061 Aluminum, consisting of a single set screw. This initial design failed due to stresses exceeding that of the set screw. To reduce the chance of failure and flywheel release, the team machined another adapter utilizing two woodruff keys and four set screws. Similarly to the initial design the adapter failed within the first few minutes of operation, releasing the rotor onto the ground below. As a result of previous failures the team performed analysis to determine initial force exerted by the engine. Following calculations, it was determined that the adapter be machined of steel, including key stock welded onto the adapter, further secured using a second plate screwed onto the bottom of the shaft. The design provided the required strength needed to withstand the initial startup force and any subsequent forces exerted by the engine.

To determine the running pressure inside the engine head, as well as within the intake, the team purchased two pressure transducers. Uncertainty of the running pressure led to the purchase of pressure transducer rated for 0-100 psi and 0-5000 psi, allowing for a wide pressure range for testing. Both transducers are Honeywell-Sensotec, 19C100PG4K and 13C5000PA4K, respectively. Initially, the team began independent tests using both pressure transducers, attempting to gather data directly from the transducer. These initial tests showed data that appeared to follow a 60-Hz sine wave, determined to be interference from components running off AC within the room. To counteract this problem the team looked to amplify the transducer output using an op-amp configuration.

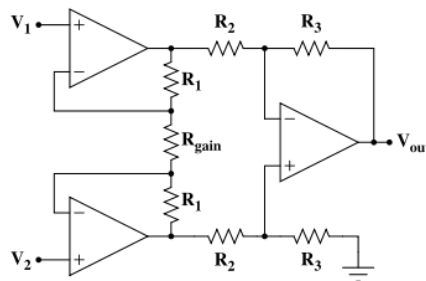


Figure 7-1: 3 Op-Amp Instrumentation Amplifier

A three op-amp configuration amplifies the differential between the negative and positive output to provide the required resolution of NI Labview. Preceding initial tests, it was determined that there was electrical noise pickup that was being amplified by the operational amplifiers. After conversations with an electrical engineer we were able to resolve the electrical noise by using an AD620, instrumentation amplifier, and adding filtering to the circuit. The circuit is composed of several capacitors, used for filtering, a 5-Volt voltage regulator, to

generate the required voltage, a Molex connector for the pressure transducer and the AD620. To acquire data from the pressure transducer the output of the AD620 was connected to a Digital to Analog converter, which would take samples from the output data at a rate of 10,000 samples per second and export it to an excel file.

To calibrate the transducers they were connected to an air tank with labview monitoring the output voltages. The tank was filled to 100-psi, and ten readings were taken from the transducer. The tank was then dropped at 10-psi increments, and ten more readings were taken. This was repeated down to 0-psi, and then repeated three times. The data was then plotted to determine a trend line relating voltage to pressure. For the 5000-psi transducer the equation is  $y = 3314.6 * x - 26.457$ , where x is the voltage (in volts) and y is the pressure (in psi). For the 100-psi transducer the equation is  $20.46 * x - .0039$ .

The LabView program was designed to be as simple as possible while providing all the functionality needed. The DAQ assistant was set up to read one channel for N samples. There were controls set on the front panel to allow the user to set the rate of samples as well as the number of samples. Once the samples are taken they are shown on a waveform graph on the VI's front panel as well as saved to an excel sheet.

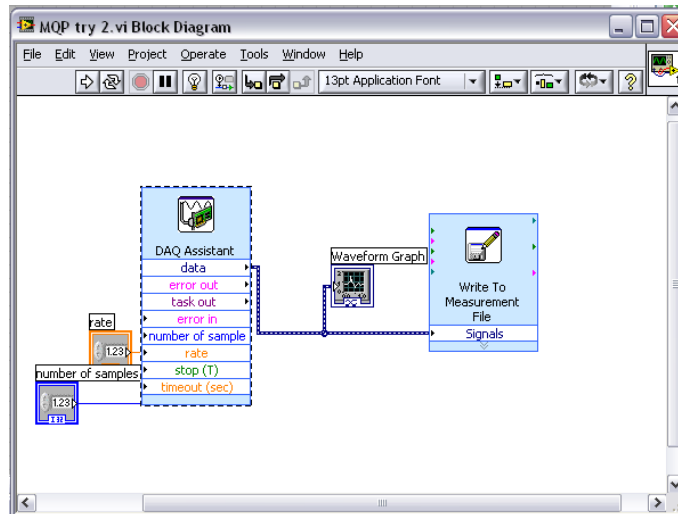


Figure 7-2: LabView Block Diagram

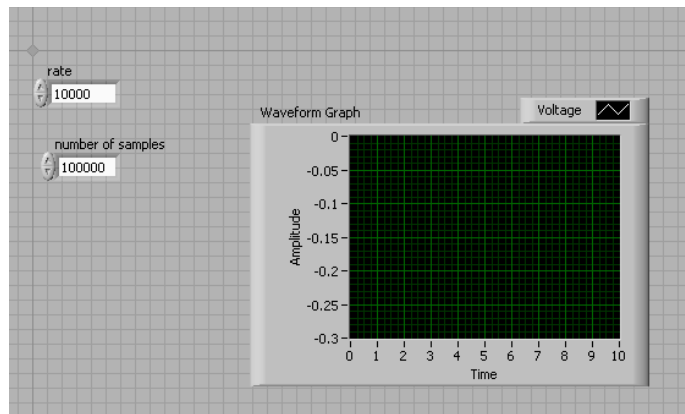


Figure 7-3: LabView Front Panel

With the circuit and Labview program developed testing could be conducted. Tests were run at 10,000 samples per second, for a total of 100,000 samples, giving ten seconds of data. Data started being recorded when the engine was started. The engine was turned off after approximately four seconds of running, allowing for enough time to spin up to full speed and provide data points throughout the engines RPM range as well as the spin down cycle. The calibration equation was applied to the data to translate voltage to pressure. The resulting

graph of pressure vs. time is shown below in Figure 7-4. All Plots of recorded data are shown in Appendix B: Data

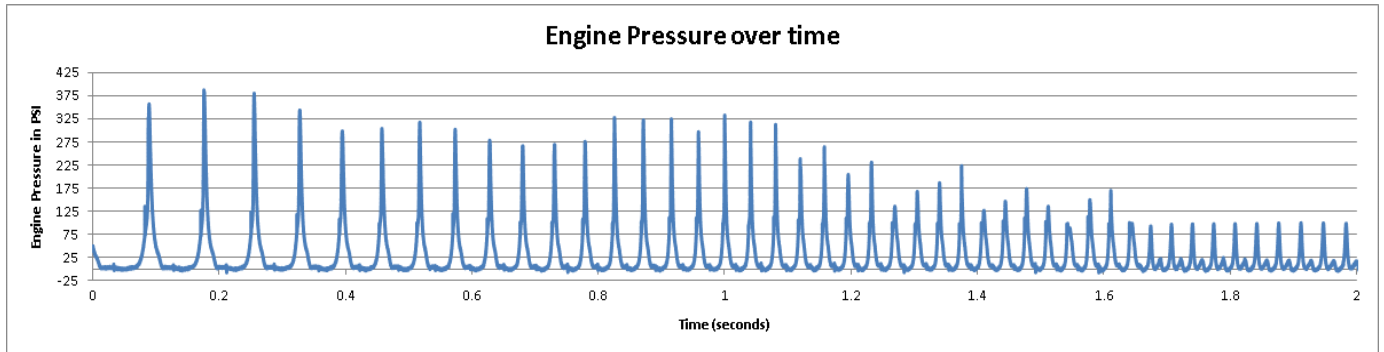


Figure 7-4: Engine Pressure over Time

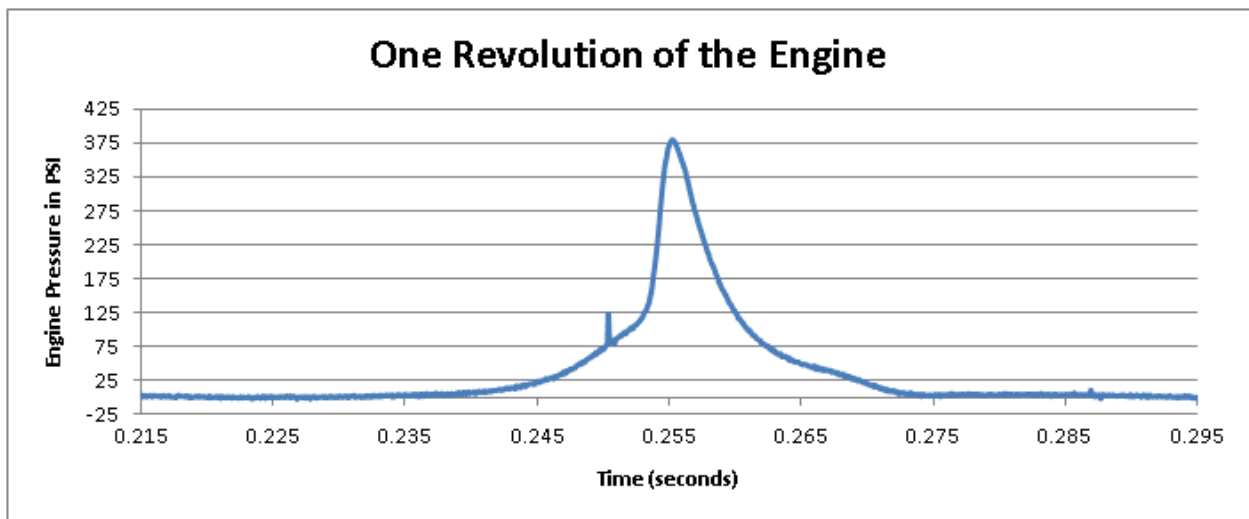


Figure 7-5: Engine Pressure for One Revolution

Also tested was the intake pressure under normal running as well as a simulated hydrostatic lock condition. This was done to allow the team to determine if the intake system was feasible. The engine was started and allowed to run the full ten seconds. The same conditions of 10,000 samples per second and 100,000 samples were set in Labview, and several tests were performed. The Recorded data is shown in Figure 7-6 and Figure 7-7.



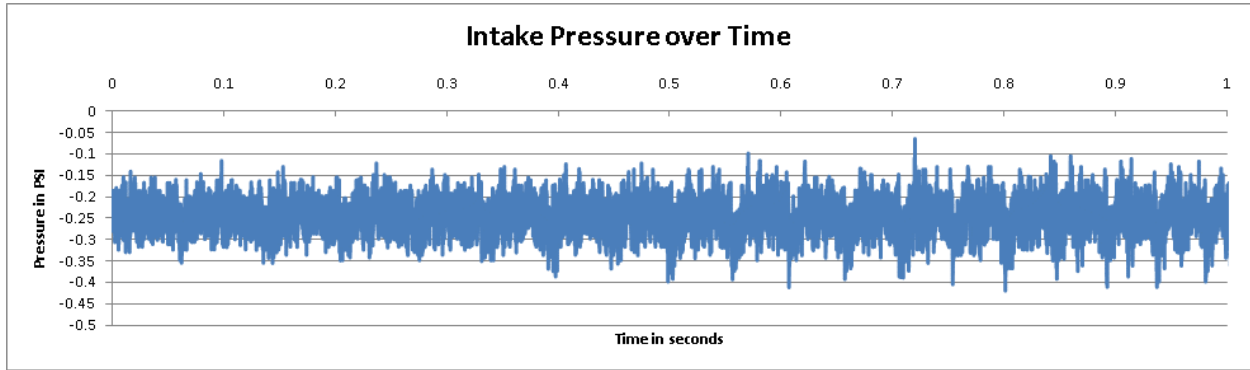


Figure 7-6: Intake Pressure over Time

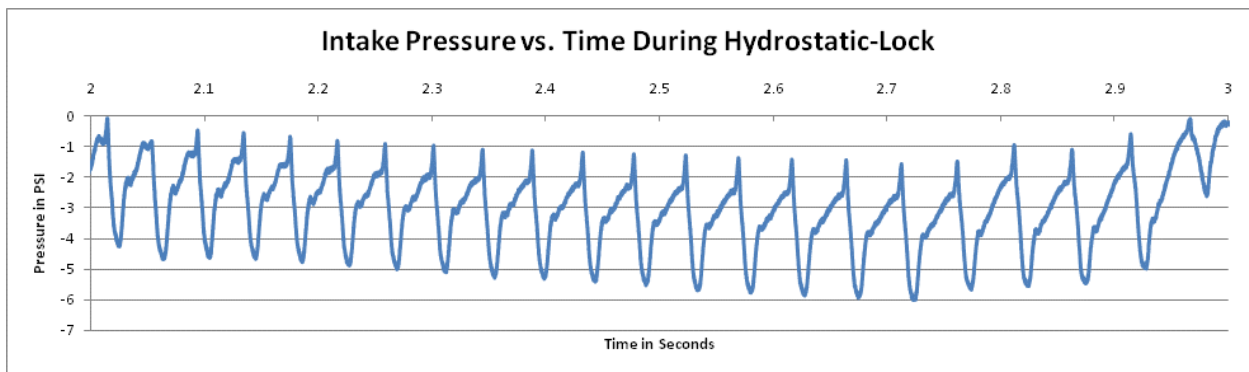


Figure 7-7: Intake Pressure over Time during Hydrostatic-Lock

### *Data Analysis*

The initial data from the engine was giving very high spikes in pressure, as shown in the Figure 7-8. These spikes were determined to be interference caused from the spark plug, due to the plug being run off of very large pulses of electricity. The spike was due to the pressure transducer being mounted in close proximity to the spark plug, sharing the same ground. Since these were skewing the recorded data, the testing setup was revised and a ground wire added to the pressure transducer connected to an external ground. With the ground wire the spikes were reduced enough that they were not interfering with the rest of the data.

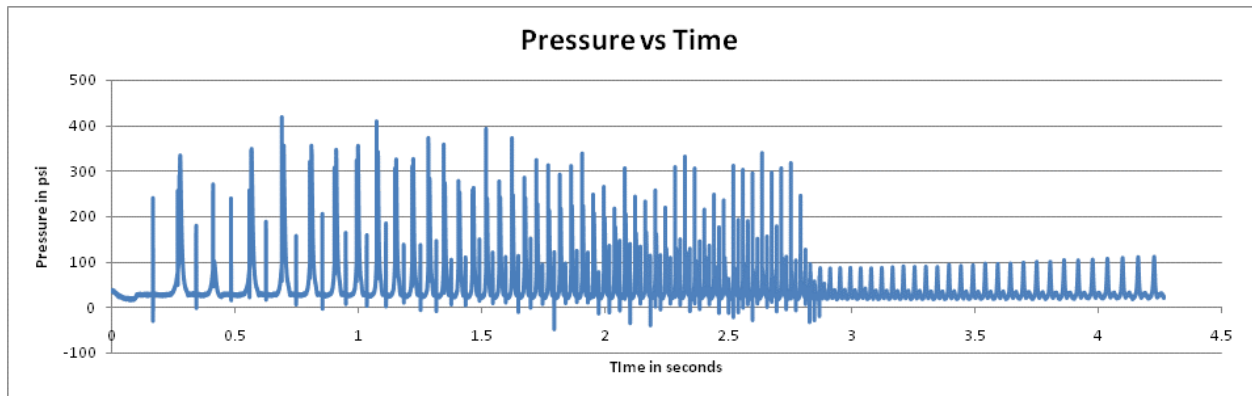


Figure 7-8: Pressure vs. Time

From all tests conducted on engine pressure, the maximum pressure spike was 380 psi, while the average was 325 psi. The pressure varied with each combustion cycle due to the nature of the simple carburetor on the Briggs and Stratton Engine, which was unable to keep the ratio of air to fuel constant with each intake cycle. Building in a safety factor of 120 psi, the release pressure was decided to be 500 psi. This value was determined to be above anything that normal running would achieve, and low enough that there would not be a substantial risk of engine damage at the time of release.

The same analysis was done to the intake pressure data. During normal running the pressure was an almost constant -0.275 psi, variation do to signal noise. With full hydrostatic-lock simulated this pressure immediately climbed to a peak of -6 psi and an average of -3 psi. Once determined that hydrostatic-locking would create a noticeable drop in pressure, the team was able to design a circuit to effectively detect hydrostatic-locking conditions. In order to allow the system to catch hydrostatic-lock early, a value of -1 psi was chosen as the system trip pressure.

The final values used for design are an internal running release pressure of 500 psi and an intake pressure of -1 psi. The engine valve will use a spring with a spring constant calculated from the release pressure. The intake will have the circuit designed to release at a pressure transducer output voltage corresponding with - 1 psi.

## Chapter 8 : Detailed Design

### Intake System

The first system to be developed is a standalone system to be mounted in the engine's intake system. This will be located before the throttle body and after the air filter with the purpose of preventing water from ever reaching the engine. The valve is almost identical to the style of a throttle body, utilizing a butterfly valve to control the passage of fluids. The valve is attached to a shaft that is rotated using a solenoid to achieve quick response times. To control the system an analog circuit was developed that constantly monitors the running intake vacuums of the system.

During normal running conditions the valve remains open, so as to not interfere with the engine's performance. If a spike in negative pressure beyond the -1psi limit is detected the valve will be closed preventing water from passing. This will also prevent air from passing, causing the engine to stall, thereby preventing the car from drawing water into the engine, preventing a hydrostatic lock condition.

The system was modeled entirely in SolidWorks, 3-D modeling allowed the team control over changes made throughout project and analysis of parts to determine the factors of safety. Each part was modeled separately and used to create an assembly. The linear actuator was also modeled using the specs provided on the manufacturer's website, allowing for virtual testing using SolidWork's built in motion analysis. This testing also allowed for component verification prior to purchase, reducing the need to modify parts from outside vendors for proper operation. All parts were modeled using normal techniques that should be easily reproduced,

the exception being the covers to hide components, which were created using lofted surfaces. The final modeled part is shown below in Figure 8-1, and all drawings are located in Appendix A.



**Figure 8-1: Final Intake System Design**

The assembly was initially designed with CNC manufacturing in mind. All parts were designed such that they could be made in WPI's Washburn shops. As the covers were designed it became apparent that the manufacturing would be beyond the capabilities of our machining knowledge. In order to improve the aesthetics of the part the covers were designed using lofts and complicated surfaces, these surfaces complicated the fixturing and machining. As a result the team looked towards rapid prototyping as this was the most economic choice before mold development. Fused Deposition Modeling (FDM) was a viable method for development, as it would allow for prototype testing before large-scale production using injection molding.

Since the system will not undergo any extreme forces the team did not perform FEA or CFD analysis on the system. The only component applying force would be the solenoid since, since the reaction force of the valve is minimal and therefore may be neglected. Solidworks was used to perform motion analysis on the solenoid assembly to determine if the limited travel could close the valve assembly.

The final system consists of a pipe with a two-inch diameter, two covers to protect the workings of the valve, a pressure transducer, a custom circuit, and a butterfly valve. The cutaway view shown below shows the placement of all components.



Figure 8-2: Intake System Cutaway

## Circuit design and development

As recent technological advances begin to dominate the engineering field focus has been placed on the design and development of more complicated, smaller components. Due to the constant demands of both society and consumer, the implementation of electronics in mechanical systems is often seen as common point; such normality may be seen in many modern products where electronic assemblies are required for effective operation.

Rapid development of Micro-electromechanical Systems (MEMS) packaging allows for the development of more complex integration of both mechanical and electrical designs in smaller packages, increasing the breadth of system design. In light of packaging, design and implementation of MEMS, the team felt that the project should exploit an electro-mechanical design. The incorporation of a mechatronics design allowed the team to increase their knowledge of electronic design while allowing for a practical, implementation of knowledge learned in previous classes. Due to the widespread implementation of mechatronics, all engineers, especially students, must be able recognize, understand and develop electronic packages for modern product design.

As in many modern products, circuits are integrated into the design to assist in the functioning of the device. Required for the intake system was a circuit that offered the ability to accurately monitor live vacuum pressure while controlling the linear actuator, which would lock the butterfly valve if the vacuum pressure exceeded a certain value. Following research into available Programmable Logic Controllers (PLC) and other programmable circuits it was determined that the team develop an analog circuit. Through the implementation of a custom analog circuit the final design could be tailored to the prototype, reducing overall size of the prototype while also reducing the final cost.

Originally developed to amplify the output of the pressure transducers, the circuit was expanded to incorporate several necessary functions. Initially constructed on a protoboard, the circuit was powered using two 9Volt batteries, connected in series, allowing for both +Vcc and – Vcc. Once power was supplied it was stepped down to +5V, using a voltage regulator to power



the Integrated Circuits (IC). Preceding research into IC's the team decided to construct the circuit using a voltage comparator. As a result of the pressure transducer monitoring intake pressure the output is negative, requiring a voltage comparator that will allow for such an input. Designed for such an application the LM311 comparator uses both positive and a negative voltage to function. The voltage comparator constantly monitors the differential between input voltages, if the positive side drops below the negative, essentially going low, the comparator switches to allow current flow. To set the switching pressure a voltage divider was implemented which would determine the switching point of the comparator. Attached to the negative lead on the comparator, as pressure decreases from increased vacuum pressure due to water intake the positive side goes low, switching the comparator. For the prototyped circuit, the linear actuator was controlled using a separate circuit running from a 12V power supply (the cars battery), actuated using a MOSFET. The MOSFET consists of three terminals, drain, gate and source. If a current is applied to the gate the switch between drain and source is completed, activating the solenoid and closing the butterfly valve.

In constructing the final circuit, several additions were made to improve adaptability and reliability for the intended purpose. Initially the circuit was powered using two 9-Volt batteries, connected in series, to achieve the required positive and negative power. While the solution is practical for powering the circuit, the power source is not ideal, requiring replacement. To counteract the problem the circuit was modified to use a DC/DC inverter, allowing the circuit to be powered off the 12V battery. The ADM660 charge pump inverter takes the +5 Volts off of the voltage regulator and converts it to -5 Volts, required to power the IC's. Through the addition of a 12V power source, the solenoid could be integrated to function

off of the same power source. To increase the reliability of the circuit both filtering and bias were added to remove any unwanted electrical noise. Additionally, a hysteresis loop was added to the voltage comparator. By adding the hysteresis loop to the voltage comparator we were able to improve the switching of the comparator, integrated within the hysteresis loop is a capacitor C10, this capacitor allows for a decay in the output signal causing the solenoid to hold for a specific period of time, as determined by the time constant.

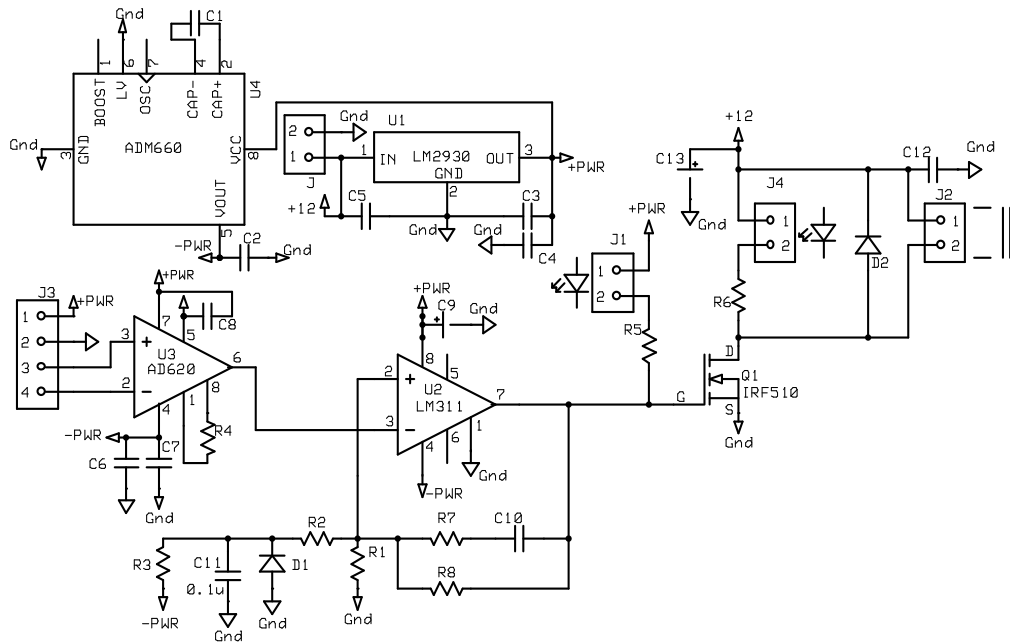


Figure 8-3: Circuit Diagram

## Spring Valve

The second system is a spring-actuated valve in the engine head. The greatest source of damage results from the pistons trying to compress water, usually damaging the connecting rods, which in turn ruin the cylinder walls. By allowing a way for this fluid and excess pressure to escape this damage can be averted. However, the required system must be able to maintain

a seal so as to not affect normal running. We decided to adapt a system used on 1830's steam locomotives where a pressure relief valve was used to release steam when pressure got too great.

From our data collection we determined the max pressure in the engine to be 380-psi. Since we wanted the system to hold at normal running pressure, a safety factor of 1.3 was built into the calculations, allowing the engine to see 500-psi before the valve would start to open. With this pressure we were able to perform calculations to determine the necessary spring constant, required to maintain an effective seal. The calculations are shown in Appendix D. A spring with a rate of 100lbf/in and a free length of one inch is chosen, with an initial compression of .25inches. Knowing the free length and the initial compression that needs to be obtained when the system is assembled, the valve assembly can be completed.

The engine head had previously been modeled to allow the implementation of a pressure transducer. This allowed for modifications to fit a valve in the place of the transducer. The valve was designed to have a .2-inch opening to the combustion chamber and a flat seat for the valve. The cap was sized such that the spring would be compressed to the required .245inches. The valve would be held in place by a threaded cap, with ANSI inch 1-14 threads.

Testing showed that the flat seat valve was not holding as desired, resulting in a design change to add a 45degree chamfer to both the valve and its corresponding seat in the engine head. The valve itself has a .25-inch diameter stem, with a .6-inch seating rim. The retaining cap has a .6inch interior as well as a .25-inch hole to allow the valve to translate only in the

direction of the valve. Figure 8-4 below show each of the pieces and drawings of all parts are in Appendix A.

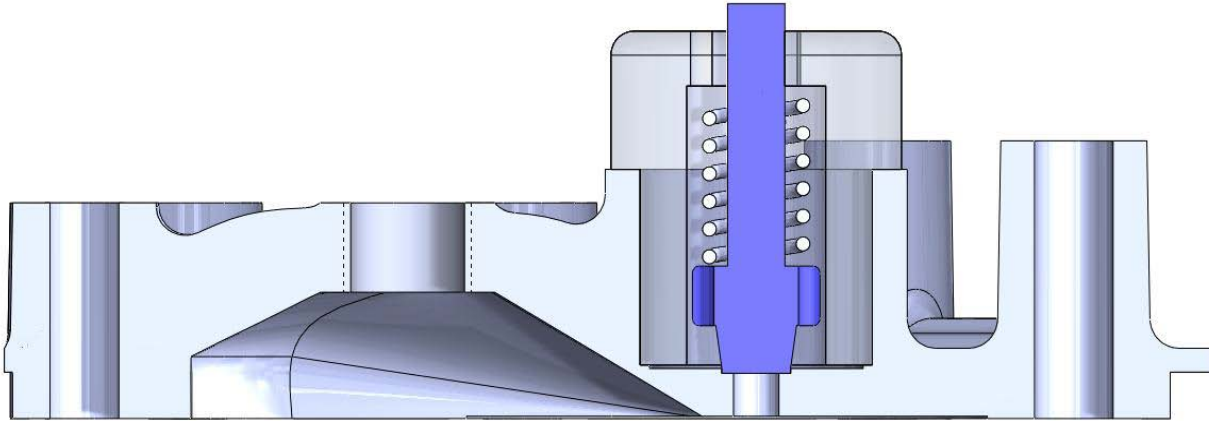


Figure 8-4: Engine Head Cutaway

For the spring controlled valve system, the team needed to run Finite Element Analysis (FEA) and Computational Fluid Dynamics (CFD). The FEA analysis on the valve system would help us ensure that under hydrostatic lock conditions the valve would not deform catastrophically. Our goal was to ensure that the system would continue to function after experiencing a hydrostatic-lock condition. Since the valve is designed to release pressure at 500-psi, all analysis was done assuming a pressure of 500-psi using ANSYS 11 for all FEA. The 500-psi assumption was based off of a SOF of 1.3 as pressure in the combustion chamber should not exceed 500-psi. The team wanted to analyze both the valve and the change on the stress distribution on the combustion chamber as a result of the addition of the exhaust port.

FEA was used to optimize the design of the valve, several variations of geometry of the valve were initially proposed. FEA was used to determine the best design, resulting in the best stress distribution per size ratio. As seen in Appendix E the tip of the valve is where the majority

of the stress on the part is distributed. The stem of the valve is a low stress member and thus its size is not critical to the structural integrity of the valve, the stems main purpose is to keep the valve oriented where the team wants it to be. In addition, the widest section of the valve, with the flow bypass slots, is dimensioned so that it can support the spring used in the system. The team also observed from the stress distribution images seen in Appendix E, that the spring support section is affected by changes in geometry. The width of the part is not a parameter that can be altered; however the team can change the thickness of the support. The effects of various geometries is shown in the figures in Appendix E, ultimately, the team chose the valve that best distributed the stress of operation while maintaining desired size constraints that are part of the teams design goals.

### **The final valve:**

As shown in Figure 8-5, the valve sees maximum stress at the corners of the tip of the valve. The maximum calculated stress of the valve is 560.14-psi. This is well within the range of the materials yield strength, which for 6061 Aluminum is 18000-psi, so the valve is not expected to fail. As expected for such a small amount of applied pressure, the expected deformations are equally as small. Shown in Figure 8-6, the calculated deformations of the valve are greatest at the corners of the tip of the valve. The calculated deformation is  $2.38 \times 10^{-5}$  inches.

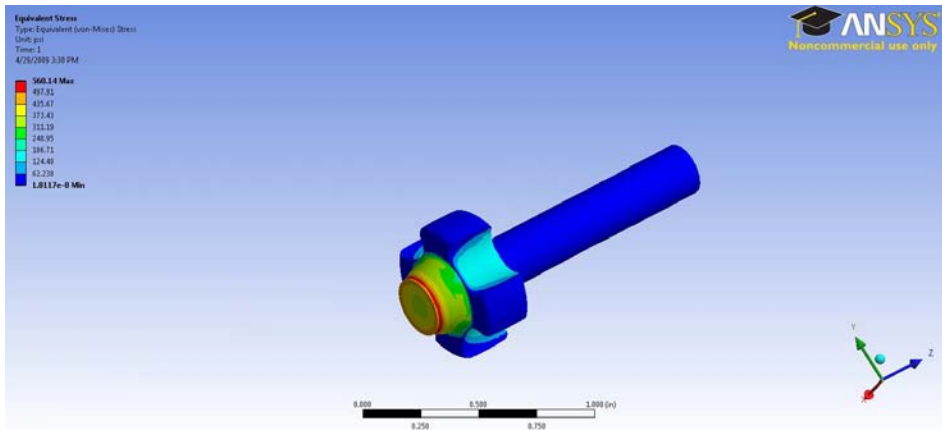


Figure 8-5: Max Stress in Valve

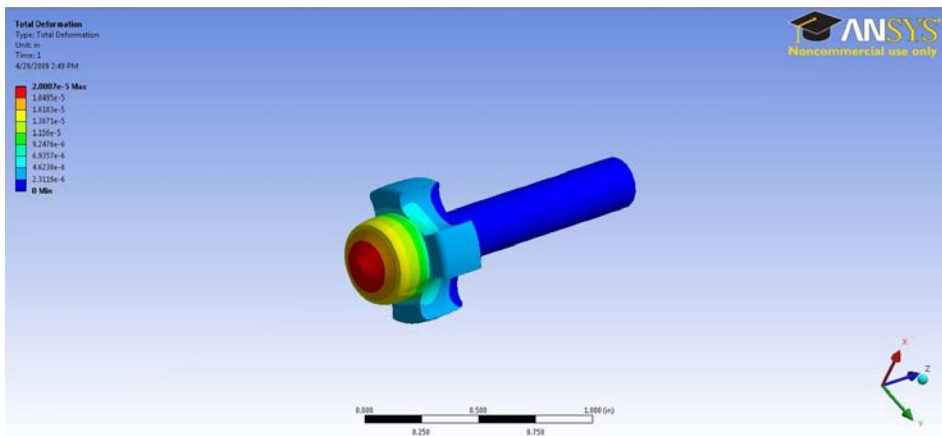


Figure 8-6: Deformation in Valve

## The final combustion chamber:

The addition of the exhaust port added stress concentrations around the area of the of the exhaust hole. As seen in figure X, the stress concentrations are strongest around the exhaust hole. In spite of the increased stress concentration, the max stress values in the engine head, located in the area immediately around the hole is 1262.4-psi, which again is less than the 18000-psi yield strength of the 6061 Aluminum used. Again, as expected for such a small amount of applied pressure, the expected deformations are equally as small. Shown in Figure 8-8, the calculated deformations of the engine head are greatest directly around the hole. The

calculated deformation is  $4.28 \times 10^{-5}$  inches. Essentially, the deformation will be almost completely negligible.

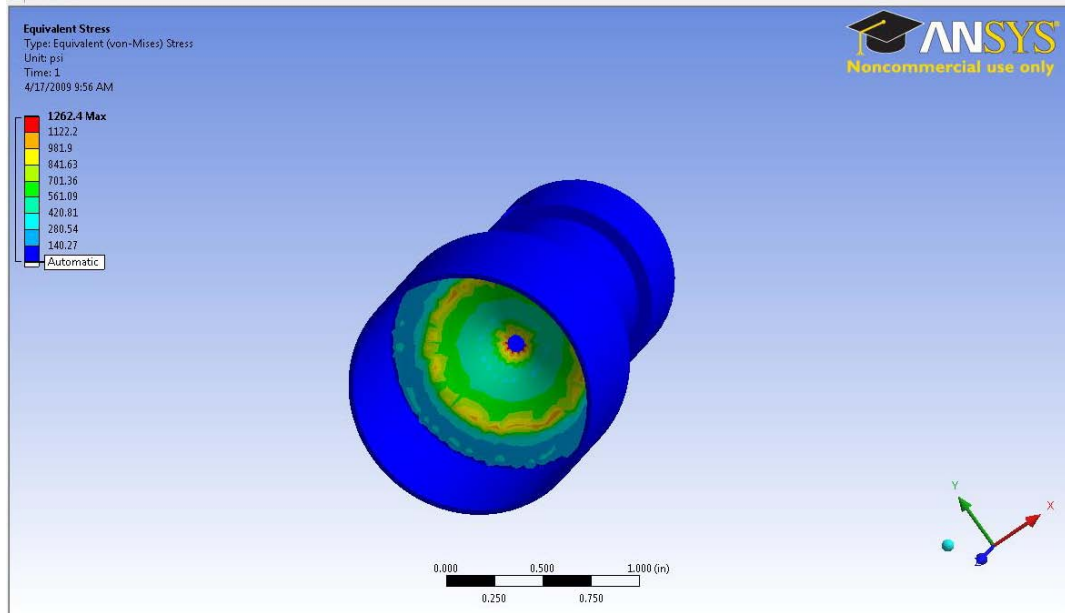


Figure 8-7: Stress in Combustion Chamber

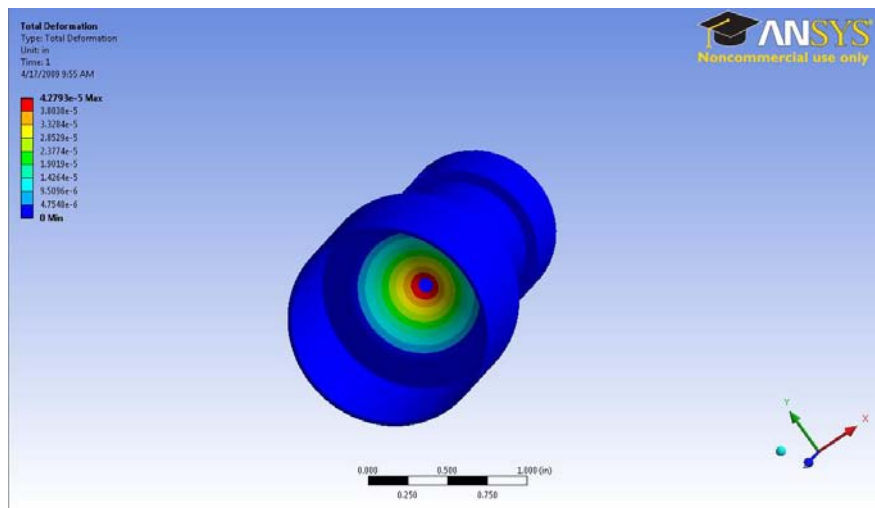


Figure 8-8: Deformations in Combustion Chamber

CFD analysis was also done on the valve system, with the goal of understanding what would be happening as the fluid was forced out of the engine through a relatively small orifice

at extremely high pressure. Ideally a dynamic model, where the valve would actuate and increase the opening as the pressure increased would be use. However for our purposes a simplified model, where the valve is always assumed to be in the fully open position will be used. For the CFD analysis, the combustion chamber with the valve opening to the valve chamber was modeled. The exhaust ports for the valve and the valve in the fully open position were not modeled. The reason for this was that they do not impact the flow that the team was trying to model. The team wanted to model the flow from the combustion chamber through the small exhaust hole, to gain a better understanding of how water at 500-psi would react. The team used the velocities and pressures gathered from the CFD analysis to help design the geometry of the valve opening. By understanding where the relative low and high pressures form, the team can design the valve to optimize the flow out of the combustion chamber under a hydrostatic-lock situation. But before we can utilize the velocity and pressure data, the team need to understand more about the characteristics of the flow, specifically, the team needs to calculate the Reynolds number, which will allow the team to understand what kind of flow exists in the valve system. FLUENT allows the team to model the Reynolds number of the flow throughout the system. As expected by the team, the flow is very turbulent. The minimum observed Reynolds number is 252000, which is significantly greater than the transition Reynolds number to turbulent flow, which is 4000.

As shown in Figure 8-9 and Figure 8-10, the velocity contour and path lines indicate that the flow in the valve is somewhat simple. The flow converges on the central hole the velocity increases, once inside the exhaust vent, the flow velocity is extremely high and is very near the maximum calculated and velocity values. The maximum observed velocity occurred inside the



larger volume of the exhaust valve system. Although the result is somewhat surprising, it is not entirely unexpected. It makes sense that the maximum velocities would occur at or very near the exit of the nozzle, which in our system; the equivalent nozzle would be the narrow opening in the engine head. The maximum calculated velocities is  $1.11 \cdot 10^5$  ft/s, although the majority of the flow is around  $5 \cdot 10^4$  ft/s. These velocities are very high and indicate that the flow in the valve will be well in excess of the speed of sound. Although the team expected very high velocities, the calculated velocities lead the team to recommend for future work that more CFD analysis be done, to verify the team's model and to further examine the flow of the system.

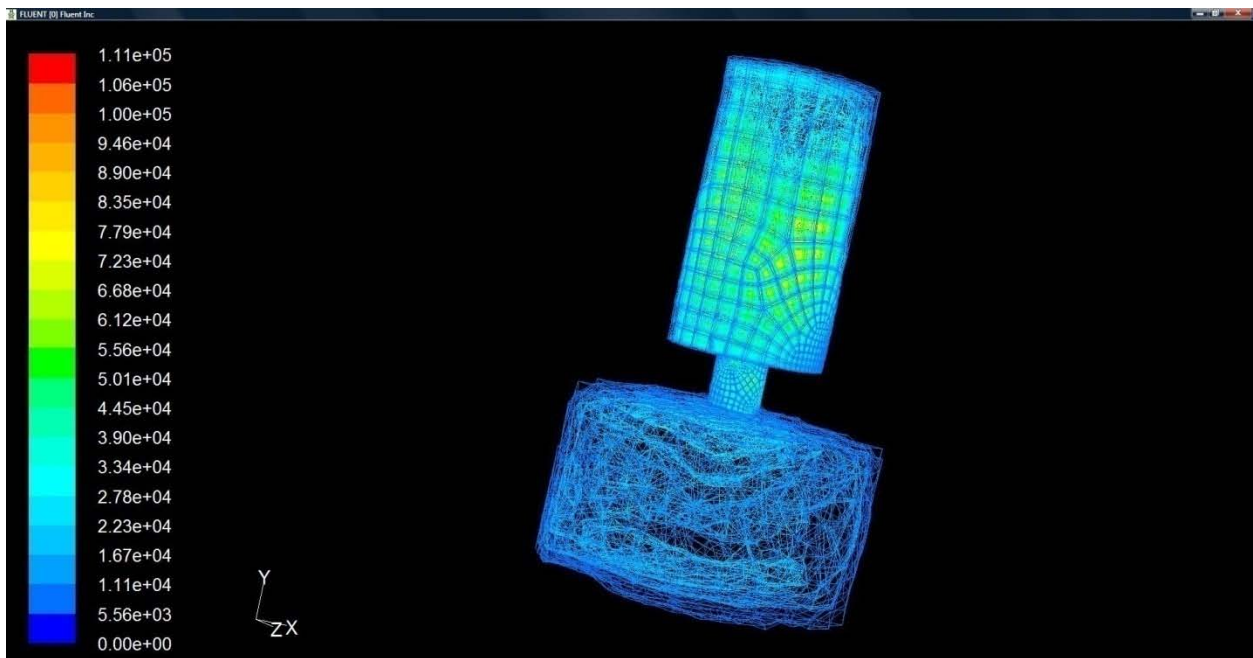


Figure 8-9: Velocity Magnitude Contours

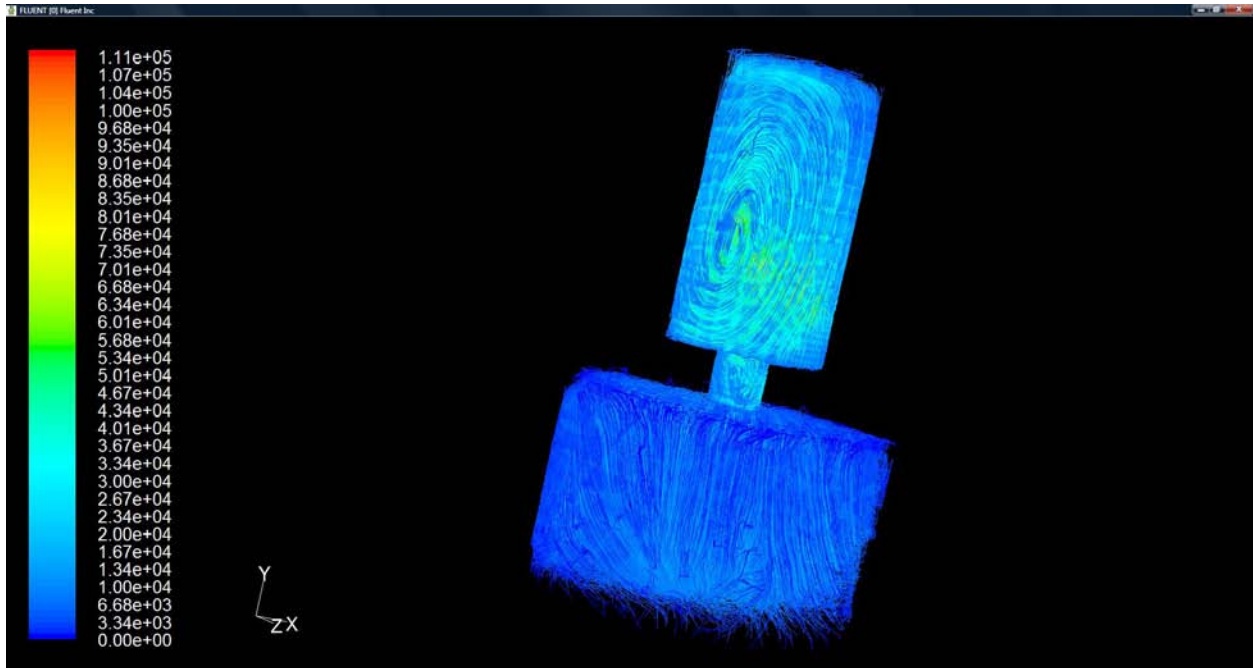


Figure 8-10: Velocity Path Lines

The team used CFD to calculate pressures in the system, and used the calculated pressures to work out where the low and high pressure areas in the system were. By knowing the areas of low and high pressure, the team can design the geometry of the valve to take advantage of the differences in pressure, because flow will always flow from areas of high pressure to areas of low pressure. As seen in Figure 8-11, there is an area of high pressure concentrated in one half of the small exit hole in the engine head. Because of the extremely turbulent flow dynamics, the pressure is not evenly distributed through the narrow exit hole. The maximum calculated pressure is  $1.68 \times 10^5$  psi, and the normal pressure is approximately  $7.5 \times 10^4$  psi. These pressures are significantly higher than expected. As a result of both the velocities and the pressures being higher than the team expected and thought to be reasonable, the team strongly recommends that any future work include further investigation

into CFD analysis of the system, which is detailed further in the recommendation section of this report.

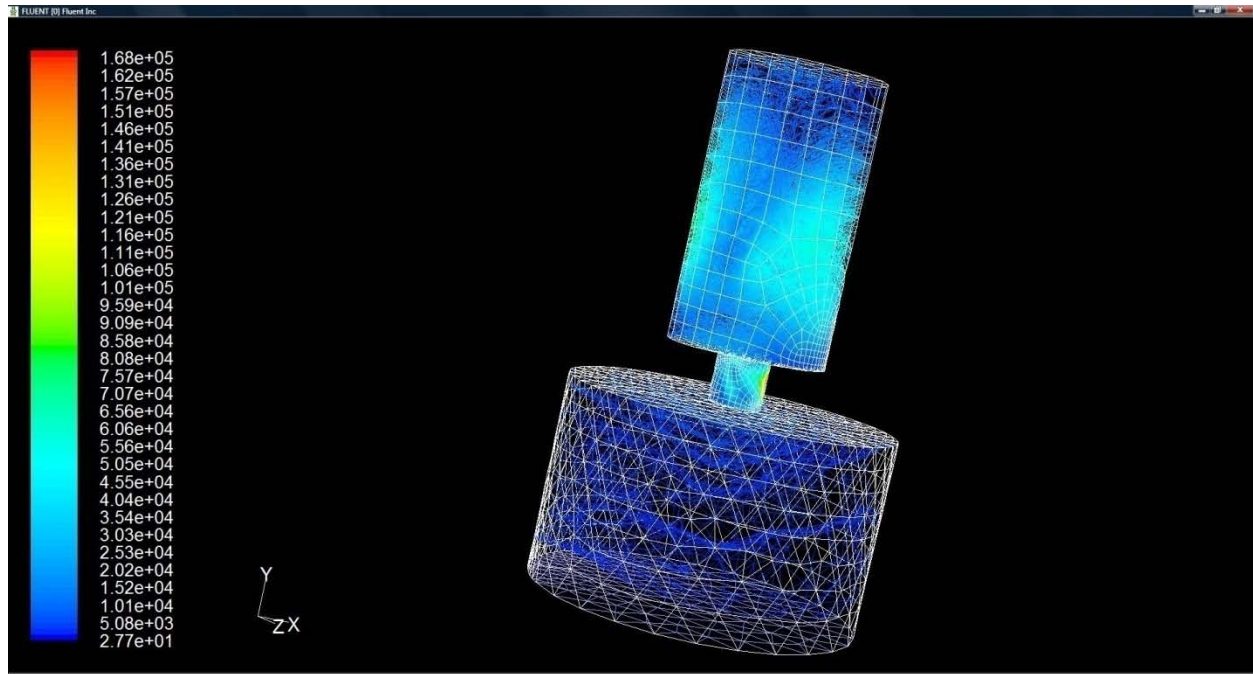


Figure 8-11: Pressure Contour

During final assembly and testing, it was discovered that due to limitations of machining tolerances, the flat tipped valve was not forming a sufficient seal and was releasing pressure much earlier than expected. The seal was poor enough that the engine would not run with the valve in place due to the valve not being able to hold a seal at normal operating pressure. To alleviate this, the team modified the valve tip geometry as well as the geometry of the base in which the valve tip sits. The geometries were changed from flat surfaces to matching chamfered edges in an effort to form a better seal with the machining tolerance limitations taken into account. The final valve system consists of a 0.2-inch diameter exit hole in the engine head; the valve dimensions are shown in Appendix A. The valve tip shape was changed from a flat head to a 45°-chamfered edge with matching seat in the engine head to ensure that the

valve would seal. The last minute change to the valve design is expected to alter the flow properties and stress distribution of both the valve and the engine head. The team expects that the pressure concentrations will be significantly altered, because of the highly turbulent flow. The flow in initial CFD analysis created areas of concentrated pressures and velocities as it passed through the small exit hole in the engine head. By changing the geometry of the exit hole, even slightly, the resulting pressure and velocity distributions would be significantly altered. The removal of the sharp edges would result in a reduction of areas of stress concentrations and would result in more evenly distributed stresses and fewer areas of high stress concentration.

## Chapter 9 : Prototype Construction

The two methods of prototype construction used for the project were CNC machining and FDM rapid prototyping. CNC stands for computer numerical controlled machining, and it was first used in the 1940's and 1950's when controls were added to manual machine tools. Modern CNC machines have the ability to create very complex surfaces with very tight tolerances. Machines offered range from simple 3 axis milling machines to 5 axis milling machines and lathes with live tooling.

Parts are first modeled in a CAD (computer aided design) program, and then imported into a CAM (computer aided manufacturing) program. The CAM program allows for the creation of tool paths, with complete control over feed rates, tolerances, and other cutting parameters. Once the tool paths are finalized the CAM program processes it and outputs machine code. The code simply gives the machine coordinates to where the tool should be moved. Also included in the code is a control for coolant, tool changes, and general information to the type of cut that is going to be performed.

The quality of the finished parts depends on a number of factors including tools used, machining speeds, and cutting parameters. Using a shorter tool will reduce the chances of chatter, improving the final surface. The shorter tools will also be able to cut at deeper increments. Each tool has a predetermined speed and feed rate to allow for the best possible cutting. These are readily available on the manufacture's website. Failure to follow these values can result in chattering, increased load on both the part as well as the machine itself.

Another factor is the order of operations for cutting. Immediately jumping from a roughing pass at a depth of cut of 0.1inches to a surfacing path will put a large amount of force on the ball mill, possibly breaking it. Enough intermediate cuts need to be put in between aggressive roughing cuts and surfacing passes. Consideration for fixturing also needs to be observed. If small contact points are holding a part the cuts need to be more conservative. If you are able to get a large contact area between the part and the vice cutting can be far more aggressive.

The machine shop in WPI's Washburn Shops housed a number of Haas CNC machines. These include 3 mini-mills, 2 SL10 lathes, a TL1 lathe, a VM3 mold making machine, a super VF4 vertical milling center, an SL20 lathe, and a mill drill center. The primary machines used for this project were the VM3, VF4 and TL1.

Rapid prototyping was first introduced in the late 1980s as a method to create parts quickly using a freeform fabrication. WPI Owns a Dimension 1200es SST printer. SST stands for soluble support technology, meaning that the support material used in the printing can be dissolved post printing. The machine works like a large inkjet printer, moving across the printing area laying small strands of ABS plastic as well as a support material, creating layers until the part is complete.

The parts are initially created in a CAD program, and then imported into the printer's software as an STL file. The STL file format defines the 3d part as just its surfaces, with no dependencies to color, texture, or other visual properties. The software then slices the part at

.01inch increments to determine the shape. Once the analysis of the parts is completed the part is sent to the printer.

The printer lays material in .01inch thick layers, using its combination of support material and ABS plastic to ensure that the part comes out as defined. The use of the support material allows for complex assemblies to be created preassembled, as all free space is filled in. Once printing is completed the parts sit in a bath to dissolve the support material, leaving just the ABS part behind.

## **Intake system**

Once the intake design had been finalized and ready for production, the team then needed to evaluate the best method for production of the prototype. The intake consisted of two parts, pressure transducer and the linear actuator, which needed to be purchased as well as seven parts that needed to be manufactured, including the pipe, the 2 covers, the butterfly valve, the rod that holds the valve in place, and there are two parts needed for the linkage, one is the linkage arm and one adapts the actuator rod. Initially it was decided that all parts, aside from the covers should be machined. However, WPI did not at the time have the facilities necessary to machine all the components. It was therefore decided that rapid prototyping would be the best method for manufacturing our prototype.

The final intake system was made almost exclusively using rapid prototyping. If this system were to go into production it would probably be made using plastic molding, so rapid prototyping is the natural first step. Due to the nature of rapid prototyping, the parts are not perfectly smooth, and therefore do not fit perfectly. Since the intake pipe was built with a

lattice structure, air is able to pass through the structure. Due to this air and water is still able to pass through even when the valve is closed off.

In an attempt to solve these problems a combination of hand fitting and coatings were used. Parts that need to move freely were sanded to allow for a smooth contact surface. The interior of the intake pipe was also coated with a spray on plastic coating. This coating serves to fill in and seal the interior wall, as well as create a full seal between the pipe and valve plate. Another method would have been to coat the rapid prototype parts in resin, which would be absorbed into the parts, filling in the voids and making the parts solid.

## Valve system

The engine valve system is comprised of four parts, a modified engine head, a valve, a spring and the valve cap. The spring can be purchased and the other three parts manufactured using WPI's CNC machine shop. Each part was modeled using Solidworks and the machine code generated by GibbsCAM.

The engine head is cut in two steps, one to cut the bottom side and the next to cut the top side, both done in either the VM3 or VF4. The valve is cut the same way in a mini-mill. The cap can be cut by hand on the TL-1 Lathe, with threads added by hand with a die or utilizing the built in programs of the TL-1. All parts are shown in the following figures.

Several engine heads needed to be made over the course of the project, each serving their own purpose. The initial head was created to test the 3D model; making sure future engine heads would function properly. The cooling fins from the stock head were eliminated, as



they would not be needed for the relatively short testing times. Testing of this head proved the model was created correctly and the engine functioned properly with it installed.

The second engine head was developed with an extrusion created to hold the pressure transducer used in testing. The hole through to the combustion chamber was created with a slight chamfer to stop flame propagation through to the transducer. This was done to keep heat to the transducer at a minimum, as the pressure transducer was not rated to the heats seen in the engine. At the time of manufacturing it was determined that the model needed to be changed in order to hold the part more securely. The contours around the sealing edge of the engine head were modified to be flush, allowing for more contact points with the vice. This reduced the chances of the part lifting out of the vice, and damaging tools, as well as the final part.

Following the pressure testing, the final head was manufactured. The head designed for the pressure transducer was modified to accommodate a cap with ANSI inch 1-14 threads. The model also had the necessary draft angles added to all cylindrical extrusions to allow for a better surface finish. The final engine head is machined from a 7075 aluminum alloy and shown in Figure 9-1.



Figure 9-1: Final Machined Engine Head

The valve was manufactured using WPI's Haas mini-mills. A piece of 6061 aluminum alloy round stock was machined down to produce the stem, then flipped and the valve seat and stabilizing seat added. The initial valve had a flat seat, however following testing it was determined that this valve was lifting on one side under pressure, releasing at a lower pressure than designed for. To remedy this, the seat was changed to a 45-degree chamfer, with a matching seat in the engine head. This allowed the valve to seat better and hold pressure.

The valve cap was machined out of a 6061-aluminum alloy. The part was machined using a combination of manual cuts and preprogrammed operations from the TL-1's controller. This allowed for tolerances to be maintained without creating machine code beforehand. Threads were added post machining using a hand die. No design changes were needed for this part.

## Chapter 10 : Prototype Testing

Following the final assembly and installment, each system had to be individually tested to validate design effectiveness. To simulate hydrostatic-locking conditions, the intake system was tested installed directly onto the intake of our engine. This insured that fluid intake would flow past the valve before entering the engine. By replicating similar operating conditions the team was able to verify the functionality of the design, as a whole, and the efficiency regarding hydrostatic-lock prevention.

Once the intake had been connected, the engine was started and allowed to run for several seconds, one of the team members then placed his hand over the opening of the intake, simulating the introduction of water. The simulation of water induction caused a spike in negative pressure. Preceding the simulation of a full hydrostatic-lock, the circuit determined a sudden change in negative pressure below that of normal operation. Once detected a relay was sent to turn on the solenoid, which is connected to the butterfly valve, closing the intake.

Testing revealed that the circuit and butterfly valve function as intended, however the activated system did not stall the engine as the team had anticipated would happen. Upon further investigation, the team discovered that the butterfly valve was not forming a perfect seal. Due to improper sealing air was able to bypass the valve, flowing into the engine, allowing for continued operation. The team concluded that this was due to the material used as well as the method in which the part was manufactured. The intake system tube and butterfly valve was constructed of rapid prototype ABS plastic. More importantly, to save material cost and manufacturing time, both parts we're made as lattice structures; due to the FDM

manufacturing process inclusions were present in the part allowing for airflow to pass through such voids, allowing for continued engine operation. As a result the systems functioned perfectly however while functioning correctly they were unable to accomplish their goal of mitigating hydrostatic-lock. The team is confident in the robustness of their design theory; however the team recognizes and addresses remedial solutions in Chapter 11.

For standalone testing of the engine head valve system, the desired experiment setup consisted of the assembled engine head installed on the existing engine. Beneficial to testing would be the inspection of gaskets, seals and other components, and if necessary replaced before testing, to ensure that there would be no undesired loss of engine pressure. The goal of the experiment is to verify that the appropriate functioning and release of the valve system, releasing pressure over 500 psi.

Due to timeline limitations, the engine head valve system was unable to be sufficiently tested. The team was able to outline its testing scenario and goals. With the engine head valve system setup as described above, the team planned to start the engine and allow it to run, making careful observations of its running characteristics to ensure that the design did not interfere with normal running. After extensive rounds of normal running testing, the team would then prepare to hydrostatic-lock the engine. To hydrostatic-lock the engine a sample of water, at a minimum slightly larger volume than the combustion volume of the engine,  $1.36 \text{ in}^2$  would be introduced by pouring swiftly into the intake of the engine. The intake system should not be connected to the engine to make adding the water easier. Great care should be taken while adding the water sample; no experimenter or valuable equipment should be facing the

engine head or the direction of the exhaust ports. Hydrostatic-locking is a violent event and if the system functions properly, water will be exiting the exhaust ports at extremely high velocities and could be hazardous. In addition, if the system fails, the most likely component to fail would be the spring controlled valve system. If catastrophic failure occurs, the cap, spring and valve could be turned into potentially hazardous projectiles. All experimenters should be very focused on the events at hand while the hydrostatic-lock condition is occurring, if the system does not mitigate hydrostatic-lock, the engine may fail violently. During the experiment any changes in engine rpm, vibration, noise, exhaust as well as changes in the system should be noted and investigated to determine if they are caused by the addition of water to the engine.

The team had planned to do full testing with both systems integrated into the engine. However due to timeframe limitations, finally testing was unable to be completed. The team was able to outline how the testing would be done, including what procedures to follow in order to obtain the ideal testing scenario.

The engine should be setup with the engine head installed as discussed earlier in this section. The intake should also be setup as described earlier in this section with the addition of a length of flexible air-tight tubing. The purpose of the tubing is the team feels it is important to test the engine at various levels of water submersion. Therefore having a flexible tube connected to the intake would make it easier to conduct the test by placing the tube in various levels of submersion, from a variety of partial submersions to full submersion.

The engine should be started and allowed to run, and then the intake tube should be placed into a reasonably sized quantity of water. Although the final experiment is at the

discretion of the experimenter, the team would recommend at least one partial submersion test be conducted, in addition to a full submersion test. Varying levels of partial submersion may also reveal relevant results and should be looked into. While conducting the experiment with water, all experimenters should be cautious. Hydrostatic-locking can be an extremely violent occurrence, and in the event that one of the design system fails to mitigate hydrostatic-lock, the engine may fail catastrophically resulting in a dangerous situation.

The important observations to make are the time delay from the introduction of water into the intake pipe until the intake valve activation; this should be a very small period of time and may in fact not be measureable by normal methods. After the introduction of water the observer should note any changes in operation. Additionally, any movement of the engine head valve, or flow out of the exhaust ports on the valve should be noted and investigated. While all of the previously described occurrences would be useful observations, the team recommends observing the engine during normal running for a reasonable period of time before initial testing. This will ensure that the experimenter is familiar with a normal engine occurrence and something that should be investigated further, as it may be a reaction to a hydrostatic-lock situation.

## Chapter 11 : Conclusions

The two hydrostatic lock mitigation systems developed were shown to act as intended by the designers in a hydrostatic lock situation. However, significant future work needs to be done to further improve the designs and their function. This is explored further in Chapter 11.

The intake system and engine spring controlled valve were both proven to be sound conceptual designs, however both required small modifications due to manufacturing errors in order to function properly and verify validity of designs. In all pressure sensitive applications the strength of the seal formed is essential to proper function. With the addition of sealant agents to specific sensitive areas of both designs, both designs were able to reliably function as intended by the design team. All parts were either machined on HAAS CNC milling machines, such as the mini-mill, VM3 and VF4, or produced by Fused Deposition Modeling Rapid Prototyping on a Dimension 1200es SST printer. If desired, the construction of all devices and experiments described in this paper can be repeated using the methods and materials described.

Despite the significant effort put into this project by the design team, a significant amount of potential work remains that could not be completed in the given time frame. As a result, there are several possible design improvements, additional analysis, further experiments and substantial testing that could be completed, given additional time. All future work is discussed in chapter 11.



Figure 11-1: CAD Model of Intake System



Figure 11-2: Final Prototype of Intake System



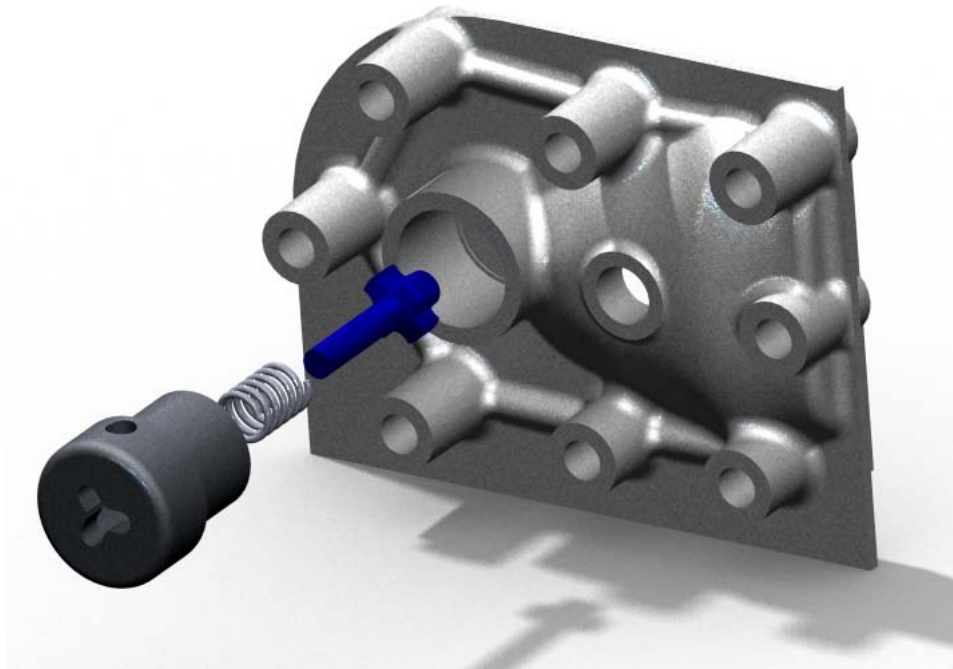


Figure 11-3: CAD Model of Engine Valve System



Figure 11-4: Final Prototype of Engine Valve System



Figure 11-5: Both Systems Installed on the Engine

## Chapter 12 : Recommendations

The most beneficial recommendation for future work is a detailed investigation into the dynamics of hydrostatic-lock. By understanding the specific dynamics of this problem, better solutions may be developed and adapted for other engines and technologies. When performing analysis into stresses during the time of hydrostatic-locking the team made an assumption that the cylinder was filled with water. Research into the compression dynamics of an air/water mixture would provide an understanding towards the conditions required to hydrostatic-lock the engine. However, due to the complex modeling required a mixed air/fuel condition the team was unable to investigate such phenomenon.

Research into the submersion of the intake filter would allow for the determination into the depth and exact conditions required for hydrostatic-lock. Due to the variations in engine design these conditions will differ from engine to engine, however the conditions may correspond depending on engine size.

### Alternative Water Detection and ECU Integration

Currently the method for detecting water is through the implementation of a pressure transducer to monitor pressure in the intake system. It would be beneficial to look into other methods that may prove more reliable and detailed information. Partially submerging the intake will not result in a very large spike in pressure, allowing for the engine to continue pulling water into the intake, potentially below the lock off pressure. By investigating additional methods to detect water, it may be possible to detect water in any concentration. If able to

develop a system to monitor the concentration of water, and relay this to the operator, the system could virtually determine the exact point at which the engine would hydrostatic-lock.

This system could also be tied into the engine management system of modern cars. This would allow the ECU to make intelligent decisions about how to handle hydrostatic-lock situations. If the sensor detects a small amount of water, the ECU could limit the throttle position, reducing the chance of pulling water into the intake due to the higher density. While this would limit power available, it would also allow the operator to navigate out of the area, at which point the throttle position could be reset.

Other benefits of integrating with the ECU include utilization of preexisting sensor to both stop the engine, and provide user alerts. Since modern engines contain preinstalled sensors for engine management, these can be utilized to improve detection. Once a hydrostatic-lock situation has been detected the ECU can stop the flow of fuel as well as spark. Combined with closing the throttle the engine would be able to spin down in approximately the same time as normally stopping the engine. The removal of fuel and spark will reduce the vacuum that draws in water, allowing the operator to move the car away from the area of trouble. The implementation of such a system reduces the need for a mechanical system, requiring additional programming to the ECU to detect and implement the system.

The status can also be displayed on the car's dash, providing the operator with feedback as to the condition of the engine. Since damage often occurs as the operator attempts to turn the engine over after hydrostatic-locking a warning system would provide information as to

when the engine would be safe to operate, therefore preventing the destruction of components.

## **Valve Seating and Sealing**

Following challenges of machining a valve to seat properly further work should be done to improve the seating surface of the release valve. To improve the seal future work may include research into valve grinding, or the addition of a ball valve. A second alternative would be to remove the valve entirely. By developing a mechanical fuse that is designed to release at a specific pressure, there would be no seating issues. The fuse could be a screw in piece, making it very easy to replace. The only downside would be the inability to start the engine post hydrostatic-lock.

## **System Improvement and modification**

Currently the system relies on the proper function of a valve to exhaust any increase in pressure. Prolonged exposure to cycling heating may lead to the weakening of the valve components, in turn leading to future failure. By replacing the valve with an electronic solenoid/linear actuator the valve could respond to changes in the intake, exhausting pressure if the system detected the intake of water.

In order to increase the efficiency of the system, if combined, the circuit may control both the intake assembly as well as the engine head valve. The concurrent functioning of both systems would prevent the possibility of hydrostatic-locking regardless of if one system failed. To implement such a system the engine head must be modified to use an electronic assembly and the circuit must be adapted to control either the solenoid or linear actuator.

To further improve the system the circuit may be modified to include a separate system for water detection. If two sensors were used, in separate sections of the intake, a circuit may be developed to monitor both areas; if one became submerged the intake could be rerouted to open a section free of water. If both sensors were submerged the intake would close itself off, stalling the engine and preventing a hydrostatic-lock condition.

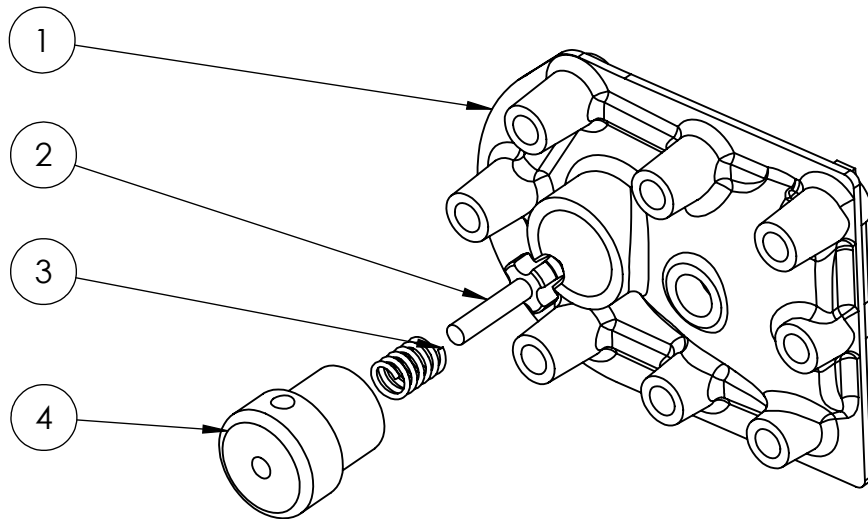
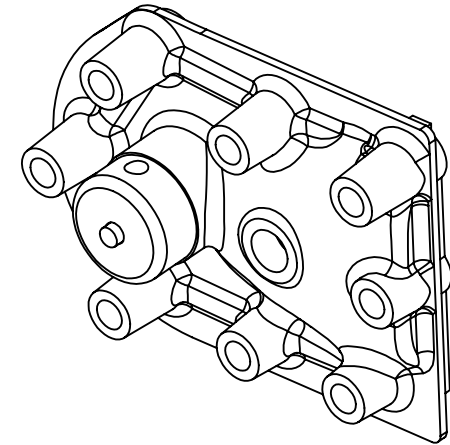
## **Adaptation for Manufacturing**

Each system needs to be modified for manufacturing. While the designs worked very well for prototyping, changes are needed to allow for mass production. The engine heads are best suited for casting, as the machining cost is extremely high due to long machining time, a result of surfacing operations. Molds need to be developed for both the aluminum casting for the engine heads, as well as the injection plastic molding for the intake system.

# Chapter 13 : Appendices

## Appendix A: Drawings

ITEM NO.	PART NUMBER	DESCRIPTION	QTY.
1	engine_head_with_valve_machine_fix	MOdified Engine Head	1
2	final valve		1
3	spring2	100lb/in spring 1 inch free length	1
4	valve cap new	Retaining Cap	1



DO NOT SCALE DRAWING	REVISION
TITLE: <b>Engine Valve System</b>	
Part Name	<b>new head</b>
	A4
SCALE:1:2	SHEET 1 OF 1



**WPI**

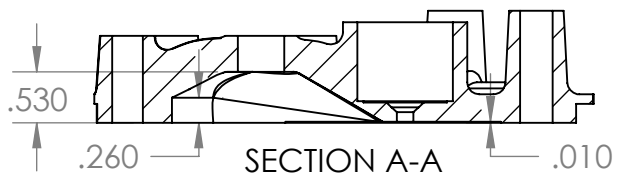
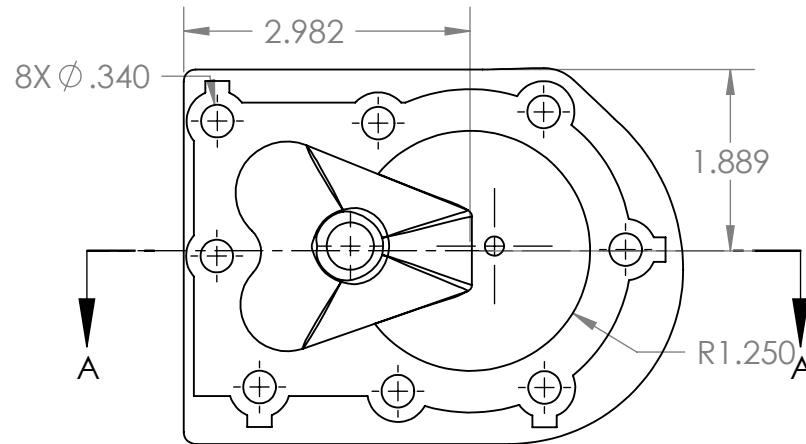
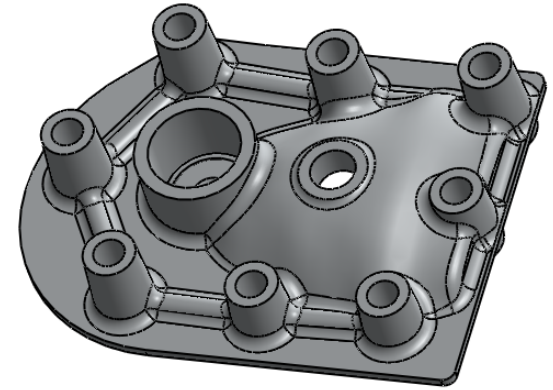
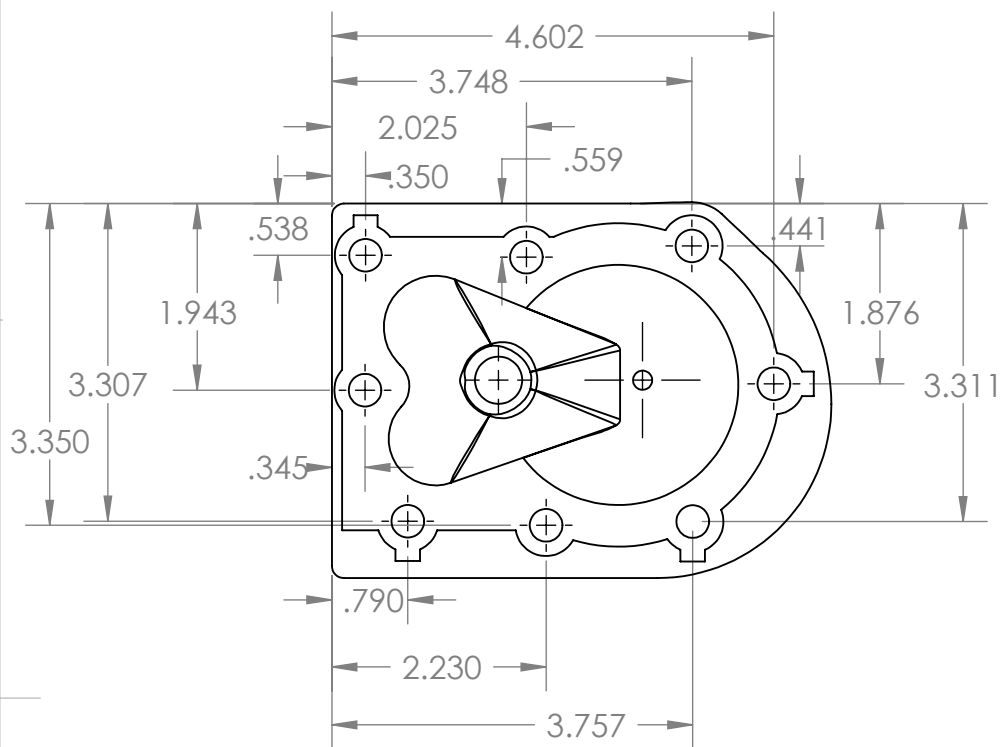
UNLESS OTHERWISE SPECIFIED:  
 DIMENSIONS ARE IN Inches  
 SURFACE FINISH:  
 TOLERANCES:  
 LINEAR:  
 ANGULAR:

DEBUR AND  
 BREAK SHARP  
 EDGES

MATERIAL:  
 Aluminum 6061

	NAME	SIGNATURE	DATE
DRAWN	Chris Egan		4/28/09





The engine head may take any form as long as the dimensions on the drawings are followed. The vital parts include the combustion chamber volume, the spacing for the bolt holes, and the location of the spark plug and valve. The volume of the Combustion Chamber is  $1.36\text{in}^2$



UNLESS OTHERWISE SPECIFIED:  
 DIMENSIONS ARE IN INCHES  
 SURFACE FINISH:  
 TOLERANCES:  
 LINEAR:  
 ANGULAR:

DEBUR AND  
 BREAK SHARP  
 EDGES

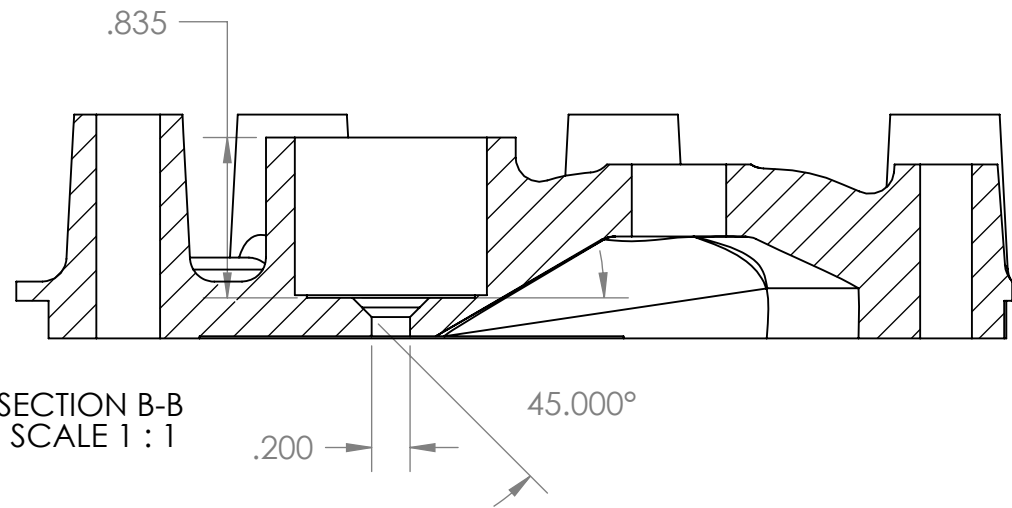
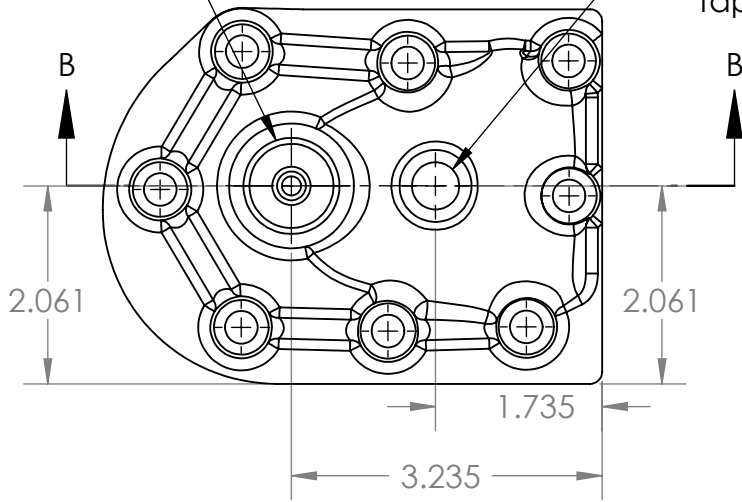
MATERIAL:  
 Aluminum 6061

NAME	SIGNATURE	DATE
DRAWN Chris Egan		4/28/09

DO NOT SCALE DRAWING	REVISION
TITLE: <b>Engine Head With Valve</b>	
Part Name engine_head_with_valve_machine_fix	A4
SCALE:1:2	SHEET 1 OF 2

ANSI Inch 1-14 Thread

Metric 14x1.25 tap



SECTION B-B  
SCALE 1 : 1

DO NOT SCALE DRAWING REVISION

TITLE:

# Engine Head with Valve

Part Name  
engine\_head\_with\_valve\_machine\_fix A4

SCALE:1:2 SHEET 2 OF 2



# WPI

UNLESS OTHERWISE SPECIFIED:  
 DIMENSIONS ARE IN INCHES  
 SURFACE FINISH:  
 TOLERANCES:  
 LINEAR:  
 ANGULAR:

DEBUR AND  
BREAK SHARP  
EDGES

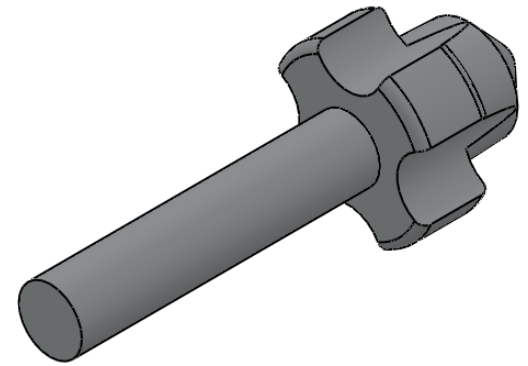
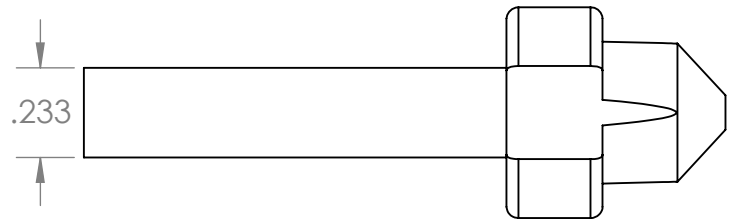
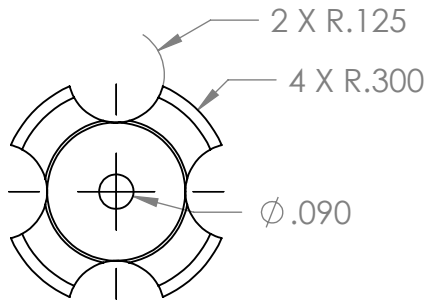
MATERIAL:  
Aluminum 6061

	NAME	SIGNATURE	DATE
DRAWN	Chris Egan		4/28/09

1 2 3 4 5 6

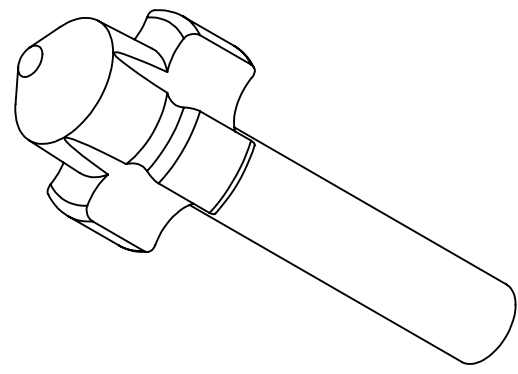
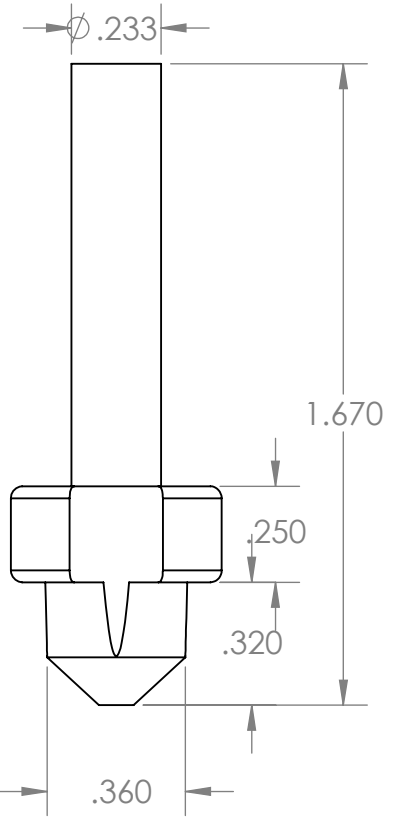
A

A



B

B



C

C

D

D



**WPI**

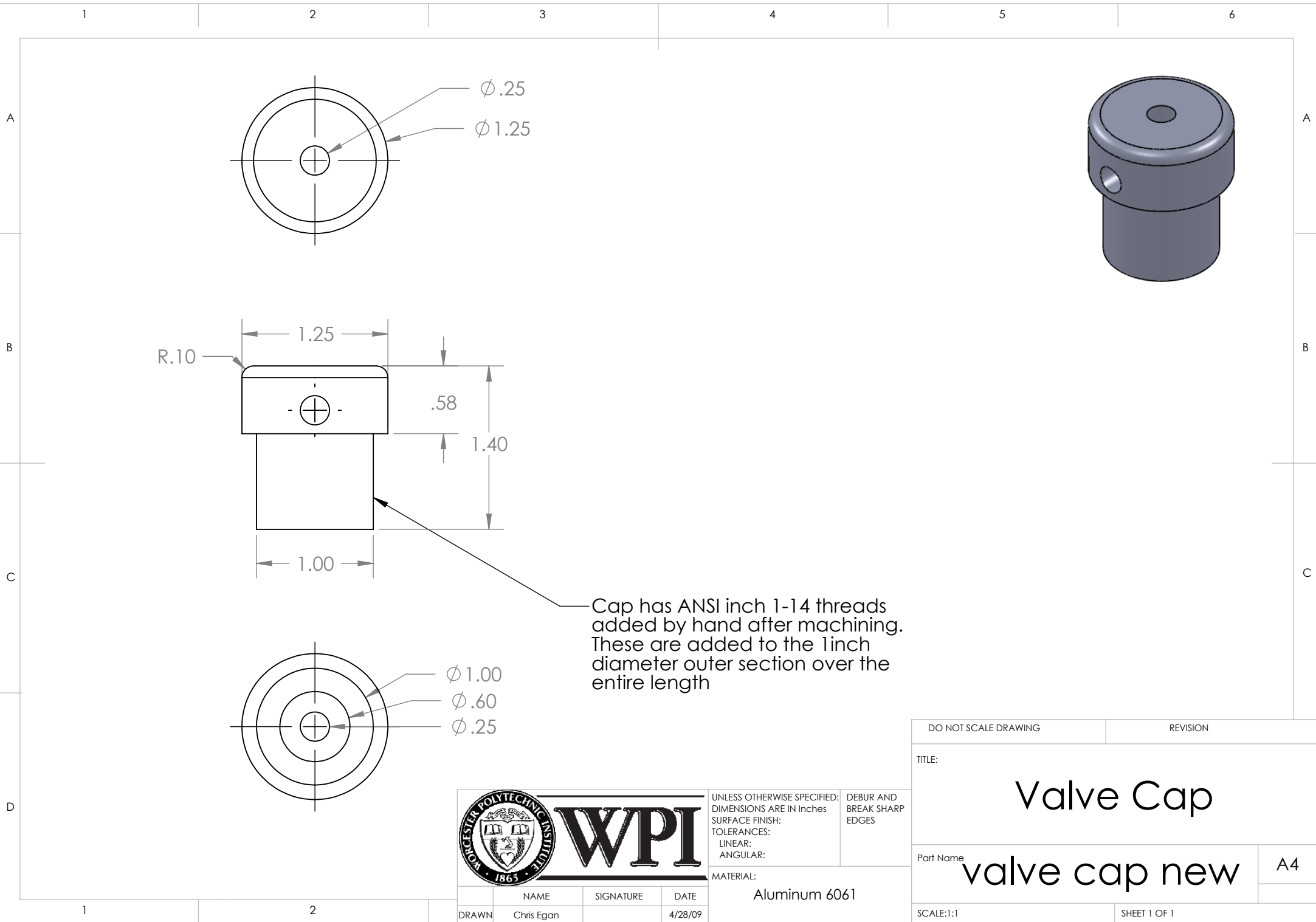
UNLESS OTHERWISE SPECIFIED:  
 DIMENSIONS ARE IN Inches  
 SURFACE FINISH:  
 TOLERANCES:  
 LINEAR:  
 ANGULAR:  
 DEBUR AND  
 BREAK SHARP  
 EDGES

MATERIAL:  
 Aluminum 6061

NAME	SIGNATURE	DATE
DRAWN Chris Egan		4/28/09

DO NOT SCALE DRAWING	REVISION
TITLE: <h1>Engine Valve</h1>	
Part Name	final valve
	A4
SCALE:2:1	SHEET 1 OF 1

1 2



**WPI**

UNLESS OTHERWISE SPECIFIED:  
 DIMENSIONS ARE IN Inches  
 SURFACE FINISH:  
 TOLERANCES:  
 LINEAR:  
 ANGULAR:

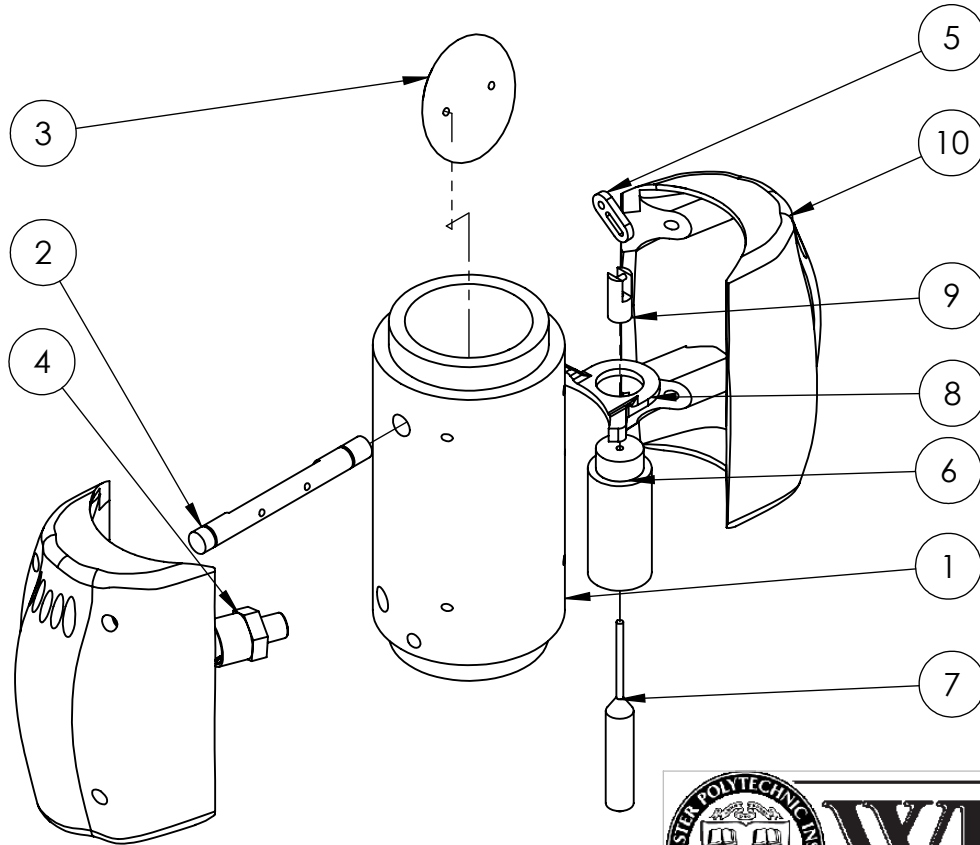
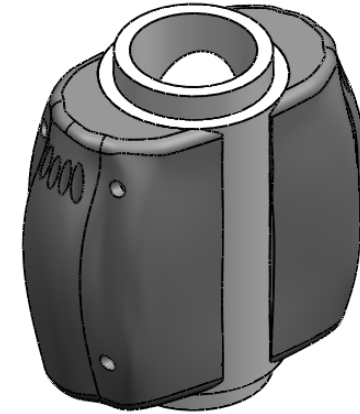
DEBUR AND  
 BREAK SHARP  
 EDGES

MATERIAL:  
 Aluminum 6061

	NAME	SIGNATURE	DATE
DRAWN	Chris Egan		4/28/09

DO NOT SCALE DRAWING		REVISION	
TITLE: <h1>Valve Cap</h1>			
Part Name <h2>valve cap new</h2>			A4
SCALE:1:1		SHEET 1 OF 1	

ITEM NO.	PART NUMBER	DESCRIPTION	QTY.
1	pipe	Intake Pipe	1
2	pin	Valve Pin	1
3	plate	Valve Plate	1
4	transducer	Pressure Transducer	1
5	slot bar	Arm to link Actuator to Valve	1
6	69905k1 body	Linear Actuator Body	1
7	69905k1 rod	Linear Actuator Pin	1
8	stand	Linear Actuator Mounting Stand	1
9	attachment	Linear Actuator Atchment	1
10	cover_transducer	Intake System Cover	2



UNLESS OTHERWISE SPECIFIED:  
 DIMENSIONS ARE IN Inches  
 SURFACE FINISH:  
 TOLERANCES:  
 LINEAR:  
 ANGULAR:

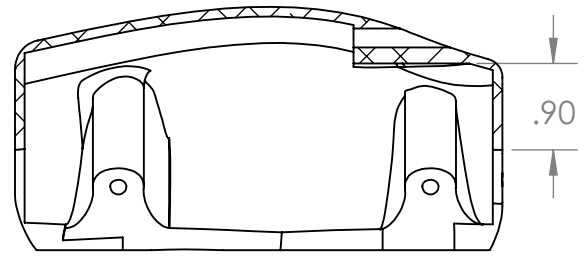
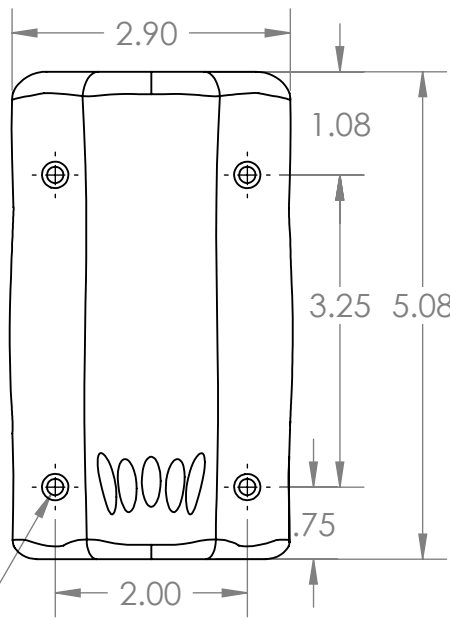
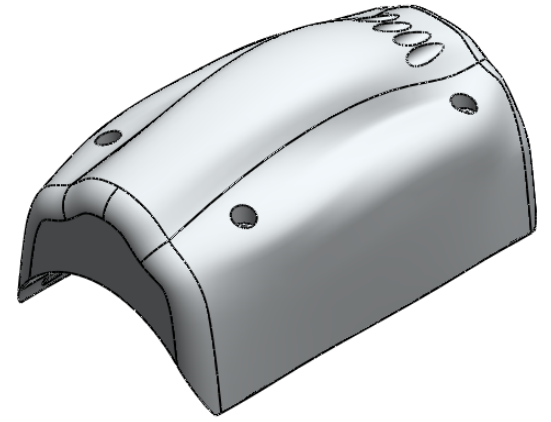
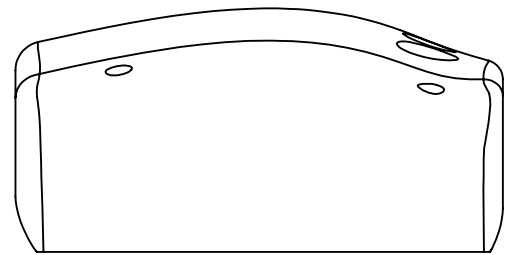
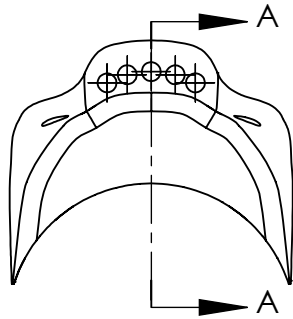
DEBUR AND  
 BREAK SHARP  
 EDGES

MATERIAL:

ABS Plastic and  
 6061 Aluminim

NAME	SIGNATURE	DATE
DRAWN Chris Egan		4/28/09

DO NOT SCALE DRAWING	REVISION
TITLE: <h1>Intake System</h1>	
Part Name <h2>standalone system</h2>	A4
SCALE:1:3	SHEET 1 OF 1



SECTION A-A

The final shape is not important as long as all shown dimensions are met. The clearance shown in the section view is important for circuit clearance.

4X  $\phi$  .17 THRU ALL  
 $\square$   $\phi$  .28  $\nabla$  .19



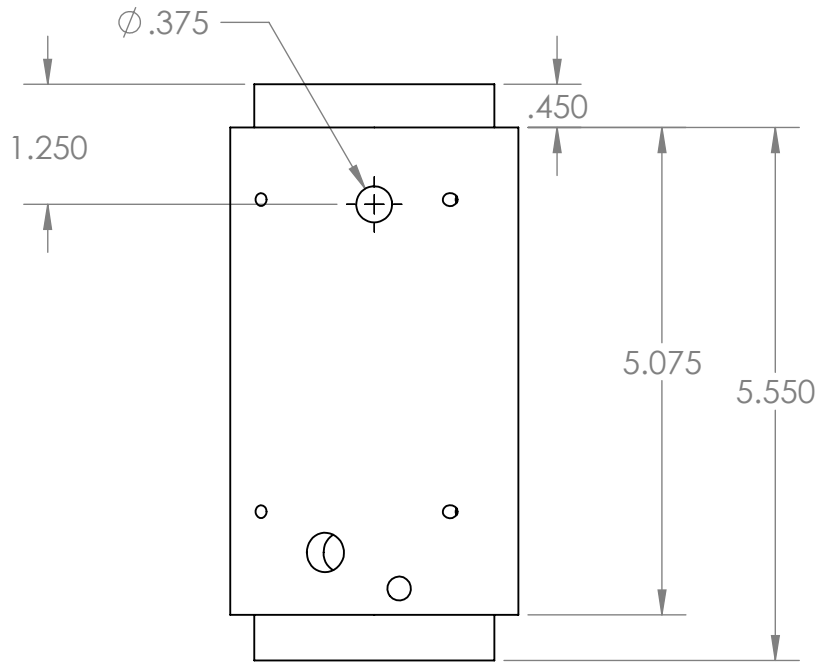
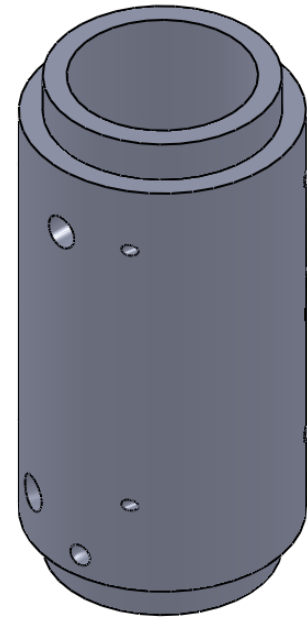
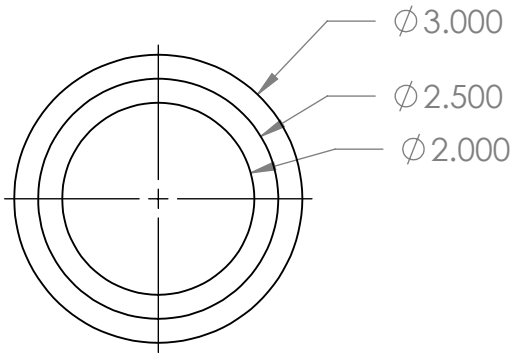
UNLESS OTHERWISE SPECIFIED:  
 DIMENSIONS ARE IN Inches  
 SURFACE FINISH:  
 TOLERANCES:  
 LINEAR:  
 ANGULAR:

DEBUR AND  
 BREAK SHARP  
 EDGES

MATERIAL:  
 Aluminum 6061

NAME	SIGNATURE	DATE
DRAWN Chris Egan		4/28/09

DO NOT SCALE DRAWING	REVISION
TITLE: <h1>Intake Cover</h1>	
Part Name <h2>cover_transducer</h2>	A4
SCALE:1:2	SHEET 1 OF 1



**WPI**

UNLESS OTHERWISE SPECIFIED:  
 DIMENSIONS ARE IN INCHES  
 SURFACE FINISH:  
 TOLERANCES:  
 LINEAR:  
 ANGULAR:

DEBUR AND  
 BREAK SHARP  
 EDGES

MATERIAL:

ABS Plastic

DO NOT SCALE DRAWING		REVISION	
TITLE: <h1>Valve Pin</h1>			
Part Name		pipe	
SCALE: 1:2		SHEET 1 OF 2	
DRAWN		A4	
Chris Egan			
4/28/09			

NAME	SIGNATURE	DATE
Chris Egan		4/28/09

A

A

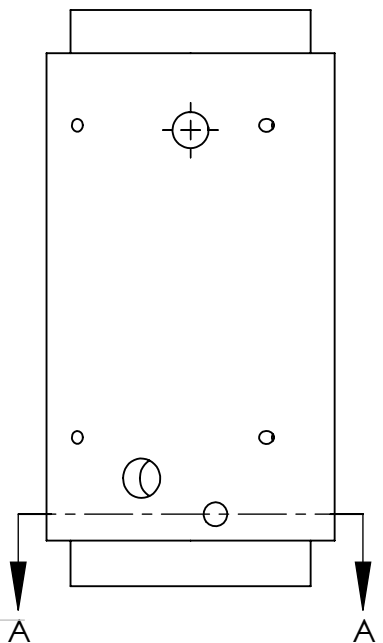
B

B

C

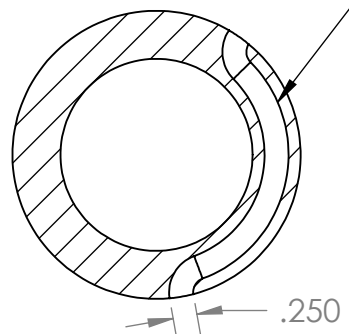
C

D



Holes for the covers are constructed on a plane 100degrees off the right plane, 10 degrees off the front plane. The holes are constructed for 6-32 screws, and are 2 inches apart centered on the part. The top set are 1.2 inches from the top of the pipe, and the second set are 3.25 below the first. The hole for the pressure transducer may be placed anywhere inside the circuit side that it does not conflict with wires. The threads are a 1/8-27.

The channel through the pipe may take any route, it is simply to allow the passage of wires from one side to the other.



SECTION A-A



**WPI**

UNLESS OTHERWISE SPECIFIED:  
 DIMENSIONS ARE IN Inches  
 SURFACE FINISH:  
 TOLERANCES:  
 LINEAR:  
 ANGULAR:  
 DEBUR AND  
 BREAK SHARP  
 EDGES

MATERIAL:  
 ABS Plastic

	NAME	SIGNATURE	DATE
DRAWN	Chris Egan		4/28/09

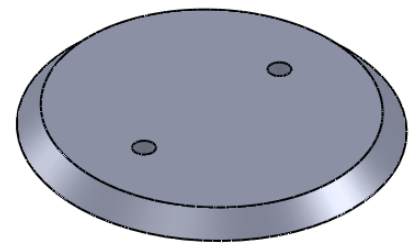
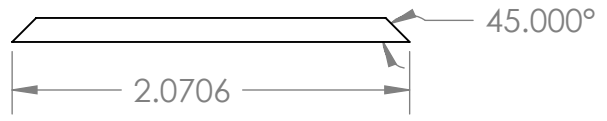
DO NOT SCALE DRAWING		REVISION	
TITLE:  <b>Valve Pin</b>			
Part Name  <b>pipe</b>			A4
SCALE:1:2		SHEET 2 OF 2	



1 2 3 4 5 6

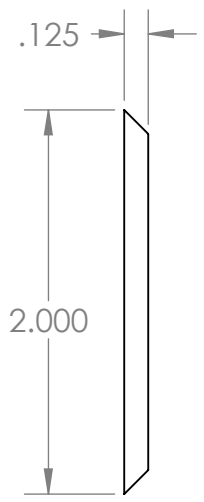
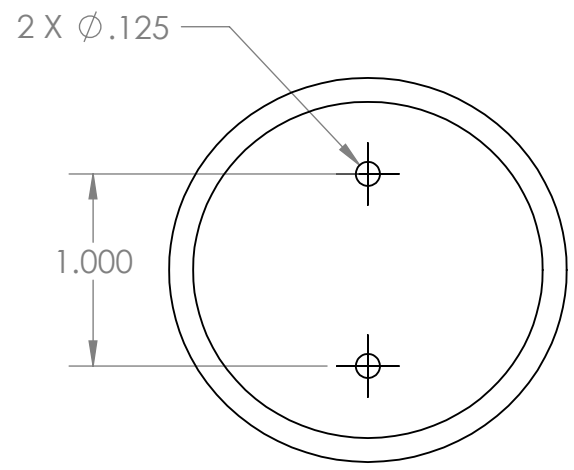
A

A



B

B



C

C

D



**WPI**

UNLESS OTHERWISE SPECIFIED:  
DIMENSIONS ARE IN INCHES  
SURFACE FINISH:  
TOLERANCES:  
LINEAR:  
ANGULAR:

DEBUR AND  
BREAK SHARP  
EDGES

MATERIAL:  
ABS Plastic

DO NOT SCALE DRAWING		REVISION	
TITLE: <h1>Valve Plate</h1>			
Part Name		plate	A4
SCALE:1:1		SHEET 1 OF 1	

1

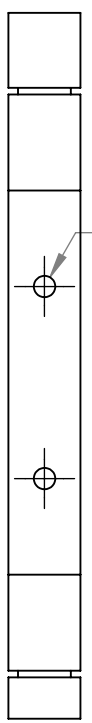
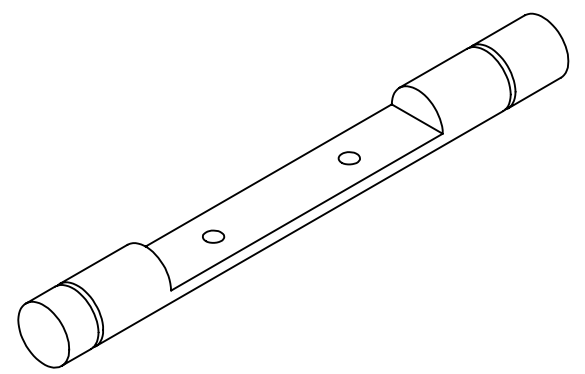
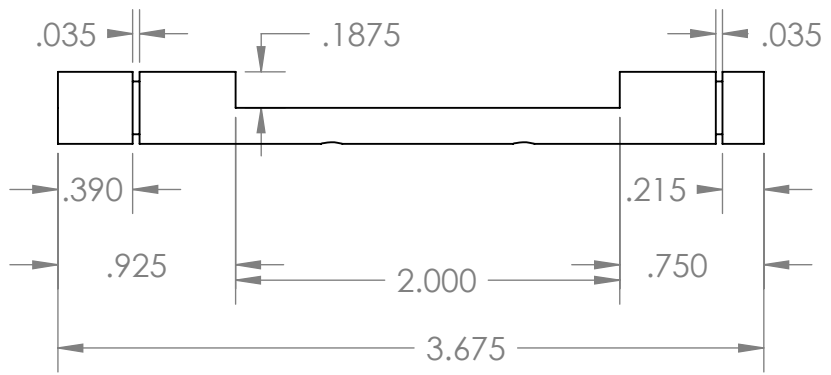
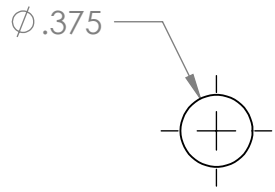
2

	NAME	SIGNATURE	DATE
DRAWN	Chris Egan		4/28/09

1 2 3 4 5 6

A  
B  
C  
D

A  
B  
C



2X  $\phi .089$  THRU ALL  
4-40 UNC THRU ALL



**WPI**

UNLESS OTHERWISE SPECIFIED:  
DIMENSIONS ARE IN INCHES  
SURFACE FINISH:  
TOLERANCES:  
LINEAR:  
ANGULAR:

DEBUR AND  
BREAK SHARP  
EDGES

MATERIAL:  
ABS Plastic

	NAME	SIGNATURE	DATE
DRAWN	Chris Egan		4/28/09

DO NOT SCALE DRAWING	REVISION
TITLE: <h1>Valve Pin</h1>	
Part Name	pin
	A4
SCALE:1:1	SHEET 1 OF 1

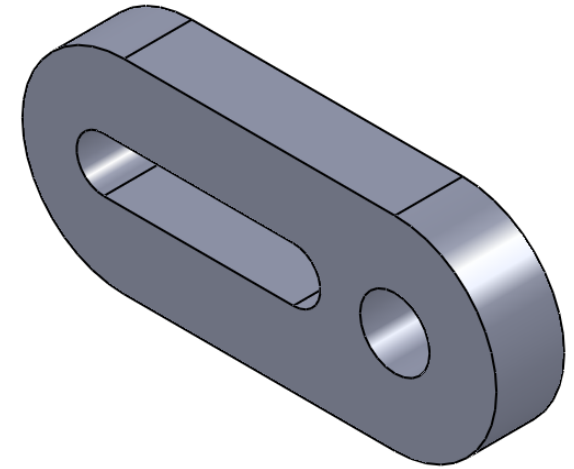
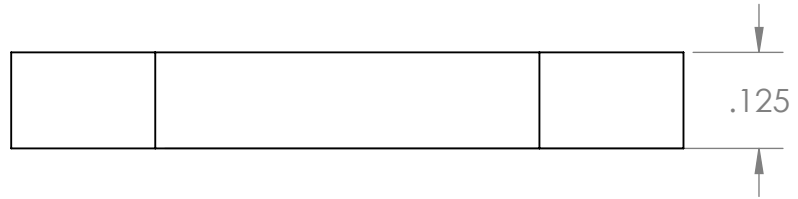
1

2

1 2 3 4 5 6

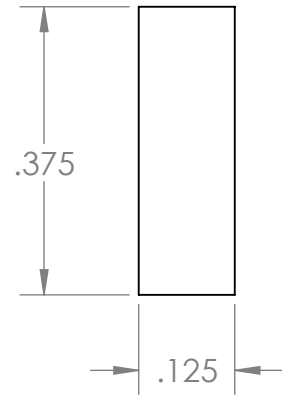
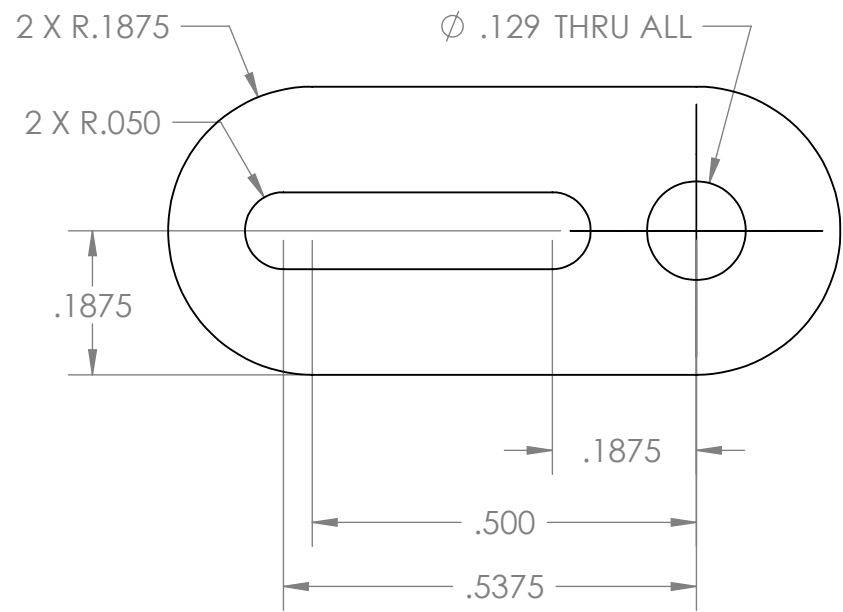
A

A



B

B

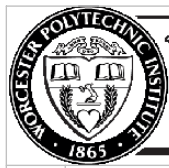


C

C

D

D



**WPI**

UNLESS OTHERWISE SPECIFIED:  
DIMENSIONS ARE IN INCHES  
SURFACE FINISH:  
TOLERANCES:  
LINEAR:  
ANGULAR:

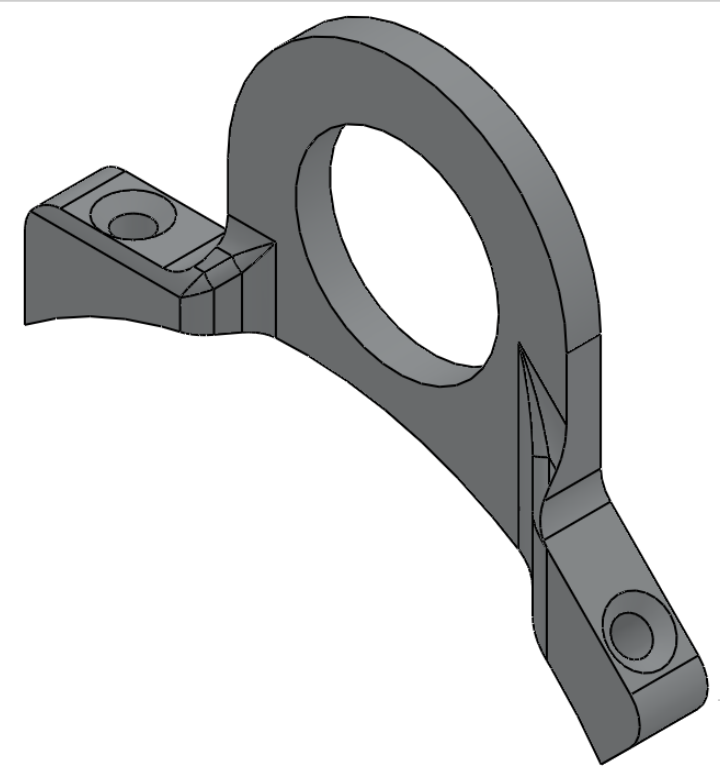
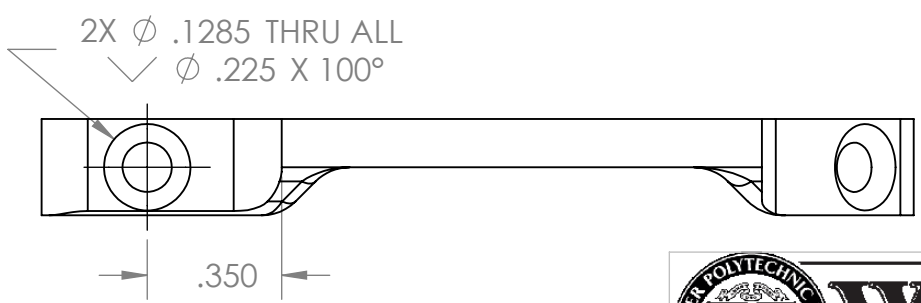
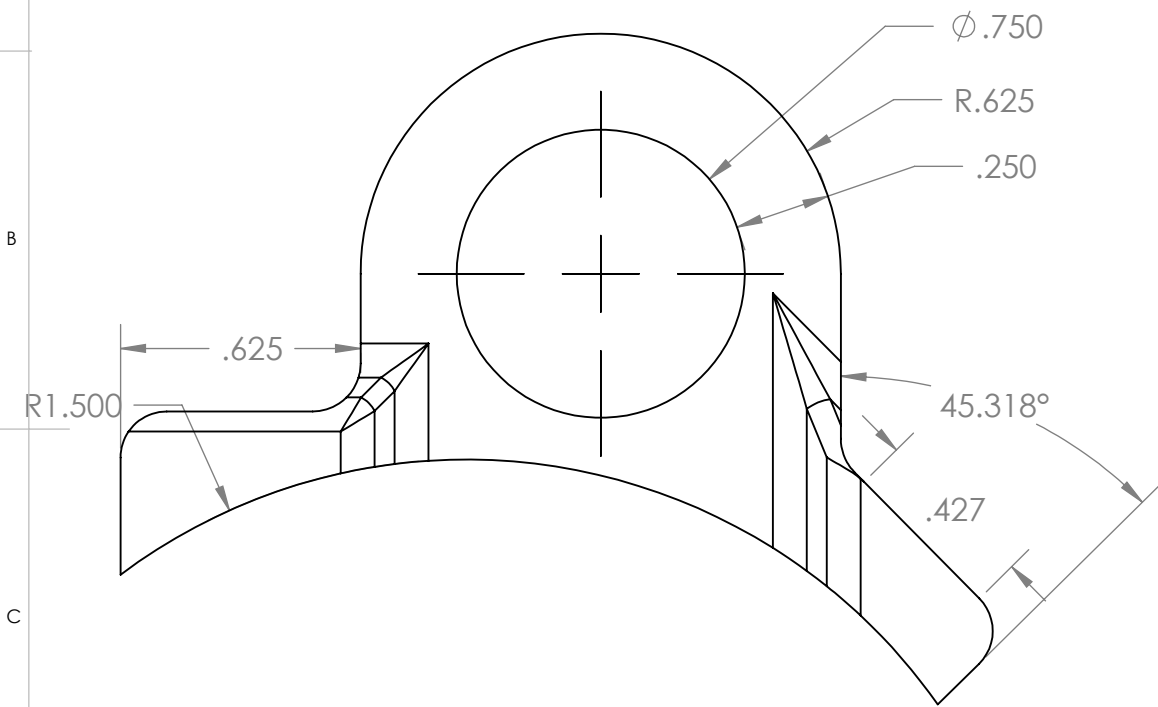
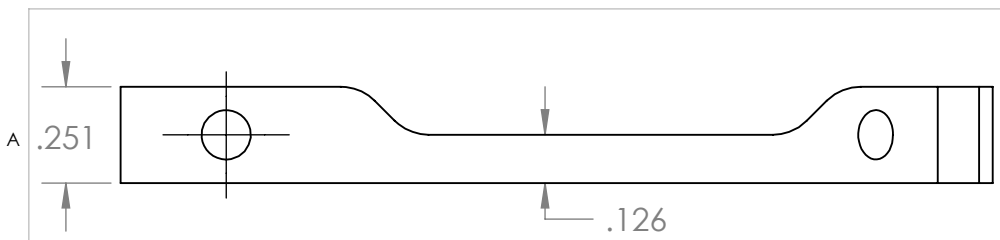
DEBUR AND  
BREAK SHARP  
EDGES

MATERIAL:  
ABS Plastic

NAME	SIGNATURE	DATE
DRAWN Chris Egan		4/28/09

DO NOT SCALE DRAWING	REVISION
TITLE: <h1>Valve Pin</h1>	
Part Name	slot bar
	A4
SCALE:4:1	SHEET 1 OF 1

1 2



Length of sides is not important as long as they match the holes on the pipe.

DO NOT SCALE DRAWING	REVISION
TITLE: <b>Transducer Stand</b>	
Part Name	<b>stand</b>
	A4
SCALE:2:1	SHEET 1 OF 1



UNLESS OTHERWISE SPECIFIED:  
 DIMENSIONS ARE IN INCHES  
 SURFACE FINISH:  
 TOLERANCES:  
 LINEAR:  
 ANGULAR:  
 MATERIAL: ABS Plastic

NAME	SIGNATURE	DATE
DRAWN Chris Egan		4/28/09

1

2

3

4

5

6

A

A

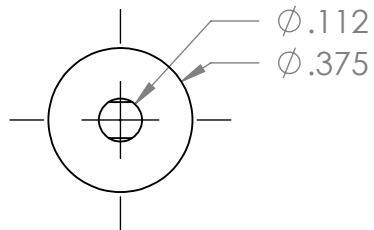
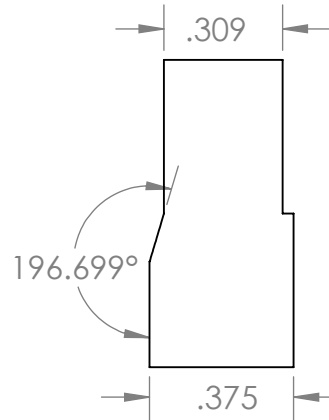
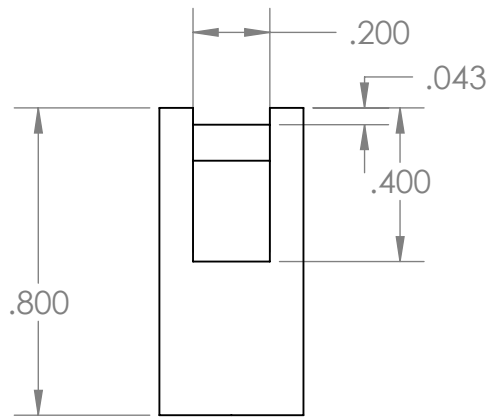
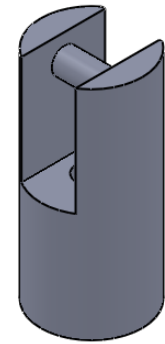
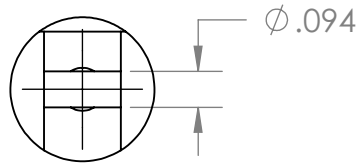
B

B

C

C

D



**WPI**

UNLESS OTHERWISE SPECIFIED:  
DIMENSIONS ARE IN INCHES  
SURFACE FINISH:  
TOLERANCES:  
LINEAR:  
ANGULAR:

DEBUR AND  
BREAK SHARP  
EDGES

MATERIAL:

Aluminum 6061

	NAME	SIGNATURE	DATE
DRAWN	Chris Egan		4/28/09

DO NOT SCALE DRAWING

REVISION

TITLE:

Transducer Attachment

Part Name

attachment

A4

SCALE:2:1

SHEET 1 OF 1

1

2

## Appendix B: Data

### Ungrounded Tests

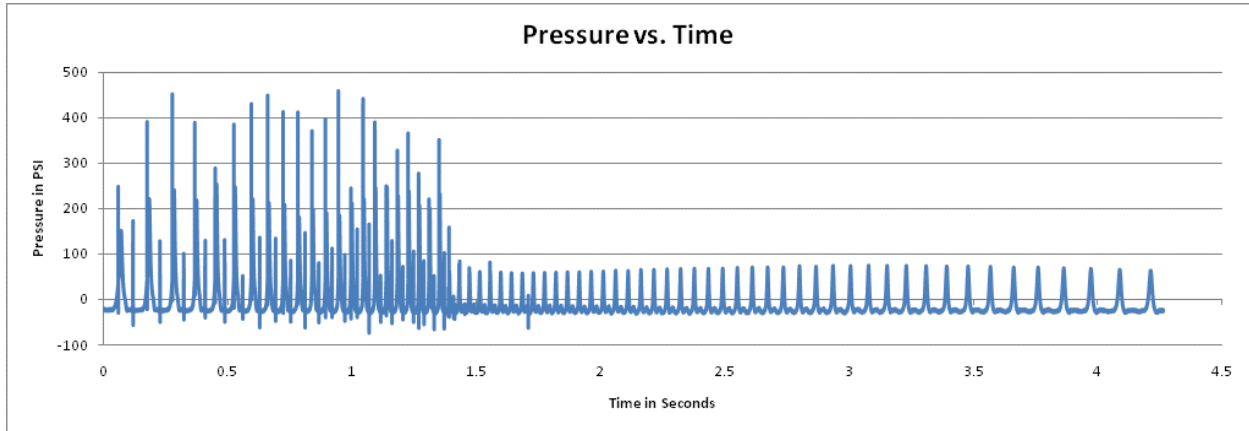


Figure 13-1: Engine Pressure Test 1

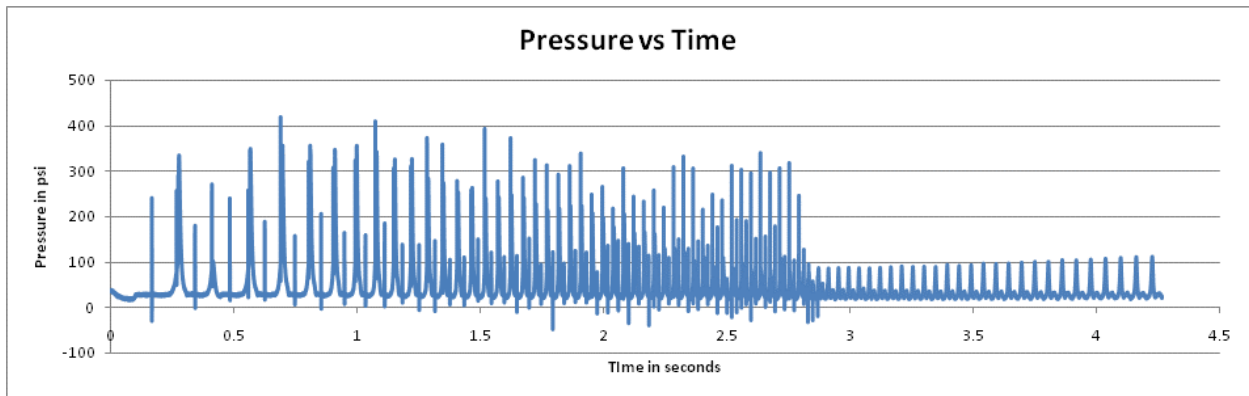


Figure 13-2: Engine Pressure Test 2

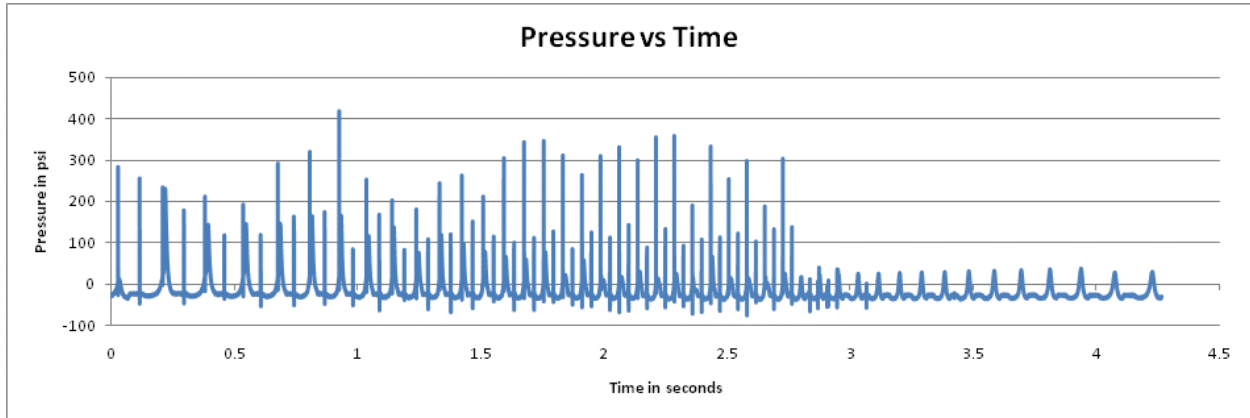


Figure 13-3: Engine Pressure Test 3

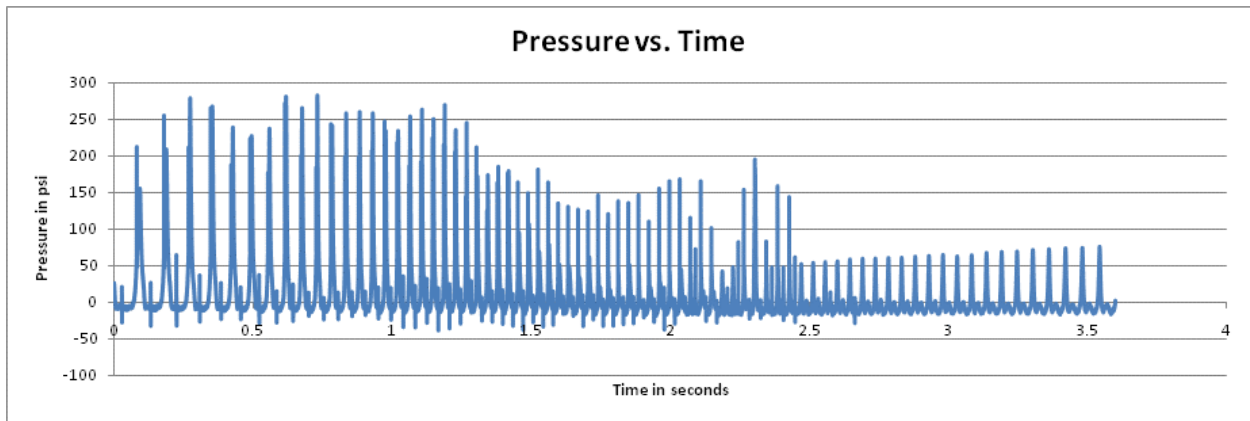


Figure 13-4: Engine Pressure Test 4

### Grounded tests

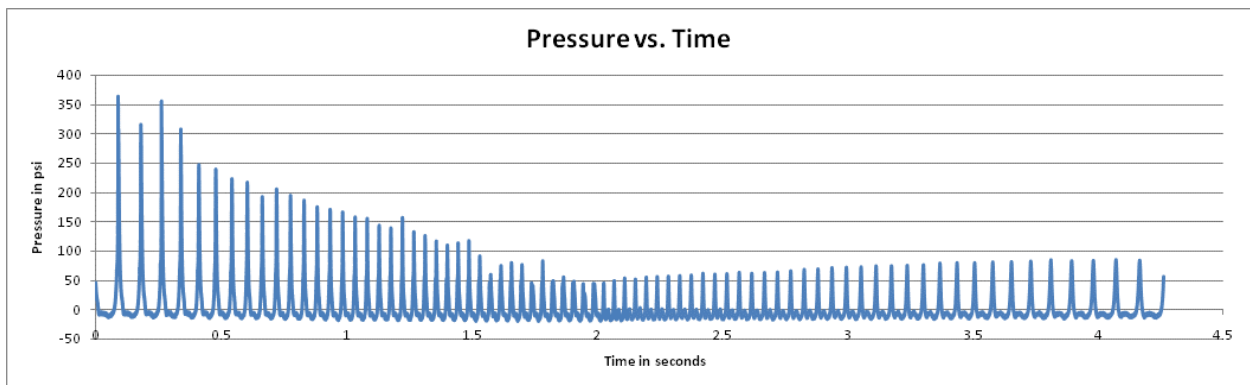


Figure 13-5: Engine Pressure Test 5

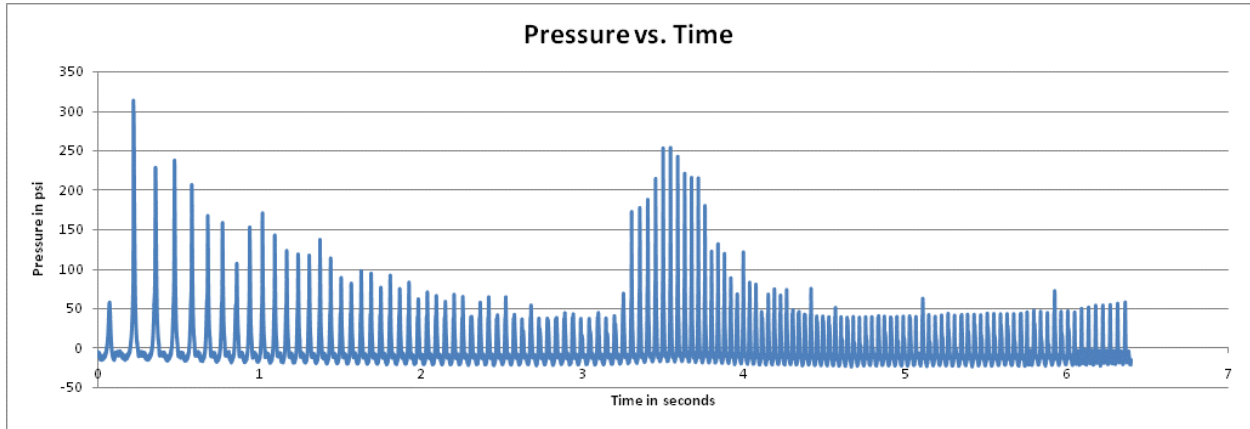


Figure 13-6: Engine Pressure Test 6

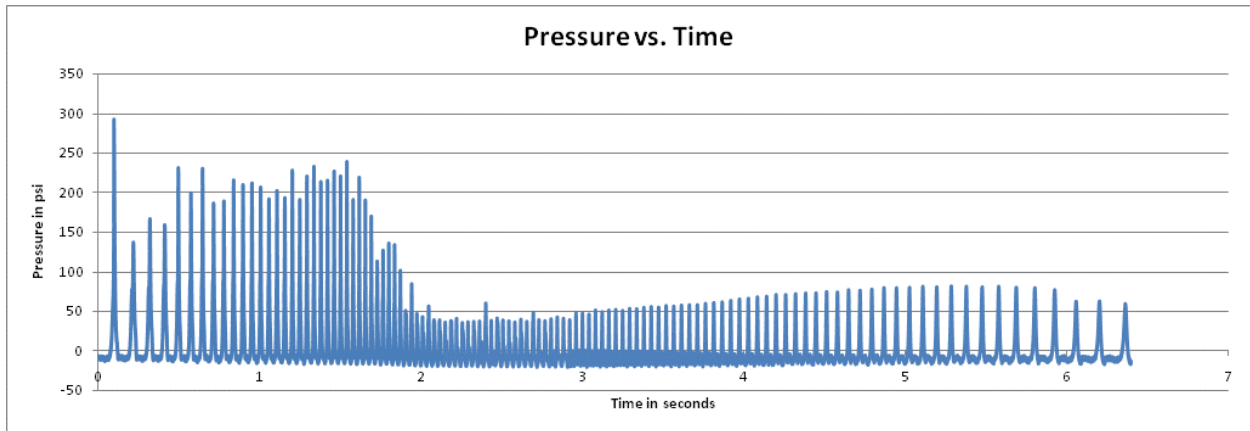


Figure 13-7: Engine Pressure Test 7

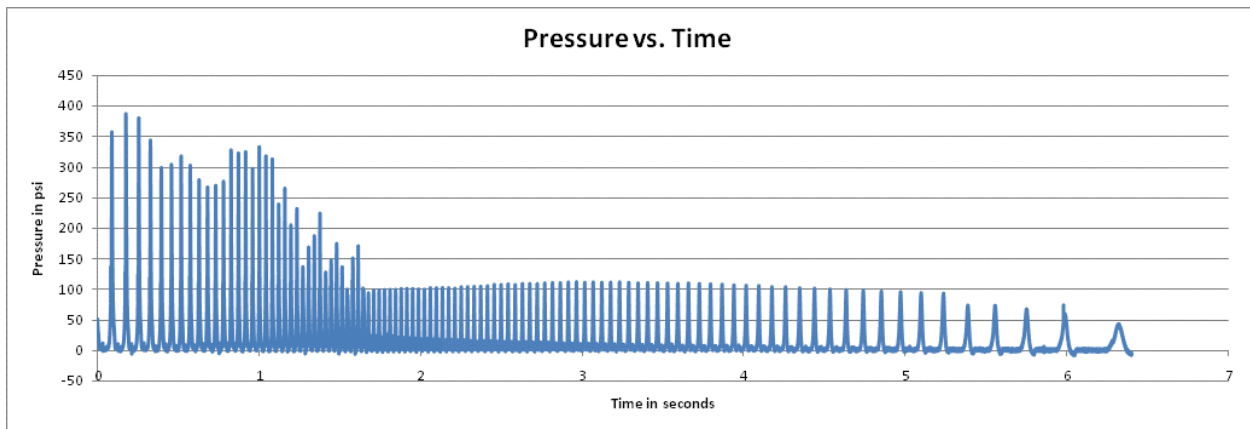


Figure 13-8: Engine Pressure Test 8



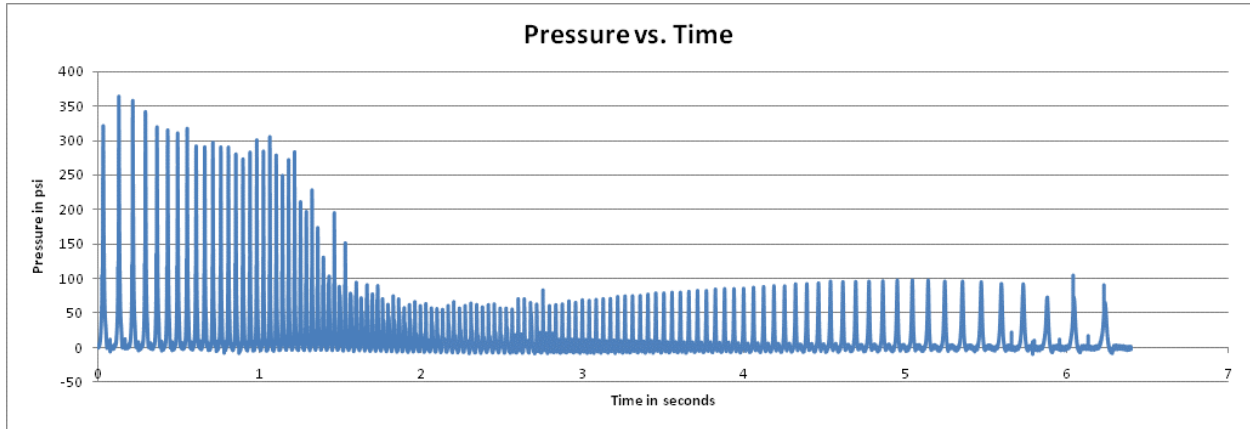


Figure 13-9: Engine Pressure Test 9

### Intake Pressure Tests

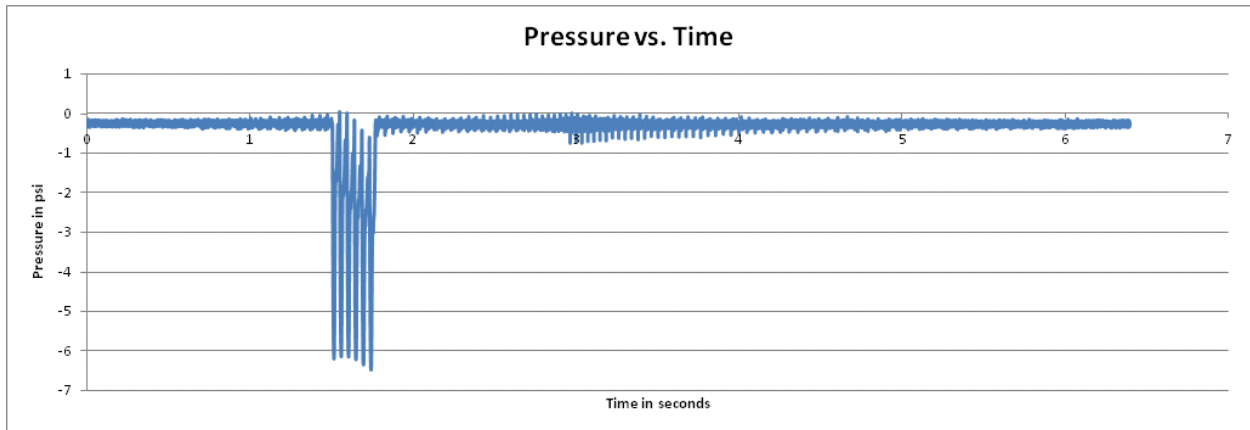


Figure 13-10: Intake Pressure with Short Hydrostatic-Lock Simulation

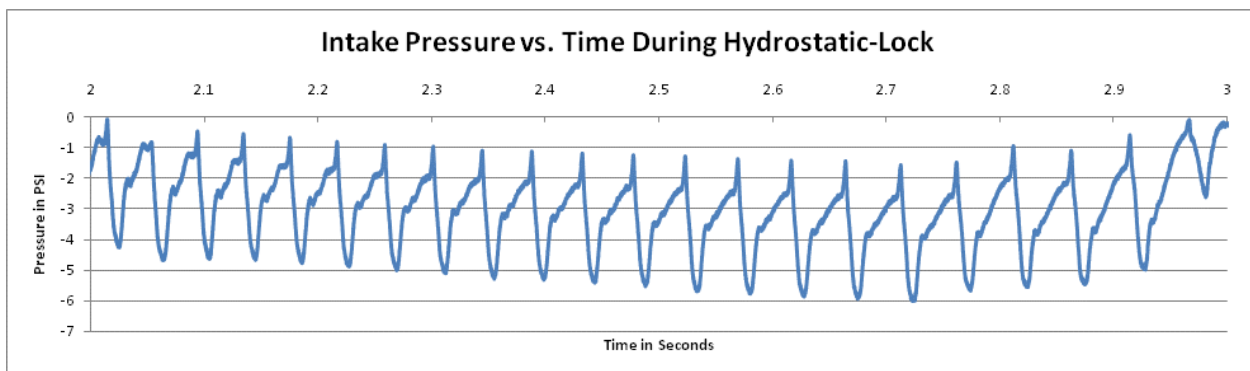


Figure 13-11: Intake Pressure with Full Hydrostatic-Lock Simulation

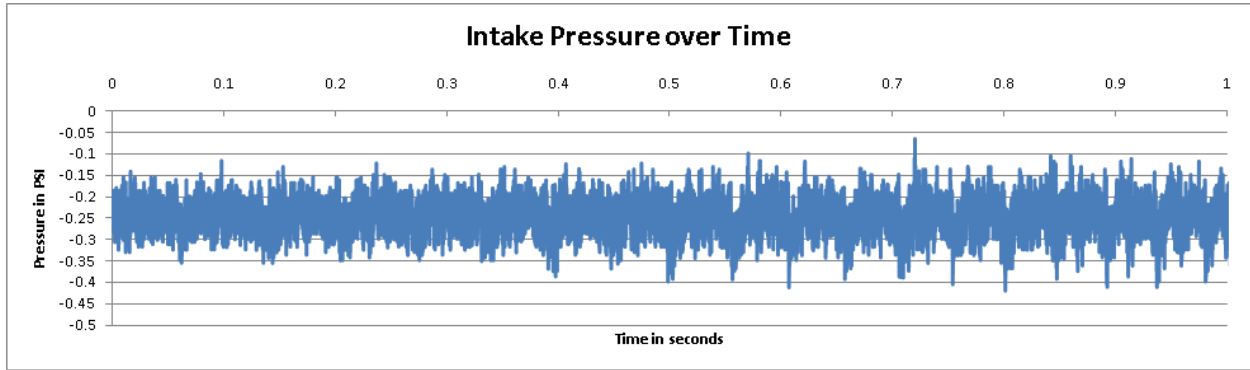


Figure 13-12: Intake Pressure Normal

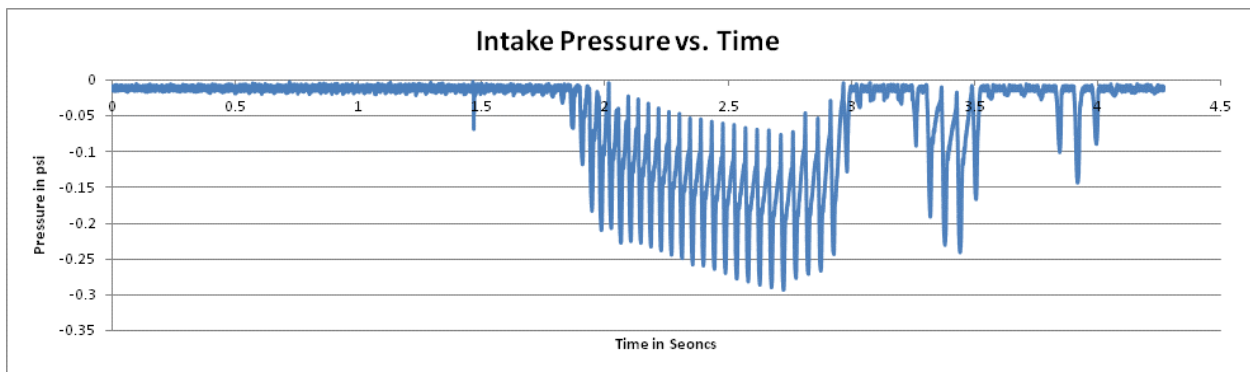


Figure 13-13: Intake Pressure with Hydrostatic-Lock Simulation

# Appendix C: Data Sheets

### FEATURES

#### Easy to use

Gain set with one external resistor  
(Gain range 1 to 10,000)

Wide power supply range ( $\pm 2.3$  V to  $\pm 18$  V)

Higher performance than 3 op amp IA designs

Available in 8-lead DIP and SOIC packaging

Low power, 1.3 mA max supply current

#### Excellent dc performance (B grade)

50  $\mu$ V max, input offset voltage

0.6  $\mu$ V/ $^{\circ}$ C max, input offset drift

1.0 nA max, input bias current

100 dB min common-mode rejection ratio (G = 10)

#### Low noise

9 nV/ $\sqrt{\text{Hz}}$  @ 1 kHz, input voltage noise

0.28  $\mu$ V p-p noise (0.1 Hz to 10 Hz)

#### Excellent ac specifications

120 kHz bandwidth (G = 100)

15  $\mu$ s settling time to 0.01%

### APPLICATIONS

Weigh scales

ECG and medical instrumentation

Transducer interface

Data acquisition systems

Industrial process controls

Battery-powered and portable equipment

### CONNECTION DIAGRAM

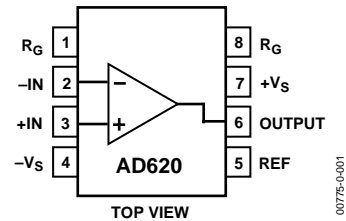


Figure 1. 8-Lead PDIP (N), CERDIP (Q), and SOIC (R) Packages

### PRODUCT DESCRIPTION

The AD620 is a low cost, high accuracy instrumentation amplifier that requires only one external resistor to set gains of 1 to 10,000. Furthermore, the AD620 features 8-lead SOIC and DIP packaging that is smaller than discrete designs and offers lower power (only 1.3 mA max supply current), making it a good fit for battery-powered, portable (or remote) applications.

The AD620, with its high accuracy of 40 ppm maximum nonlinearity, low offset voltage of 50  $\mu$ V max, and offset drift of 0.6  $\mu$ V/ $^{\circ}$ C max, is ideal for use in precision data acquisition systems, such as weigh scales and transducer interfaces. Furthermore, the low noise, low input bias current, and low power of the AD620 make it well suited for medical applications, such as ECG and noninvasive blood pressure monitors.

The low input bias current of 1.0 nA max is made possible with the use of Superbeta processing in the input stage. The AD620 works well as a preamplifier due to its low input voltage noise of 9 nV/ $\sqrt{\text{Hz}}$  at 1 kHz, 0.28  $\mu$ V p-p in the 0.1 Hz to 10 Hz band, and 0.1 pA/ $\sqrt{\text{Hz}}$  input current noise. Also, the AD620 is well suited for multiplexed applications with its settling time of 15  $\mu$ s to 0.01%, and its cost is low enough to enable designs with one in-amp per channel.

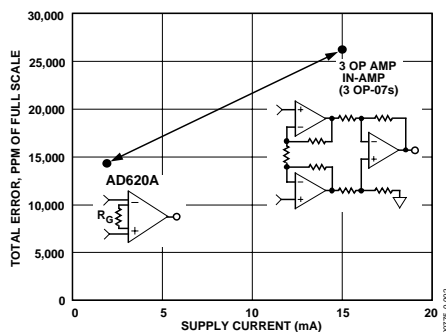


Figure 2. Three Op Amp IA Designs vs. AD620

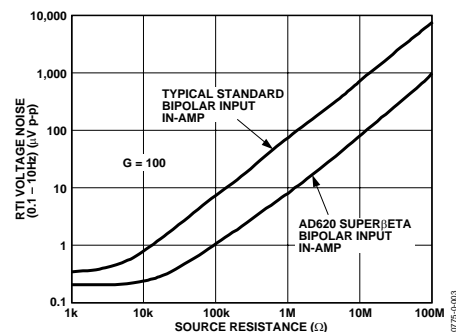


Figure 3. Total Voltage Noise vs. Source Resistance

### Rev. G

Information furnished by Analog Devices is believed to be accurate and reliable. However, no responsibility is assumed by Analog Devices for its use, nor for any infringements of patents or other rights of third parties that may result from its use. Specifications subject to change without notice. No license is granted by implication or otherwise under any patent or patent rights of Analog Devices. Trademarks and registered trademarks are the property of their respective owners.

## TABLE OF CONTENTS

Specifications .....	3	Input Protection .....	16
Absolute Maximum Ratings .....	5	RF Interference .....	16
ESD Caution .....	5	Common-Mode Rejection.....	17
Typical Performance Characteristics .....	7	Grounding.....	17
Theory of Operation .....	13	Ground Returns for Input Bias Currents.....	18
Gain Selection.....	16	Outline Dimensions.....	19
Input and Output Offset Voltage .....	16	Ordering Guide .....	20
Reference Terminal .....	16		

## REVISION HISTORY

### 12/04—Rev. F to Rev. G

Updated Format.....	Universal
Change to Features.....	1
Change to Product Description.....	1
Changes to Specifications.....	3
Added Metallization Photograph.....	4
Replaced Figure 4-Figure 6 .....	6
Replaced Figure 15 .....	7
Replaced Figure 33 .....	10
Replaced Figure 34 and Figure 35 .....	10
Replaced Figure 37 .....	10
Changes to Table 3 .....	13
Changes to Figure 41 and Figure 42 .....	14
Changes to Figure 43 .....	15
Change to Figure 44.....	17
Changes to Input Protection section .....	15
Deleted Figure 9.....	15
Changes to RF Interference section .....	15
Edit to Ground Returns for Input Bias Currents section.....	17
Added AD620CHIPS to Ordering Guide .....	19

### 7/03—Data Sheet changed from REV. E to REV. F

Edit to FEATURES.....	1
Changes to SPECIFICATIONS .....	2
Removed AD620CHIPS from ORDERING GUIDE .....	4
Removed METALLIZATION PHOTOGRAPH.....	4
Replaced TPCs 1–3 .....	5
Replaced TPC 12 .....	6
Replaced TPC 30 .....	9
Replaced TPCs 31 and 32.....	10
Replaced Figure 4.....	10
Changes to Table I.....	11
Changes to Figures 6 and 7 .....	12
Changes to Figure 8 .....	13
Edited INPUT PROTECTION section.....	13
Added new Figure 9.....	13
Changes to RF INTERFACE section .....	14
Edit to GROUND RETURNS FOR INPUT BIAS CURRENTS section.....	15
Updated OUTLINE DIMENSIONS.....	16

# SPECIFICATIONS

Typical @ 25°C,  $V_S = \pm 15$  V, and  $R_L = 2$  k $\Omega$ , unless otherwise noted.

Table 1.

Parameter	Conditions	AD620A			AD620B			AD620S <sup>1</sup>			Unit
		Min	Typ	Max	Min	Typ	Max	Min	Typ	Max	
GAIN	$G = 1 + (49.4 \text{ k}\Omega/R_G)$										
Gain Range		1		10,000	1		10,000	1		10,000	
Gain Error <sup>2</sup>	$V_{OUT} = \pm 10$ V										
G = 1			0.03	0.10		0.01	0.02		0.03	0.10	%
G = 10			0.15	0.30		0.10	0.15		0.15	0.30	%
G = 100			0.15	0.30		0.10	0.15		0.15	0.30	%
G = 1000			0.40	0.70		0.35	0.50		0.40	0.70	%
Nonlinearity	$V_{OUT} = -10$ V to $+10$ V										
G = 1–1000	$R_L = 10$ k $\Omega$		10	40		10	40		10	40	ppm
G = 1–100	$R_L = 2$ k $\Omega$		10	95		10	95		10	95	ppm
Gain vs. Temperature	G = 1			10			10			10	ppm/°C
	Gain > 1 <sup>2</sup>			–50			–50			–50	ppm/°C
VOLTAGE OFFSET	(Total RTI Error = $V_{OSI} + V_{OSO}/G$ )										
Input Offset, $V_{OSI}$	$V_S = \pm 5$ V to $\pm 15$ V		30	125		15	50		30	125	$\mu$ V
Overtemperature	$V_S = \pm 5$ V to $\pm 15$ V			185			85			225	$\mu$ V
Average TC	$V_S = \pm 5$ V to $\pm 15$ V		0.3	1.0		0.1	0.6		0.3	1.0	$\mu$ V/°C
Output Offset, $V_{OSO}$	$V_S = \pm 15$ V		400	1000		200	500		400	1000	$\mu$ V
	$V_S = \pm 5$ V			1500			750			1500	$\mu$ V
Overtemperature	$V_S = \pm 5$ V to $\pm 15$ V			2000			1000			2000	$\mu$ V
Average TC	$V_S = \pm 5$ V to $\pm 15$ V		5.0	15		2.5	7.0		5.0	15	$\mu$ V/°C
Offset Referred to the Input vs. Supply (PSR)	$V_S = \pm 2.3$ V to $\pm 18$ V										
G = 1		80	100		80	100		80	100		dB
G = 10		95	120		100	120		95	120		dB
G = 100		110	140		120	140		110	140		dB
G = 1000		110	140		120	140		110	140		dB
INPUT CURRENT											
Input Bias Current			0.5	2.0		0.5	1.0		0.5	2	nA
Overtemperature				2.5			1.5			4	nA
Average TC			3.0			3.0			8.0		pA/°C
Input Offset Current			0.3	1.0		0.3	0.5		0.3	1.0	nA
Overtemperature				1.5			0.75			2.0	nA
Average TC			1.5			1.5			8.0		pA/°C
INPUT											
Input Impedance											
Differential			10  2			10  2			10  2		G $\Omega$ _pF
Common-Mode			10  2			10  2			10  2		G $\Omega$ _pF
Input Voltage Range <sup>3</sup>	$V_S = \pm 2.3$ V to $\pm 5$ V	$-V_S + 1.9$		$+V_S - 1.2$	$-V_S + 1.9$		$+V_S - 1.2$	$-V_S + 1.9$		$+V_S - 1.2$	V
Overtemperature	$V_S = \pm 5$ V to $\pm 18$ V	$-V_S + 2.1$		$+V_S - 1.3$	$-V_S + 2.1$		$+V_S - 1.3$	$-V_S + 2.1$		$+V_S - 1.3$	V
		$-V_S + 1.9$		$+V_S - 1.4$	$-V_S + 1.9$		$+V_S - 1.4$	$-V_S + 1.9$		$+V_S - 1.4$	V
Overtemperature		$-V_S + 2.1$		$+V_S - 1.4$	$-V_S + 2.1$		$+V_S + 2.1$	$-V_S + 2.3$		$+V_S - 1.4$	V

# AD620

Parameter	Conditions	AD620A			AD620B			AD620S <sup>1</sup>			Unit
		Min	Typ	Max	Min	Typ	Max	Min	Typ	Max	
Common-Mode Rejection											
Ratio DC to 60 Hz with 1 k $\Omega$ Source Imbalance	$V_{CM} = 0\text{ V to } \pm 10\text{ V}$										
G = 1		73	90		80	90		73	90		dB
G = 10		93	110		100	110		93	110		dB
G = 100		110	130		120	130		110	130		dB
G = 1000		110	130		120	130		110	130		dB
OUTPUT											
Output Swing	$R_L = 10\text{ k}\Omega$ $V_S = \pm 2.3\text{ V}$ to $\pm 5\text{ V}$	$-V_S + 1.1$	$+V_S - 1.2$		$-V_S + 1.1$	$+V_S - 1.2$		$-V_S + 1.1$	$+V_S - 1.2$		V
Overtemperature		$-V_S + 1.4$	$+V_S - 1.3$		$-V_S + 1.4$	$+V_S - 1.3$		$-V_S + 1.6$	$+V_S - 1.3$		V
Overtemperature	$V_S = \pm 5\text{ V}$ to $\pm 18\text{ V}$	$-V_S + 1.2$	$+V_S - 1.4$		$-V_S + 1.2$	$+V_S - 1.4$		$-V_S + 1.2$	$+V_S - 1.4$		V
Short Circuit Current		$-V_S + 1.6$	$+V_S - 1.5$		$-V_S + 1.6$	$+V_S - 1.5$		$-V_S + 2.3$	$+V_S - 1.5$		V
		$\pm 18$			$\pm 18$			$\pm 18$			mA
DYNAMIC RESPONSE											
Small Signal -3 dB Bandwidth	10 V Step										
G = 1		1000			1000			1000			kHz
G = 10		800			800			800			kHz
G = 100		120			120			120			kHz
G = 1000		12			12			12			kHz
Slew Rate		0.75	1.2		0.75	1.2		0.75	1.2		V/ $\mu$ s
Settling Time to 0.01%											
G = 1-100		15			15			15			$\mu$ s
G = 1000		150			150			150			$\mu$ s
NOISE											
Voltage Noise, 1 kHz	$Total\ RTI\ Noise = \sqrt{(e_{ni}^2) + (e_{no}/G)^2}$										
Input, Voltage Noise, $e_{ni}$		9	13		9	13		9	13		nV/ $\sqrt{\text{Hz}}$
Output, Voltage Noise, $e_{no}$		72	100		72	100		72	100		nV/ $\sqrt{\text{Hz}}$
RTI, 0.1 Hz to 10 Hz	$f = 1\text{ kHz}$										
G = 1		3.0			3.0 6.0			3.0 6.0			$\mu$ V p-p
G = 10		0.55			0.55 0.8			0.55 0.8			$\mu$ V p-p
G = 100-1000		0.28			0.28 0.4			0.28 0.4			$\mu$ V p-p
Current Noise		100			100			100			fA/ $\sqrt{\text{Hz}}$
0.1 Hz to 10 Hz		10			10			10			pA p-p
REFERENCE INPUT											
$R_{IN}$	$V_{IN+}, V_{REF} = 0$	20			20			20			k $\Omega$
$I_{IN}$		50	60		50	60		50	60		$\mu$ A
Voltage Range		$-V_S + 1.6$	$+V_S - 1.6$		$-V_S + 1.6$	$+V_S - 1.6$		$-V_S + 1.6$	$+V_S - 1.6$		V
Gain to Output		$1 \pm 0.0001$			$1 \pm 0.0001$			$1 \pm 0.0001$			
POWER SUPPLY											
Operating Range <sup>4</sup>	$V_S = \pm 2.3\text{ V}$ to $\pm 18\text{ V}$	$\pm 2.3$	$\pm 18$		$\pm 2.3$	$\pm 18$		$\pm 2.3$	$\pm 18$		V
Quiescent Current		0.9	1.3		0.9	1.3		0.9	1.3		mA
Overtemperature		1.1	1.6		1.1	1.6		1.1	1.6		mA
TEMPERATURE RANGE											
For Specified Performance		$-40\text{ to }+85$			$-40\text{ to }+85$			$-55\text{ to }+125$			$^{\circ}\text{C}$

<sup>1</sup> See Analog Devices military data sheet for 883B tested specifications.

<sup>2</sup> Does not include effects of external resistor  $R_G$ .

<sup>3</sup> One input grounded.  $G = 1$ .

<sup>4</sup> This is defined as the same supply range that is used to specify PSR.

## ABSOLUTE MAXIMUM RATINGS

Table 2.

Parameter	Rating
Supply Voltage	$\pm 18$ V
Internal Power Dissipation <sup>1</sup>	650 mW
Input Voltage (Common-Mode)	$\pm V_S$
Differential Input Voltage	25 V
Output Short-Circuit Duration	Indefinite
Storage Temperature Range (Q)	-65°C to +150°C
Storage Temperature Range (N, R)	-65°C to +125°C
Operating Temperature Range	
AD620 (A, B)	-40°C to +85°C
AD620 (S)	-55°C to +125°C
Lead Temperature Range (Soldering 10 seconds)	300°C

Stresses above those listed under Absolute Maximum Ratings may cause permanent damage to the device. This is a stress rating only; functional operation of the device at these or any other conditions above those indicated in the operational section of this specification is not implied. Exposure to absolute maximum rating conditions for extended periods may affect device reliability.

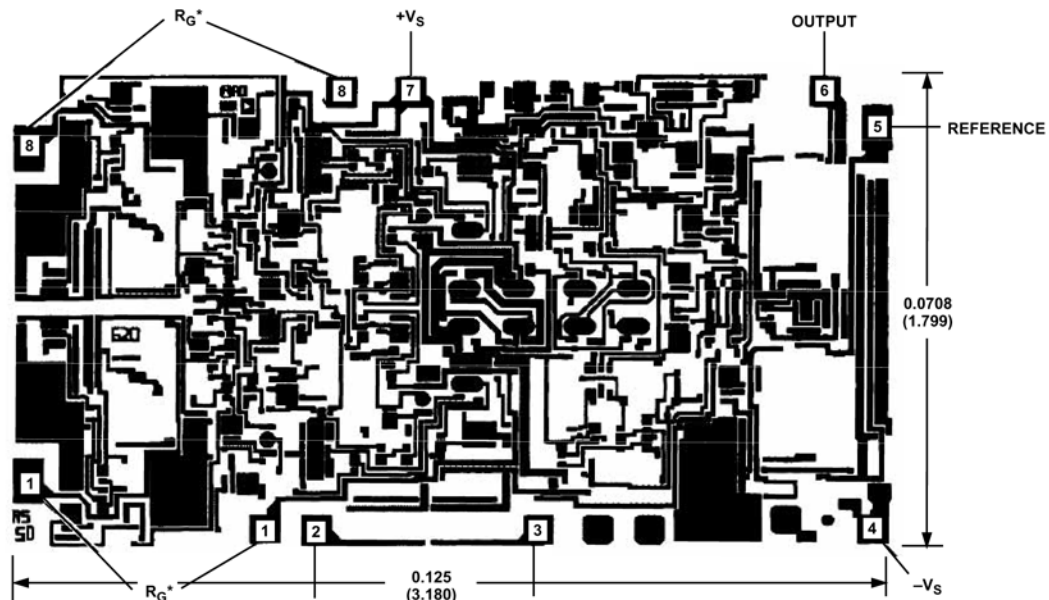
<sup>1</sup> Specification is for device in free air:  
 8-Lead Plastic Package:  $\theta_{JA} = 95^\circ\text{C}$   
 8-Lead CERDIP Package:  $\theta_{JA} = 110^\circ\text{C}$   
 8-Lead SOIC Package:  $\theta_{JA} = 155^\circ\text{C}$

### ESD CAUTION

ESD (electrostatic discharge) sensitive device. Electrostatic charges as high as 4000 V readily accumulate on the human body and test equipment and can discharge without detection. Although this product features proprietary ESD protection circuitry, permanent damage may occur on devices subjected to high energy electrostatic discharges. Therefore, proper ESD precautions are recommended to avoid performance degradation or loss of functionality.







\*FOR CHIP APPLICATIONS: THE PADS 1 $R_G$  AND 8 $R_G$  MUST BE CONNECTED IN PARALLEL TO THE EXTERNAL GAIN REGISTER  $R_G$ . DO NOT CONNECT THEM IN SERIES TO  $R_G$ . FOR UNITY GAIN APPLICATIONS WHERE  $R_G$  IS NOT REQUIRED, THE PADS 1 $R_G$  MAY SIMPLY BE BONDED TOGETHER, AS WELL AS THE PADS 8 $R_G$ .

00775-0-004

Figure 4. Metallization Photograph.  
Dimensions shown in inches and (mm).

Contact sales for latest dimensions.

# TYPICAL PERFORMANCE CHARACTERISTICS

(@ 25°C,  $V_s = \pm 15\text{ V}$ ,  $R_L = 2\text{ k}\Omega$ , unless otherwise noted.)

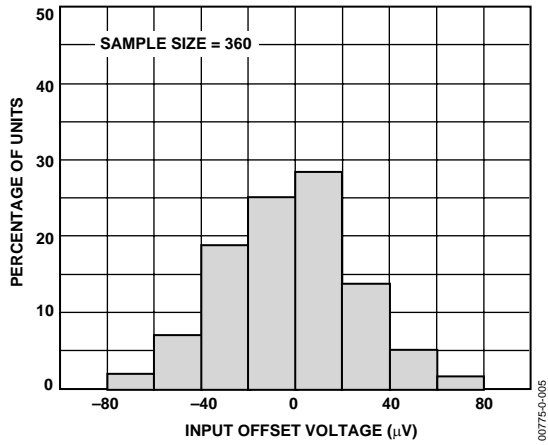


Figure 5. Typical Distribution of Input Offset Voltage

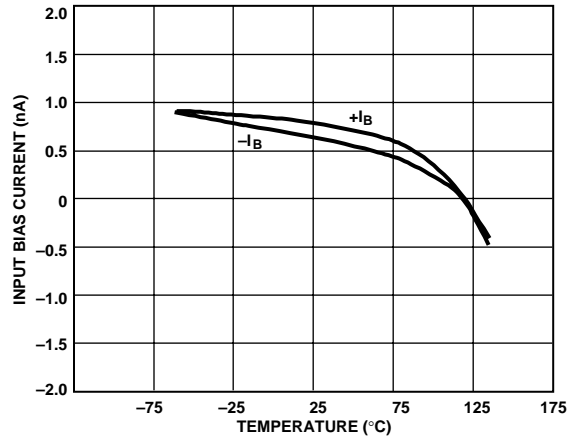


Figure 8. Input Bias Current vs. Temperature

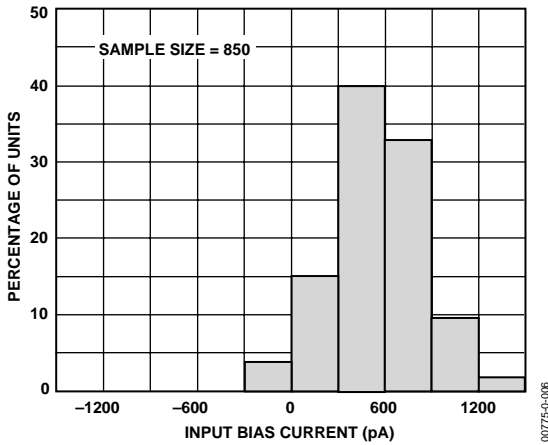


Figure 6. Typical Distribution of Input Bias Current

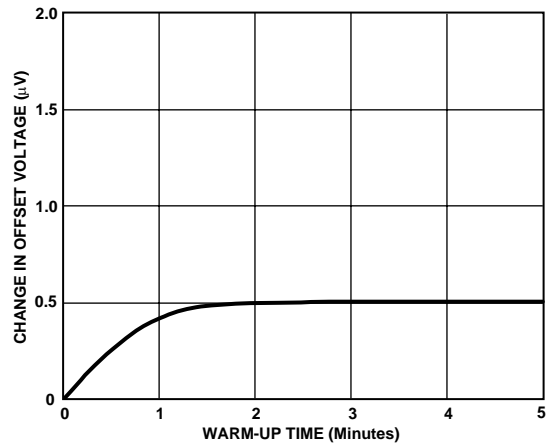


Figure 9. Change in Input Offset Voltage vs. Warm-Up Time

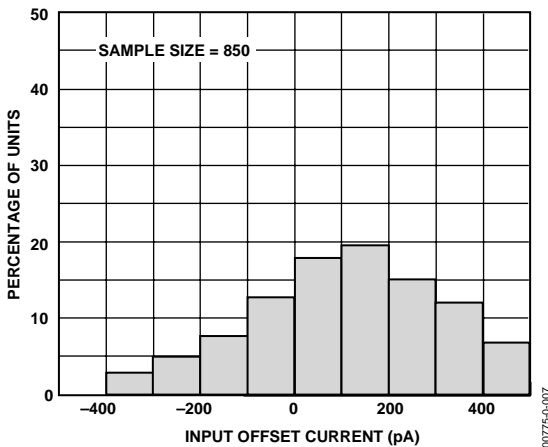


Figure 7. Typical Distribution of Input Offset Current

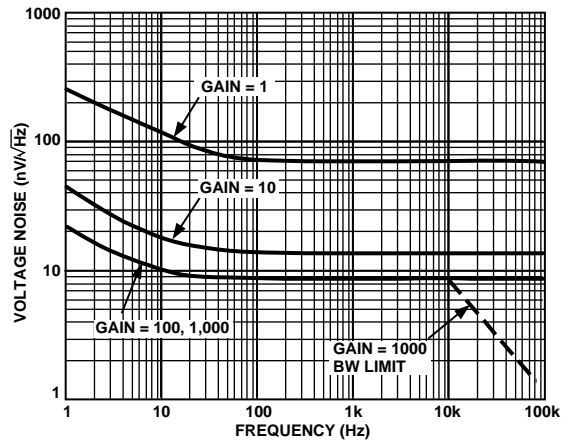


Figure 10. Voltage Noise Spectral Density vs. Frequency ( $G = 1-1000$ )

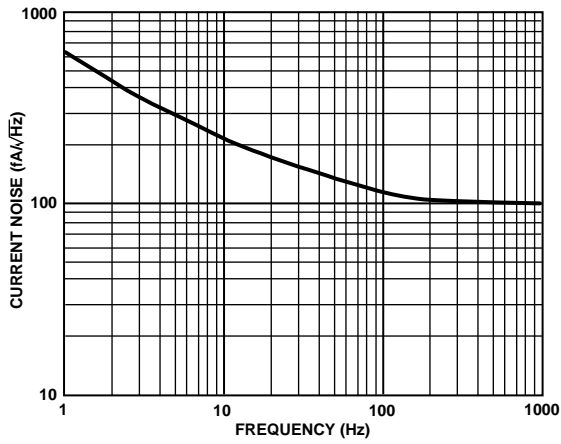


Figure 11. Current Noise Spectral Density vs. Frequency

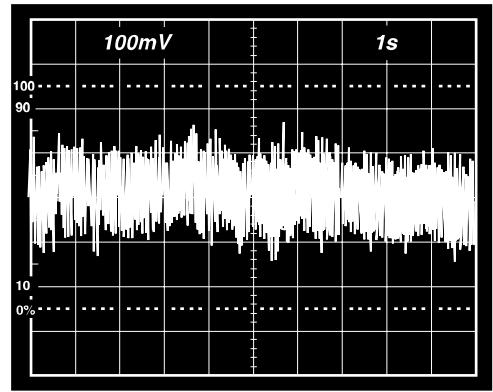


Figure 14. 0.1 Hz to 10 Hz Current Noise, 5 pA/Div

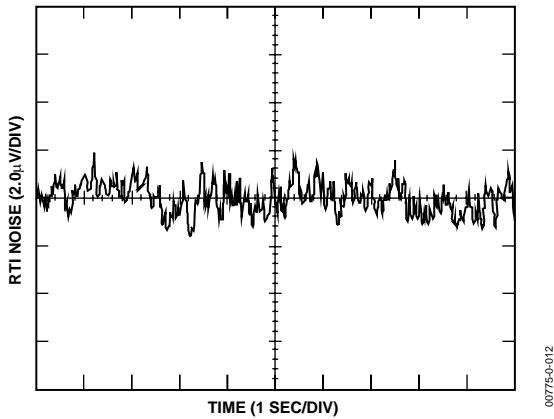


Figure 12. 0.1 Hz to 10 Hz RTI Voltage Noise ( $G = 1$ )

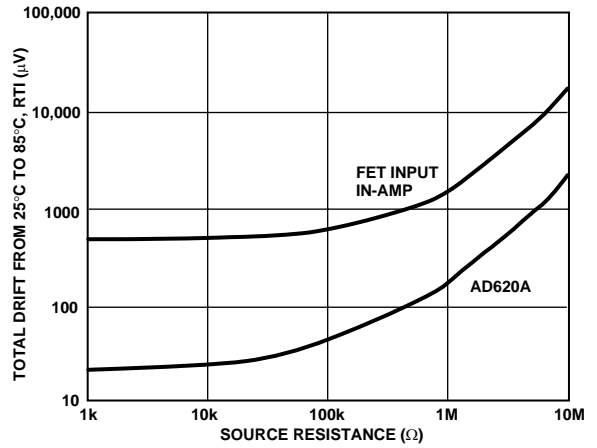


Figure 15. Total Drift vs. Source Resistance

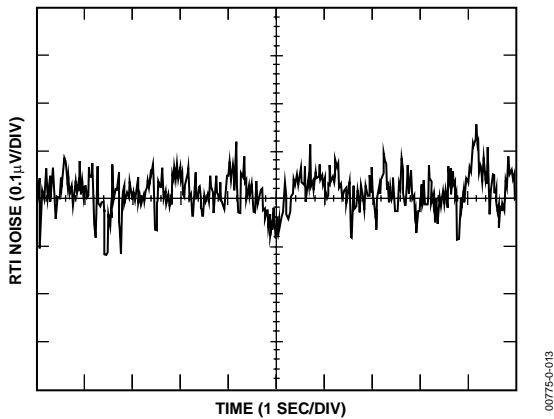


Figure 13. 0.1 Hz to 10 Hz RTI Voltage Noise ( $G = 1000$ )

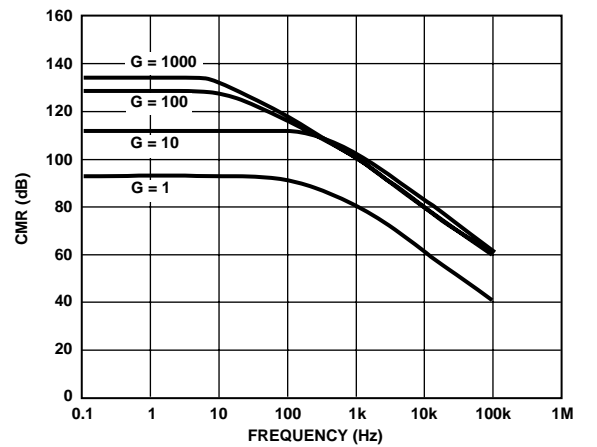


Figure 16. Typical CMR vs. Frequency, RTI, Zero to 1 kΩ Source Imbalance

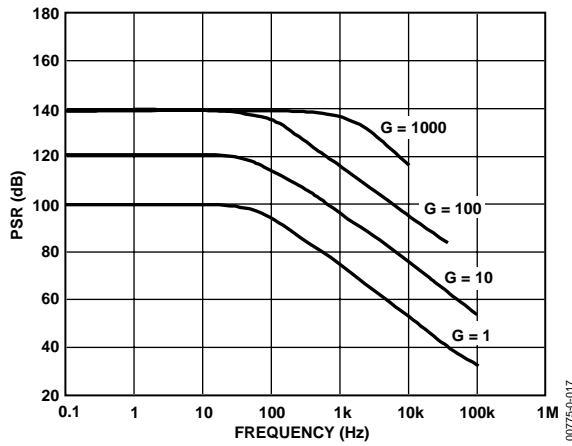


Figure 17. Positive PSR vs. Frequency, RTI (G = 1–1000)

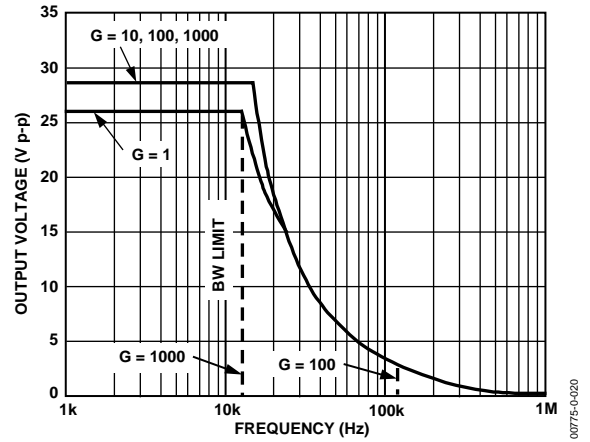


Figure 20. Large Signal Frequency Response

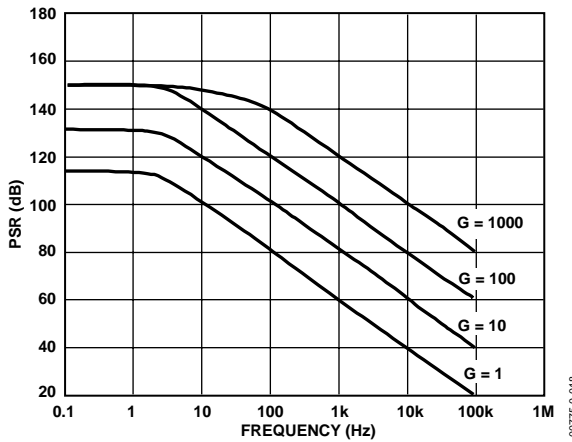


Figure 18. Negative PSR vs. Frequency, RTI (G = 1–1000)

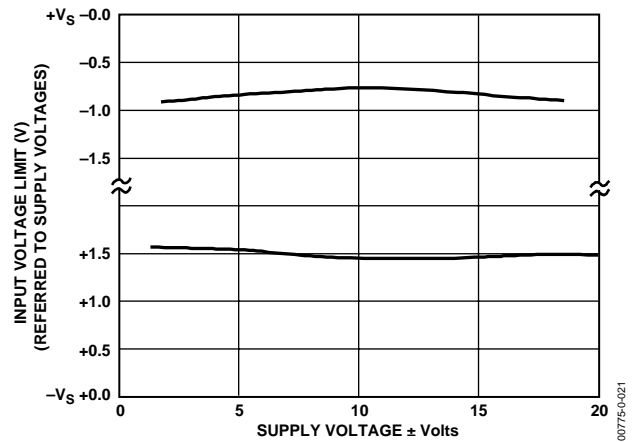


Figure 21. Input Voltage Range vs. Supply Voltage, G = 1

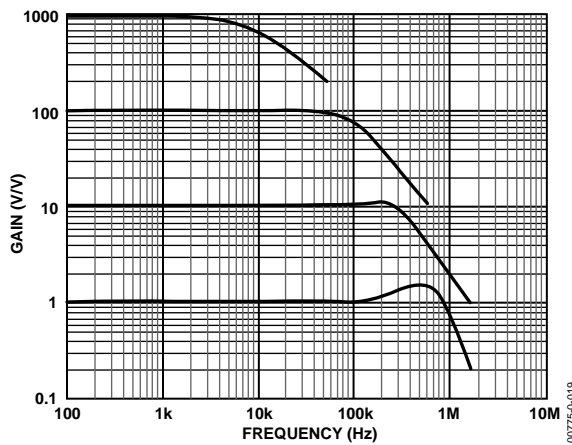


Figure 19. Gain vs. Frequency

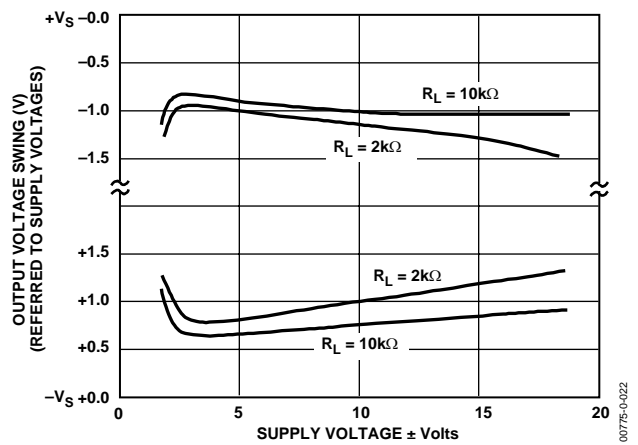


Figure 22. Output Voltage Swing vs. Supply Voltage, G = 10

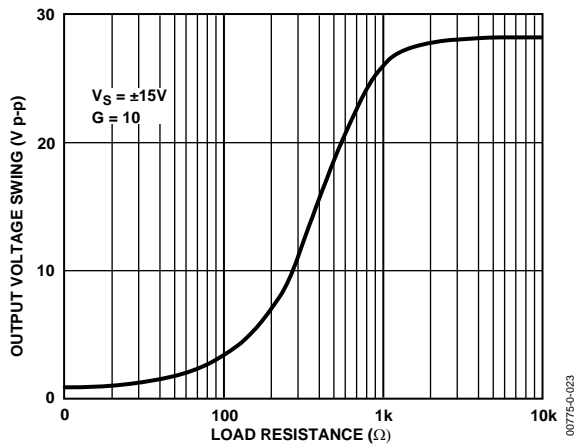


Figure 23. Output Voltage Swing vs. Load Resistance

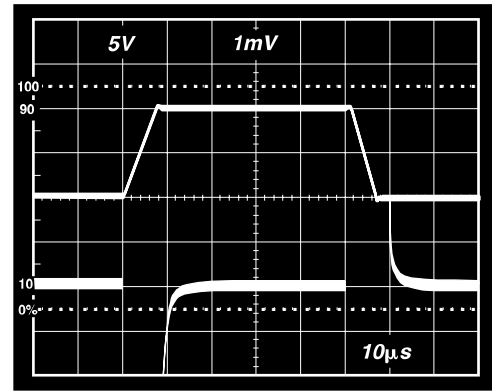


Figure 26. Large Signal Response and Settling Time,  $G = 10$  ( $0.5 \text{ mV} = 0.01\%$ )

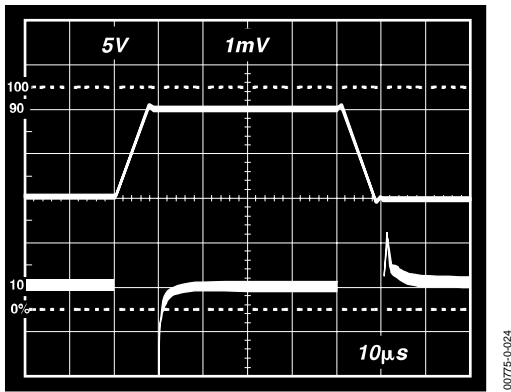


Figure 24. Large Signal Pulse Response and Settling Time  
 $G = 1$  ( $0.5 \text{ mV} = 0.01\%$ )

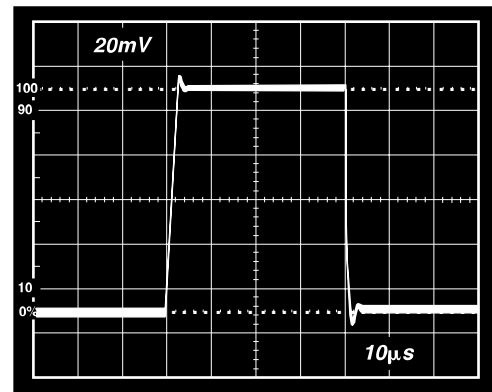


Figure 27. Small Signal Response,  $G = 10$ ,  $R_L = 2 \text{ k}\Omega$ ,  $C_L = 100 \text{ pF}$

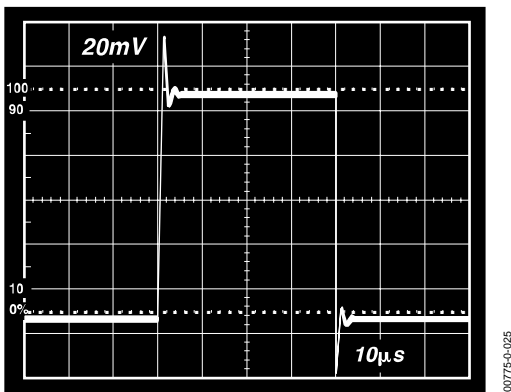


Figure 25. Small Signal Response,  $G = 1$ ,  $R_L = 2 \text{ k}\Omega$ ,  $C_L = 100 \text{ pF}$

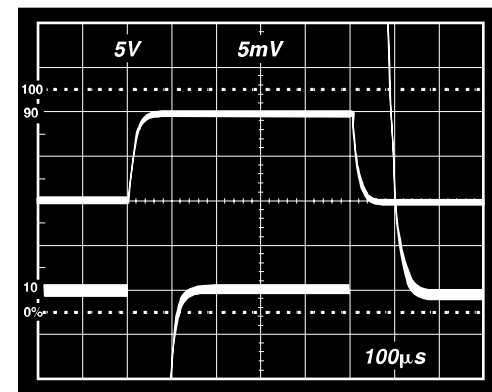


Figure 28. Large Signal Response and Settling Time,  $G = 100$  ( $0.5 \text{ mV} = 0.01\%$ )

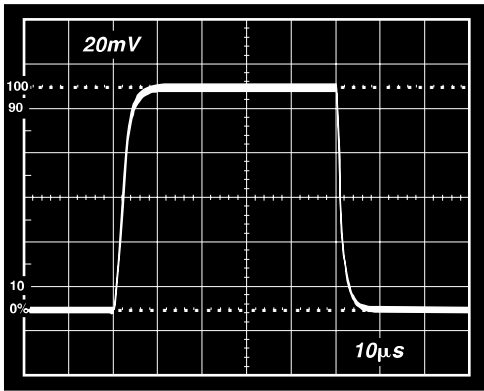


Figure 29. Small Signal Pulse Response,  $G = 100$ ,  $R_L = 2\text{ k}\Omega$ ,  $C_L = 100\text{ pF}$

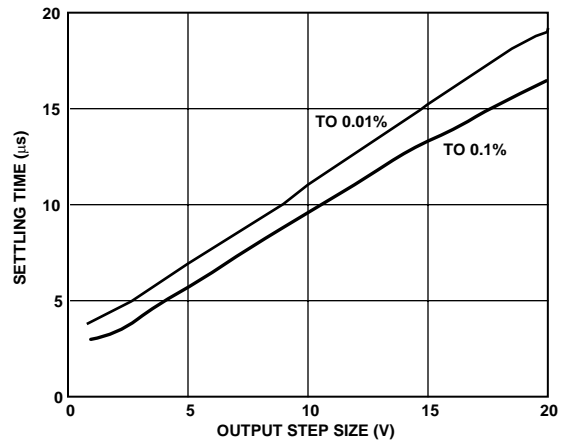


Figure 32. Settling Time vs. Step Size ( $G = 1$ )

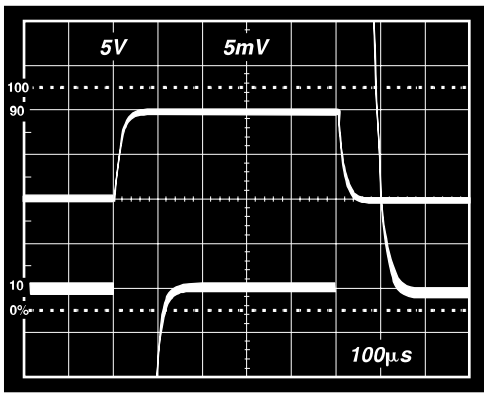


Figure 30. Large Signal Response and Settling Time,  $G = 1000$  ( $0.5\text{ mV} = 0.01\%$ )

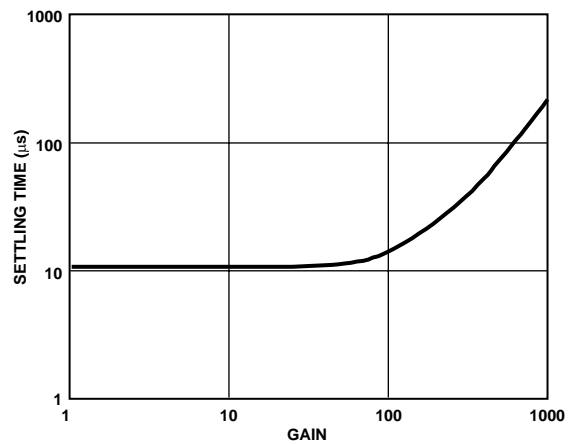


Figure 33. Settling Time to 0.01% vs. Gain, for a 10V Step

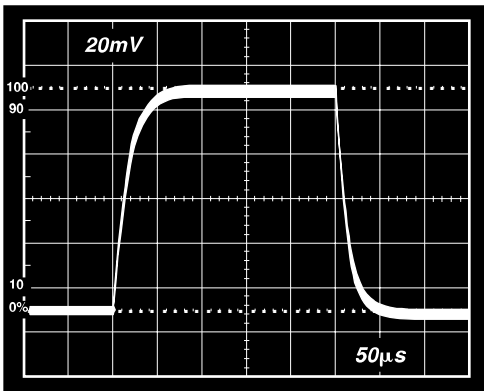


Figure 31. Small Signal Pulse Response,  $G = 1000$ ,  $R_L = 2\text{ k}\Omega$ ,  $C_L = 100\text{ pF}$

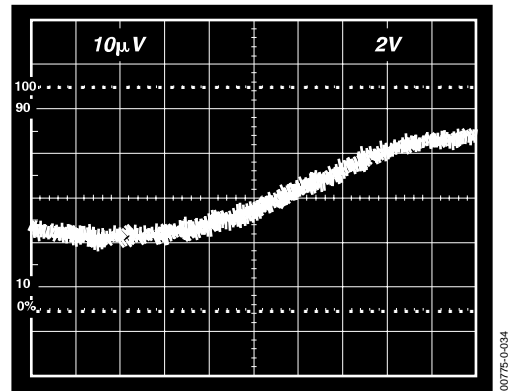
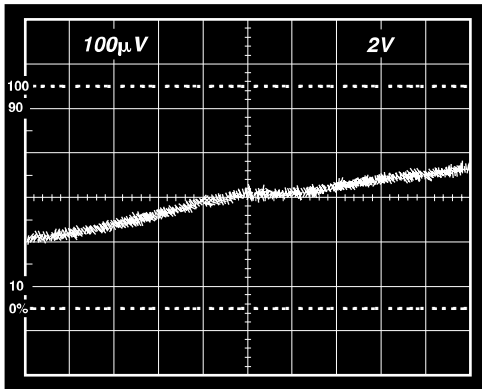


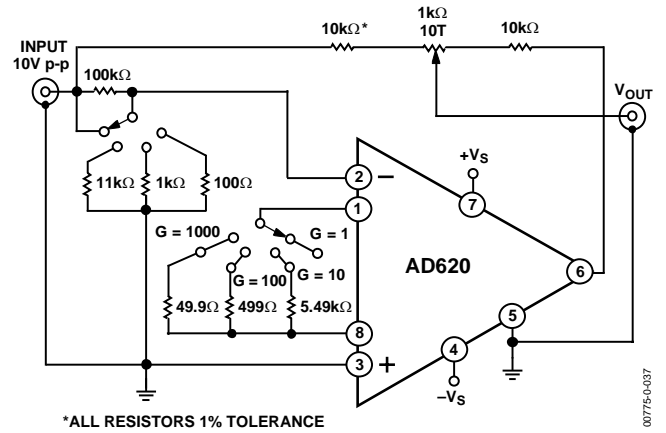
Figure 34. Gain Nonlinearity,  $G = 1$ ,  $R_L = 10\text{ k}\Omega$  ( $10\text{ }\mu\text{V} = 1\text{ ppm}$ )

# AD620



00775-0-035

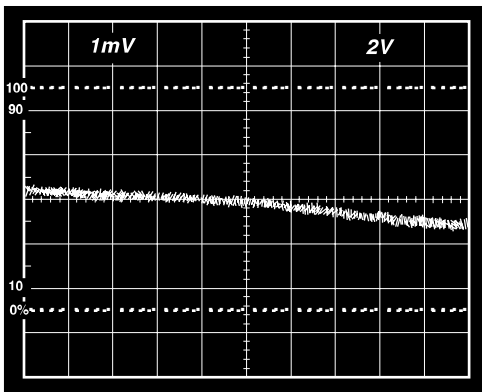
Figure 35. Gain Nonlinearity,  $G = 100$ ,  $R_L = 10\text{ k}\Omega$   
( $100\ \mu\text{V} = 10\text{ ppm}$ )



\*ALL RESISTORS 1% TOLERANCE

00775-0-037

Figure 37. Settling Time Test Circuit



00775-0-036

Figure 36. Gain Nonlinearity,  $G = 1000$ ,  $R_L = 10\text{ k}\Omega$   
( $1\text{ mV} = 100\text{ ppm}$ )

## THEORY OF OPERATION

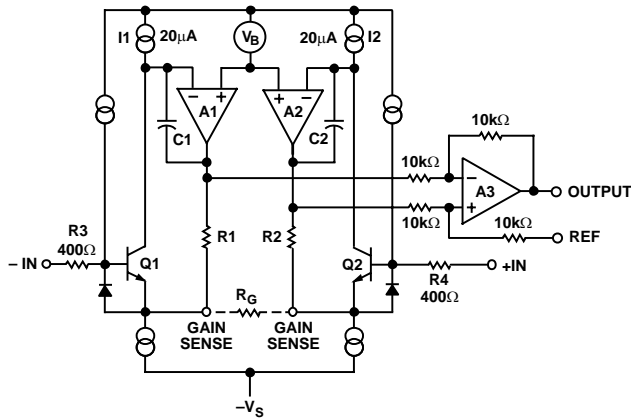


Figure 38. Simplified Schematic of AD620

The AD620 is a monolithic instrumentation amplifier based on a modification of the classic three op amp approach. Absolute value trimming allows the user to program gain *accurately* (to 0.15% at  $G = 100$ ) with only one resistor. Monolithic construction and laser wafer trimming allow the tight matching and tracking of circuit components, thus ensuring the high level of performance inherent in this circuit.

The input transistors Q1 and Q2 provide a single differential-pair bipolar input for high precision (Figure 38), yet offer 10× lower input bias current thanks to Superβ processing. Feedback through the Q1-A1-R1 loop and the Q2-A2-R2 loop maintains constant collector current of the input devices Q1 and Q2, thereby impressing the input voltage across the external gain setting resistor  $R_G$ . This creates a differential gain from the inputs to the A1/A2 outputs given by  $G = (R1 + R2)/R_G + 1$ . The unity-gain subtractor, A3, removes any common-mode signal, yielding a single-ended output referred to the REF pin potential.

The value of  $R_G$  also determines the transconductance of the preamp stage. As  $R_G$  is reduced for larger gains, the transconductance increases asymptotically to that of the input transistors. This has three important advantages: (a) Open-loop gain is boosted for increasing programmed gain, thus reducing gain related errors. (b) The gain-bandwidth product (determined by C1 and C2 and the preamp transconductance) increases with programmed gain, thus optimizing frequency response. (c) The input voltage noise is reduced to a value of 9 nV/√Hz, determined mainly by the collector current and base resistance of the input devices.

The internal gain resistors, R1 and R2, are trimmed to an absolute value of 24.7 kΩ, allowing the gain to be programmed accurately with a single external resistor.

The gain equation is then

$$G = \frac{49.4k\Omega}{R_G} + 1$$

$$R_G = \frac{49.4k\Omega}{G-1}$$

### **Make vs. Buy: a Typical Bridge Application Error Budget**

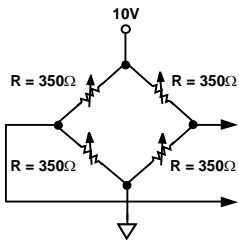
The AD620 offers improved performance over “homebrew” three op amp IA designs, along with smaller size, fewer components, and 10× lower supply current. In the typical application, shown in Figure 39, a gain of 100 is required to amplify a bridge output of 20 mV full-scale over the industrial temperature range of -40°C to +85°C. Table 3 shows how to calculate the effect various error sources have on circuit accuracy.



# AD620

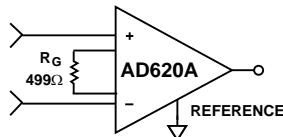
Regardless of the system in which it is being used, the AD620 provides greater accuracy at low power and price. In simple systems, absolute accuracy and drift errors are by far the most significant contributors to error. In more complex systems with an intelligent processor, an autogain/autozero cycle will remove all absolute accuracy and drift errors, leaving only the resolution errors of gain, nonlinearity, and noise, thus allowing full 14-bit accuracy.

Note that for the homebrew circuit, the OP07 specifications for input voltage offset and noise have been multiplied by  $\sqrt{2}$ . This is because a three op amp type in-amp has two op amps at its inputs, both contributing to the overall input error.



PRECISION BRIDGE TRANSDUCER

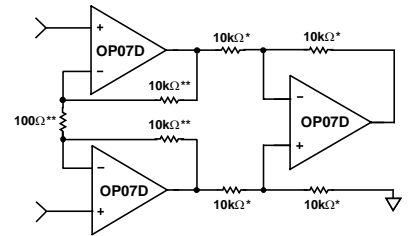
00775-0-039



AD620A MONOLITHIC INSTRUMENTATION AMPLIFIER, G = 100

SUPPLY CURRENT = 1.3mA MAX

00775-0-040



"HOMEBREW" IN-AMP, G = 100  
 \*0.02% RESISTOR MATCH, 3ppm/°C TRACKING  
 \*\*DISCRETE 1% RESISTOR, 100ppm/°C TRACKING  
 SUPPLY CURRENT = 15mA MAX

00775-0-041

Figure 39. Make vs. Buy

Table 3. Make vs. Buy Error Budget

Error Source	AD620 Circuit Calculation	"Homebrew" Circuit Calculation	Error, ppm of Full Scale	
			AD620	Homebrew
<b>ABSOLUTE ACCURACY</b> at $T_A = 25^\circ\text{C}$				
Input Offset Voltage, $\mu\text{V}$	125 $\mu\text{V}/20\text{ mV}$	$(150\ \mu\text{V} \times \sqrt{2})/20\text{ mV}$	6,250	10,607
Output Offset Voltage, $\mu\text{V}$	1000 $\mu\text{V}/100\text{ mV}/20\text{ mV}$	$((150\ \mu\text{V} \times 2)/100)/20\text{ mV}$	500	150
Input Offset Current, nA	2 nA $\times 350\ \Omega/20\text{ mV}$	$(6\text{ nA} \times 350\ \Omega)/20\text{ mV}$	18	53
CMR, dB	110 dB(3.16 ppm) $\times 5\text{ V}/20\text{ mV}$	$(0.02\% \text{ Match} \times 5\text{ V})/20\text{ mV}/100$	791	500
Total Absolute Error			7,559	11,310
<b>DRIFT TO 85°C</b>				
Gain Drift, ppm/°C	$(50\text{ ppm} + 10\text{ ppm}) \times 60^\circ\text{C}$	100 ppm/°C Track $\times 60^\circ\text{C}$	3,600	6,000
Input Offset Voltage Drift, $\mu\text{V}/^\circ\text{C}$	1 $\mu\text{V}/^\circ\text{C} \times 60^\circ\text{C}/20\text{ mV}$	$(2.5\ \mu\text{V}/^\circ\text{C} \times \sqrt{2} \times 60^\circ\text{C})/20\text{ mV}$	3,000	10,607
Output Offset Voltage Drift, $\mu\text{V}/^\circ\text{C}$	15 $\mu\text{V}/^\circ\text{C} \times 60^\circ\text{C}/100\text{ mV}/20\text{ mV}$	$(2.5\ \mu\text{V}/^\circ\text{C} \times 2 \times 60^\circ\text{C})/100\text{ mV}/20\text{ mV}$	450	150
Total Drift Error			7,050	16,757
<b>RESOLUTION</b>				
Gain Nonlinearity, ppm of Full Scale	40 ppm	40 ppm	40	40
Typ 0.1 Hz to 10 Hz Voltage Noise, $\mu\text{V p-p}$	0.28 $\mu\text{V p-p}/20\text{ mV}$	$(0.38\ \mu\text{V p-p} \times \sqrt{2})/20\text{ mV}$	14	27
Total Resolution Error			54	67
Grand Total Error			14,663	28,134

G = 100,  $V_s = \pm 15\text{ V}$ .

(All errors are min/max and referred to input.)

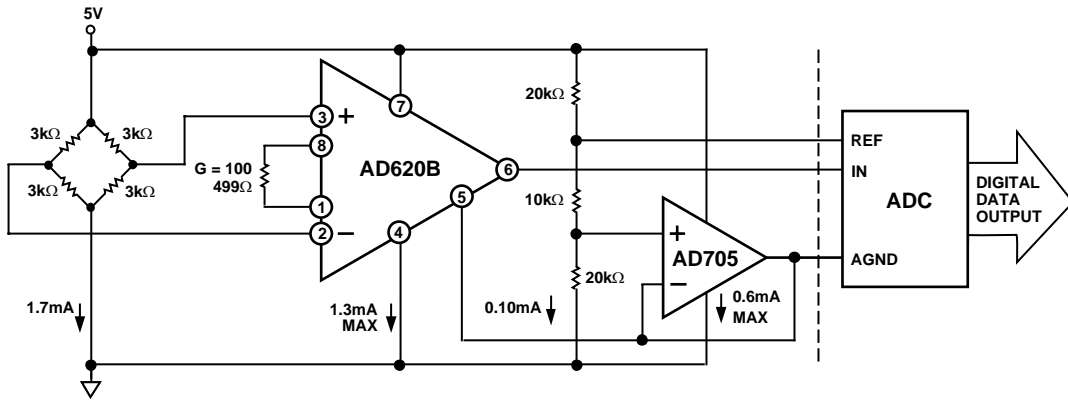


Figure 40. A Pressure Monitor Circuit that Operates on a 5 V Single Supply

00775-0-042

**Pressure Measurement**

Although useful in many bridge applications, such as weigh scales, the AD620 is especially suitable for higher resistance pressure sensors powered at lower voltages where small size and low power become more significant.

Figure 40 shows a 3 kΩ pressure transducer bridge powered from 5 V. In such a circuit, the bridge consumes only 1.7 mA. Adding the AD620 and a buffered voltage divider allows the signal to be conditioned for only 3.8 mA of total supply current.

Small size and low cost make the AD620 especially attractive for voltage output pressure transducers. Since it delivers low noise and drift, it will also serve applications such as diagnostic noninvasive blood pressure measurement.

**Medical ECG**

The low current noise of the AD620 allows its use in ECG monitors (Figure 41) where high source resistances of 1 MΩ or higher are not uncommon. The AD620's low power, low supply voltage requirements, and space-saving 8-lead mini-DIP and SOIC package offerings make it an excellent choice for battery-powered data recorders.

Furthermore, the low bias currents and low current noise, coupled with the low voltage noise of the AD620, improve the dynamic range for better performance.

The value of capacitor C1 is chosen to maintain stability of the right leg drive loop. Proper safeguards, such as isolation, must be added to this circuit to protect the patient from possible harm.

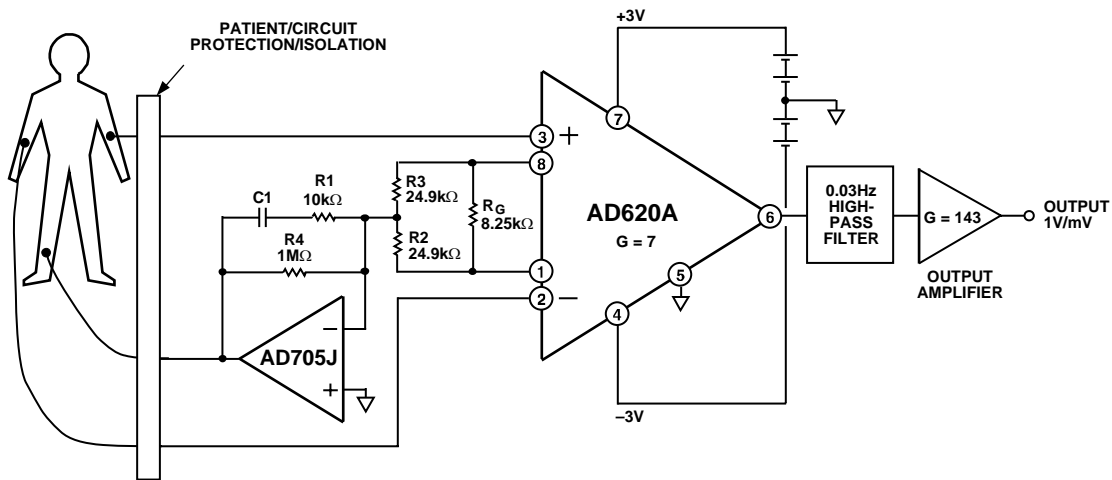


Figure 41. A Medical ECG Monitor Circuit

00775-0-043

# AD620

## Precision V-I Converter

The AD620, along with another op amp and two resistors, makes a precision current source (Figure 42). The op amp buffers the reference terminal to maintain good CMR. The output voltage,  $V_x$ , of the AD620 appears across  $R_1$ , which converts it to a current. This current, less only the input bias current of the op amp, then flows out to the load.

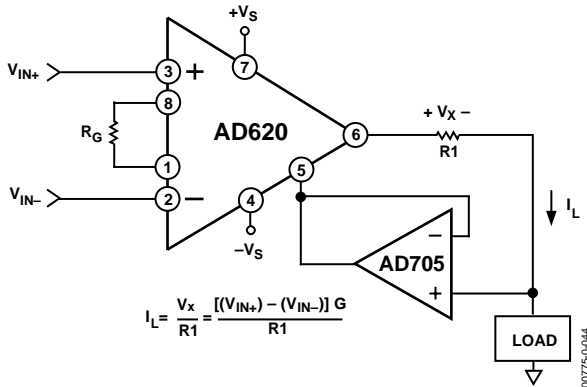


Figure 42. Precision Voltage-to-Current Converter (Operates on 1.8 mA,  $\pm 3$  V)

## GAIN SELECTION

The AD620's gain is resistor-programmed by  $R_G$ , or more precisely, by whatever impedance appears between Pins 1 and 8. The AD620 is designed to offer accurate gains using 0.1% to 1% resistors. Table 4 shows required values of  $R_G$  for various gains. Note that for  $G = 1$ , the  $R_G$  pins are unconnected ( $R_G = \infty$ ). For any arbitrary gain,  $R_G$  can be calculated by using the formula:

$$R_G = \frac{49.4k\Omega}{G - 1}$$

To minimize gain error, avoid high parasitic resistance in series with  $R_G$ ; to minimize gain drift,  $R_G$  should have a low TC—less than 10 ppm/ $^{\circ}$ C—for the best performance.

Table 4. Required Values of Gain Resistors

1% Std Table Value of $R_G(\Omega)$	Calculated Gain	0.1% Std Table Value of $R_G(\Omega)$	Calculated Gain
49.9 k	1.990	49.3 k	2.002
12.4 k	4.984	12.4 k	4.984
5.49 k	9.998	5.49 k	9.998
2.61 k	19.93	2.61 k	19.93
1.00 k	50.40	1.01 k	49.91
499	100.0	499	100.0
249	199.4	249	199.4
100	495.0	98.8	501.0
49.9	991.0	49.3	1,003.0

## INPUT AND OUTPUT OFFSET VOLTAGE

The low errors of the AD620 are attributed to two sources, input and output errors. The output error is divided by  $G$  when referred to the input. In practice, the input errors dominate at high gains, and the output errors dominate at low gains. The total  $V_{OS}$  for a given gain is calculated as

$$\text{Total Error RTI} = \text{input error} + (\text{output error}/G)$$

$$\text{Total Error RTO} = (\text{input error} \times G) + \text{output error}$$

## REFERENCE TERMINAL

The reference terminal potential defines the zero output voltage and is especially useful when the load does not share a precise ground with the rest of the system. It provides a direct means of injecting a precise offset to the output, with an allowable range of 2 V within the supply voltages. Parasitic resistance should be kept to a minimum for optimum CMR.

## INPUT PROTECTION

The AD620 features 400  $\Omega$  of series thin film resistance at its inputs and will safely withstand input overloads of up to  $\pm 15$  V or  $\pm 60$  mA for several hours. This is true for all gains and power on and off, which is particularly important since the signal source and amplifier may be powered separately. For longer time periods, the current should not exceed 6 mA ( $I_{IN} \leq V_{IN}/400 \Omega$ ). For input overloads beyond the supplies, clamping the inputs to the supplies (using a low leakage diode such as an FD333) will reduce the required resistance, yielding lower noise.

## RF INTERFERENCE

All instrumentation amplifiers rectify small out of band signals. The disturbance may appear as a small dc voltage offset. High frequency signals can be filtered with a low pass R-C network placed at the input of the instrumentation amplifier. Figure 43 demonstrates such a configuration. The filter limits the input signal according to the following relationship:

$$\text{FilterFreq}_{DIFF} = \frac{1}{2\pi R(2C_D + C_C)}$$

$$\text{FilterFreq}_{CM} = \frac{1}{2\pi RC_C}$$

where  $C_D \geq 10C_C$ .

$C_D$  affects the difference signal.  $C_C$  affects the common-mode signal. Any mismatch in  $R \times C_C$  will degrade the AD620's CMRR. To avoid inadvertently reducing CMRR-bandwidth performance, make sure that  $C_C$  is at least one magnitude smaller than  $C_D$ . The effect of mismatched  $C_C$ s is reduced with a larger  $C_D:C_C$  ratio.

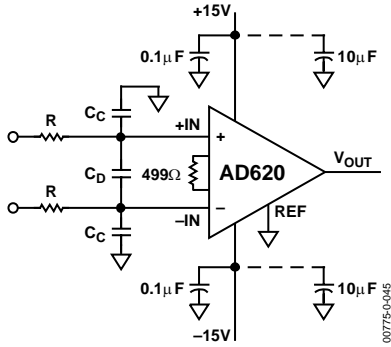


Figure 43. Circuit to Attenuate RF Interference

**COMMON-MODE REJECTION**

Instrumentation amplifiers, such as the AD620, offer high CMR, which is a measure of the change in output voltage when both inputs are changed by equal amounts. These specifications are usually given for a full-range input voltage change and a specified source imbalance.

For optimal CMR, the reference terminal should be tied to a low impedance point, and differences in capacitance and resistance should be kept to a minimum between the two inputs. In many applications, shielded cables are used to minimize noise; for best CMR over frequency, the shield should be properly driven. Figure 44 and Figure 45 show active data guards that are configured to improve ac common-mode rejections by “bootstrapping” the capacitances of input cable shields, thus minimizing the capacitance mismatch between the inputs.

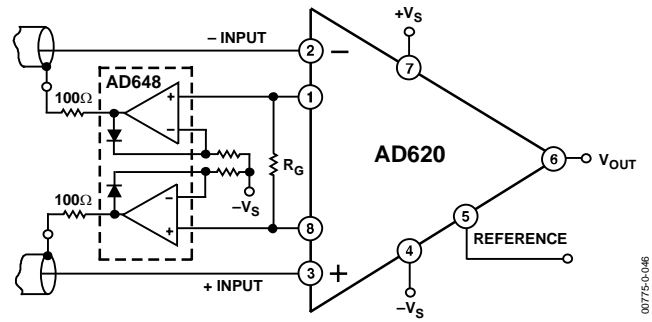


Figure 44. Differential Shield Driver

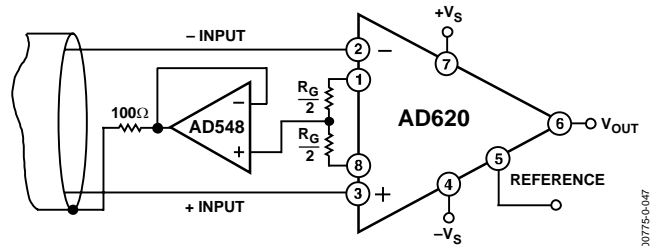


Figure 45. Common-Mode Shield Driver

**GROUNDING**

Since the AD620 output voltage is developed with respect to the potential on the reference terminal, it can solve many grounding problems by simply tying the REF pin to the appropriate “local ground.”

To isolate low level analog signals from a noisy digital environment, many data-acquisition components have separate analog and digital ground pins (Figure 46). It would be convenient to use a single ground line; however, current through ground wires and PC runs of the circuit card can cause hundreds of millivolts of error. Therefore, separate ground returns should be provided to minimize the current flow from the sensitive points to the system ground. These ground returns must be tied together at some point, usually best at the ADC package shown in Figure 46.

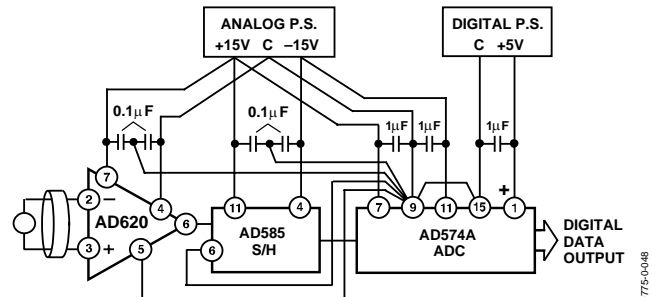


Figure 46. Basic Grounding Practice

# AD620

## GROUND RETURNS FOR INPUT BIAS CURRENTS

Input bias currents are those currents necessary to bias the input transistors of an amplifier. There must be a direct return path for these currents. Therefore, when amplifying “floating” input sources, such as transformers or ac-coupled sources, there must be a dc path from each input to ground, as shown in Figure 47, Figure 48, and Figure 49. Refer to *A Designer’s Guide to Instrumentation Amplifiers* (free from Analog Devices) for more information regarding in-amp applications.

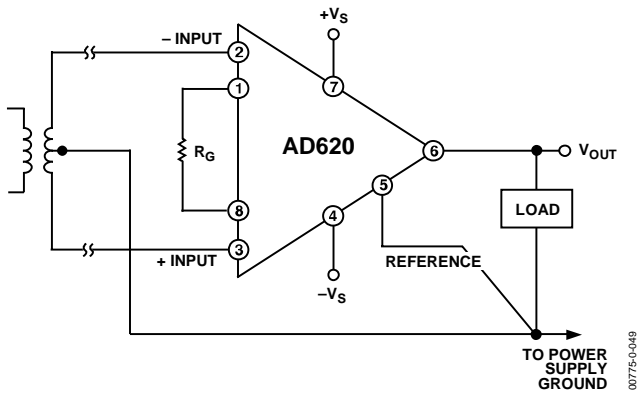


Figure 47. Ground Returns for Bias Currents with Transformer-Coupled Inputs

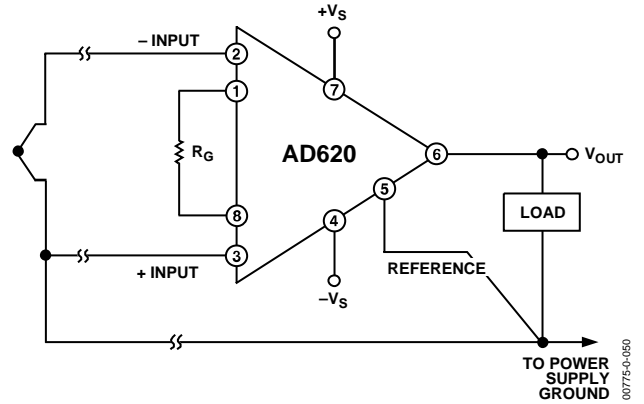


Figure 48. Ground Returns for Bias Currents with Thermocouple Inputs

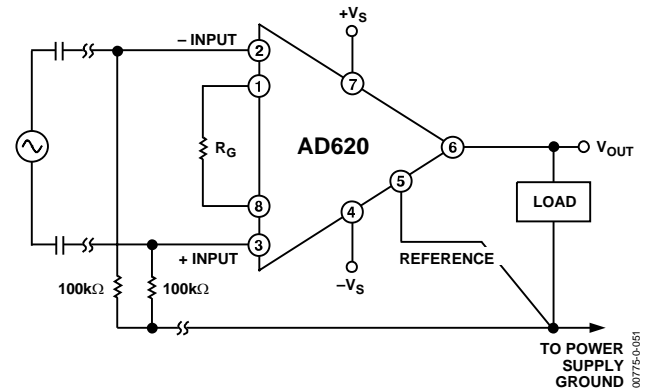
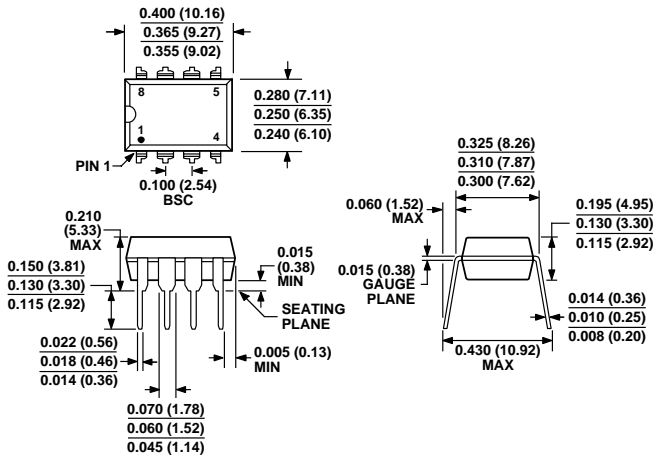


Figure 49. Ground Returns for Bias Currents with AC-Coupled Inputs

# OUTLINE DIMENSIONS

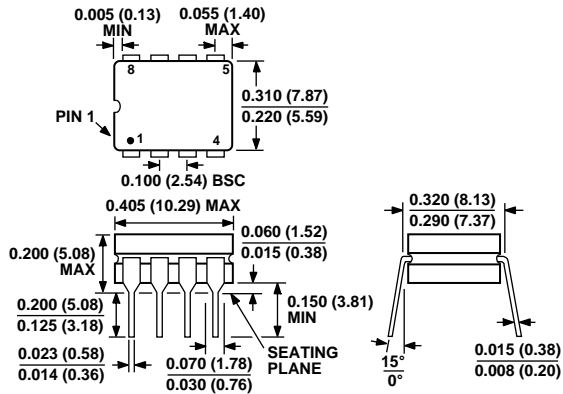


COMPLIANT TO JEDEC STANDARDS MS-001-BA  
 CONTROLLING DIMENSIONS ARE IN INCHES; MILLIMETER DIMENSIONS (IN PARENTHESES) ARE ROUNDED-OFF INCH EQUIVALENTS FOR REFERENCE ONLY AND ARE NOT APPROPRIATE FOR USE IN DESIGN. CORNER LEADS MAY BE CONFIGURED AS WHOLE OR HALF LEADS.

Figure 50. 8-Lead Plastic Dual In-Line Package [PDIP]

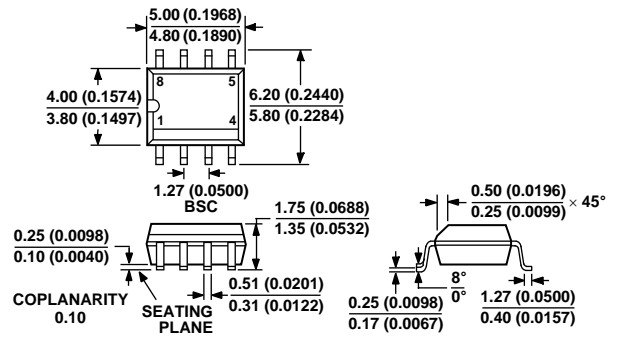
Narrow Body (N-8).

Dimensions shown in inches and (millimeters)



CONTROLLING DIMENSIONS ARE IN INCHES; MILLIMETER DIMENSIONS (IN PARENTHESES) ARE ROUNDED-OFF INCH EQUIVALENTS FOR REFERENCE ONLY AND ARE NOT APPROPRIATE FOR USE IN DESIGN

Figure 51. 8-Lead Ceramic Dual In-Line Package [CERDIP] (Q-8)  
 Dimensions shown in inches and (millimeters)



COMPLIANT TO JEDEC STANDARDS MS-012AA  
 CONTROLLING DIMENSIONS ARE IN MILLIMETERS; INCH DIMENSIONS (IN PARENTHESES) ARE ROUNDED-OFF MILLIMETER EQUIVALENTS FOR REFERENCE ONLY AND ARE NOT APPROPRIATE FOR USE IN DESIGN

Figure 52. 8-Lead Standard Small Outline Package [SOIC]

Narrow Body (R-8)

Dimensions shown in millimeters and (inches)

# AD620

## ORDERING GUIDE

Model	Temperature Range	Package Option <sup>1</sup>
AD620AN	-40°C to +85°C	N-8
AD620ANZ <sup>2</sup>	-40°C to +85°C	N-8
AD620BN	-40°C to +85°C	N-8
AD620BNZ <sup>2</sup>	-40°C to +85°C	N-8
AD620AR	-40°C to +85°C	R-8
AD620ARZ <sup>2</sup>	-40°C to +85°C	R-8
AD620AR-REEL	-40°C to +85°C	13" REEL
AD620ARZ-REEL <sup>2</sup>	-40°C to +85°C	13" REEL
AD620AR-REEL7	-40°C to +85°C	7" REEL
AD620ARZ-REEL7 <sup>2</sup>	-40°C to +85°C	7" REEL
AD620BR	-40°C to +85°C	R-8
AD620BRZ <sup>2</sup>	-40°C to +85°C	R-8
AD620BR-REEL	-40°C to +85°C	13" REEL
AD620BRZ-RL <sup>2</sup>	-40°C to +85°C	13" REEL
AD620BR-REEL7	-40°C to +85°C	7" REEL
AD620BRZ-R7 <sup>2</sup>	-40°C to +85°C	7" REEL
AD620ACHIPS	-40°C to +85°C	Die Form
AD620SQ/883B	-55°C to +125°C	Q-8

<sup>1</sup> N = Plastic DIP; Q = CERDIP; R = SOIC.

<sup>2</sup> Z = Pb-free part.

## ADM660/ADM8660

### FEATURES

**ADM660:** Inverts or Doubles Input Supply Voltage  
**ADM8660:** Inverts Input Supply Voltage  
**100 mA Output Current**  
**Shutdown Function (ADM8660)**  
**2.2  $\mu\text{F}$  or 10  $\mu\text{F}$  Capacitors**  
**0.3 V Drop at 30 mA Load**  
**+1.5 V to +7 V Supply**  
**Low Power CMOS: 600  $\mu\text{A}$  Quiescent Current**  
**Selectable Charge Pump Frequency (25 kHz/120 kHz)**  
**Pin Compatible Upgrade for MAX660, MAX665, ICL7660**  
**Available in 16-Lead TSSOP Package**

### APPLICATIONS

**Handheld Instruments**  
**Portable Computers**  
**Remote Data Acquisition**  
**Op Amp Power Supplies**

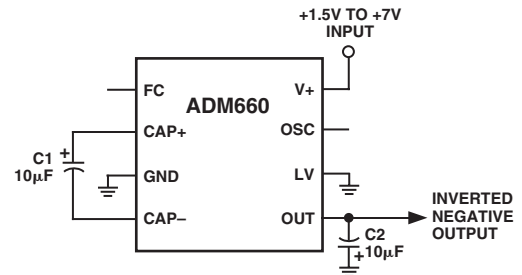
### GENERAL DESCRIPTION

The ADM660/ADM8660 is a charge-pump voltage converter that can be used to either invert the input supply voltage giving  $V_{\text{OUT}} = -V_{\text{IN}}$  or double it (ADM660 only) giving  $V_{\text{OUT}} = 2 \times V_{\text{IN}}$ . Input voltages ranging from +1.5 V to +7 V can be inverted into a negative -1.5 V to -7 V output supply. This inverting scheme is ideal for generating a negative rail in single power supply systems. Only two small external capacitors are needed for the charge pump. Output currents up to 50 mA with greater than 90% efficiency are achievable, while 100 mA achieves greater than 80% efficiency.

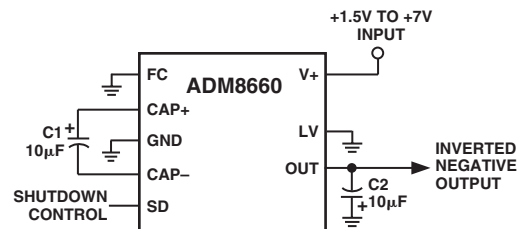
A Frequency Control (FC) input pin is used to select either 25 kHz or 120 kHz charge-pump operation. This is used to optimize capacitor size and quiescent current. With 25 kHz selected, a 10  $\mu\text{F}$  external capacitor is suitable, while with 120 kHz the capacitor may be reduced to 2.2  $\mu\text{F}$ . The oscillator frequency on the ADM660 can also be controlled with an external capacitor connected to the OSC input or by driving this input with an external clock. In applications where a higher supply voltage is desired it is possible to use the ADM660 to double the input voltage. With input voltages from 2.5 V to 7 V, output voltages from 5 V to 14 V are achievable with up to 100 mA output current.

The ADM8660 features a low power shutdown (SD) pin instead of the external oscillator (OSC) pin. This can be used to disable the device and reduce the quiescent current to 300 nA.

### TYPICAL CIRCUIT CONFIGURATIONS



Voltage Inverter Configuration (ADM660)



Voltage Inverter Configuration with Shutdown (ADM8660)

The ADM660 is a pin compatible upgrade for the MAX660, MAX665, ICL7660, and LTC1046.

The ADM660/ADM8660 is available in 8-lead DIP and narrow-body SOIC. The ADM660 is also available in a 16-lead TSSOP package.

### ADM660/ADM8660 Options

Option	ADM660	ADM8660
Inverting Mode	Y	Y
Doubling Mode	Y	N
External Oscillator	Y	N
Shutdown	N	Y
Package Options		
R-8	Y	Y
N-8	Y	Y
RU-16	Y	N

### REV. B

Information furnished by Analog Devices is believed to be accurate and reliable. However, no responsibility is assumed by Analog Devices for its use, nor for any infringements of patents or other rights of third parties that may result from its use. No license is granted by implication or otherwise under any patent or patent rights of Analog Devices. Trademarks and registered trademarks are the property of their respective companies.



# ADM660/ADM8660—SPECIFICATIONS (V+ = +5 V, C1, C2 = 10 $\mu$ F, \* T<sub>A</sub> = T<sub>MIN</sub> to T<sub>MAX</sub>, unless otherwise noted.)

Parameter	Min	Typ	Max	Unit	Test Conditions/Comments
Input Voltage, V+	3.5		7.0	V	R <sub>L</sub> = 1 k $\Omega$ Inverting Mode, LV = Open
	1.5		7.0	V	Inverting Mode, LV = GND
	2.5		7.0	V	Doubling Mode, LV = OUT
Supply Current		0.6	1	mA	No Load FC = Open (ADM660), GND (ADM8660)
		2.5	4.5	mA	FC = V+, LV = Open
Output Current	100			mA	
Output Resistance (ADM660)		9	15	$\Omega$	I <sub>L</sub> = 100 mA
Output Resistance (ADM8660)		9	15	$\Omega$	I <sub>L</sub> = 100 mA, T <sub>A</sub> = 25°C
Output Resistance (ADM8660)			16.5	$\Omega$	I <sub>L</sub> = 100 mA, T <sub>A</sub> = -40°C to +85°C
Charge-Pump Frequency		25		kHz	FC = Open (ADM660), GND (ADM8660)
		120		kHz	FC = V+
OSC Input Current		$\pm 5$		$\mu$ A	FC = Open (ADM660), GND (ADM8660)
		$\pm 25$		$\mu$ A	FC = V+
Power Efficiency (FC = Open) (ADM660)	90	94		%	R <sub>L</sub> = 1 k $\Omega$ Connected from V+ to OUT
Power Efficiency (FC = Open) (ADM8660)	90	94		%	R <sub>L</sub> = 1 k $\Omega$ Connected from V+ to OUT, T <sub>A</sub> = +25°C
Power Efficiency (FC = Open) (ADM8660)	88.5			%	R <sub>L</sub> = 1 k $\Omega$ Connected from V+ to OUT, T <sub>A</sub> = -40°C to +85°C
Power Efficiency (FC = Open) (ADM660)	90	93		%	R <sub>L</sub> = 500 $\Omega$ Connected from OUT to GND
Power Efficiency (FC = Open) (ADM8660)	90	93		%	R <sub>L</sub> = 500 $\Omega$ Connected from OUT to GND, T <sub>A</sub> = +25°C
Power Efficiency (FC = Open) (ADM8660)	88.5			%	R <sub>L</sub> = 500 $\Omega$ Connected from OUT to GND, T <sub>A</sub> = -40°C to +85°C
Power Efficiency (FC = Open)		81.5		%	I <sub>L</sub> = 100 mA to GND
Voltage Conversion Efficiency	99	99.96		%	No Load
Shutdown Supply Current, I <sub>SHDN</sub>		0.3	5	$\mu$ A	ADM8660, SHDN = V+
Shutdown Input Voltage, V <sub>SHDN</sub>	2.4			V	SHDN High = Disabled
			0.8	V	SHDN Low = Enabled
Shutdown Exit Time		500		$\mu$ s	I <sub>L</sub> = 100 mA

\*C1 and C2 are low ESR (<0.2  $\Omega$ ) electrolytic capacitors.  
High ESR degrade performance.

Specifications subject to change without notice.

## ABSOLUTE MAXIMUM RATINGS\*

(T<sub>A</sub> = +25°C, unless otherwise noted.)

Input Voltage (V+ to GND, GND to OUT) . . . . .	+7.5 V
LV Input Voltage . . . . . (OUT – 0.3 V) to (V+, +0.3 V)	
FC and OSC Input Voltage . . . . . (OUT – 0.3 V) or (V+, –6 V) to (V+, +0.3 V)	
OUT, V+ Output Current (Continuous) . . . . .	120 mA
Output Short Circuit Duration to GND . . . . .	10 secs
Power Dissipation, N-8 . . . . . (Derate 8.3 mW/°C above +50°C)	625 mW
θ <sub>JA</sub> , Thermal Impedance . . . . .	120°C/W
Power Dissipation, R-8 . . . . . (Derate 6 mW/°C above +50°C)	450 mW
θ <sub>JA</sub> , Thermal Impedance . . . . .	170°C/W

Power Dissipation, RU-16 . . . . . (Derate 6 mW/°C above +50°C)	500 mW
θ <sub>JA</sub> , Thermal Impedance . . . . .	158°C/W
Operating Temperature Range	
Industrial (A Version) . . . . .	–40°C to +85°C
Storage Temperature Range . . . . .	–65°C to +150°C
Lead Temperature Range (Soldering 10 sec) . . . . .	+300°C
Vapor Phase (60 sec) . . . . .	+215°C
Infrared (15 sec) . . . . .	+220°C
ESD Rating . . . . .	>2000 V

\*This is a stress rating only; functional operation of the device at these or any other conditions above those indicated in the operation section of this specification is not implied. Exposure to absolute maximum rating conditions for extended periods may affect device reliability.

## ORDERING GUIDE

Model	Temperature Range	Package Options*
ADM660AN	–40°C to +85°C	N-8
ADM660AR	–40°C to +85°C	R-8
ADM660ARU	–40°C to +85°C	RU-16
ADM8660AN	–40°C to +85°C	N-8
ADM8660AR	–40°C to +85°C	R-8

\*N = Plastic DIP; RU = Thin Shrink Small Outline; RN = Small Outline.

## CAUTION

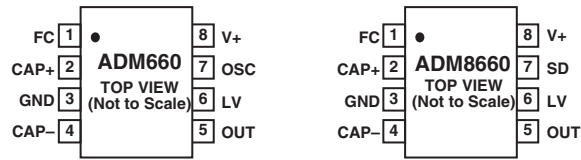
ESD (electrostatic discharge) sensitive device. Electrostatic charges as high as 4000 V readily accumulate on the human body and test equipment and can discharge without detection. Although the ADM660/ADM8660 features proprietary ESD protection circuitry, permanent damage may occur on devices subjected to high energy electrostatic discharges. Therefore, proper ESD precautions are recommended to avoid performance degradation or loss of functionality.



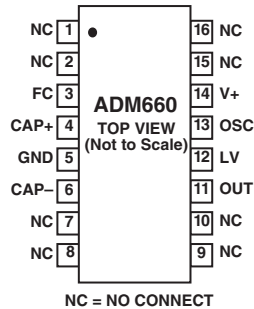
# ADM660/ADM8660

## PIN CONNECTIONS

### 8-Lead



### 16-Lead



## PIN FUNCTION DESCRIPTIONS

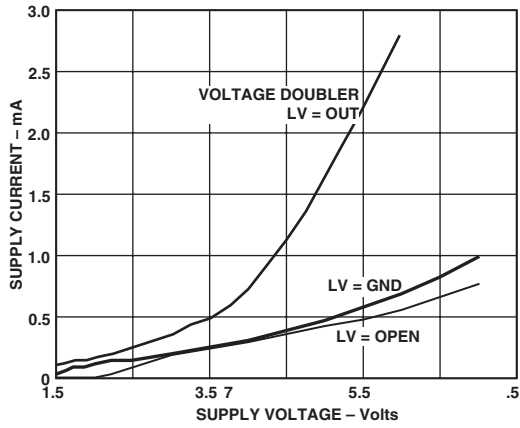
### Inverter Configuration

Mnemonic	Function
FC	Frequency Control Input for Internal Oscillator and Charge Pump. With FC = Open (ADM660) or connected to GND (ADM8660), $f_{CP} = 25$ kHz; with FC = V+, $f_{CP} = 120$ kHz.
CAP+	Positive Charge-Pump Capacitor Terminal.
GND	Power Supply Ground.
CAP-	Negative Charge-Pump Capacitor Terminal.
OUT	Output, Negative Voltage.
LV	Low Voltage Operation Input. Connect to GND when input voltage is less than 3.5 V. Above 3.5 V, LV may be connected to GND or left unconnected.
OSC	ADM660: Oscillator Control Input. OSC is connected to an internal 15 pF capacitor. An external capacitor may be connected to slow the oscillator. An external oscillator may also be used to overdrive OSC. The charge-pump frequency is equal to 1/2 the oscillator frequency.
SD	ADM8660: Shutdown Control Input. This input, when high, is used to disable the charge pump thereby reducing the power consumption.
V+	Positive Power Supply Input.

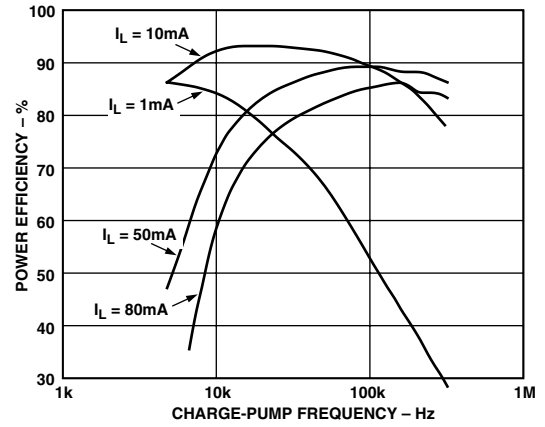
### Doubler Configuration (ADM660 Only)

Mnemonic	Function
FC	Frequency Control Input for Internal Oscillator and Charge Pump. With FC = Open, $f_{CP} = 25$ kHz; with FC = V+, $f_{CP} = 120$ kHz.
CAP+	Positive Charge-Pump Capacitor Terminal.
GND	Positive Input Supply.
CAP-	Negative Charge-Pump Capacitor Terminal.
OUT	Ground.
LV	Low Voltage Operation Input. Connect to OUT.
OSC	Must be left unconnected in this mode.
V+	Doubled Positive Output.

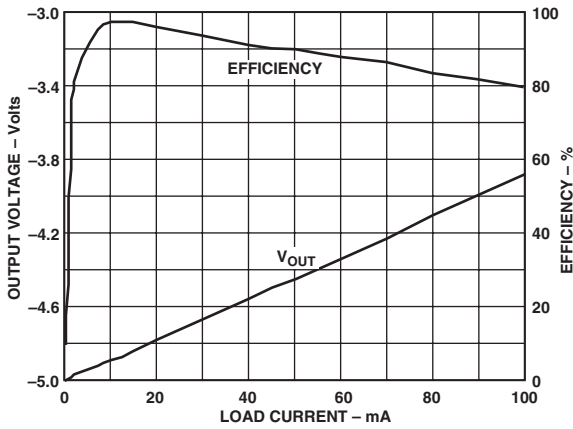
# Typical Performance Characteristics—ADM660/ADM8660



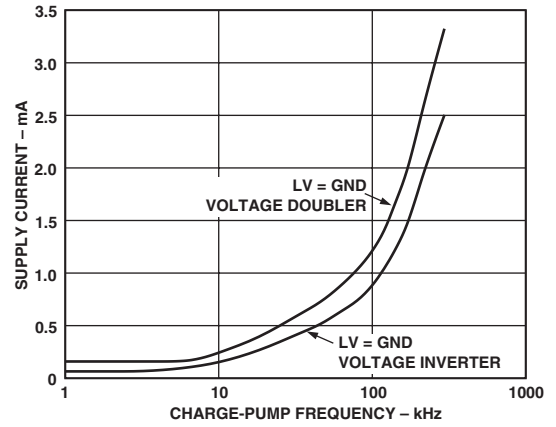
TPC 1. Power Supply Current vs. Voltage



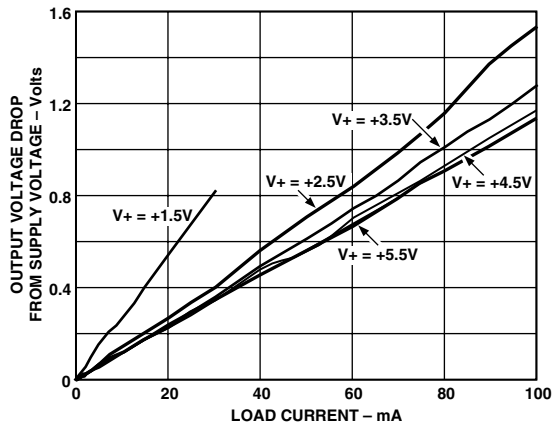
TPC 4. Efficiency vs. Charge-Pump Frequency



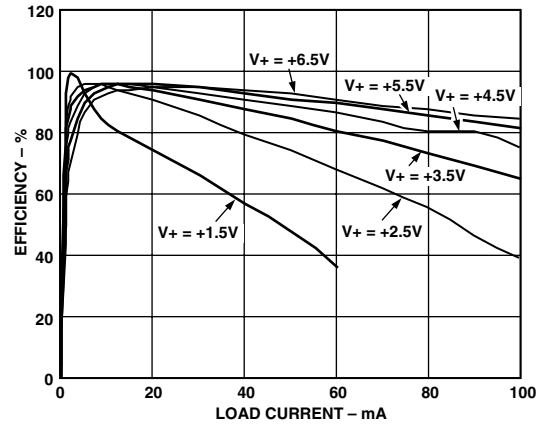
TPC 2. Output Voltage and Efficiency vs. Load Current



TPC 5. Power Supply Current vs. Charge-Pump Frequency

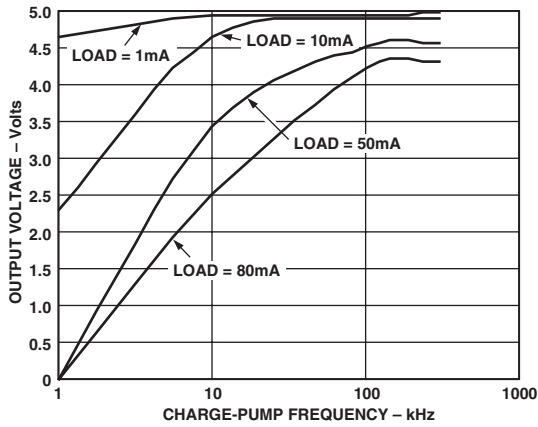


TPC 3. Output Voltage Drop vs. Load Current

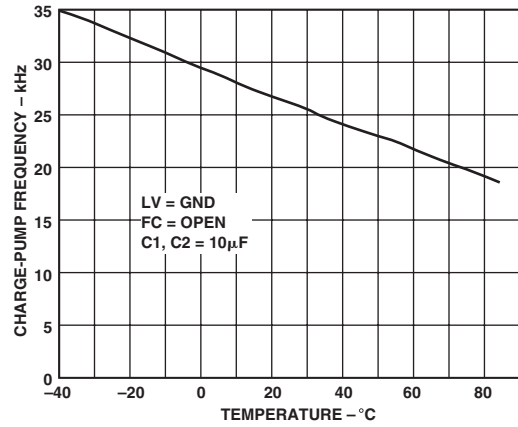


TPC 6. Power Efficiency vs. Load Current

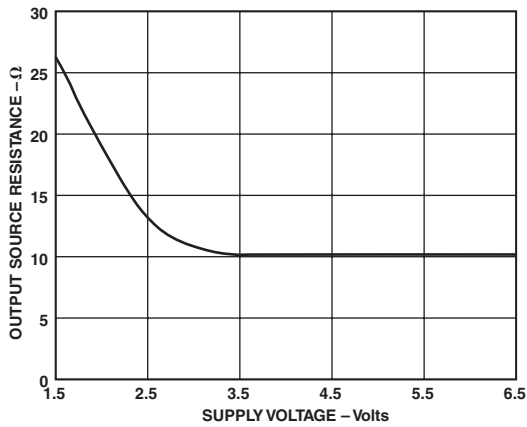
# ADM660/ADM8660



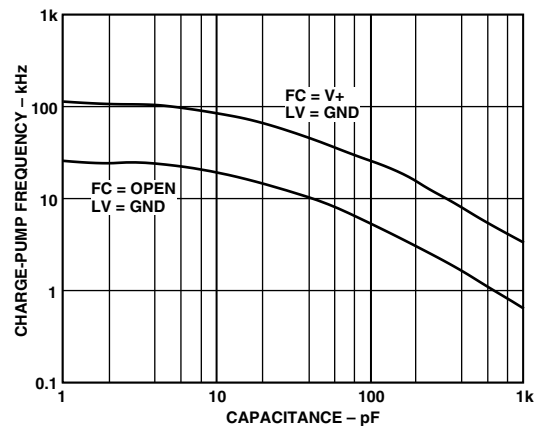
TPC 7. Output Voltage vs. Charge-Pump Frequency



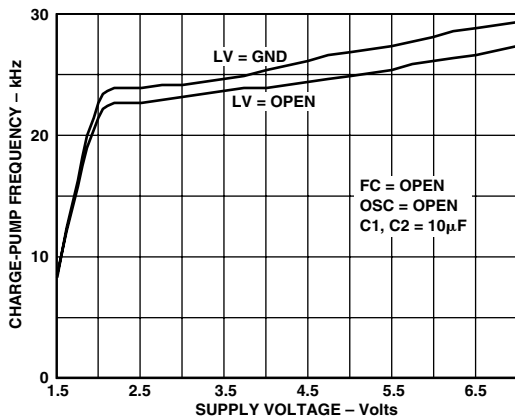
TPC 10. Charge-Pump Frequency vs. Temperature



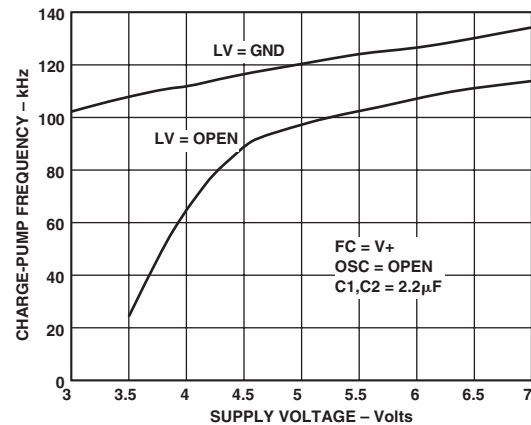
TPC 8. Output Source Resistance vs. Supply Voltage



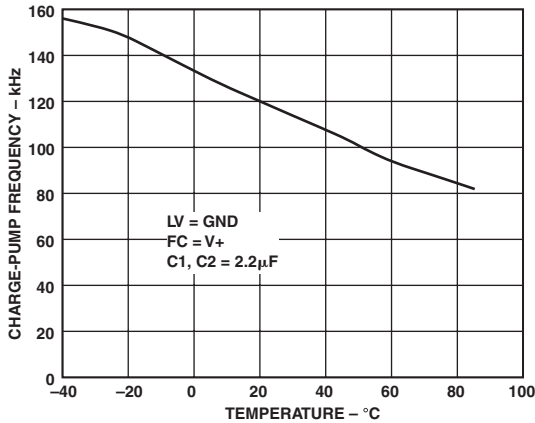
TPC 11. Charge-Pump Frequency vs. External Capacitance



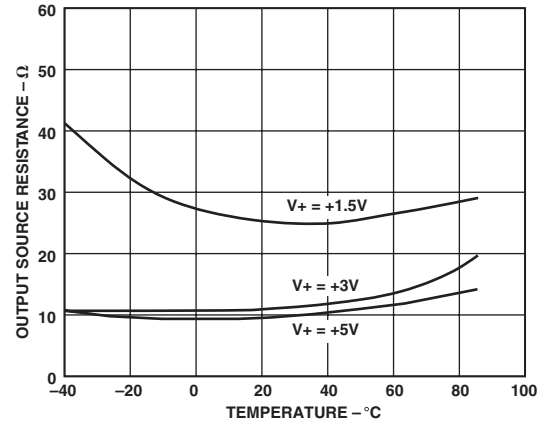
TPC 9. Charge-Pump Frequency vs. Supply Voltage



TPC 12. Charge-Pump Frequency vs. Supply Voltage



TPC 13. Charge-Pump Frequency vs. Temperature



TPC 14. Output Resistance vs. Temperature

### GENERAL INFORMATION

The ADM660/ADM8660 is a switched capacitor voltage converter that can be used to invert the input supply voltage. The ADM660 can also be used in a voltage doubling mode. The voltage conversion task is achieved using a switched capacitor technique using two external charge storage capacitors. An on-board oscillator and switching network transfers charge between the charge storage capacitors. The basic principle behind the voltage conversion scheme is illustrated in Figures 1 and 2.

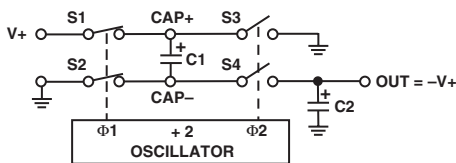


Figure 1. Voltage Inversion Principle

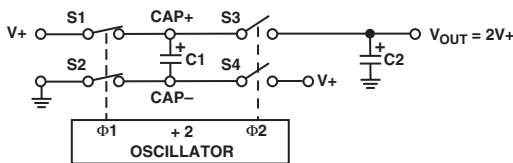


Figure 2. Voltage Doubling Principle

Figure 1 shows the voltage inverting configuration, while Figure 2 shows the configuration for voltage doubling. An oscillator generating antiphase signals  $\phi_1$  and  $\phi_2$  controls switches S1, S2, and S3, S4. During  $\phi_1$ , switches S1 and S2 are closed charging C1 up to the voltage at V+. During  $\phi_2$ , S1 and S2 open and S3 and S4 close. With the voltage inverter configuration during  $\phi_2$ , the positive terminal of C1 is connected to GND via S3 and the negative terminal of C1 connects to  $V_{OUT}$  via S4. The net result is voltage inversion at  $V_{OUT}$  wrt GND. Charge on C1 is transferred to C2 during  $\phi_1$ . Capacitor C2 maintains this voltage during  $\phi_2$ . The charge transfer efficiency depends on the on-resistance of the switches, the frequency at which they are being switched, and also on the equivalent series resistance (ESR) of the external capacitors. The reason for this is explained in the following section. For maximum efficiency, capacitors with low ESR are, therefore, recommended.

The voltage doubling configuration reverses some of the connections, but the same principle applies.

### Switched Capacitor Theory of Operation

As already described, the charge pump on the ADM660/ADM8660 uses a switched capacitor technique in order to invert or double the input supply voltage. Basic switched capacitor theory is discussed below.

A switched capacitor building block is illustrated in Figure 3. With the switch in position A, capacitor C1 will charge to voltage V1. The total charge stored on C1 is  $q_1 = C_1V_1$ . The switch is then flipped to position B discharging C1 to voltage V2. The charge remaining on C1 is  $q_2 = C_1V_2$ . The charge transferred to the output V2 is, therefore, the difference between  $q_1$  and  $q_2$ , so  $\Delta q = q_1 - q_2 = C_1(V_1 - V_2)$ .

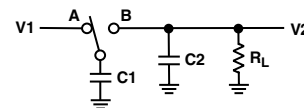


Figure 3. Switched Capacitor Building Block

As the switch is toggled between A and B at a frequency  $f$ , the charge transfer per unit time or current is:

$$I = f(\Delta q) = f(C_1)(V_1 - V_2)$$

Therefore,

$$I = (V_1 - V_2)/(1/fC_1) = (V_1 - V_2)/(R_{EQ})$$

where  $R_{EQ} = 1/fC_1$

The switched capacitor may, therefore, be replaced by an equivalent resistance whose value is dependent on both the capacitor size and the switching frequency. This explains why lower capacitor values may be used with higher switching frequencies. It should be remembered that as the switching frequency is increased the power consumption will increase due to some charge being lost at each switching cycle. As a result, at high frequencies, the power efficiency starts decreasing. Other losses include the resistance of the internal switches and the equivalent series resistance (ESR) of the charge storage capacitors.

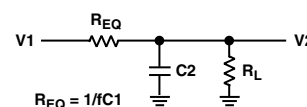


Figure 4. Switched Capacitor Equivalent Circuit

# ADM660/ADM8660

## Inverting Negative Voltage Generator

Figures 5 and 6 show the ADM660/ADM8660 configured to generate a negative output voltage. Input supply voltages from 1.5 V up to 7 V are allowable. For supply voltage less than 3 V, LV must be connected to GND. This bypasses the internal regulator circuitry and gives best performance in low voltage applications. With supply voltages greater than 3 V, LV may be either connected to GND or left open. Leaving it open facilitates direct substitution for the ICL7660.

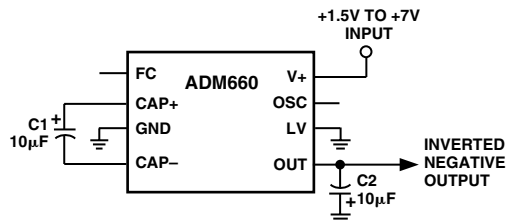


Figure 5. ADM660 Voltage Inverter Configuration

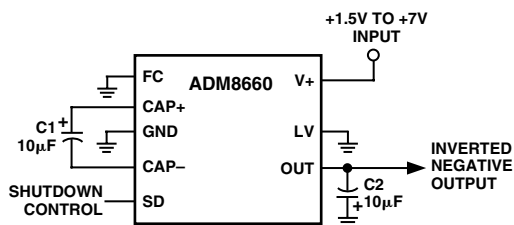


Figure 6. ADM8660 Voltage Inverter Configuration

## OSCILLATOR FREQUENCY

The internal charge-pump frequency may be selected to be either 25 kHz or 120 kHz using the Frequency Control (FC) input. With FC unconnected (ADM660) or connected to GND (ADM8660), the internal charge pump runs at 25 kHz while, if FC is connected to V+, the frequency is increased by a factor of five. Increasing the frequency allows smaller capacitors to be used for equivalent performance or, if the capacitor size is unchanged, it results in lower output impedance and ripple.

If a charge-pump frequency other than the two fixed values is desired, this is made possible by the OSC input, which can either have a capacitor connected to it or be overdriven by an external clock. Refer to the Typical Performance Characteristics, which shows the variation in charge-pump frequency versus capacitor size. The charge-pump frequency is one-half the oscillator frequency applied to the OSC pin.

If an external clock is used to overdrive the oscillator, its levels should swing to within 100 mV of V+ and GND. A CMOS driver is, therefore, suitable. When OSC is overdriven, FC has no effect but LV must be grounded.

Note that overdriving is permitted only in the voltage inverter configuration.

Table I. ADM660 Charge-Pump Frequency Selection

FC	OSC	Charge Pump	C1, C2
Open	Open	25 kHz	10 µF
V+	Open	120 kHz	2.2 µF
Open or V+	Ext Cap	See Typical Characteristics	
Open	Ext CLK	Ext CLK Frequency/2	

Table II. ADM8660 Charge-Pump Frequency Selection

FC	OSC	Charge Pump	C1, C2
GND	Open	25 kHz	10 µF
V+	Open	120 kHz	2.2 µF
GND or V+	Ext Cap	See Typical Characteristics	
GND	Ext CLK	Ext CLK Frequency/2	

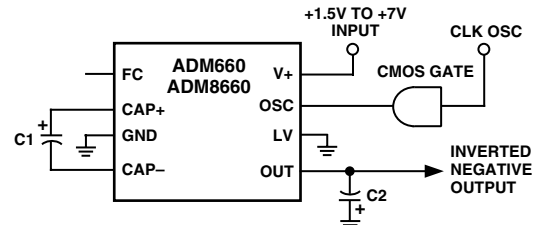


Figure 7. ADM660/ADM8660 External Oscillator

## Voltage Doubling Configuration

Figure 8 shows the ADM660 configured to generate increased output voltages. As in the inverting mode, only two external capacitors are required. The doubling function is achieved by reversing some connections to the device. The input voltage is applied to the GND pin and V+ is used as the output. Input voltages from 2.5 V to 7 V are allowable. In this configuration, pins LV, OUT must be connected to GND.

The unloaded output voltage in this configuration is  $2(V_{IN})$ . Output resistance and ripple are similar to the voltage inverting configuration.

**Note that the ADM8660 cannot be used in the voltage doubling configuration.**

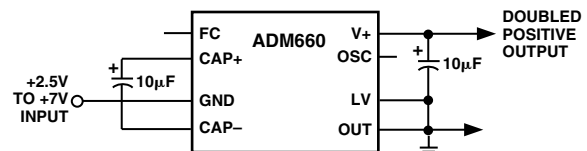


Figure 8. Voltage Doubler Configuration

## Shutdown Input

The ADM8660 contains a shutdown input that can be used to disable the device and thus reduce the power consumption. A logic high level on the SD input shuts the device down reducing the quiescent current to 0.3 µA. During shutdown, the output voltage goes to 0 V. Therefore, ground referenced loads are not powered during this state. When exiting shutdown, it takes several cycles (approximately 500 µs) for the charge pump to reach its final value. If the shutdown function is not being used, then SD should be hardwired to GND.

## Capacitor Selection

The optimum capacitor value selection depends the charge-pump frequency. With 25 kHz selected, 10 µF capacitors are recommended, while with 120 kHz selected, 2.2 µF capacitors may be used. Other frequencies allow other capacitor values to be used. For maximum efficiency in all cases, it is recommended that capacitors with low ESR are used for the charge-pump. Low ESR capacitors give both the lowest output resistance and lowest ripple voltage. High output resistance degrades the overall power efficiency and causes voltage drops, especially at high output



current levels. The ADM660/ADM8660 is tested using low ESR, 10  $\mu\text{F}$ , capacitors for both C1 and C2. Smaller values of C1 increase the output resistance, while increasing C1 will reduce the output resistance. The output resistance is also dependent on the internal switches on resistance as well as the capacitors ESR, so the effect of increasing C1 becomes negligible past a certain point.

Figure 9 shows how the output resistance varies with oscillator frequency for three different capacitor values. At low oscillator frequencies, the output impedance is dominated by the  $1/f_C$  term. This explains why the output impedance is higher for smaller capacitance values. At high oscillator frequencies, the  $1/f_C$  term becomes insignificant and the output impedance is dominated by the internal switches on resistance. From an output impedance viewpoint, therefore, there is no benefit to be gained from using excessively large capacitors.

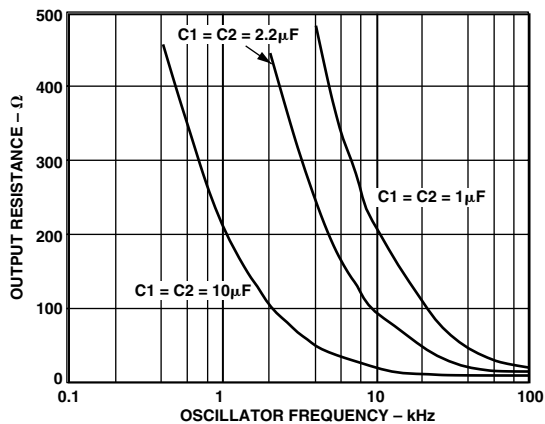


Figure 9. Output Impedance vs. Oscillator Frequency

### Capacitor C2

The output capacitor size C2 affects the output ripple. Increasing the capacitor size reduces the peak-to-peak ripple. The ESR affects both the output impedance and the output ripple. Reducing the ESR reduces the output impedance and ripple. For convenience it is recommended that both C1 and C2 be the same value.

Table III. Capacitor Selection

Charge-Pump Frequency	Capacitor C1, C2
25 kHz	10 $\mu\text{F}$
120 kHz	2.2 $\mu\text{F}$

### Power Efficiency and Oscillator Frequency Trade-Off

While higher switching frequencies allow smaller capacitors to be used for equivalent performance, or improved performance with the same capacitors, there is a trade-off to consider. As the oscillator frequency is increased, the quiescent current increases. This happens as a result of a finite charge being lost at each switching cycle. The charge loss per unit cycle at very high frequencies can be significant, thereby reducing the power efficiency. Since the power efficiency is also degraded at low oscillator frequencies due to an increase in output impedance, this means that there is an optimum frequency band for maximum power transfer. Refer to the Typical Performance Characteristics section.

### Bypass Capacitor

The ac impedance of the ADM660/ADM8660 may be reduced by using a bypass capacitor on the input supply. This capacitor should be connected between the input supply and GND. It will provide instantaneous current surges as required. Suitable capacitors of 0.1  $\mu\text{F}$  or greater may be used.





# Revision History

<b>Location</b>	<b>Page</b>
<b>12/02—Data Sheet changed from REV. A to REV. B.</b>	
Renumbered TPCs and Figures .....	UNIVERSAL
Edits to SPECIFICATIONS .....	2
Updated ABSOLUTE MAXIMUM RATINGS .....	3
Updated OUTLINE DIMENSIONS .....	10





T-39.09

**N-Channel Enhancement-Mode Vertical DMOS Power FETs**

**Ordering Information**

BV <sub>DSS</sub> / BV <sub>DGS</sub>	R <sub>DS(ON)</sub> (max)	I <sub>D(ON)</sub> (min)	Order Number / Package
			TO-220
100V	0.6Ω	4.0A	IRF510
60V	0.6Ω	4.0A	IRF511
100V	0.8Ω	3.5A	IRF512
60V	0.8Ω	3.5A	IRF513

**Features**

- Freedom from secondary breakdown
- Low power drive requirement
- Ease of paralleling
- Low C<sub>ISS</sub> and fast switching speeds
- Excellent thermal stability
- Integral Source-Drain diode
- High input impedance and high gain
- Complementary N- and P-Channel devices

**Advanced DMOS Technology**

These enhancement-mode (normally-off) power transistors utilize a vertical DMOS structure and Supertex's well-proven silicon-gate manufacturing process. This combination produces devices with the power handling capabilities of bipolar transistors and with the high input impedance and negative temperature coefficient inherent in MOS devices. Characteristic of all MOS structures, these devices are free from thermal runaway and thermally-induced secondary breakdown.

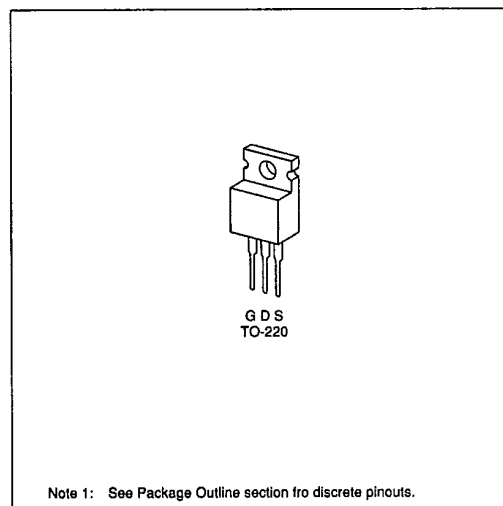
Supertex Vertical DMOS Power FETs are ideally suited to a wide range of switching and amplifying applications where high breakdown voltage, high input impedance, low input capacitance, and fast switching speeds are desired.

**Applications**

- Motor control
- Converters
- Amplifiers
- Switches
- Power supply circuits
- Drivers (Relays, Hammers, Solenoids, Lamps, Memories, Displays, Bipolar Transistors, etc.)

**Package Options**

(Note 1)



**Absolute Maximum Ratings**

Drain-to-Source Voltage	BV <sub>DSS</sub>
Drain-to-Gate Voltage	BV <sub>DGS</sub>
Gate-to-Source Voltage	± 20V
Operating and Storage Temperature	-55°C to +150°C
Soldering Temperature*	300°C

\*Distance of 1.6 mm from case for 10 seconds.

**Thermal Characteristics**

T-39-09

Package	I <sub>D</sub> (continuous)*	I <sub>D</sub> (pulsed)*	Power Dissipation @ T <sub>C</sub> = 25°C	θ <sub>JC</sub> °C/W	θ <sub>JA</sub> °C/W	I <sub>DR</sub>	I <sub>DRM</sub> *
IRF510	4.0A	16.0A	20W	80	6.4	4.0A	16.0A
IRF511	4.0A	16.0A	20W	80	6.4	4.0A	16.0A
IRF512	3.5A	14.0A	20W	80	6.4	3.5A	14.0A
IRF513	3.5A	14.0A	20W	80	6.4	3.5A	14.0A

\*I<sub>D</sub> (continuous) is limited by max rated T<sub>J</sub>.

**Electrical Characteristics (@ 25°C unless otherwise specified)**

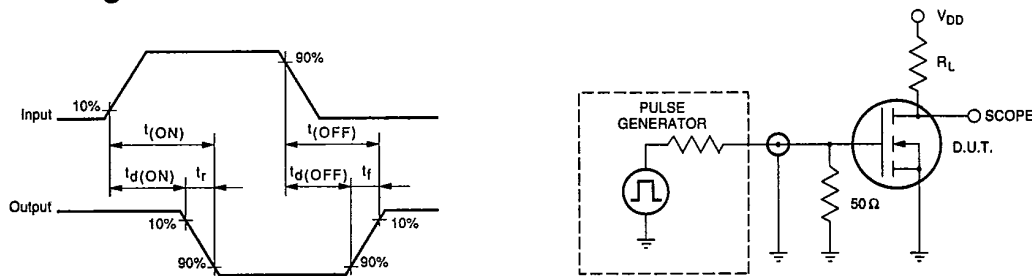
(Notes 1 and 2)

Symbol	Parameter	Min	Typ	Max	Unit	Conditions
BV <sub>DSS</sub>	Drain-to-Source Breakdown Voltage	IRF510, IRF512 100			V	V <sub>GS</sub> = 0, I <sub>D</sub> = 250μA
		IRF511, IRF513 60				
V <sub>GS(th)</sub>	Gate Threshold Voltage	2.0		4.0	V	V <sub>GS</sub> = V <sub>DS</sub> , I <sub>D</sub> = 250μA
I <sub>GSS</sub>	Gate Body Leakage			500	nA	V <sub>GS</sub> = ±20V, V <sub>DS</sub> = 0
I <sub>DSS</sub>	Zero Gate Voltage Drain Current			250 1000	μA	V <sub>GS</sub> = 0, V <sub>DS</sub> = Max Rating V <sub>GS</sub> = 0, V <sub>DS</sub> = 0.8 Max Rating T <sub>C</sub> = 125°C
I <sub>D(ON)</sub>	ON-State Drain Current	IRF510, IRF511 4.0			A	V <sub>GS</sub> = 10V V <sub>DS</sub> > I <sub>D(ON)</sub> × R <sub>DS(ON)</sub> Max Rating
		IRF512, IRF513 3.5				
R <sub>DS(ON)</sub>	Static Drain-to-Source ON-State Resistance			0.6 0.8	Ω	V <sub>GS</sub> = 10V, I <sub>D</sub> = 2.0A
		IRF510, IRF511				
		IRF512, IRF513				
G <sub>FS</sub>	Forward Transconductance	1.0	1.5		Ω	V <sub>DS</sub> > I <sub>D(ON)</sub> × R <sub>DS(ON)</sub> Max Rating I <sub>D</sub> = 2.0A
C <sub>ISS</sub>	Input Capacitance			150	pF	V <sub>GS</sub> = 0, V <sub>DS</sub> = 25V f = 1 MHz
C <sub>OSS</sub>	Common Source Output Capacitance			100		
C <sub>RSS</sub>	Reverse Transfer Capacitance			25		
t <sub>d(ON)</sub>	Turn-ON Delay Time			20	ns	V <sub>DD</sub> = 0.5BV <sub>DSS</sub> I <sub>D</sub> = 2.0A R <sub>S</sub> = 50Ω
t <sub>r</sub>	Rise Time			25		
t <sub>d(OFF)</sub>	Turn-OFF Delay Time			25		
t <sub>f</sub>	Fall Time			20		
V <sub>SD</sub>	Diode Forward Voltage Drop	IRF510, IRF511 2.5		2.0		
		IRF512, IRF513				V <sub>GS</sub> = 0, I <sub>SD</sub> = 4.0A V <sub>GS</sub> = 0, I <sub>SD</sub> = 3.5A
t <sub>rr</sub>	Reverse Recovery Time		230		ns	T <sub>J</sub> = 150°C, I <sub>SD</sub> = 4.0A, dI <sub>F/dt</sub> = 100A/μS

Note 1: All D.C. parameters 100% tested at 25°C unless otherwise stated. (Pulse test: 300μs pulse, 2% duty cycle.)

Note 2: All A.C. parameters sample tested.

**Switching Waveforms and Test Circuit**



This datasheet has been download from:

[www.datasheetcatalog.com](http://www.datasheetcatalog.com)

Datasheets for electronics components.

# LM2930

## 3-Terminal Positive Regulator

### General Description

The LM2930 3-terminal positive regulator features an ability to source 150 mA of output current with an input-output differential of 0.6V or less. Efficient use of low input voltages obtained, for example, from an automotive battery during cold crank conditions, allows 5V circuitry to be properly powered with supply voltages as low as 5.6V. Familiar regulator features such as current limit and thermal overload protection are also provided.

Designed originally for automotive applications, the LM2930 and all regulated circuitry are protected from reverse battery installations or 2 battery jumps. During line transients, such as a load dump (40V) when the input voltage to the regulator can momentarily exceed the specified maximum operating voltage, the regulator will automatically shut down to protect both internal circuits and the load. The LM2930 cannot be harmed by temporary mirror-image insertion.

Fixed outputs of 5V and 8V are available in the plastic TO-220 and TO-263 power packages.

### Features

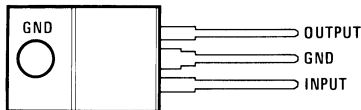
- Input-output differential less than 0.6V
- Output current in excess of 150 mA
- Reverse battery protection
- 40V load dump protection
- Internal short circuit current limit
- Internal thermal overload protection
- Mirror-image insertion protection
- P+ Product Enhancement tested

### Voltage Range

- |                |    |
|----------------|----|
| ■ LM2930T-5.0: | 5V |
| ■ LM2930T-8.0: | 8V |
| ■ LM2930S-5.0: | 5V |
| ■ LM2930S-8.0: | 8V |

### Connection Diagram

(TO-220)  
Plastic Package



00553901

Front View

Order Number LM2930T-5.0 or LM2930T-8.0  
See NS Package Number T03B

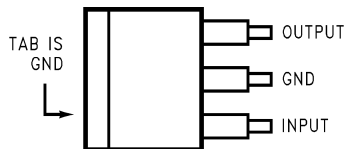


00553908

Side View

Order Number LM2930S-5.0 or LM2930S-8.0  
See NS Package Number TS3B

### (TO-263) Plastic Surface-Mount Package



00553907

Top View

**Absolute Maximum Ratings** (Note 1)

If Military/Aerospace specified devices are required, please contact the National Semiconductor Sales Office/Distributors for availability and specifications.

Input Voltage	
Operating Range	26V
Overvoltage Protection	40V
Reverse Voltage (100 ms)	-12V

Reverse Voltage (DC)	-6V
Internal Power Dissipation (Note 2)	Internally Limited
Operating Temperature Range	-40°C to +85°C
Maximum Junction Temperature	125°C
Storage Temperature Range	-65°C to +150°C
Lead Temp. (Soldering, 10 seconds)	230°C

**Electrical Characteristics** (Note 3)

LM2930-5.0  $V_{IN}=14V$ ,  $I_O=150\text{ mA}$ ,  $T_J=25^\circ\text{C}$  (Note 6),  $C_2=10\text{ }\mu\text{F}$ , unless otherwise specified

Parameter	Conditions	Typ	Tested Limit (Note 4)	Design Limit (Note 5)	Unit
Output Voltage		5	5.3 4.7		$V_{MAX}$ $V_{MIN}$
	$6V \leq V_{IN} \leq 26V$ , $5\text{ mA} \leq I_O \leq 150\text{ mA}$ $-40^\circ\text{C} \leq T_J \leq 125^\circ\text{C}$			5.5 4.5	$V_{MAX}$ $V_{MIN}$
Line Regulation	$9V \leq V_{IN} \leq 16V$ , $I_O=5\text{ mA}$	7	25		$\text{mV}_{MAX}$
	$6V \leq V_{IN} \leq 26V$ , $I_O=5\text{ mA}$	30	80		$\text{mV}_{MAX}$
Load Regulation	$5\text{ mA} \leq I_O \leq 150\text{ mA}$	14	50		$\text{mV}_{MAX}$
Output Impedance	$100\text{ mA}_{DC}$ & $10\text{ mA}_{rms}$ , 100 Hz–10 kHz	200			$\text{m}\Omega$
Quiescent Current	$I_O=10\text{ mA}$	4	7		$\text{mA}_{MAX}$
	$I_O=150\text{ mA}$	18	40		$\text{mA}_{MAX}$
Output Noise Voltage	10 Hz–100 kHz	140			$\mu\text{V}_{rms}$
Long Term Stability		20			$\text{mV}/1000\text{ hr}$
Ripple Rejection	$f_O=120\text{ Hz}$	56			dB
Current Limit		400	700 150		$\text{mA}_{MAX}$ $\text{mA}_{MIN}$
Dropout Voltage	$I_O=150\text{ mA}$	0.32	0.6		$V_{MAX}$
Output Voltage Under Transient Conditions	$-12V \leq V_{IN} \leq 40V$ , $R_L=100\Omega$		5.5 -0.3		$V_{MAX}$ $V_{MIN}$

**Electrical Characteristics** (Note 3)

LM2930-8.0 ( $V_{IN}=14V$ ,  $I_O=150\text{ mA}$ ,  $T_J=25^\circ\text{C}$  (Note 6),  $C_2=10\text{ }\mu\text{F}$ , unless otherwise specified)

Parameter	Conditions	Typ	Tested Limit (Note 4)	Design Limit (Note 5)	Unit
Output Voltage		8	8.5 7.5		$V_{MAX}$ $V_{MIN}$
	$9.4V \leq V_{IN} \leq 26V$ , $5\text{ mA} \leq I_O \leq 150\text{ mA}$ , $-40^\circ\text{C} \leq T_J \leq 125^\circ\text{C}$			8.8 7.2	$V_{MAX}$ $V_{MIN}$
Line Regulation	$9.4V \leq V_{IN} \leq 16V$ , $I_O=5\text{ mA}$	12	50		$\text{mV}_{MAX}$
	$9.4V \leq V_{IN} \leq 26V$ , $I_O=5\text{ mA}$	50	100		$\text{mV}_{MAX}$
Load Regulation	$5\text{ mA} \leq I_O \leq 150\text{ mA}$	25	50		$\text{mV}_{MAX}$
Output Impedance	$100\text{ mA}_{DC}$ & $10\text{ mA}_{rms}$ , 100 Hz–10 kHz	300			$\text{m}\Omega$
Quiescent Current	$I_O=10\text{ mA}$	4	7		$\text{mA}_{MAX}$
	$I_O=150\text{ mA}$	18	40		$\text{mA}_{MAX}$
Output Noise Voltage	10 Hz–100 kHz	170			$\mu\text{V}_{rms}$
Long Term Stability		30			$\text{mV}/1000\text{ hr}$
Ripple Rejection	$f_O=120\text{ Hz}$	52			dB



## Electrical Characteristics (Note 3) (Continued)

LM2930-8.0 ( $V_{IN}=14V$ ,  $I_O=150\text{ mA}$ ,  $T_J=25^\circ\text{C}$  (Note 6),  $C_2=10\ \mu\text{F}$ , unless otherwise specified)

Parameter	Conditions	Typ	Tested Limit (Note 4)	Design Limit (Note 5)	Unit
Current Limit		400	700 150		$\text{mA}_{\text{MAX}}$ $\text{mA}_{\text{MIN}}$
Dropout Voltage	$I_O=150\text{ mA}$	0.32	0.6		$V_{\text{MAX}}$
Output Voltage Under Transient Conditions	$-12V \leq V_{IN} \leq 40V$ , $R_L=100\Omega$		8.8 -0.3		$V_{\text{MAX}}$ $V_{\text{MIN}}$

**Note 1:** Absolute Maximum Ratings indicate limits beyond which damage to the device may occur. Operating ratings indicate conditions for which the device is functional, but do not guarantee specific performance limits. Electrical Characteristics state DC and AC electrical specifications under particular test conditions which guarantee specific performance limits. This assumes that the device is within the Operating Ratings. Specifications are not guaranteed for parameters where no limit is given, however, the typical value is a good indication of device performance.

**Note 2:** Thermal resistance without a heat sink for junction to case temperature is  $3^\circ\text{C/W}$  and for case to ambient temperature is  $50^\circ\text{C/W}$  for the TO-220,  $73^\circ\text{C/W}$  for the TO-263. If the TO-263 package is used, the thermal resistance can be reduced by increasing the P.C. board copper area thermally connected to the package. Using 0.5 square inches of copper area,  $\theta_{JA}$  is  $50^\circ\text{C/W}$ ; with 1 square inch of copper area,  $\theta_{JA}$  is  $37^\circ\text{C/W}$ ; and with 1.6 or more square inches of copper area,  $\theta_{JA}$  is  $32^\circ\text{C/W}$ .

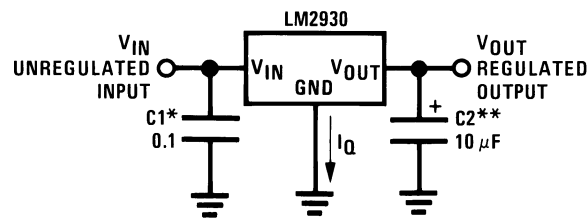
**Note 3:** All characteristics are measured with a capacitor across the input of  $0.1\ \mu\text{F}$  and a capacitor across the output of  $10\ \mu\text{F}$ . All characteristics except noise voltage and ripple rejection ratio are measured using pulse techniques ( $t_{PW} \leq 10\text{ ms}$ , duty cycle  $\leq 5\%$ ). Output voltage changes due to changes in internal temperature must be taken into account separately.

**Note 4:** Guaranteed and 100% production tested.

**Note 5:** Guaranteed (but not 100% production tested) over the operating temperature and input current ranges. These limits are not used to calculate outgoing quality levels.

**Note 6:** To ensure constant junction temperature, low duty cycle pulse testing is used.

## Typical Application

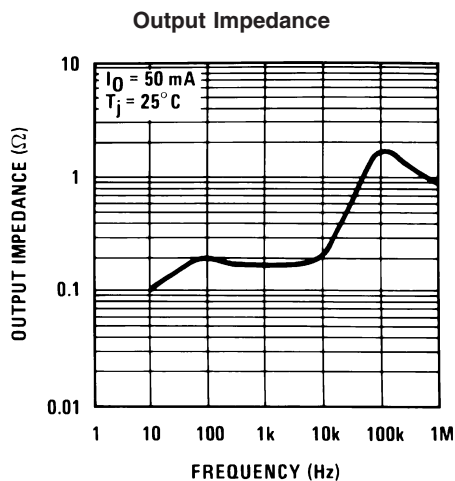


00553905

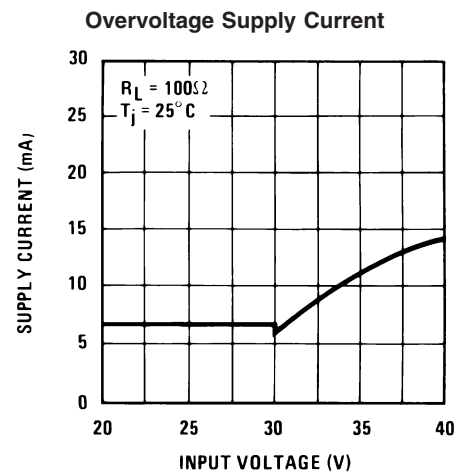
\*Required if regulator is located far from power supply filter.

\*\* $C_{OUT}$  must be at least  $10\ \mu\text{F}$  to maintain stability. May be increased without bound to maintain regulation during transients. Locate as close as possible to the regulator. This capacitor must be rated over the same operating temperature range as the regulator. The equivalent series resistance (ESR) of this capacitor should be less than  $1\ \Omega$  over the expected operating temperature range.

## Typical Performance Characteristics



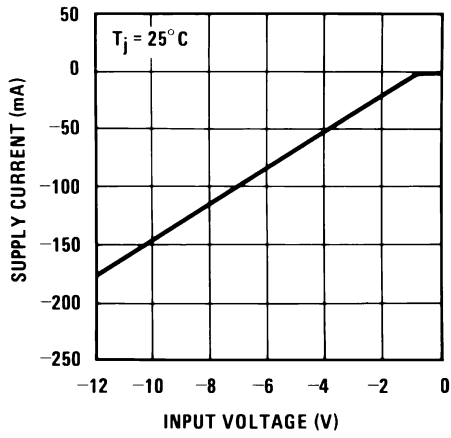
00553911



00553912

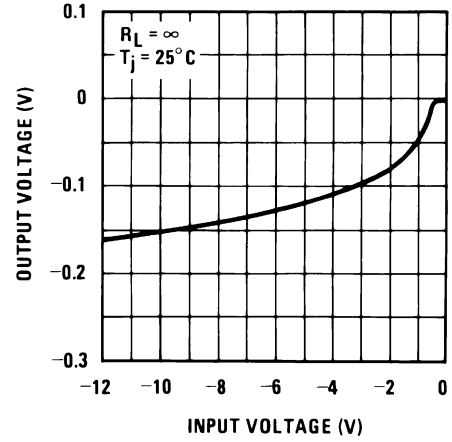
Typical Performance Characteristics (Continued)

Reverse Supply Current



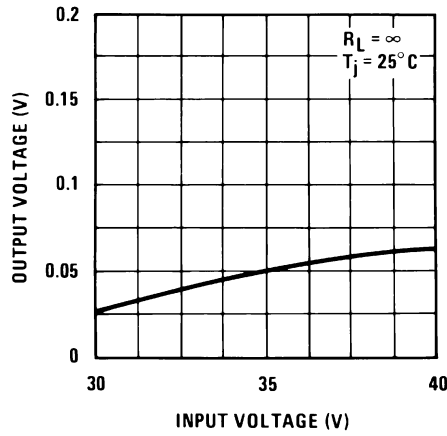
00553913

Output at Reverse Supply



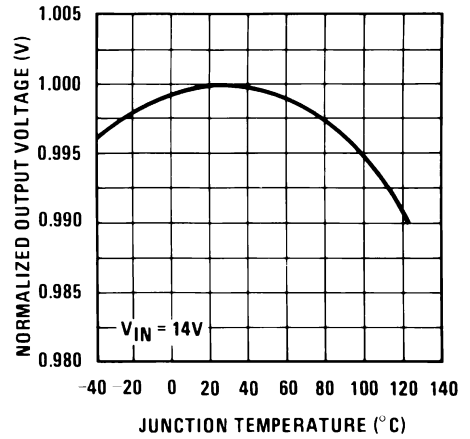
00553914

Output at Overvoltage



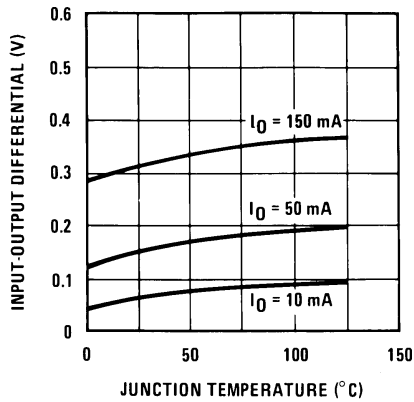
00553915

Output Voltage (Normalized to 1V at  $T_j=25^\circ\text{C}$ )



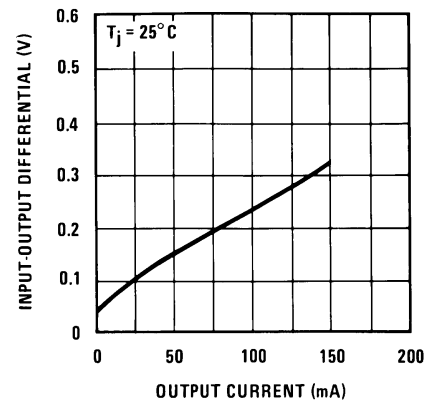
00553916

Dropout Voltage



00553917

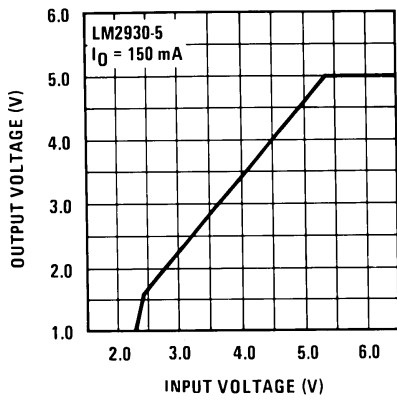
Dropout Voltage



00553918

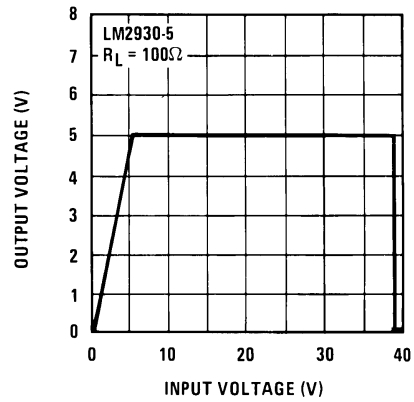
# Typical Performance Characteristics (Continued)

Low Voltage Behavior



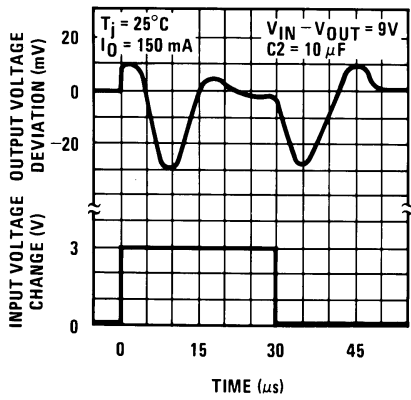
00553919

High Voltage Behavior



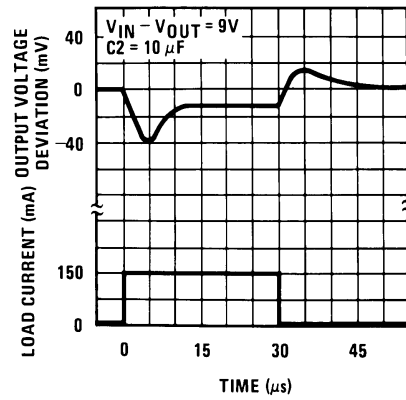
00553920

Line Transient Response



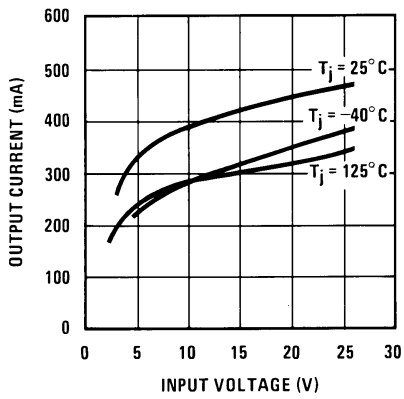
00553921

Load Transient Response



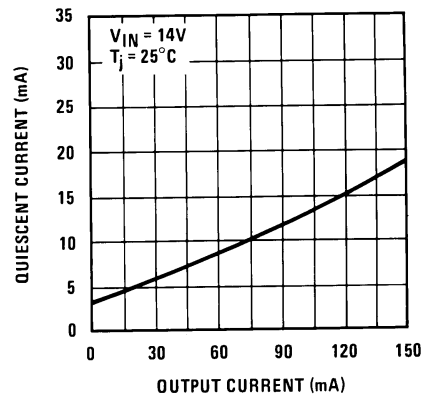
00553922

Peak Output Current



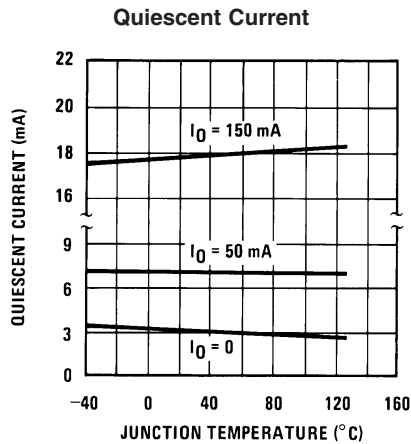
00553923

Quiescent Current

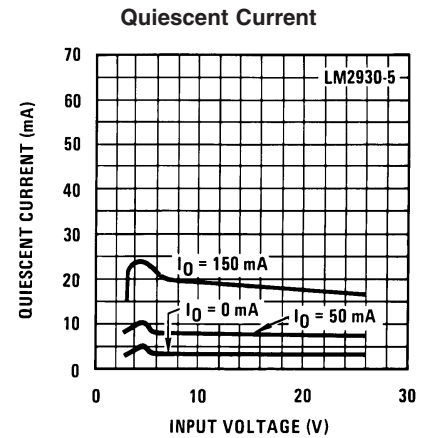


00553924

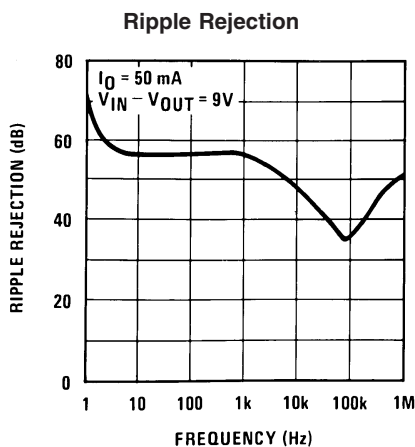
## Typical Performance Characteristics (Continued)



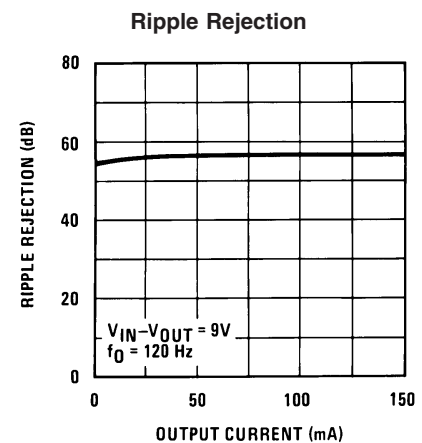
00553925



00553926



00553927



00553928

## Definition of Terms

**Dropout Voltage:** The input-output voltage differential at which the circuit ceases to regulate against further reduction in input voltage. Measured when the output voltage has dropped 100 mV from the nominal value obtained at 14V input, dropout voltage is dependent upon load current and junction temperature.

**Input Voltage:** The DC voltage applied to the input terminals with respect to ground.

**Input-Output Differential:** The voltage difference between the unregulated input voltage and the regulated output voltage for which the regulator will operate.

**Line Regulation:** The change in output voltage for a change in the input voltage. The measurement is made under conditions of low dissipation or by using pulse techniques such that the average chip temperature is not significantly affected.

**Load Regulation:** The change in output voltage for a change in load current at constant chip temperature.

**Long Term Stability:** Output voltage stability under accelerated life-test conditions after 1000 hours with maximum rated voltage and junction temperature.

**Output Noise Voltage:** The rms AC voltage at the output, with constant load and no input ripple, measured over a specified frequency range.

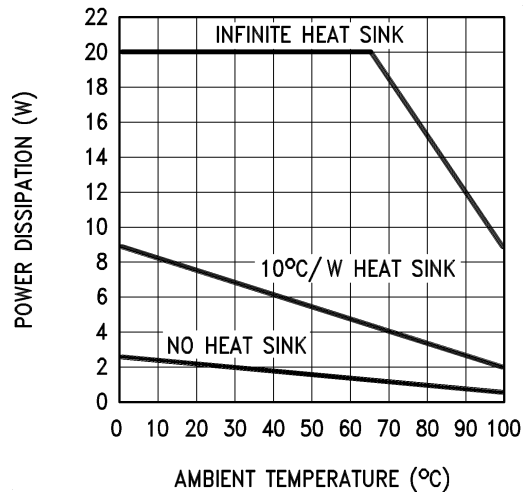
**Quiescent Current:** That part of the positive input current that does not contribute to the positive load current. The regulator ground lead current.

**Ripple Rejection:** The ratio of the peak-to-peak input ripple voltage to the peak-to-peak output ripple voltage.

**Temperature Stability of  $V_O$ :** The percentage change in output voltage for a thermal variation from room temperature to either temperature extreme.

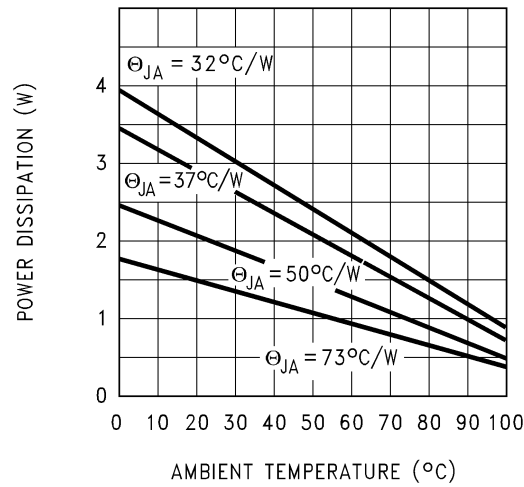
Definition of Terms (Continued)

Maximum Power Dissipation (TO-220)



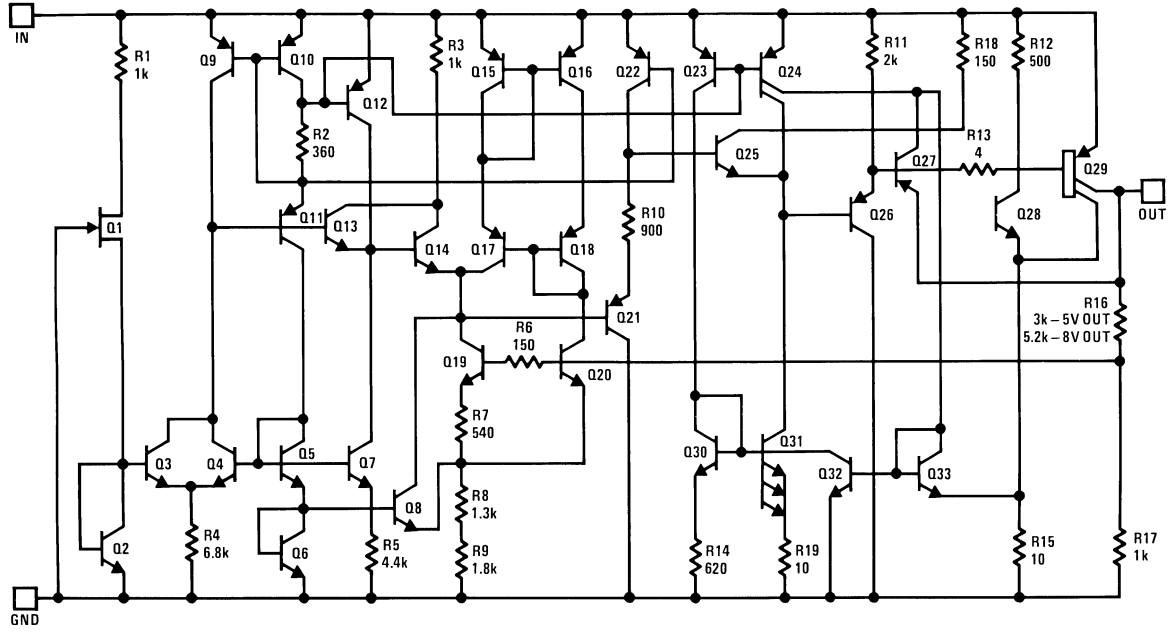
00553906

Maximum Power Dissipation (TO-263) (Note 2)



00553909

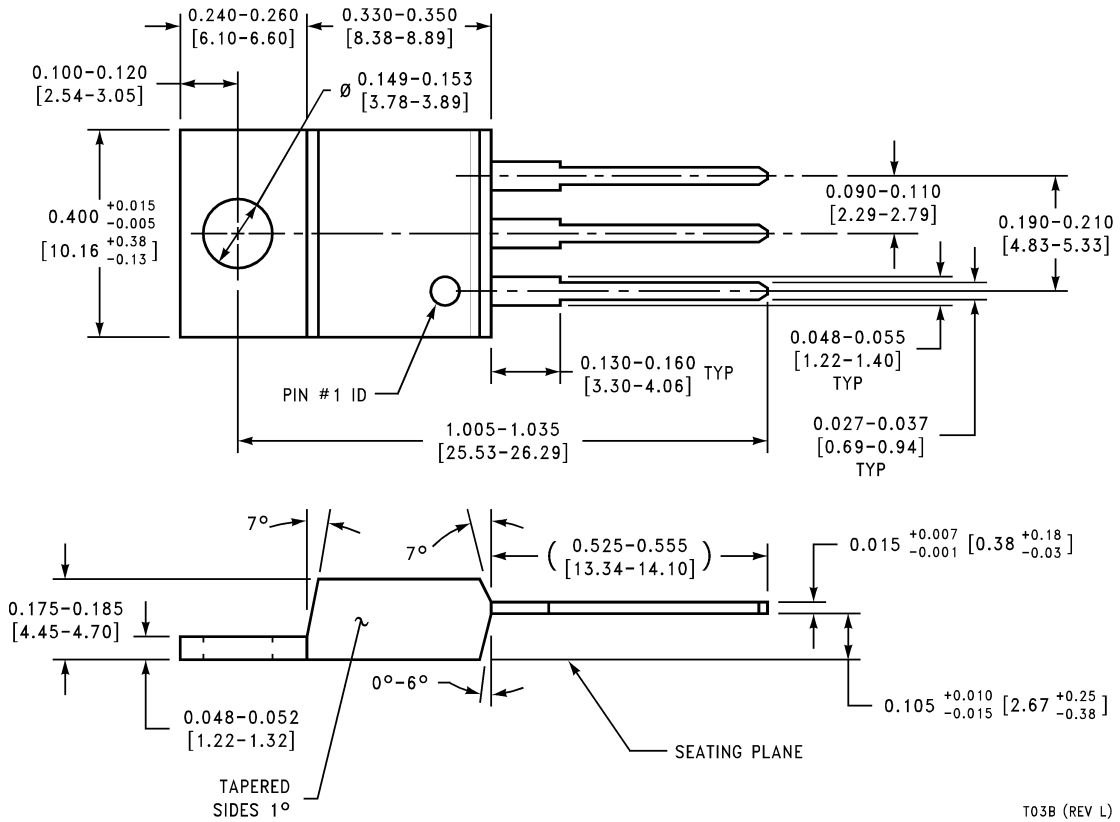
# Schematic Diagram



00553910

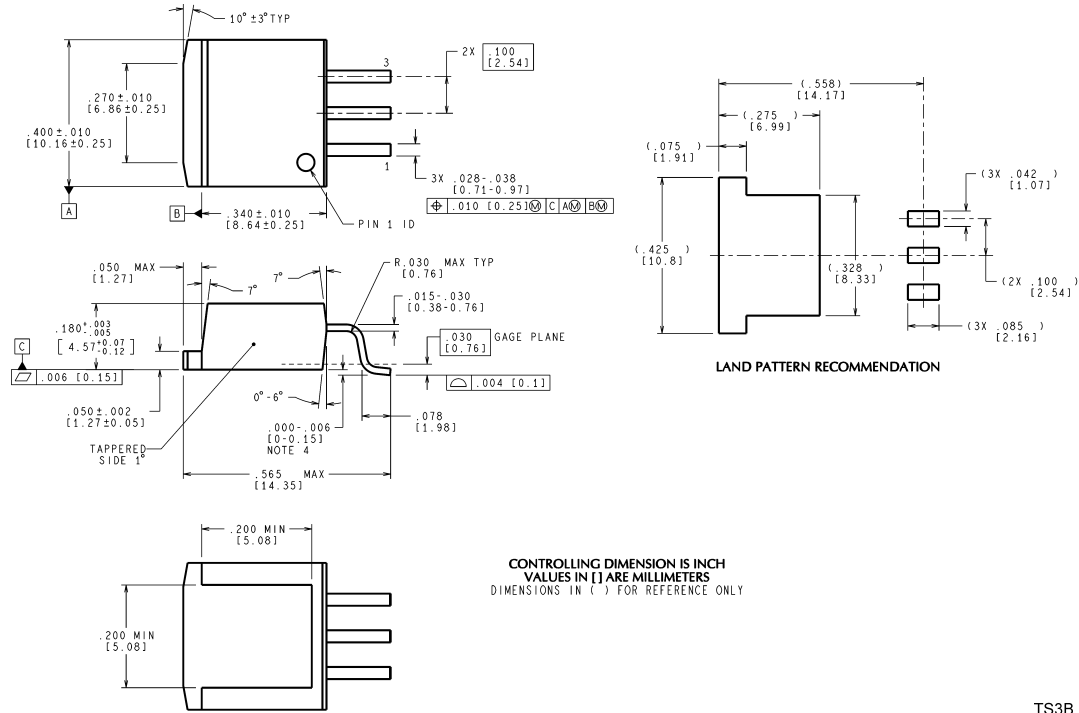
**Physical Dimensions** inches (millimeters)

unless otherwise noted



**TO-220 3-Lead Molded Package**  
**Order Number LM2930T-5.0 or LM2930T-8.0**  
**NS Package Number T03B**

**Physical Dimensions** inches (millimeters) unless otherwise noted (Continued)



**TO-263 3-Lead Plastic Surface Mount Package**  
**Order Number LM2930S-5.0 or LM2930S-8.0**  
**NS Package Number TS3B**

TS3B (Rev F)

National does not assume any responsibility for use of any circuitry described, no circuit patent licenses are implied and National reserves the right at any time without notice to change said circuitry and specifications.

For the most current product information visit us at [www.national.com](http://www.national.com).

**LIFE SUPPORT POLICY**


NATIONAL'S PRODUCTS ARE NOT AUTHORIZED FOR USE AS CRITICAL COMPONENTS IN LIFE SUPPORT DEVICES OR SYSTEMS WITHOUT THE EXPRESS WRITTEN APPROVAL OF THE PRESIDENT AND GENERAL COUNSEL OF NATIONAL SEMICONDUCTOR CORPORATION. As used herein:

1. Life support devices or systems are devices or systems which, (a) are intended for surgical implant into the body, or (b) support or sustain life, and whose failure to perform when properly used in accordance with instructions for use provided in the labeling, can be reasonably expected to result in a significant injury to the user.
2. A critical component is any component of a life support device or system whose failure to perform can be reasonably expected to cause the failure of the life support device or system, or to affect its safety or effectiveness.

**BANNED SUBSTANCE COMPLIANCE**

National Semiconductor manufactures products and uses packing materials that meet the provisions of the Customer Products Stewardship Specification (CSP-9-111C2) and the Banned Substances and Materials of Interest Specification (CSP-9-111S2) and contain no "Banned Substances" as defined in CSP-9-111S2.

Leadfree products are RoHS compliant.

 **National Semiconductor**  
**Americas Customer Support Center**  
 Email: [new.feedback@nsc.com](mailto:new.feedback@nsc.com)  
 Tel: 1-800-272-9959

**National Semiconductor**  
**Europe Customer Support Center**  
 Fax: +49 (0) 180-530 85 86  
 Email: [europe.support@nsc.com](mailto:europe.support@nsc.com)  
 Deutsch Tel: +49 (0) 69 9508 6208  
 English Tel: +44 (0) 870 24 0 2171  
 Français Tel: +33 (0) 1 41 91 8790

**National Semiconductor**  
**Asia Pacific Customer Support Center**  
 Email: [ap.support@nsc.com](mailto:ap.support@nsc.com)

**National Semiconductor**  
**Japan Customer Support Center**  
 Fax: 81-3-5639-7507  
 Email: [jpn.feedback@nsc.com](mailto:jpn.feedback@nsc.com)  
 Tel: 81-3-5639-7560



# LM111/LM211/LM311 Voltage Comparator

## 1.0 General Description

The LM111, LM211 and LM311 are voltage comparators that have input currents nearly a thousand times lower than devices like the LM106 or LM710. They are also designed to operate over a wider range of supply voltages: from standard  $\pm 15V$  op amp supplies down to the single 5V supply used for IC logic. Their output is compatible with RTL, DTL and TTL as well as MOS circuits. Further, they can drive lamps or relays, switching voltages up to 50V at currents as high as 50 mA.

Both the inputs and the outputs of the LM111, LM211 or the LM311 can be isolated from system ground, and the output can drive loads referred to ground, the positive supply or the negative supply. Offset balancing and strobe capability are provided and outputs can be wire OR'ed. Although slower than the LM106 and LM710 (200 ns response time vs 40 ns)

the devices are also much less prone to spurious oscillations. The LM111 has the same pin configuration as the LM106 and LM710.

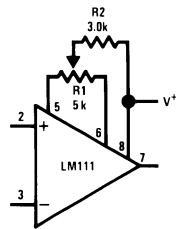
The LM211 is identical to the LM111, except that its performance is specified over a  $-25^{\circ}C$  to  $+85^{\circ}C$  temperature range instead of  $-55^{\circ}C$  to  $+125^{\circ}C$ . The LM311 has a temperature range of  $0^{\circ}C$  to  $+70^{\circ}C$ .

## 2.0 Features

- Operates from single 5V supply
- Input current: 150 nA max. over temperature
- Offset current: 20 nA max. over temperature
- Differential input voltage range:  $\pm 30V$
- Power consumption: 135 mW at  $\pm 15V$

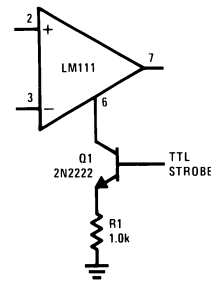
## 3.0 Typical Applications (Note 3)

**Offset Balancing**



00570436

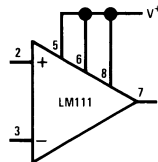
**Strobing**



00570437

**Note:** Do Not Ground Strobe Pin. Output is turned off when current is pulled from Strobe Pin.

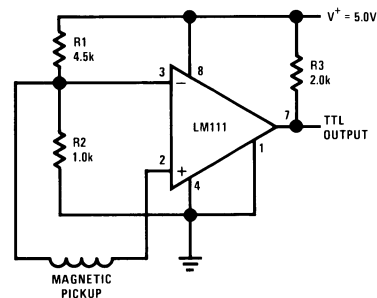
**Increasing Input Stage Current (Note 1)**



00570438

**Note 1:** Increases typical common mode slew from  $7.0V/\mu s$  to  $18V/\mu s$ .

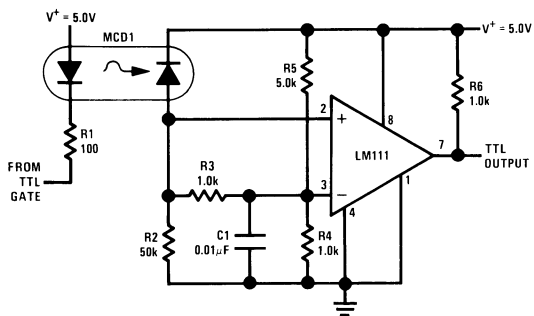
**Detector for Magnetic Transducer**



00570439

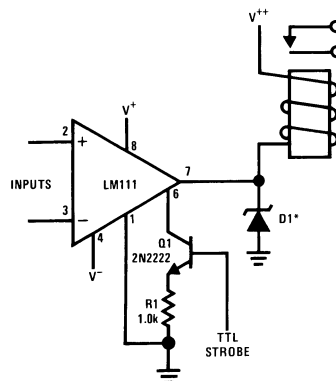
### 3.0 Typical Applications (Note 3) (Continued)

**Digital Transmission Isolator**



00570440

**Relay Driver with Strobe**

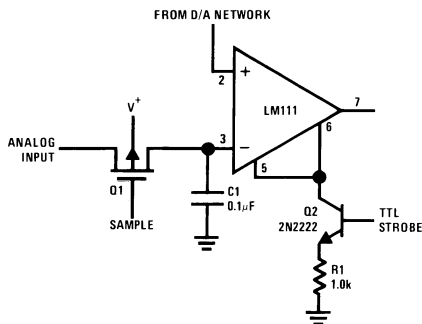


00570441

\*Absorbs inductive kickback of relay and protects IC from severe voltage transients on V<sup>+</sup> line.

**Note:** Do Not Ground Strobe Pin.

**Strobing off Both Input and Output Stages (Note 2)**



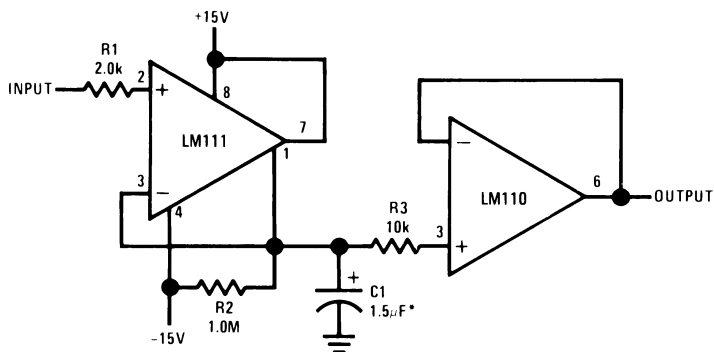
00570442

**Note:** Do Not Ground Strobe Pin.

**Note 2:** Typical input current is 50 pA with inputs strobed off.

**Note 3:** Pin connections shown on schematic diagram and typical applications are for H08 metal can package.

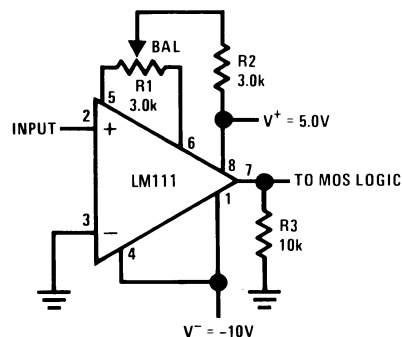
**Positive Peak Detector**



00570423

\*Solid tantalum

**Zero Crossing Detector Driving MOS Logic**



00570424

## 4.0 Absolute Maximum Ratings for the LM111/LM211 (Note 10)

If Military/Aerospace specified devices are required, please contact the National Semiconductor Sales Office/Distributors for availability and specifications.

Total Supply Voltage ( $V_{S4}$ )	36V
Output to Negative Supply Voltage ( $V_{74}$ )	50V
Ground to Negative Supply Voltage ( $V_{14}$ )	30V
Differential Input Voltage	$\pm 30V$
Input Voltage (Note 4)	$\pm 15V$
Output Short Circuit Duration	10 sec
Operating Temperature Range	

LM111	-55°C to 125°C
LM211	-25°C to 85°C
Lead Temperature (Soldering, 10 sec)	260°C
Voltage at Strobe Pin	$V^+ - 5V$
Soldering Information	
Dual-In-Line Package	
Soldering (10 seconds)	260°C
Small Outline Package	
Vapor Phase (60 seconds)	215°C
Infrared (15 seconds)	220°C
See AN-450 "Surface Mounting Methods and Their Effect on Product Reliability" for other methods of soldering surface mount devices.	
ESD Rating (Note 11)	300V

## Electrical Characteristics (Note 6) for the LM111 and LM211

Parameter	Conditions	Min	Typ	Max	Units
Input Offset Voltage (Note 7)	$T_A=25^\circ\text{C}$ , $R_S \leq 50\text{k}$		0.7	3.0	mV
Input Offset Current	$T_A=25^\circ\text{C}$		4.0	10	nA
Input Bias Current	$T_A=25^\circ\text{C}$		60	100	nA
Voltage Gain	$T_A=25^\circ\text{C}$	40	200		V/mV
Response Time (Note 8)	$T_A=25^\circ\text{C}$		200		ns
Saturation Voltage	$V_{IN} \leq -5\text{ mV}$ , $I_{OUT} = 50\text{ mA}$ $T_A=25^\circ\text{C}$		0.75	1.5	V
Strobe ON Current (Note 9)	$T_A=25^\circ\text{C}$		2.0	5.0	mA
Output Leakage Current	$V_{IN} \geq 5\text{ mV}$ , $V_{OUT} = 35V$ $T_A=25^\circ\text{C}$ , $I_{STROBE} = 3\text{ mA}$		0.2	10	nA
Input Offset Voltage (Note 7)	$R_S \leq 50\text{ k}$			4.0	mV
Input Offset Current (Note 7)				20	nA
Input Bias Current				150	nA
Input Voltage Range	$V^+ = 15V$ , $V^- = -15V$ , Pin 7 Pull-Up May Go To 5V	-14.5	13.8, -14.7	13.0	V
Saturation Voltage	$V^+ \geq 4.5V$ , $V^- = 0$ $V_{IN} \leq -6\text{ mV}$ , $I_{OUT} \leq 8\text{ mA}$		0.23	0.4	V
Output Leakage Current	$V_{IN} \geq 5\text{ mV}$ , $V_{OUT} = 35V$		0.1	0.5	$\mu\text{A}$
Positive Supply Current	$T_A=25^\circ\text{C}$		5.1	6.0	mA
Negative Supply Current	$T_A=25^\circ\text{C}$		4.1	5.0	mA

**Note 4:** This rating applies for  $\pm 15$  supplies. The positive input voltage limit is 30V above the negative supply. The negative input voltage limit is equal to the negative supply voltage or 30V below the positive supply, whichever is less.

**Note 5:** The maximum junction temperature of the LM111 is 150°C, while that of the LM211 is 110°C. For operating at elevated temperatures, devices in the H08 package must be derated based on a thermal resistance of 165°C/W, junction to ambient, or 20°C/W, junction to case. The thermal resistance of the dual-in-line package is 110°C/W, junction to ambient.

**Note 6:** These specifications apply for  $V_S = \pm 15V$  and Ground pin at ground, and  $-55^\circ\text{C} \leq T_A \leq +125^\circ\text{C}$ , unless otherwise stated. With the LM211, however, all temperature specifications are limited to  $-25^\circ\text{C} \leq T_A \leq +85^\circ\text{C}$ . The offset voltage, offset current and bias current specifications apply for any supply voltage from a single 5V supply up to  $\pm 15V$  supplies.

**Note 7:** The offset voltages and offset currents given are the maximum values required to drive the output within a volt of either supply with a 1 mA load. Thus, these parameters define an error band and take into account the worst-case effects of voltage gain and  $R_S$ .

**Note 8:** The response time specified (see definitions) is for a 100 mV input step with 5 mV overdrive.

**Note 9:** This specification gives the range of current which must be drawn from the strobe pin to ensure the output is properly disabled. Do not short the strobe pin to ground; it should be current driven at 3 to 5 mA.

**Note 10:** Refer to RETS111X for the LM111H, LM111J and LM111J-8 military specifications.

**Note 11:** Human body model, 1.5 k $\Omega$  in series with 100 pF.

## 5.0 Absolute Maximum Ratings for the LM311 (Note 12)

If Military/Aerospace specified devices are required, please contact the National Semiconductor Sales Office/Distributors for availability and specifications.

Total Supply Voltage ( $V_{S4}$ )	36V
Output to Negative Supply Voltage ( $V_{74}$ )	40V
Ground to Negative Supply Voltage ( $V_{14}$ )	30V
Differential Input Voltage	$\pm 30V$
Input Voltage (Note 13)	$\pm 15V$
Power Dissipation (Note 14)	500 mW
ESD Rating (Note 19)	300V

Output Short Circuit Duration	10 sec
Operating Temperature Range	0° to 70°C
Storage Temperature Range	-65°C to 150°C
Lead Temperature (soldering, 10 sec)	260°C
Voltage at Strobe Pin	$V^+ - 5V$
Soldering Information	
Dual-In-Line Package	
Soldering (10 seconds)	260°C
Small Outline Package	
Vapor Phase (60 seconds)	215°C
Infrared (15 seconds)	220°C
See AN-450 "Surface Mounting Methods and Their Effect on Product Reliability" for other methods of soldering surface mount devices.	

## Electrical Characteristics (Note 15) for the LM311

Parameter	Conditions	Min	Typ	Max	Units
Input Offset Voltage (Note 16)	$T_A = 25^\circ C, R_S \leq 50k$		2.0	7.5	mV
Input Offset Current (Note 16)	$T_A = 25^\circ C$		6.0	50	nA
Input Bias Current	$T_A = 25^\circ C$		100	250	nA
Voltage Gain	$T_A = 25^\circ C$	40	200		V/mV
Response Time (Note 17)	$T_A = 25^\circ C$		200		ns
Saturation Voltage	$V_{IN} \leq -10$ mV, $I_{OUT} = 50$ mA $T_A = 25^\circ C$		0.75	1.5	V
Strobe ON Current (Note 18)	$T_A = 25^\circ C$		2.0	5.0	mA
Output Leakage Current	$V_{IN} \geq 10$ mV, $V_{OUT} = 35V$ $T_A = 25^\circ C, I_{STROBE} = 3$ mA $V^- = \text{Pin } 1 = -5V$		0.2	50	nA
Input Offset Voltage (Note 16)	$R_S \leq 50K$			10	mV
Input Offset Current (Note 16)				70	nA
Input Bias Current				300	nA
Input Voltage Range		-14.5	13.8, -14.7	13.0	V
Saturation Voltage	$V^+ \geq 4.5V, V^- = 0$ $V_{IN} \leq -10$ mV, $I_{OUT} \leq 8$ mA		0.23	0.4	V
Positive Supply Current	$T_A = 25^\circ C$		5.1	7.5	mA
Negative Supply Current	$T_A = 25^\circ C$		4.1	5.0	mA

**Note 12:** "Absolute Maximum Ratings indicate limits beyond which damage to the device may occur. Operating Ratings indicate conditions for which the device is functional, but do not guarantee specific performance limits."

**Note 13:** This rating applies for  $\pm 15V$  supplies. The positive input voltage limit is 30V above the negative supply. The negative input voltage limit is equal to the negative supply voltage or 30V below the positive supply, whichever is less.

**Note 14:** The maximum junction temperature of the LM311 is 110°C. For operating at elevated temperature, devices in the H08 package must be derated based on a thermal resistance of 165°C/W, junction to ambient, or 20°C/W, junction to case. The thermal resistance of the dual-in-line package is 100°C/W, junction to ambient.

**Note 15:** These specifications apply for  $V_S = \pm 15V$  and Pin 1 at ground, and  $0^\circ C < T_A < +70^\circ C$ , unless otherwise specified. The offset voltage, offset current and bias current specifications apply for any supply voltage from a single 5V supply up to  $\pm 15V$  supplies.

**Note 16:** The offset voltages and offset currents given are the maximum values required to drive the output within a volt of either supply with 1 mA load. Thus, these parameters define an error band and take into account the worst-case effects of voltage gain and  $R_S$ .

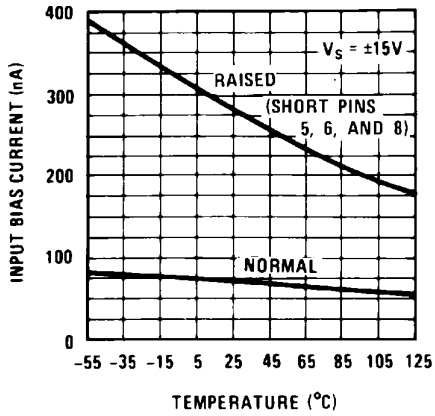
**Note 17:** The response time specified (see definitions) is for a 100 mV input step with 5 mV overdrive.

**Note 18:** This specification gives the range of current which must be drawn from the strobe pin to ensure the output is properly disabled. Do not short the strobe pin to ground; it should be current driven at 3 to 5 mA.

**Note 19:** Human body model, 1.5 k $\Omega$  in series with 100 pF.

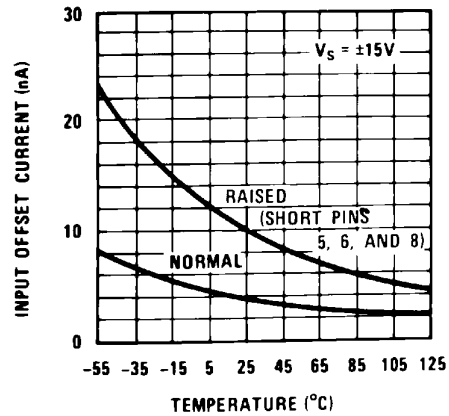
## 6.0 LM111/LM211 Typical Performance Characteristics

Input Bias Current



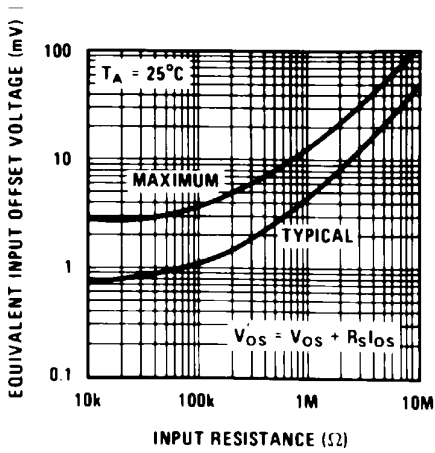
00570443

Input Bias Current



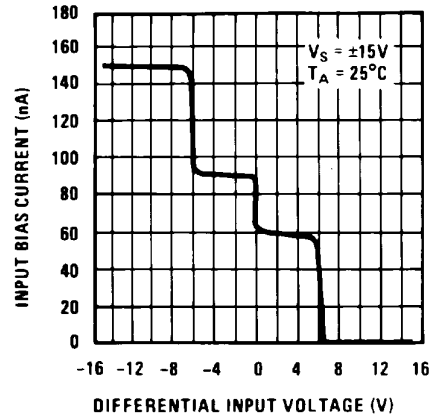
00570444

Input Bias Current



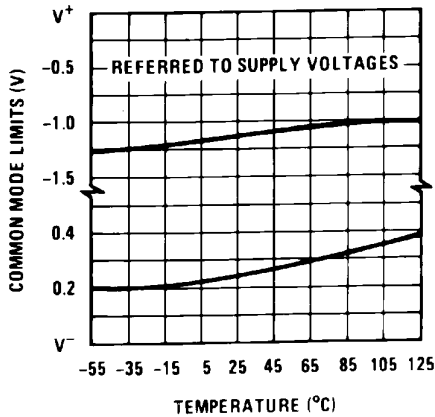
00570445

Input Bias Current



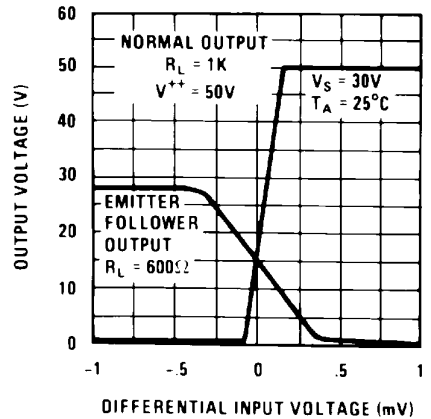
00570446

Input Bias Current



00570447

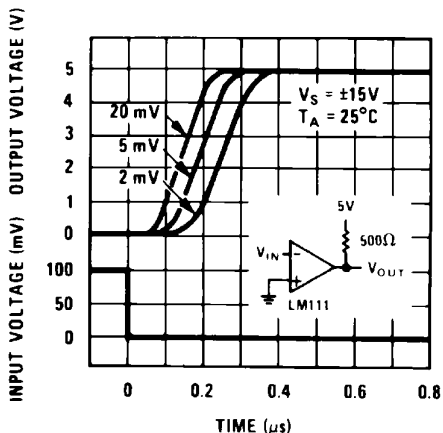
Input Bias Current



00570448

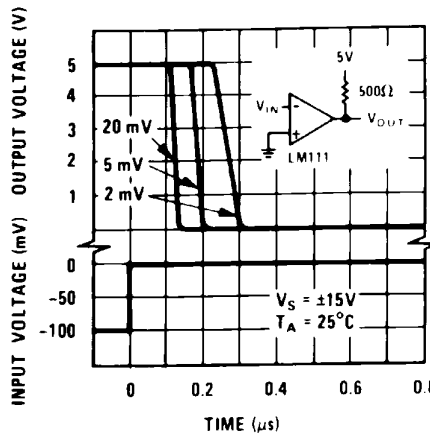
## 6.0 LM111/LM211 Typical Performance Characteristics (Continued)

Input Bias Current  
Input Overdrives



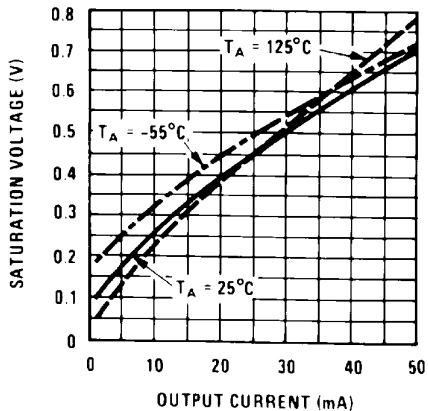
00570449

Input Bias Current  
Input Overdrives



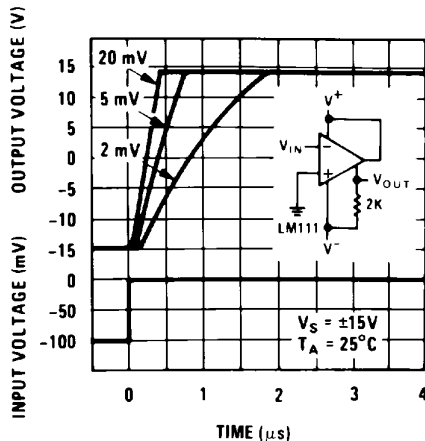
00570450

Input Bias Current



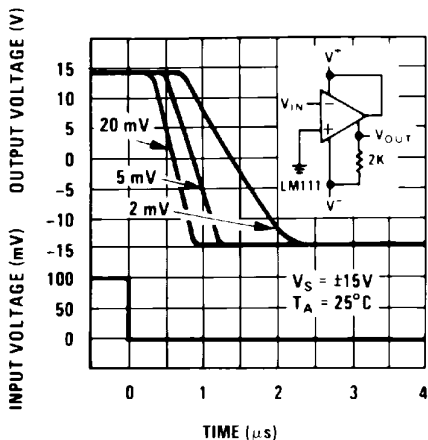
00570451

Response Time for Various  
Input Overdrives



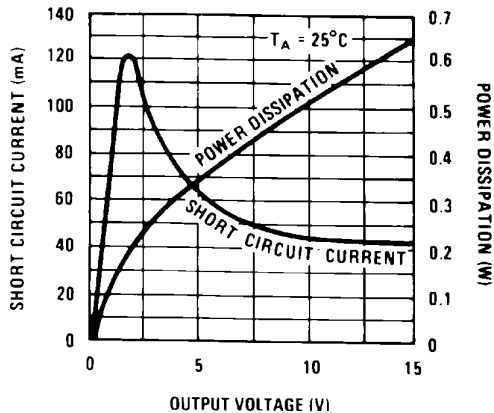
00570452

Response Time for Various  
Input Overdrives



00570453

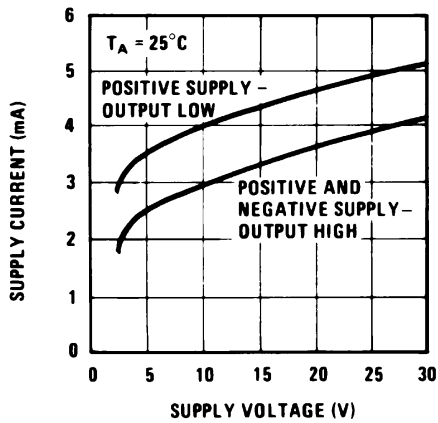
Output Limiting Characteristics



00570454

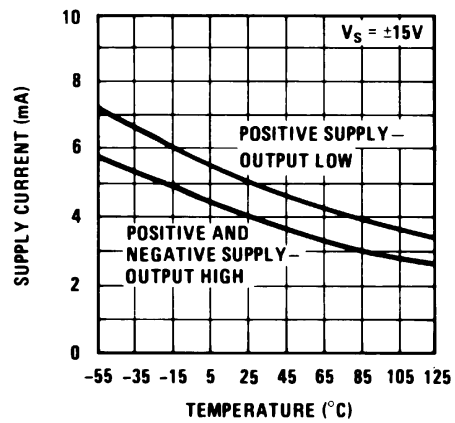
## 6.0 LM111/LM211 Typical Performance Characteristics (Continued)

Supply Current



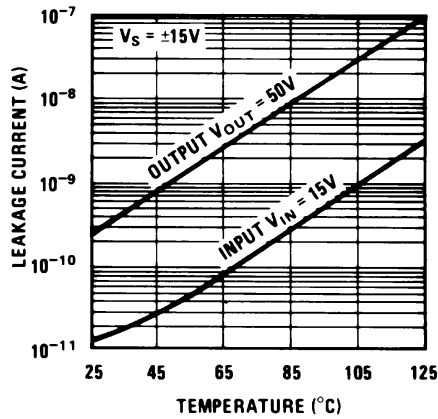
00570455

Supply Current



00570456

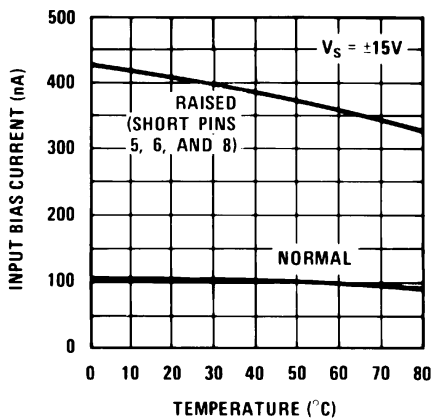
Leakage Currents



00570457

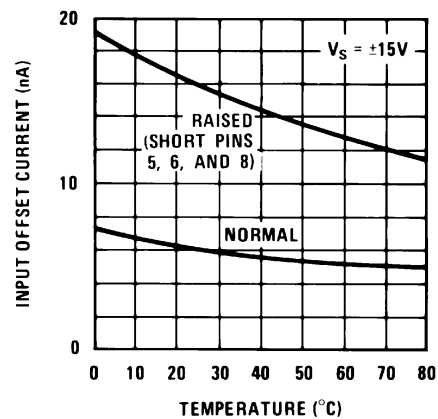
## 7.0 LM311 Typical Performance Characteristics

Input Bias Current



00570458

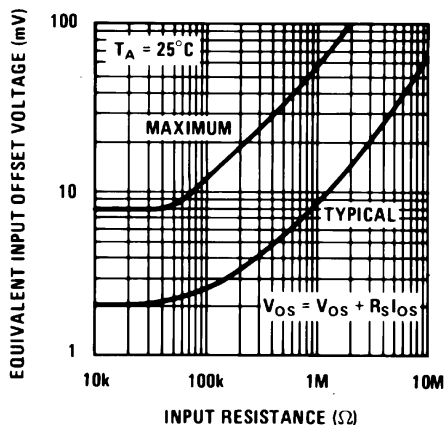
Input Offset Current



00570459

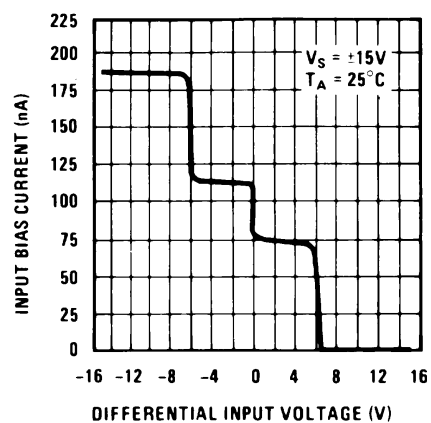
## 7.0 LM311 Typical Performance Characteristics (Continued)

Offset Error



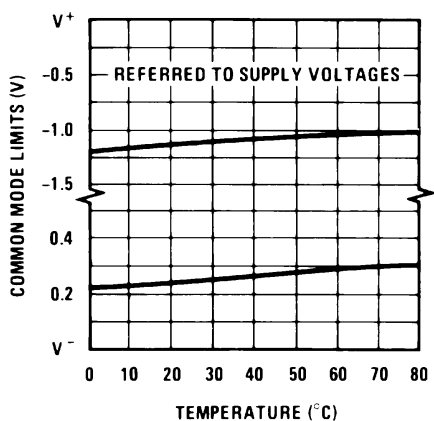
00570460

Input Characteristics



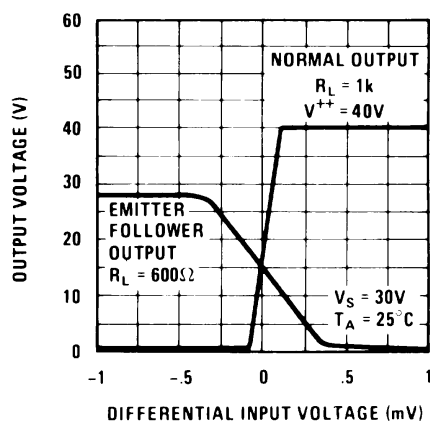
00570461

Common Mode Limits



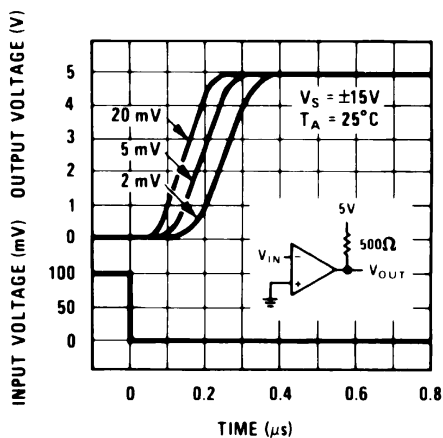
00570462

Transfer Function



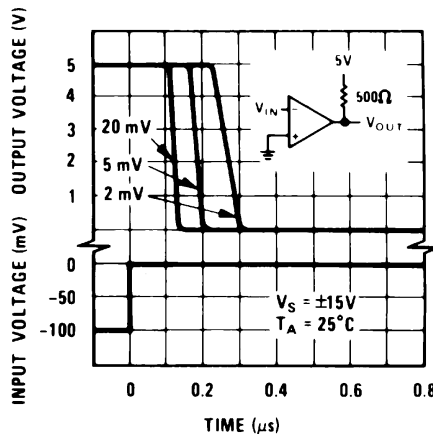
00570463

Response Time for Various Input Overdrives



00570464

Response Time for Various Input Overdrives

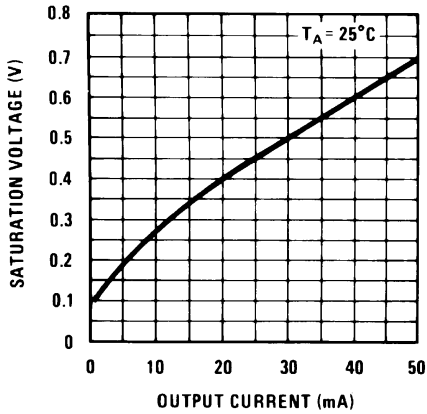


00570465



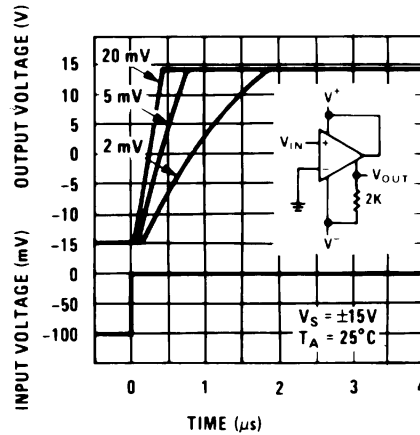
# 7.0 LM311 Typical Performance Characteristics (Continued)

Output Saturation Voltage



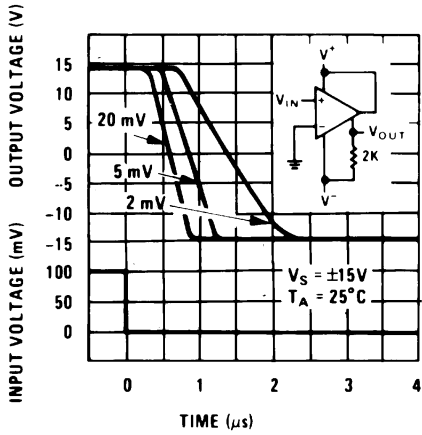
00570466

Response Time for Various Input Overdrives



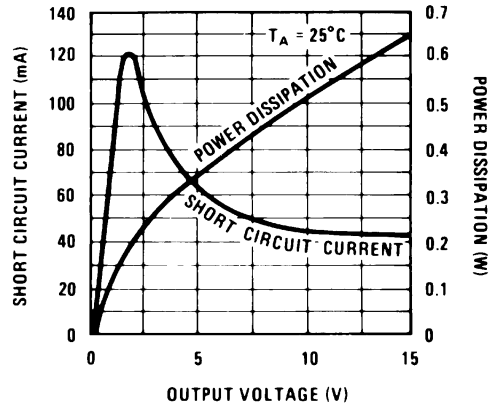
00570467

Response Time for Various Input Overdrives



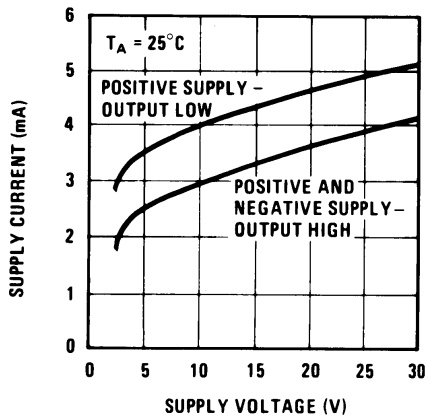
00570468

Output Limiting Characteristics



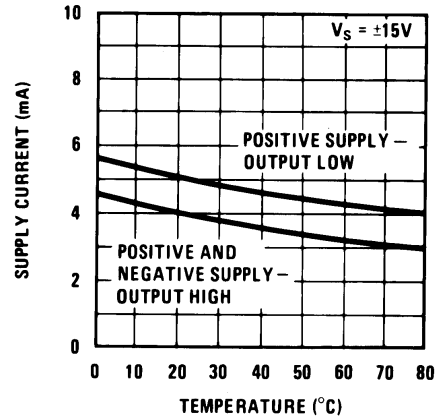
00570469

Supply Current



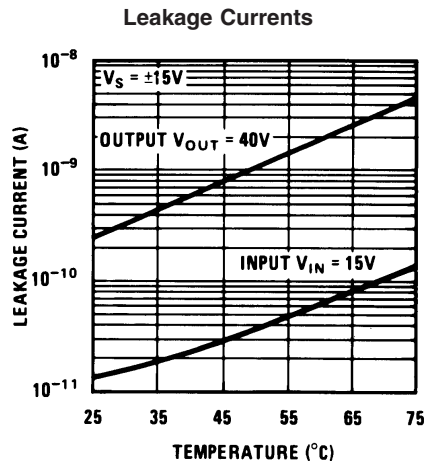
00570470

Supply Current



00570471

## 7.0 LM311 Typical Performance Characteristics (Continued)



00570472

## 8.0 Application Hints

### 8.1 CIRCUIT TECHNIQUES FOR AVOIDING OSCILLATIONS IN COMPARATOR APPLICATIONS

When a high-speed comparator such as the LM111 is used with fast input signals and low source impedances, the output response will normally be fast and stable, assuming that the power supplies have been bypassed (with 0.1  $\mu$ F disc capacitors), and that the output signal is routed well away from the inputs (pins 2 and 3) and also away from pins 5 and 6.

However, when the input signal is a voltage ramp or a slow sine wave, or if the signal source impedance is high (1 k $\Omega$  to 100 k $\Omega$ ), the comparator may burst into oscillation near the crossing-point. This is due to the high gain and wide bandwidth of comparators like the LM111. To avoid oscillation or instability in such a usage, several precautions are recommended, as shown in *Figure 1* below.

1. The trim pins (pins 5 and 6) act as unwanted auxiliary inputs. If these pins are not connected to a trim-pot, they should be shorted together. If they are connected to a trim-pot, a 0.01  $\mu$ F capacitor C1 between pins 5 and 6 will minimize the susceptibility to AC coupling. A smaller capacitor is used if pin 5 is used for positive feedback as in *Figure 1*.
2. Certain sources will produce a cleaner comparator output waveform if a 100 pF to 1000 pF capacitor C2 is connected directly across the input pins.
3. When the signal source is applied through a resistive network,  $R_S$ , it is usually advantageous to choose an  $R_S$  of substantially the same value, both for DC and for dynamic (AC) considerations. Carbon, tin-oxide, and metal-film resistors have all been used successfully in comparator input circuitry. Inductive wirewound resistors are not suitable.
4. When comparator circuits use input resistors (eg. summing resistors), their value and placement are particularly important. In all cases the body of the resistor should be close to the device or socket. In other words there should be very little lead length or printed-circuit foil run between comparator and resistor to radiate or pick up signals. The same applies to capacitors, pots, etc. For example, if  $R_S=10$  k $\Omega$ , as little as 5 inches of

lead between the resistors and the input pins can result in oscillations that are very hard to damp. Twisting these input leads tightly is the only (second best) alternative to placing resistors close to the comparator.

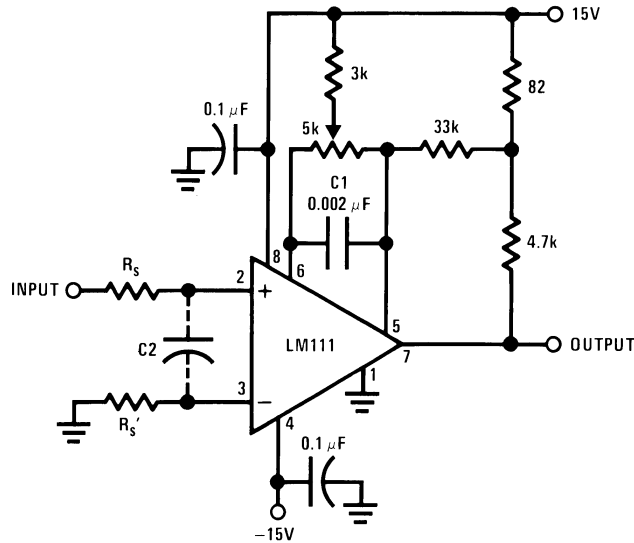
5. Since feedback to almost any pin of a comparator can result in oscillation, the printed-circuit layout should be engineered thoughtfully. Preferably there should be a groundplane under the LM111 circuitry, for example, one side of a double-layer circuit card. Ground foil (or, positive supply or negative supply foil) should extend between the output and the inputs, to act as a guard. The foil connections for the inputs should be as small and compact as possible, and should be essentially surrounded by ground foil on all sides, to guard against capacitive coupling from any high-level signals (such as the output). If pins 5 and 6 are not used, they should be shorted together. If they are connected to a trim-pot, the trim-pot should be located, at most, a few inches away from the LM111, and the 0.01  $\mu$ F capacitor should be installed. If this capacitor cannot be used, a shielding printed-circuit foil may be advisable between pins 6 and 7. The power supply bypass capacitors should be located within a couple inches of the LM111. (Some other comparators require the power-supply bypass to be located immediately adjacent to the comparator.)
6. It is a standard procedure to use hysteresis (positive feedback) around a comparator, to prevent oscillation, and to avoid excessive noise on the output because the comparator is a good amplifier for its own noise. In the circuit of *Figure 2*, the feedback from the output to the positive input will cause about 3 mV of hysteresis. However, if  $R_S$  is larger than 100 $\Omega$ , such as 50 k $\Omega$ , it would not be reasonable to simply increase the value of the positive feedback resistor above 510 k $\Omega$ . The circuit of *Figure 3* could be used, but it is rather awkward. See the notes in paragraph 7 below.

## 8.0 Application Hints (Continued)

7. When both inputs of the LM111 are connected to active signals, or if a high-impedance signal is driving the positive input of the LM111 so that positive feedback would be disruptive, the circuit of *Figure 1* is ideal. The positive feedback is to pin 5 (one of the offset adjustment pins). It is sufficient to cause 1 to 2 mV hysteresis and sharp transitions with input triangle waves from a few Hz to hundreds of kHz. The positive-feedback signal across the 82Ω resistor swings 240 mV below the posi-

tive supply. This signal is centered around the nominal voltage at pin 5, so this feedback does not add to the  $V_{OS}$  of the comparator. As much as 8 mV of  $V_{OS}$  can be trimmed out, using the 5 kΩ pot and 3 kΩ resistor as shown.

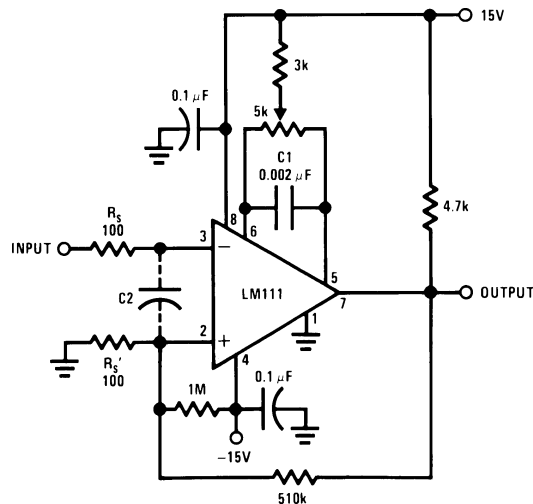
8. These application notes apply specifically to the LM111, LM211, LM311, and LF111 families of comparators, and are applicable to all high-speed comparators in general, (with the exception that not all comparators have trim pins).



00570429

Pin connections shown are for LM111H in the H08 hermetic package

**FIGURE 1. Improved Positive Feedback**

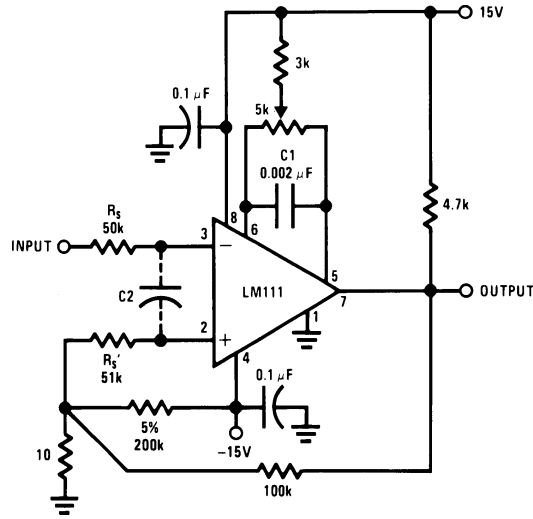


00570430

Pin connections shown are for LM111H in the H08 hermetic package

**FIGURE 2. Conventional Positive Feedback**

## 8.0 Application Hints (Continued)

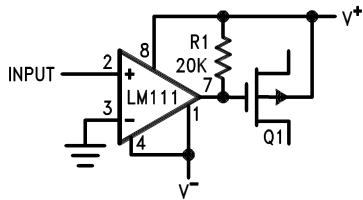


00570431

FIGURE 3. Positive Feedback with High Source Resistance

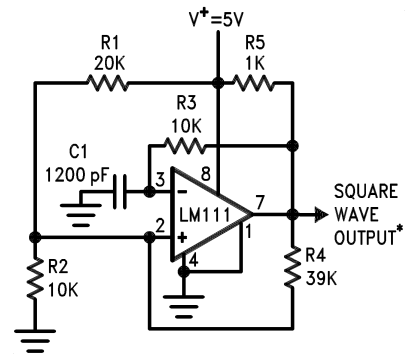
## 9.0 Typical Applications (Pin numbers refer to H08 package)

### Zero Crossing Detector Driving MOS Switch



00570413

### 100 kHz Free Running Multivibrator

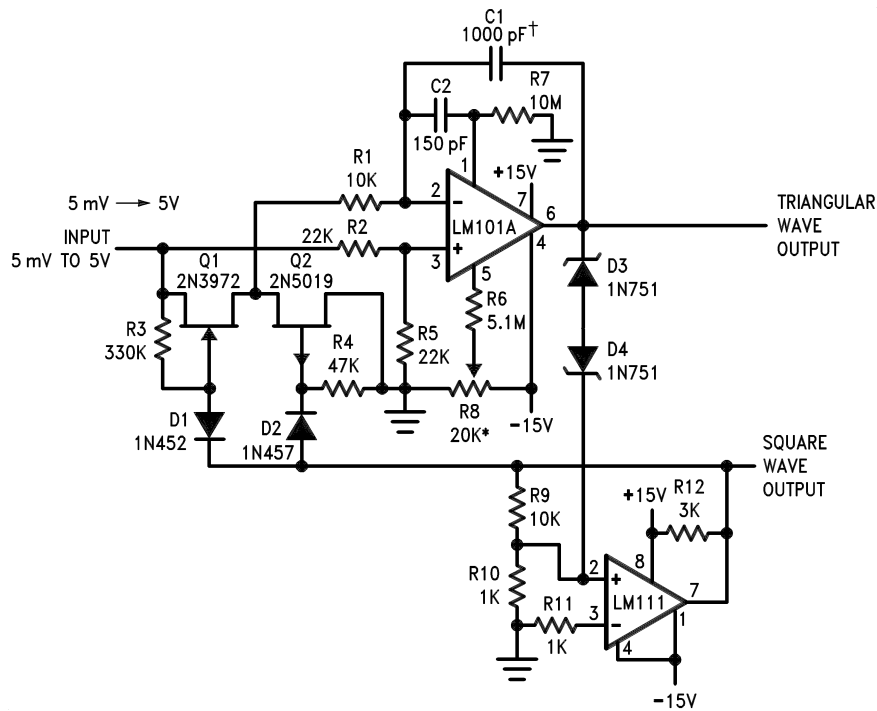


00570414

\*TTL or DTL fanout of two

## 9.0 Typical Applications (Pin numbers refer to H08 package) (Continued)

### 10 Hz to 10 kHz Voltage Controlled Oscillator

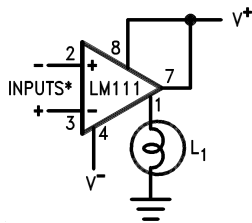


00570415

\*Adjust for symmetrical square wave time when  $V_{IN} = 5 \text{ mV}$

†Minimum capacitance 20 pF Maximum frequency 50 kHz

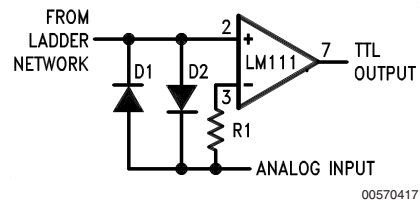
### Driving Ground-Referred Load



00570416

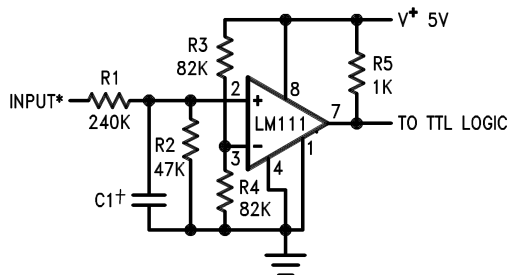
\*Input polarity is reversed when using pin 1 as output.

### Using Clamp Diodes to Improve Response



00570417

### TTL Interface with High Level Logic



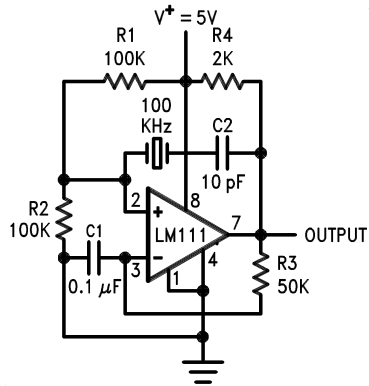
00570418

\*Values shown are for a 0 to 30V logic swing and a 15V threshold.

†May be added to control speed and reduce susceptibility to noise spikes.

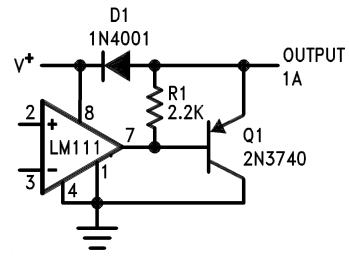
## 9.0 Typical Applications (Pin numbers refer to H08 package) (Continued)

**Crystal Oscillator**



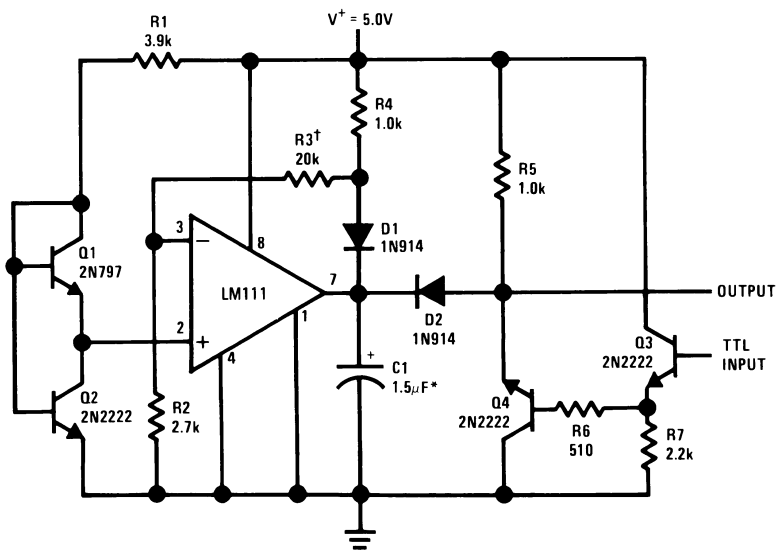
00570419

**Comparator and Solenoid Driver**



00570420

**Precision Squarer**



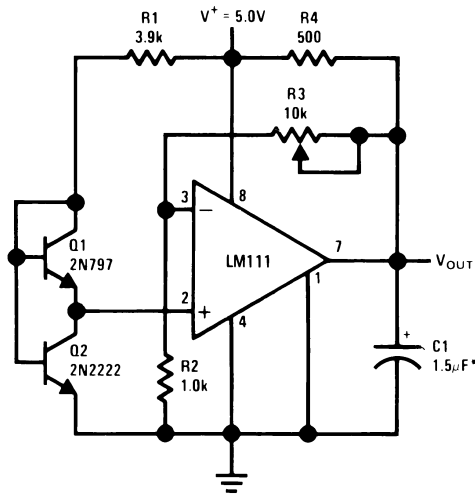
00570421

\*Solid tantalum

†Adjust to set clamp level

## 9.0 Typical Applications (Pin numbers refer to H08 package) (Continued)

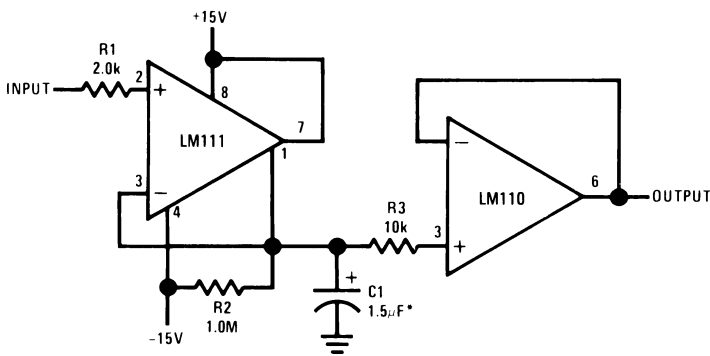
### Low Voltage Adjustable Reference Supply



00570422

\*Solid tantalum

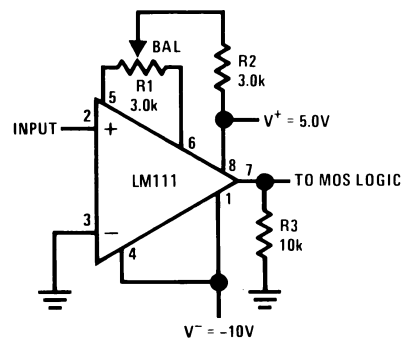
### Positive Peak Detector



00570423

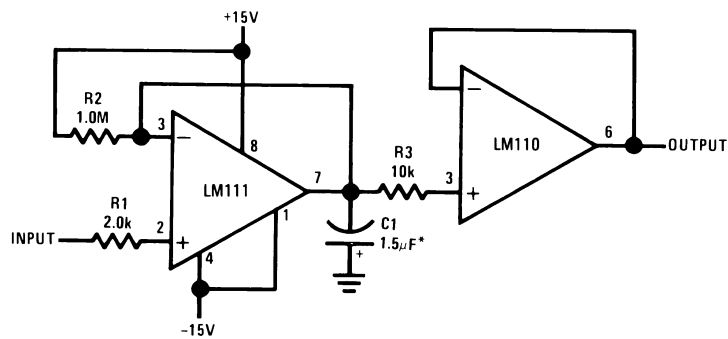
\*Solid tantalum

### Zero Crossing Detector Driving MOS Logic



00570424

### Negative Peak Detector

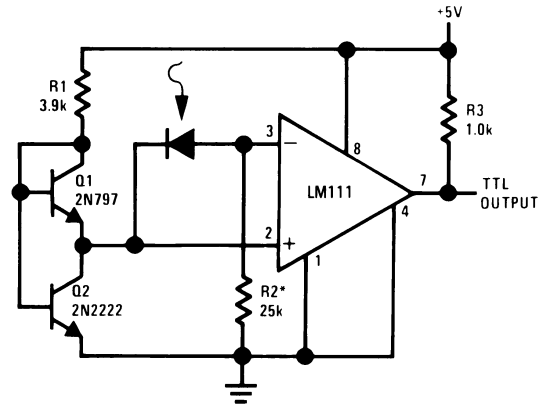


00570425

\*Solid tantalum

## 9.0 Typical Applications (Pin numbers refer to H08 package) (Continued)

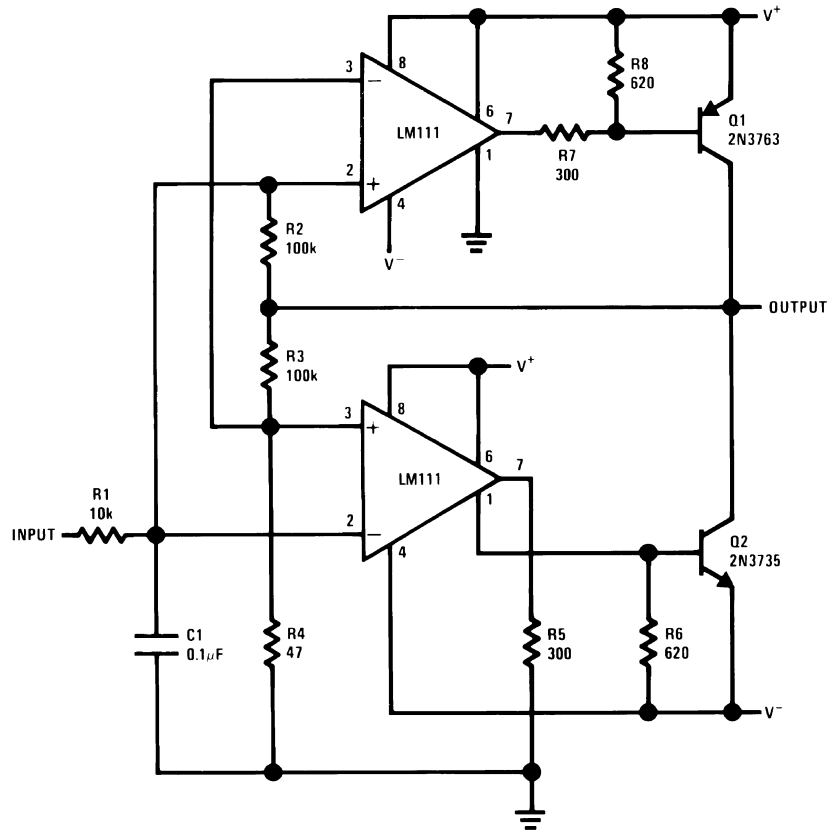
### Precision Photodiode Comparator



00570426

\*R2 sets the comparison level. At comparison, the photodiode has less than 5 mV across it, decreasing leakages by an order of magnitude.

### Switching Power Amplifier

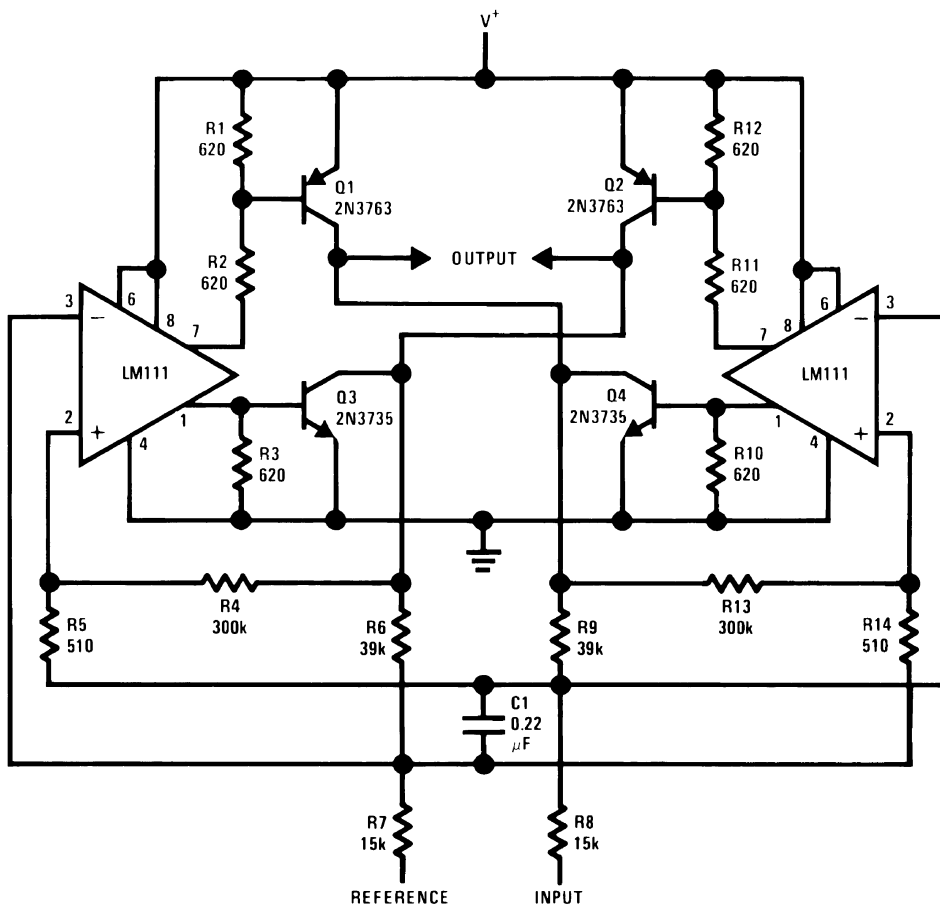


00570427



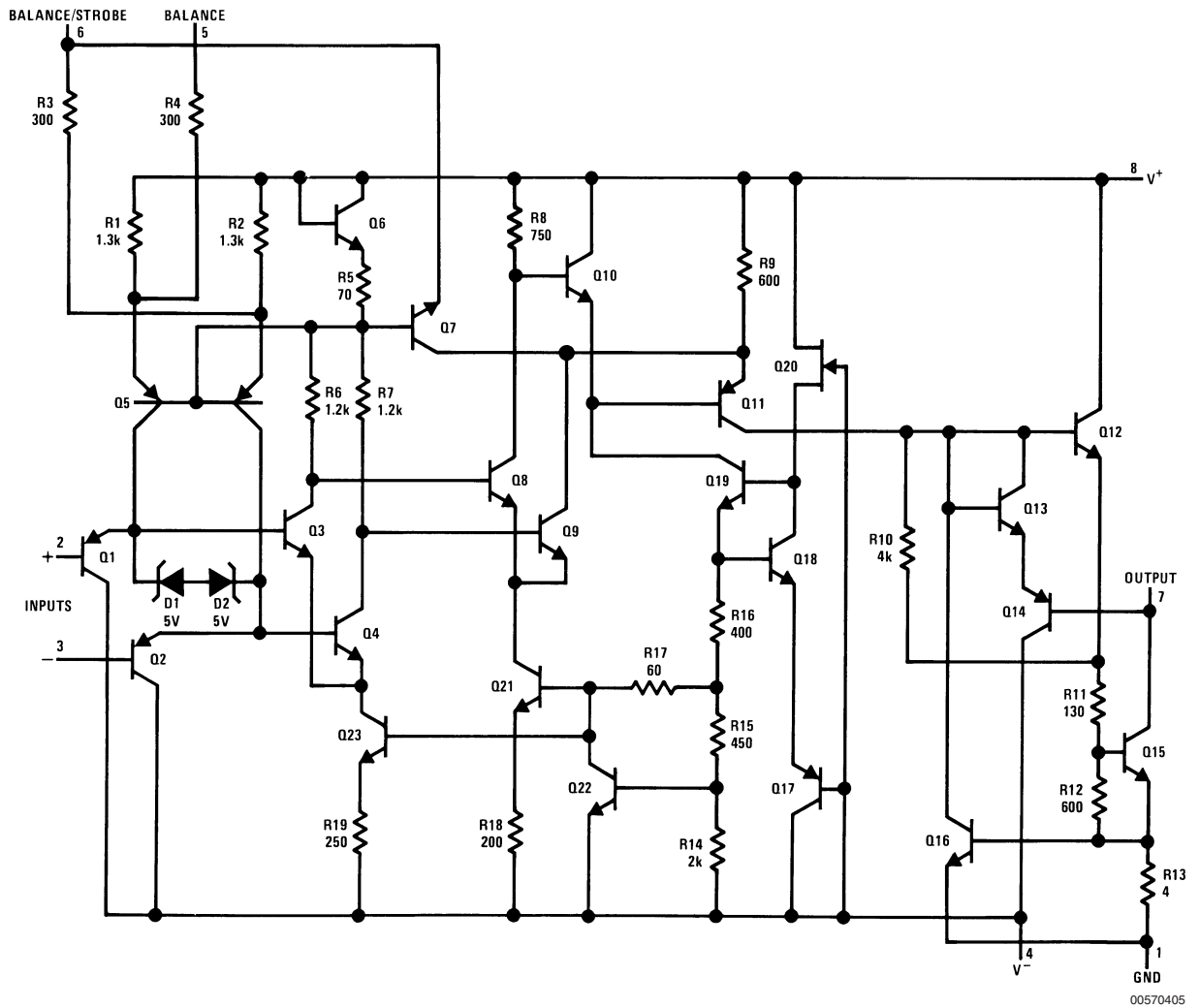
9.0 Typical Applications (Pin numbers refer to H08 package) (Continued)

Switching Power Amplifier



00570428

# 10.0 Schematic Diagram (Note 20)

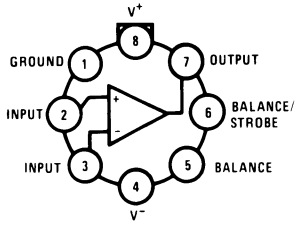


**Note 20:** Pin connections shown on schematic diagram are for H08 package.

00570405

# 11.0 Connection Diagrams

**Metal Can Package**



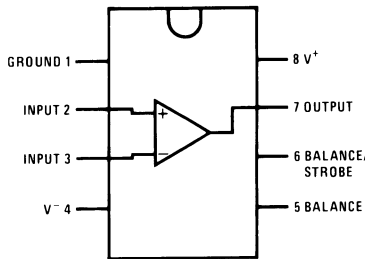
00570406

**Note:** Pin 4 connected to case

**Top View**

**Order Number LM111H, LM111H/883(Note 21) , LM211H or LM311H**  
**See NS Package Number H08C**

**Dual-In-Line Package**

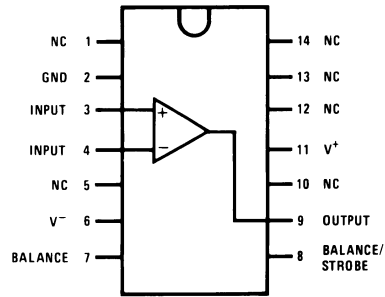


00570434

**Top View**

**Order Number LM111J-8, LM111J-8/883(Note 21),**  
**LM311M, LM311MX or LM311N**  
**See NS Package Number J08A, M08A or N08E**

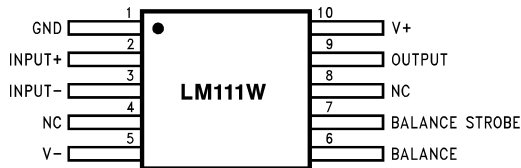
**Dual-In-Line Package**



00570435

**Top View**

**Order Number LM111J/883(Note 21)**  
**See NS Package Number J14A or N14A**



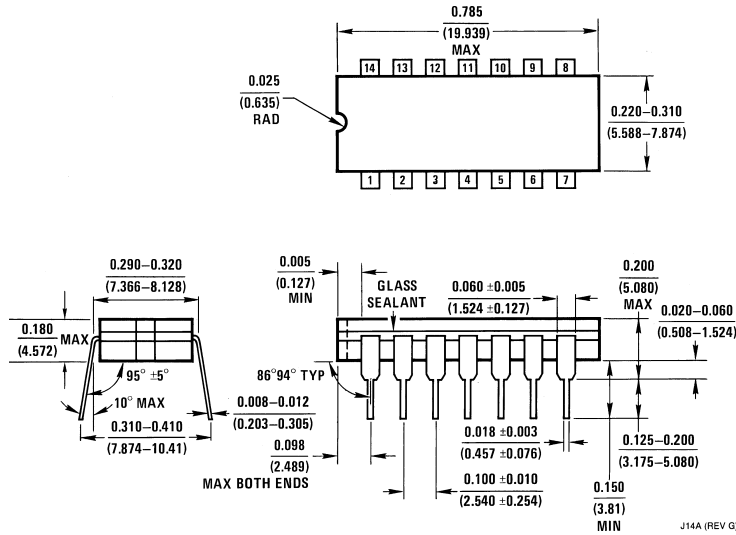
00570433

**Order Number LM111W/883(Note 21), LM111WG/883**  
**See NS Package Number W10A, WG10A**

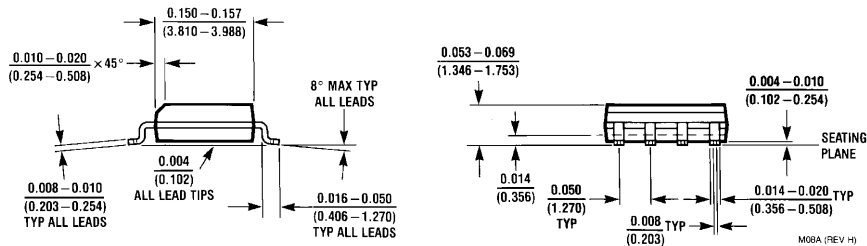
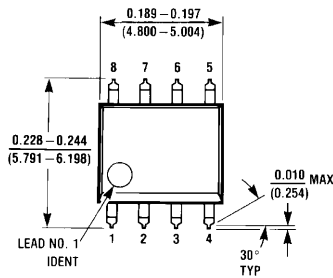
**Note 21:** Also available per JM38510/10304



**12.0 Physical Dimensions** inches (millimeters) unless otherwise noted (Continued)

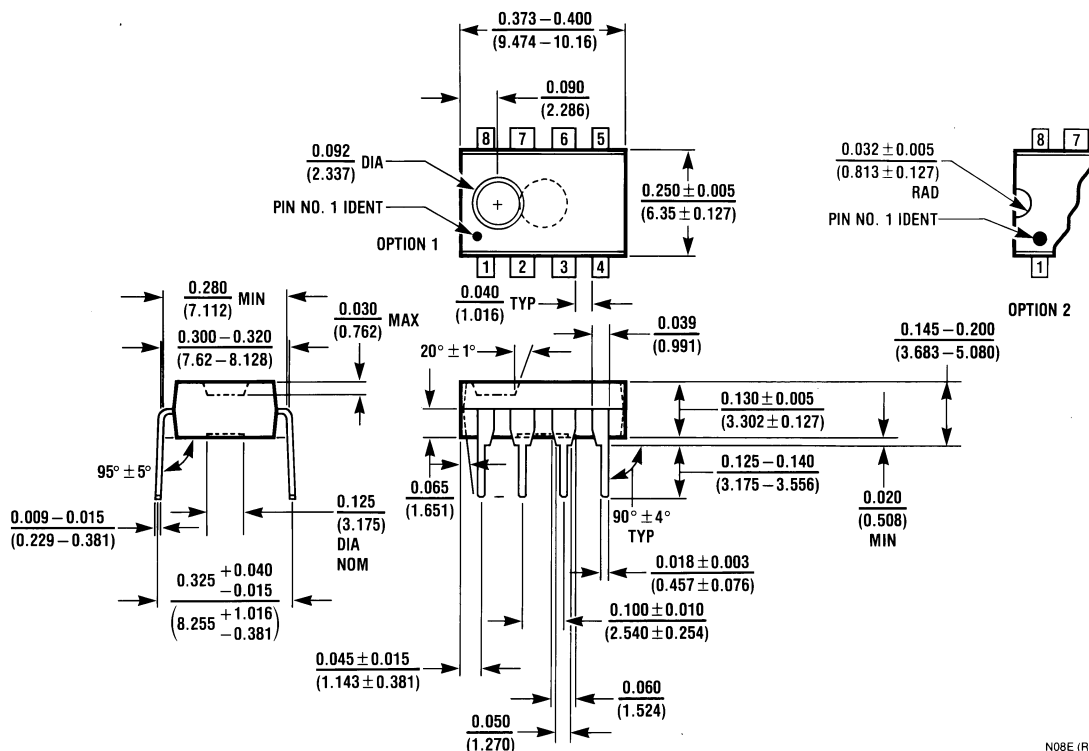


**Dual-In-Line Package (J)**  
**Order Number LM111J/883**  
**NS Package Number J14A**



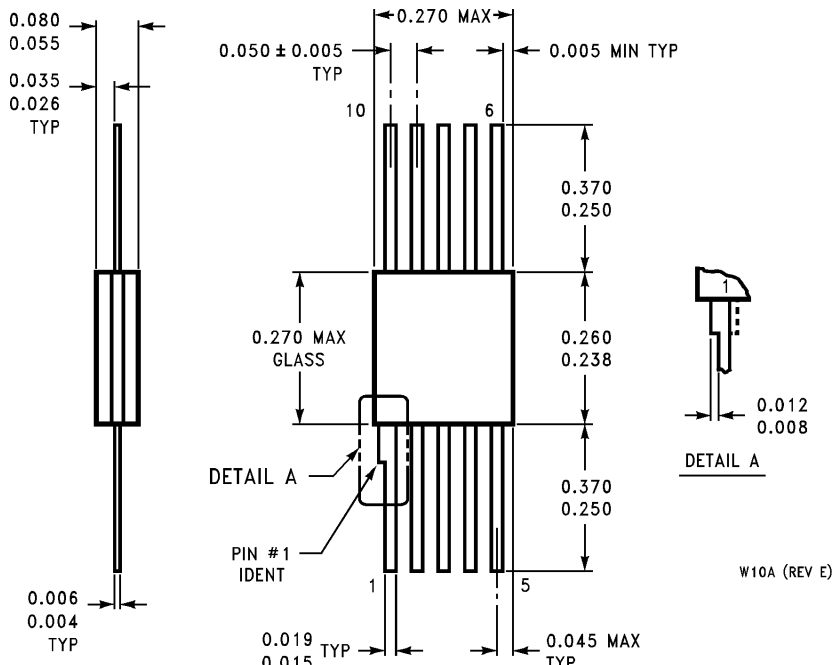
**Dual-In-Line Package (M)**  
**Order Number LM311M, LM311MX**  
**NS Package Number M08A**

## 12.0 Physical Dimensions inches (millimeters) unless otherwise noted (Continued)



Dual-In-Line Package (N)  
 Order Number LM311N  
 NS Package Number N08E

N08E (REV F)



Order Number LM111W/883, LM111WG/883  
 NS Package Number W10A, WG10A

W10A (REV E)

## Notes

National does not assume any responsibility for use of any circuitry described, no circuit patent licenses are implied and National reserves the right at any time without notice to change said circuitry and specifications.

For the most current product information visit us at [www.national.com](http://www.national.com).

### LIFE SUPPORT POLICY

NATIONAL'S PRODUCTS ARE NOT AUTHORIZED FOR USE AS CRITICAL COMPONENTS IN LIFE SUPPORT DEVICES OR SYSTEMS WITHOUT THE EXPRESS WRITTEN APPROVAL OF THE PRESIDENT AND GENERAL COUNSEL OF NATIONAL SEMICONDUCTOR CORPORATION. As used herein:

1. Life support devices or systems are devices or systems which, (a) are intended for surgical implant into the body, or (b) support or sustain life, and whose failure to perform when properly used in accordance with instructions for use provided in the labeling, can be reasonably expected to result in a significant injury to the user.
2. A critical component is any component of a life support device or system whose failure to perform can be reasonably expected to cause the failure of the life support device or system, or to affect its safety or effectiveness.

### BANNED SUBSTANCE COMPLIANCE

National Semiconductor certifies that the products and packing materials meet the provisions of the Customer Products Stewardship Specification (CSP-9-111C2) and the Banned Substances and Materials of Interest Specification (CSP-9-111S2) and contain no "Banned Substances" as defined in CSP-9-111S2.



**National Semiconductor**  
**Americas Customer**  
**Support Center**  
 Email: [new.feedback@nsc.com](mailto:new.feedback@nsc.com)  
 Tel: 1-800-272-9959

**National Semiconductor**  
**Europe Customer Support Center**  
 Fax: +49 (0) 180-530 85 86  
 Email: [europa.support@nsc.com](mailto:europa.support@nsc.com)  
 Deutsch Tel: +49 (0) 69 9508 6208  
 English Tel: +44 (0) 870 24 0 2171  
 Français Tel: +33 (0) 1 41 91 8790

**National Semiconductor**  
**Asia Pacific Customer**  
**Support Center**  
 Email: [ap.support@nsc.com](mailto:ap.support@nsc.com)

**National Semiconductor**  
**Japan Customer Support Center**  
 Fax: 81-3-5639-7507  
 Email: [jpn.feedback@nsc.com](mailto:jpn.feedback@nsc.com)  
 Tel: 81-3-5639-7560

## Appendix D:

### Calculations

## Engine Hydrolock Mitigation Spring and Flywheel calculations

#### Exerted Forces

$$\text{compression}_{\text{init}} := .25\text{in}$$

$$\text{Pressure}_{\text{running}} := 400\text{psi}$$

$$\text{Pressure}_{\text{hold}} := 500\text{psi}$$

$$F_{\text{upward}} - F_{\text{spring}} = 0$$

$$F_{\text{spring}} = \text{compression}_{\text{init}} \cdot k$$

$$F_{\text{upward}} - \text{compression}_{\text{init}} \cdot k = 0$$

$$F_{\text{upward}} = k \cdot \text{compression}_{\text{init}}$$

#### Required spring dimensions

$$\text{len}_{\text{free}} := 1\text{in} \quad \text{rod}_{\text{diam}} := .233\text{in}$$

$$\text{wire}_{\text{diam}} := .059\text{in}$$

$$\text{len}_{\text{solid}} := .490\text{in}$$

$$r := .125\text{in}$$

$$A := \pi \cdot r^2 = 0.049 \cdot \text{in}^2$$

$$x := .5\text{in}$$

$$k_{\text{real}} := 100 \frac{\text{lbf}}{\text{in}}$$

$$F_{\text{hold}} := \text{Pressure}_{\text{hold}} \cdot A = 109.176\text{N}$$

$$\text{spring}_{\text{constant}} := \frac{F_{\text{hold}}}{\text{compression}_{\text{init}}} = 98.175 \cdot \frac{\text{lbf}}{\text{in}}$$

$$\text{init}_{\text{compression}_{\text{real}}} := \frac{F_{\text{hold}}}{k_{\text{real}}} = 0.245 \cdot \text{in}$$

$$\text{len}_{\text{init}_{\text{comp}}} := \text{len}_{\text{free}} - \text{compression}_{\text{init}} = 0.75\text{in}$$

$$\text{len}_{\text{init}_{\text{comp}}} - \text{wire}_{\text{diam}} = 0.691 \cdot \text{in}$$

$$\text{len}_{\text{free}} - \text{init}_{\text{compression}_{\text{real}}} = 0.755 \cdot \text{in}$$



$$\text{len}_{\text{free}} - \text{init}_{\text{compression}} - \text{real} - \text{wire}_{\text{diam}} = 0.696 \cdot \text{in}$$

Full release pressure

$$P_{\text{fr}} := \frac{k_{\text{real}} \cdot (\text{len}_{\text{free}} - \text{len}_{\text{solid}})}{A} = 1.039 \times 10^3 \cdot \text{psi}$$

$$k_{\text{real}} \cdot \text{len}_{\text{solid}} = 49 \cdot \text{lbf}$$

$$k_{\text{real}} \cdot .245 \text{in} = 24.5 \cdot \text{lbf}$$

$$k_{\text{real}} \cdot (\text{len}_{\text{free}} - \text{len}_{\text{solid}}) = 51 \cdot \text{lbf}$$

$$\text{len}_{\text{free}} - \text{len}_{\text{solid}} = 0.51 \cdot \text{in}$$

### Calculations to determine max forces exerted on flywheel adapter systems

$$F_m := 10 \text{lb} \quad A_{\text{pin}} := .2 \cdot 4 \text{in} = 2.032 \times 10^{-3} \text{m}^2$$

$$r_m := 5 \text{in}$$

$$I := F_m \cdot r^2 = 5.013 \times 10^{-3} \text{m}^2 \cdot \text{slug}$$

$$\alpha := 3000 \cdot \frac{\text{rev}}{\text{s} \cdot \text{min}} = 314.159 \frac{1}{\text{s}^2}$$

$$\alpha_T := \alpha = 314.159 \frac{1}{\text{s}^2} \cdot \text{rad}$$

$$\text{Torque} := \alpha_T \cdot I = 166.243 \frac{\text{m}}{\text{s}^2} \cdot \text{ft} \cdot \text{lb}$$

$$\tau := \frac{\text{Torque}}{A_{\text{pin}}} = 1.131 \times 10^4 \text{N}$$

Calculate max torsional shear on bolt

$$r_{\text{bolt}} := \frac{3}{8} \cdot \quad J := \frac{\pi}{2} \cdot r_{\text{bolt}}^2$$

$$\tau_{\text{tor}} := \frac{\text{Torque} \cdot r_{\text{bolt}}}{J} = 3.072 \times 10^3 \text{N}$$

Max shear on the 5 bolt adapter

$$\tau_{\text{adp}} := \frac{\text{Torque}}{A_{\text{adp}}} = 614.466 \text{ N}$$
$$A_{\text{adp}} := \left[ 2\pi \cdot \left(\frac{1}{8}\right)^2 + 2\pi \cdot \frac{1}{8} \cdot .25 \right] \cdot 5 \cdot \text{in}$$

Using both systems

$$A_{\text{total}} := A_{\text{adp}} + A_{\text{pin}} = 0.039 \text{ m}$$

$$\tau_{\text{total}} := \frac{\text{Torque}}{A_{\text{total}}} = 582.806 \text{ N}$$

## Appendix E: Analysis

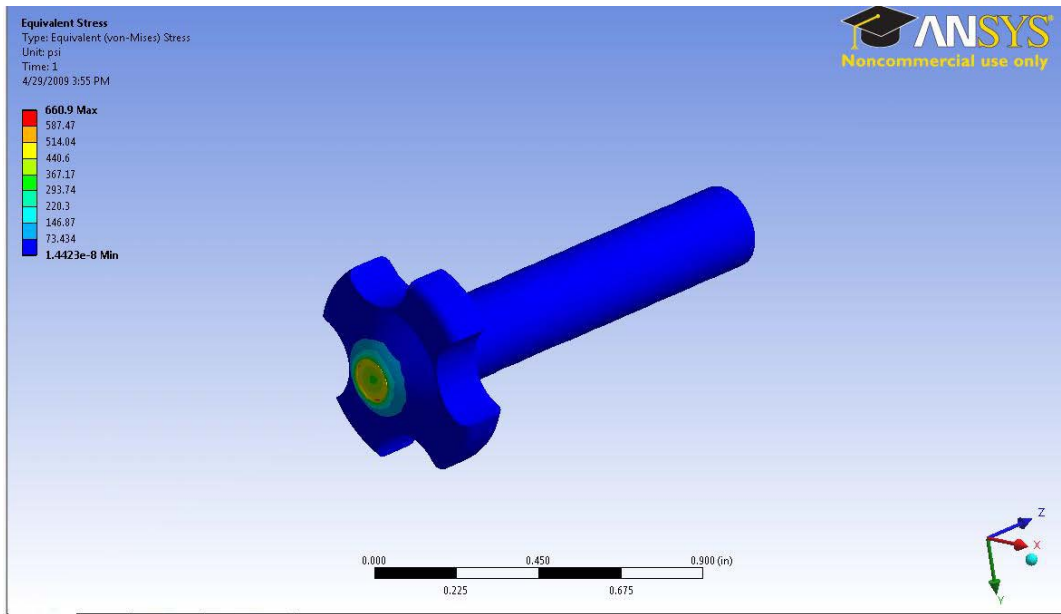


Figure 13-14: Valve Variation 1

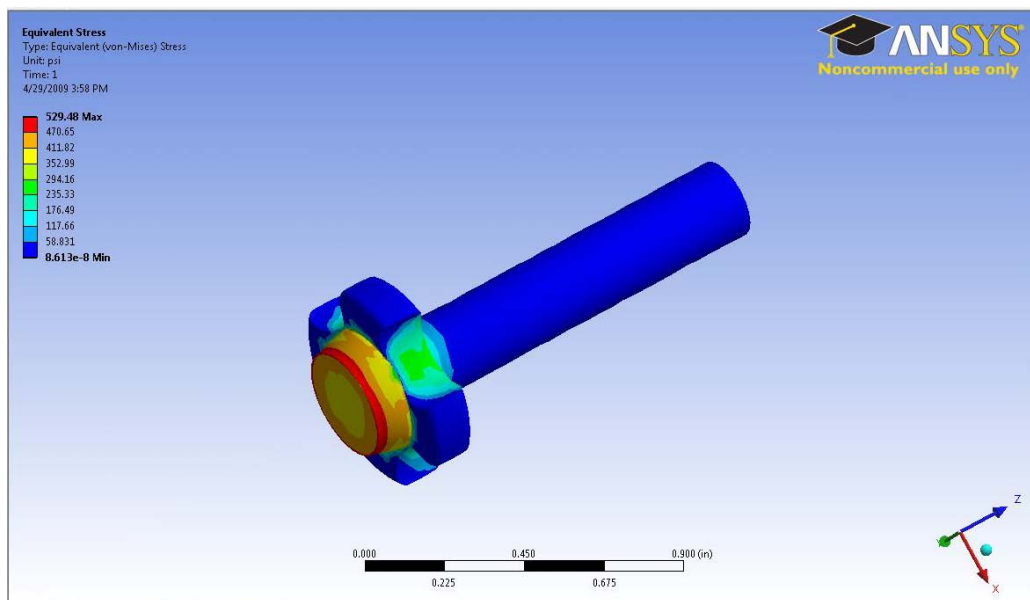


Figure 13-15: Valve Variation 2

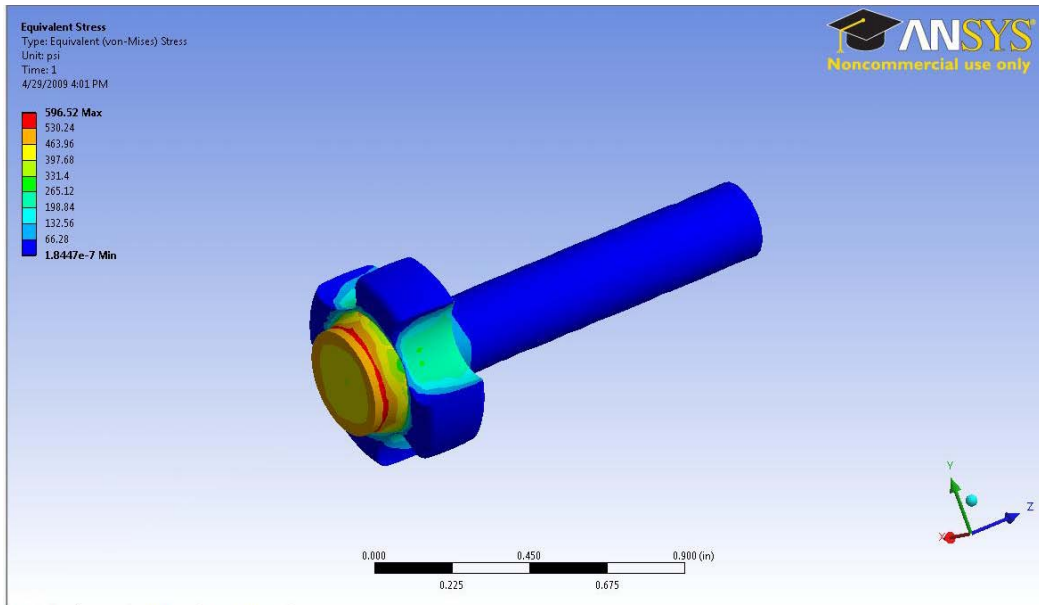


Figure 13-16: Valve Variation 3

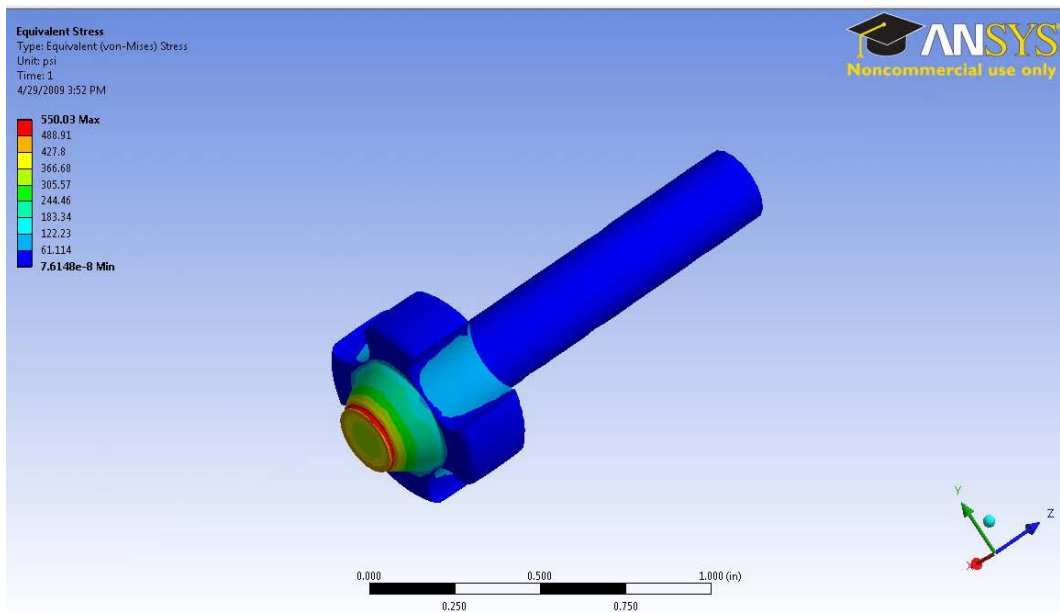


Figure 13-17: Valve Variation 4

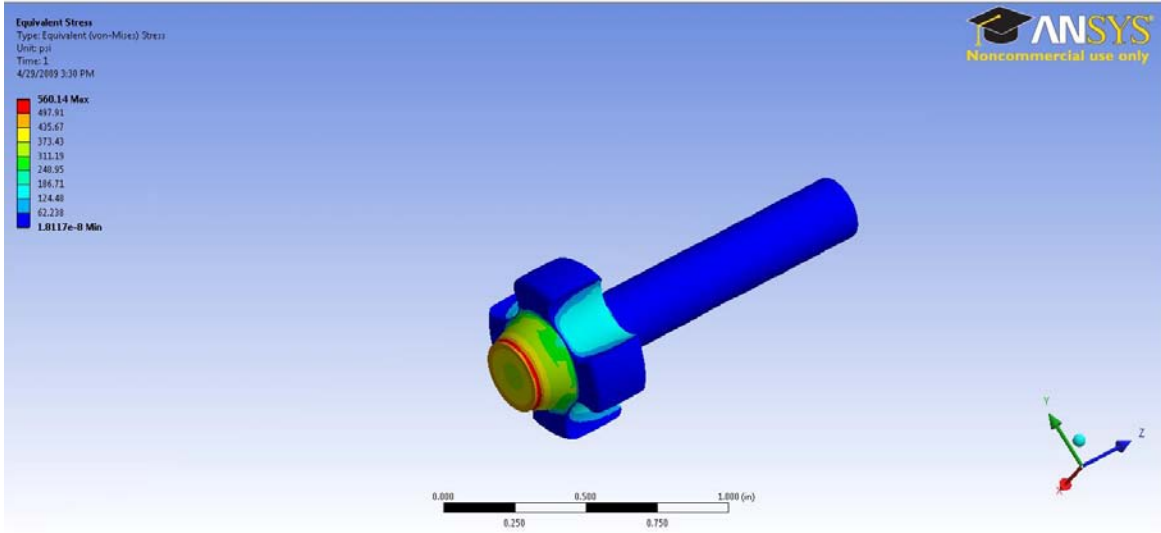
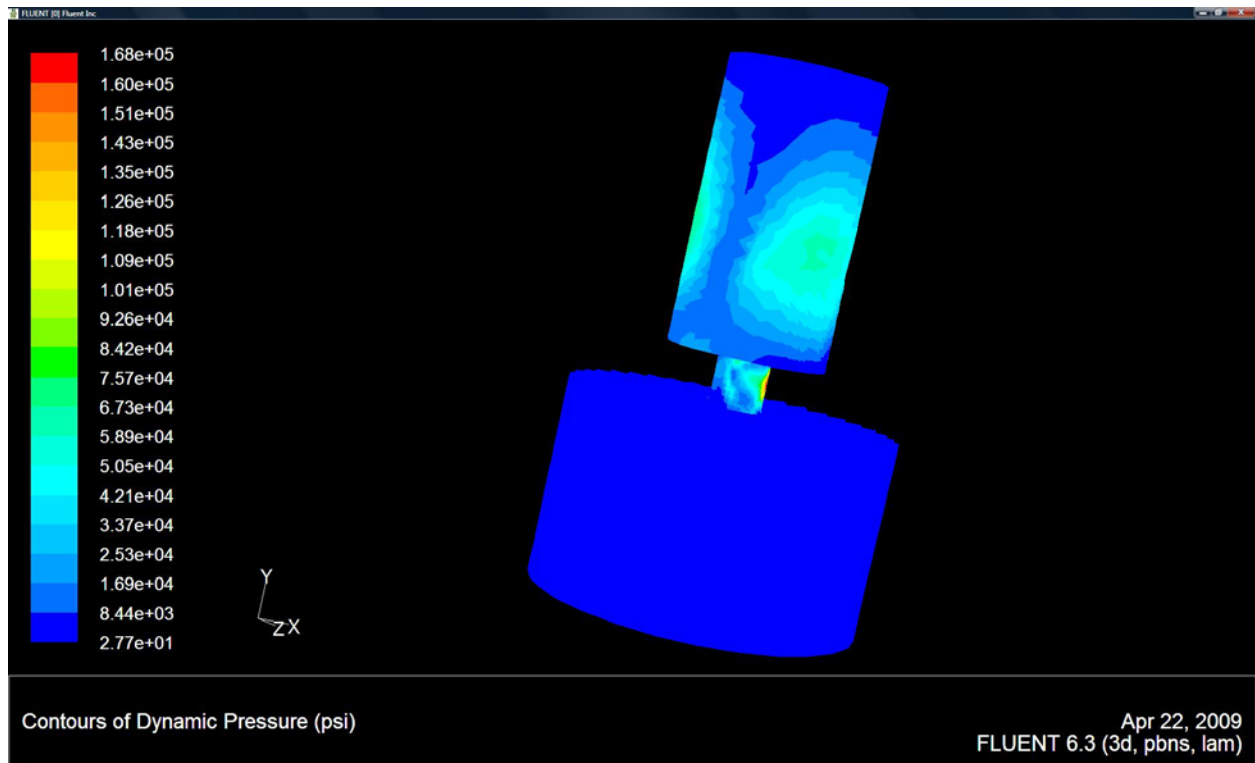
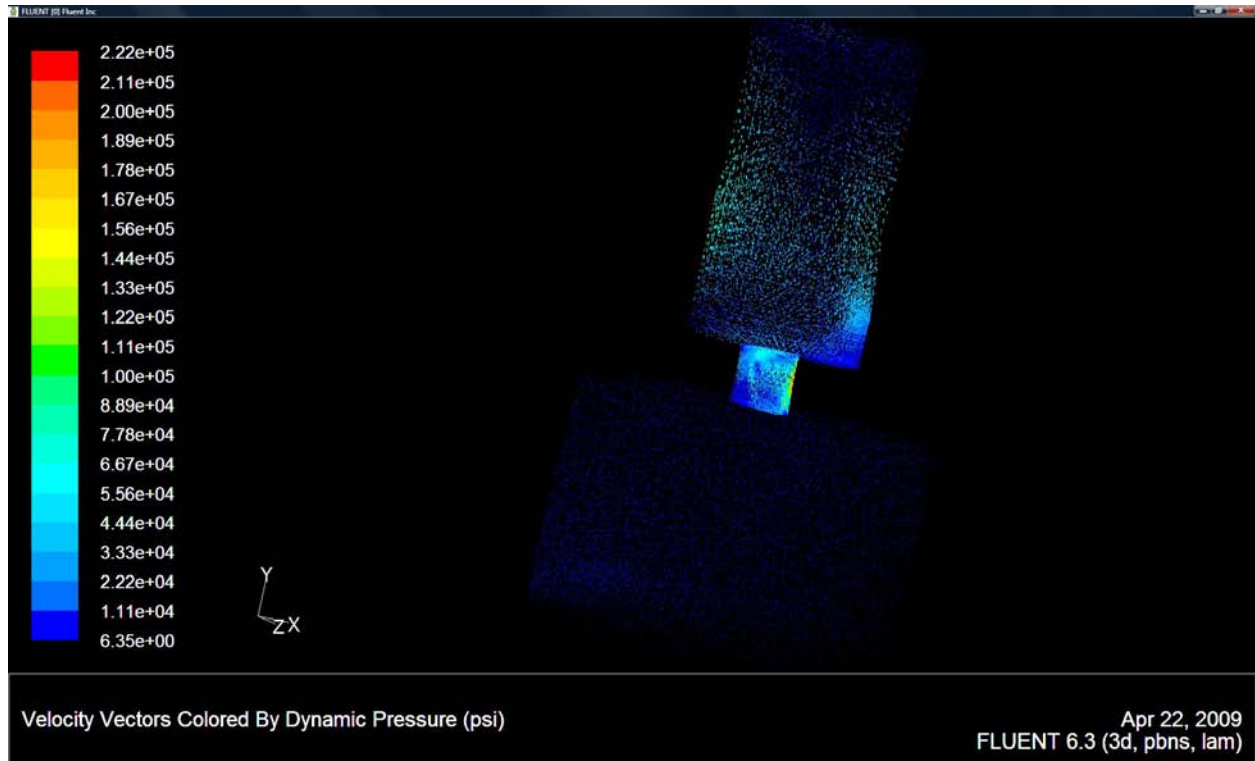
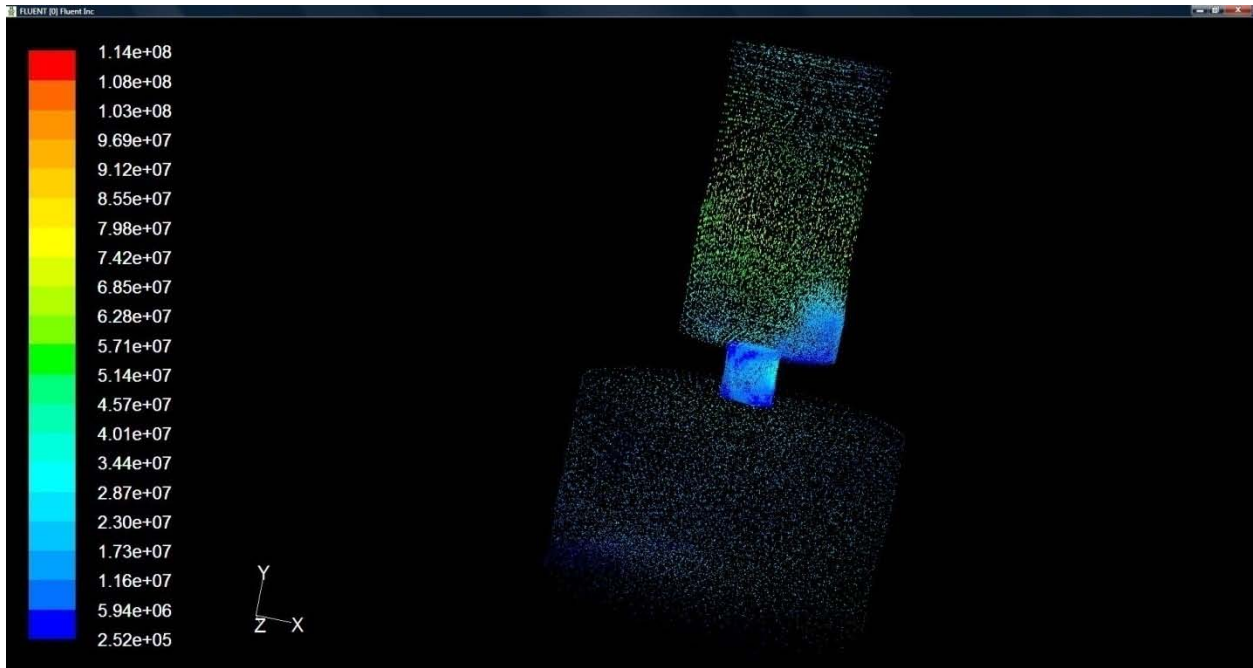


Figure 13-18: Final Valve

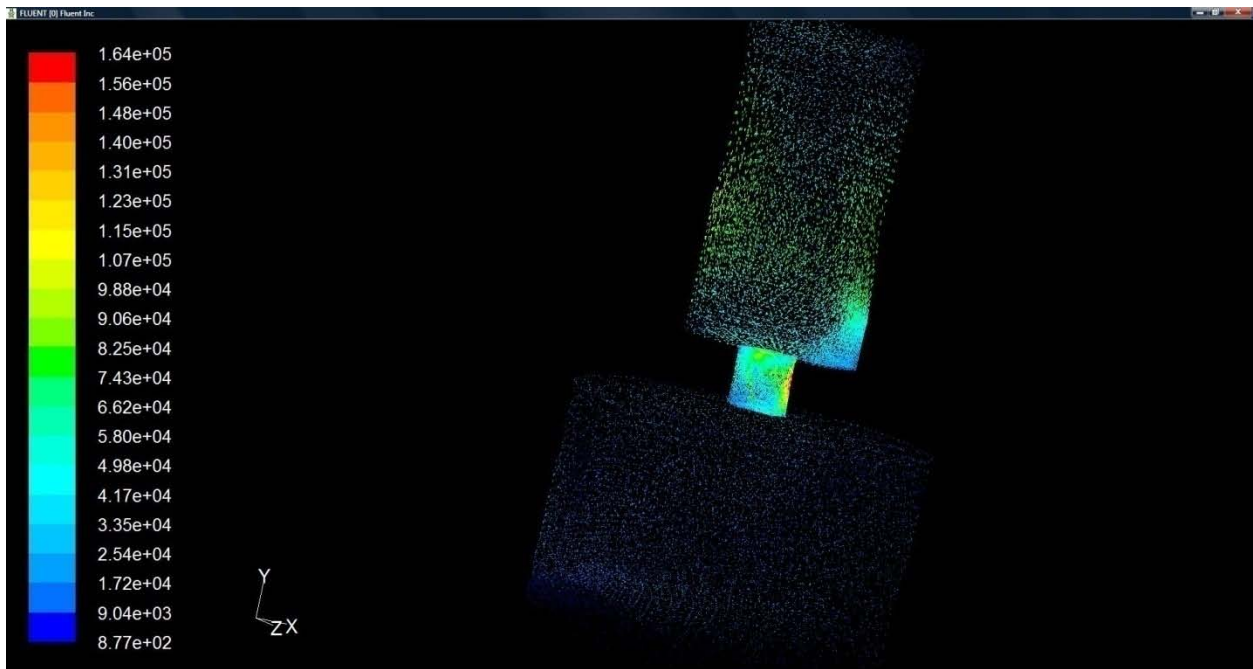
## Appendix F: Analysis





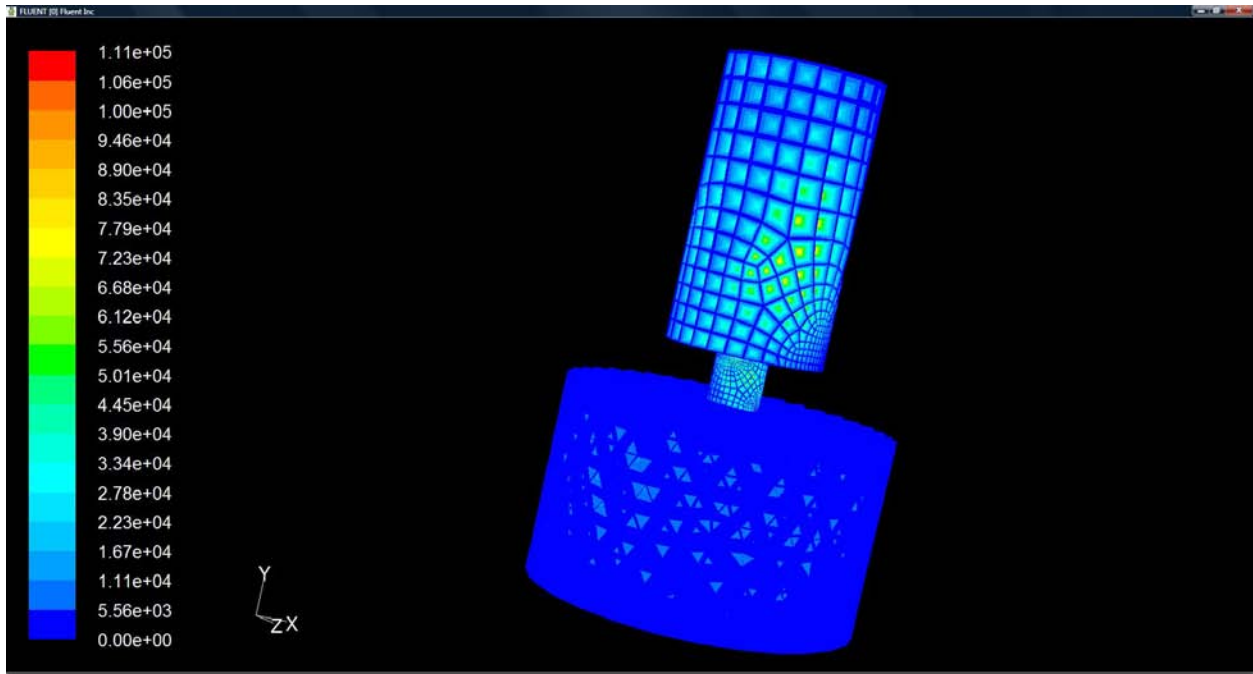
Velocity Vectors Colored By Cell Reynolds Number

Apr 22, 2009  
FLUENT 6.3 (3d, pbns, lam)



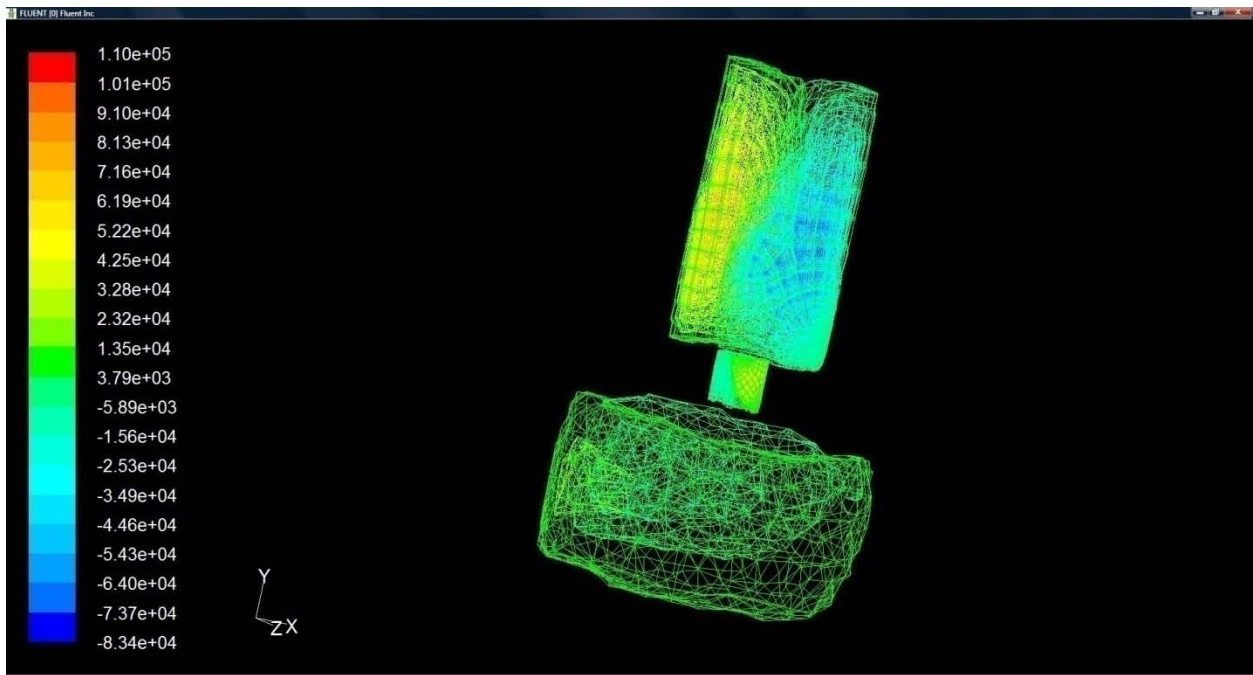
Velocity Vectors Colored By Velocity Magnitude (ft/s)

Apr 22, 2009  
FLUENT 6.3 (3d, pbns, lam)



Contours of Velocity Magnitude (ft/s)

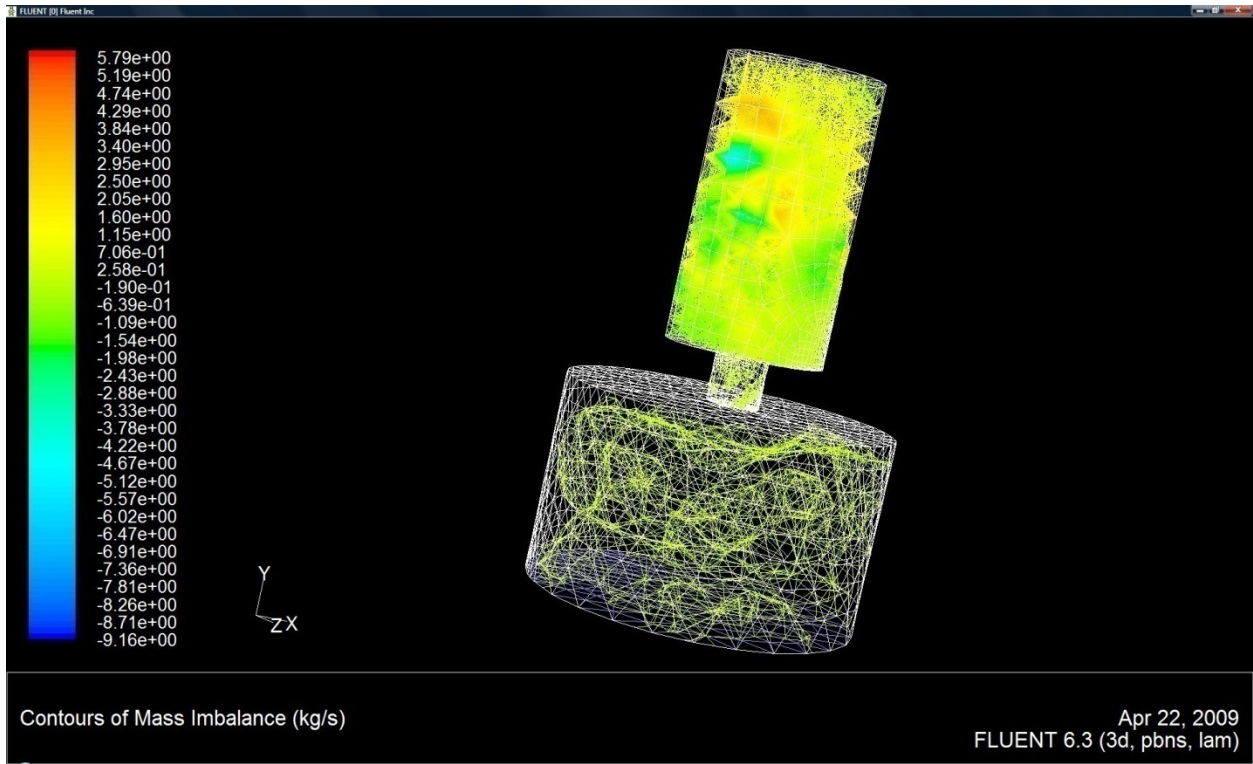
Apr 22, 2009  
FLUENT 6.3 (3d, pbns, lam)



Contours of Y Velocity (ft/s)

Apr 22, 2009  
FLUENT 6.3 (3d, pbns, lam)





## Bibliography

(Williams)(Pease)(Voltage Comparator Information And Circuits, 2009)

*About.com: Inventors.* (n.d.). Retrieved October 2008, from The History of the Automobile: <http://inventors.about.com/library/weekly/aacarsgasa.htm>

Atkins, R. D. (April, 2009). *An introduction to Engine Testing and Development.* SAE International.

*Basic Engine Dynamics Slideshow.* (2004, December 11). Retrieved September 2009, from WPI Motorsports Forum: <http://users.wpi.edu/~wpimotor/cgi-bin/yabb2/YaBB.pl>

Beyon, J. Y. (September 2000). *LabVIEW Programming, Data Acquisition and Analysis.* Prentice Hall PTR.

Dennis K. Lieu, S. S. *Visualization, Modeling, and Graphics for Engineering Design.* Thomson.

Duncan A. Grant, J. G. (1989). *Power MOSFET Theory and Applications.* Wiley-Interscience.

Hambley, A. R. *Electrical Engineering Principles and Applications.* Pearson Prentice Hall.

Johnson, G. W. (1997). *LabVIEW Graphical Programming.* Mcgraw-Hill.

Mihura, B. (June 26, 2001). *LabVIEW for data acquisition.* Prentice Hall PTR.

Moaveni, S. *Finite Element Analysis Theory and Application with ANSYS*. Mankato, Minnesota, USA: Pearson Prentice Hall.

Norton, R. L. *Design of Machinery*. Worcester, MA, USA: Mc Graw Hill.

Norton, R. L. *Machine Design an integrated approach* . Worcester, MA: Mc Graw Hill.

Oberg, J. H. *Machinery's Handbook 28*. (R. H. Christopher McCauley, Ed.) Industrial Press.

Pease, R. *Troubleshooting Analog Circuits*. EDN Magazine.

Ritter, D. J. (December 15, 2001). *LabVIEW GUI Essential Techniques*. McGraw-Hill Professional Publishing.

Stuart, R. (2007). *A Descriptive History of The Steam Engine*. Kessinger Publishing.

Thomas G. Beckwith, R. D. *Mechanical Measurements*. Pearson Prentice Hall.

*Voltage Comparator Information And Circuits*. (2009, 2 15). Retrieved from Voltage Comparators: <http://home.cogeco.ca/~rpaisley4/Comparators.html>

William H. Roadstrum, D. H. (1994). *Electrical Engineering for all Engineers*. Wiley.

William Strunk Jr., E. W. *The Elements of Style*. Longman.

Williams, J. *Analog Circuit Design: Art, Science and Personalities* . EDN Magazine.

(Basic Engine Dynamics Slideshow, 2004)